Molecular and genetic characterisation of a non-canonical auxin signalling mechanism

by

André Kuhn

September 2019

A thesis submitted to the University of East Anglia
for the degree of
Doctor of Philosophy

University of East Anglia
John Innes Centre

This thesis is dedicated to my son Daniel.

Abstract

Developmental programmes within multicellular organisms originate from a single cell that proliferates into numerous cells ultimately differentiating to make up specialized tissues and organs. Tight temporal and spatial regulation of the genes involved in these processes is essential for proper development of the organism. In plants, the hormone auxin controls almost all aspects of plant development through the gene regulatory properties of Auxin Response Factors (ARFs). Plant hormone signalling is most commonly based on de-repression via degradation of transcriptional repressors. Recently, a non-canonical signalling mechanism for the plant hormone auxin in organ development was uncovered in which the auxin has a direct effect on the activity of a transcription factor complex towards its downstream targets. In this pathway, ETTIN (ETT/ARF3) is a pivotal component. This thesis reports that ETT binds auxin directly and acts as a receptor in non-canonical auxin signalling to modulate gene expression, independently of the canonical auxin signalling machinery. Due to this direct auxin-effect on ETT, this pathway is reminiscent of animal hormonal pathways that often involve direct transcription factor-hormone interactions that modulate gene expression. In addition, this thesis identified that auxin has a direct and ETT-dependent effect on the chromatin environment of ETT-target genes. This is another feature reminiscent of hormonal signalling in animals and in agreement with ETT physically interacting with several chromatin modifying complexes in an auxin-sensitive manner. Above all this thesis identified that binding of the auxin molecule leads to ETTIN dissociating from co-repressor proteins of the TOPLESS/TOPLESS-RELATED family followed by histone acetylation and induction of target gene expression. Finally, using targeted mutations of ETT-binding cis-regulatory elements, I dissected the importance of these elements for the spatio-temporal regulation of ETT-target genes. Together, unlike canonical auxin signalling, this non-canonical auxin signalling provides an instantly reversible expression switch required for precise polarity establishment during gynoecium development.

Acknowledgements

My story at the John Innes Centre started almost exactly ten years ago, when I spend a three-month work experience internship in the group of Prof. Michael Lenhard. This internship got me interested in plant developmental biology and inspired me to enrol at Wageningen University to pursuit a degree in biology. A couple of years later, in 2013, I returned to the John Innes Centre this time for a three-month master internship in the group of Prof. Lars Østergaard. I found a welcoming group and in Lars a very supportive and enthusiastic supervisor. After completing this internship, I hoped to be able to return for my PhD-project. Fortunately, Lars was equally keen to have me back so that after finishing my master project in 2015 I could return for my PhD-project.

Therefore, I first would like to thank Lars, for his enthusiasm, support, and guidance throughout the years. Thank you for all the opportunities and freedom you have given me to grow not only as a scientist but also as a person during my PhD. I could not have asked for a better supervisor.
I would also like to thank my secondary supervisor, Prof. Caroline Dean, for her insight, encouragement and where necessary critical feedback. Further, I would like to thank the BBSRC and NRP DTP programme for funding my PhD.

I also want to thank my former MSc-thesis supervisor, Prof. Dolf Weijers who got me excited about auxin biology. Dolf has always been a great mentor and given valuable advice throughout my PhD. Thank you for this, Dolf, and thank you for giving me the opportunity to meet with you and your group to discuss science whenever I am in the Netherlands.

This work would not have been possible without the help of the many people who have contributed to this project in many different ways e.g. by sharing seeds or other materials.
I want to thank Dr. Stefan Kepinski at the University of Leeds for hosting me in his lab and the fruitful collaboration establishing ETT as an auxin binding protein. In particular I want to thank Dr. Sigurd Ramans Harborough with who I performed the NMR-experiments and who analysed the data. Thank you for your time and patience. Furthermore, I want to thank Heather McLaughlin, Dr. Kelley Gallagher and Dr. Felix Ramos Leon for their help with protein purification. I also need to acknowledge Aurelia Stahl and Bethany Runciman, two students that I have supervised and that contributed to this thesis.

A special thanks to Dr. Laila Moubayidin, who has been one of the few people who has been here for the entire duration of my project. Thank you, Laila for your critical yet open mind, the stimulating scientific and non-scientific discussions and for always keeping me motivated particularly when things felt overwhelming. You are an inspiration to every scientist, and I am

grateful to have been able to see you grow throughout the years into a group leader. I wish you all the best for the future inside and outside the lab.

A big thank you to Nicola Stacey and Heather McLaughlin for proof-reading this thesis.

I have been extremely lucky during my PhD to be part of a fantastic lab group. Although the group changed a lot since I first visited in 2013, it always remained a truly lovely group of people at work and outside of work. Thank you to Heather, Mikki, Billy, Łukasz, Yang, Sophia, Marie, Yuli, Xinran, Bhavani and Laila with who I have had the pleasure of sharing an office with over the last four years and who have become good friends. Generally, I have not been short of friendship during the last four years. Especially, I want to thank Mikki and Sylvain, two friends who started the PhD with me on the same day. Thank you for your friendship and moral support over the last four years – we have been through it all together.

Of course, I want to thank the people in my life that know me best, my family; especially my mum, my dad and my brother Stephan for all their love and support.

Liebe Mama, lieber Papa; euren Beitrag zum Erfolg dieser Doktorarbeit ist kaum zu überschätzen. Ohne euch wäre ich nicht da, wo ich heute bin. Ihr habt mir gezeigt wie faszinierend die Welt um uns herum ist und habt dadurch mein Interesse daran geweckt zu verstehen wie die Dinge um uns herum funktionieren. Ihr habt mich immer ermutigt Neues auszuprobieren und mich gelehrt Fragen zu stellen. Auch wenn es nicht immer einfach war, habt ihr mich, seit ich ein kleiner Junge war, immer unterstützt, auch wenn Andere an mir gezweifelt haben. Für eure Liebe, eure Unterstützung und euren unerschütterlichen Glauben an mich bin ich euch unendlich dankbar.

Finally, I would like to dedicate this thesis to two special people in my life: my wife Paola and my little son Daniel. Daniel, you are my motivation to be a better me every day.
Paola you have been with me since the start. I am a lucky man to have you by my side. You are my safe harbour. I know it has not always been easy for you in the last years, but I am grateful for all your support, your love and your optimism. The completion of this PhD-thesis would not have been possible without you and your support; especially in the last few months. Gracias, amorcito!

André Kuhn
John Innes Centre, Norwich
September 2019

Contents

List of Figures and Tables

Chapter 1

Introduction

Plants and animals occur in a wide variety of shapes and forms containing numerous specialised tissues and organs that originate from a single cell. Understanding how developmental programmes co-ordinate morphogenesis of complex organisms from single cells has fascinated developmental biologists for over a century. Differences in morphology and behaviour between different species are determined by the cells that make their tissues and organs. Yet, all cells within an organism do not differ in the genetic material they contain but in the set of genes which are expressed. Throughout development, mobile signals called morphogens control changes in gene expression that coordinate cell differentiation, tissue formation and organogenesis.

Angiosperms - flowering plants - have evolved an enormous variety of morphologies that enable them to occupy a wide range of different habitats, lifestyles and symbioses with other organisms. The term angiosperm derives from the Greek words “angeion” which means “vessel” and the word “sperma” meaning “seed” describing the evolution of the gynoecium. The gynoecium is an organ enclosing the ovules - the future offspring - of the plant and distinguishes angiosperms from all other phyla of the plant kingdom (Scutt et al., 2006). Gynoecia exist in countless shapes and forms across species and develop specialised structures which aid pollinator selection, fertilisation and seed dispersal (Langowski et al., 2016; Scutt et al., 2006; Seymour et al., 2013). This diversification and adaptation of the gynoecium manifested the angiosperms evolutionary success. Upon fertilisation, ovules develop into seeds and gynoecia develop into fruits. Both seed and fruit properties, such as size or fleshiness, affect the seed dispersal strategy of the individual species. Many angiosperm species rely on animals for their dispersal and vice versa; many animals rely on fruits as a major source of nutrition (Seymour et al., 2013).

Humans have depended on fruits as a nutritional food for 100,000s of years. During the Neolithic Revolution about 10,000s years ago, humans began to domesticate and modify the size and shape of fruits and seeds of wild plants species, breeding our

modern crops. Technological advances and the immediate need to increase agricultural production worldwide led to the so-called Green Revolution of the twentieth century. Although the Green Revolution, at the beginning was driven by innovations in agricultural technology, chemistry, breeding and farming practises (Borlaug, 1983; Brummer et al., 2011), it coincided with ground-breaking progress in various fields of biology with advances in the field of genetics such as the (re-) discovery of the Mendelian principles of inheritance (Bateson, 1903), chromosomes and their role in inheritance (Morgan, 1911) and chromosome recombination (Creighton and McClintock, 1931). Additionally, the emerging field of molecular biology led to the discovery of DNA as the carrier of genetic information (Avery et al., 1944; Hershey and Chase, 1952), the structure of the DNA-double helix (Watson and Crick, 1953) and other observations that were collectively summarised in the “central dogma of molecular biology” (Crick, 1970). The combination of genetics and molecular biology have had tremendous impact on both developmental biology and plant breeding.

In the first half of the twentieth century, physiological studies identified some plant-borne chemical compounds, known as phytohormones, that can alter both plant morphogenesis and plant responses to different stimuli (Went, 1937; Wetmore and Wardlaw, 1951). Since then, plant developmental biologists demonstrated that the phytohormone auxin controls most aspects of plant development using a combination of plant physiology and molecular genetics (Benjamins and Scheres, 2008; Vanneste and Friml, 2009).

Meanwhile, conventional breeding aimed towards maximising yield through phenotypic selection was conducted and has more recently been complemented by molecular tools. By selecting for desirable characteristics based on phenotype, breeders were selecting genotypes that partitioned more of their biomass into harvestable plant products. An example for that is the achievement of higher grain

yield in wheat by selecting dwarfed genotypes that invest less in biomass into the stem (Hedden, 2003). Although conventional breeding efforts have doubled yields of most staple crops over the last 50 year, there has been no substantial yield improvement since the beginning of the twenty-first century (Long et al., 2015). However, due to a growing population and the challenges of climate change, this situation is unsustainable for providing food security in the future (Long et al., 2015). Among the many reasons that led to the yield plateau, one may be that even modern breeding methods are based on cycles of observation and selection, whereas the genes behind the traits and pathways that regulate them remain largely unknown. Additionally, most economically important traits such as yield, taste, and growth are determined by many genes that each have a small additive effect, and modern breeding methods are highly inefficient in selecting for these small effects (Cabrera-Bosquet et al., 2012). Consequently, there is an increasing interest in gathering basic knowledge on plant growth and organ morphogenesis to understand the mechanisms underlying plant development and their regulation (Rodríguez-Leal et al., 2017; Soyk et al., 2017; Vanhaeren et al., 2016; Zhu et al., 2018). Therefore, understanding regulation of fruit development in detail will not only improve the basic knowledge of plant development but may also contribute to future advances in crop improvement.

The hormonal and genetic basis of gynoecium development has been studied in detail in the model species *Arabidopsis thaliana*. It is evident that the phytohormone auxin has an essential role in gynoecium initiation and patterning throughout its development (Deb et al., 2018; Moubayidin and Østergaard, 2017). An AUXIN RESPONSE FACTOR (ARF) transcription factor (TF) called ETTIN (ETT) is critical in orchestrating the developmental programs during the formation of gynoecia via the translation of auxin signals into differential gene expression (Nemhauser et al., 2000; Sessions et al., 1997; Sessions, 1995). The signalling pathway by which ARFs mediate auxin signals is well known as a typical plant hormone-signalling pathway

that it is based on the de-repression of target genes via the degradation of transcriptional repressors (Kelley and Estelle, 2012). Recently, an alternative auxin signalling mechanism has been uncovered that appears fundamentally different. ETT is a pivotal component of this pathway that appears to be crucial to establish gynoecium polarity (Simonini et al., 2016). However, the molecular mechanism remains elusive.

Using the *Arabidopsis* gynoecium as the model, this thesis aims to shed light on the molecular mechanism by which this alternative auxin-signalling pathway perceives and transduces auxin stimuli to generate a transcriptional output.

The following sections will review the relevant literature concerning regulation of transcription and organ formation before addressing the scope of this thesis.

Gene regulation in multicellular organisms

Multicellular organisms originate from a single cell (i.e. a fertilised oocyte) that proliferates into numerous cells ultimately differentiating to make up specialised tissues and organs required to successfully complete the organism's life cycle. The information for the underlying developmental programs is encoded by the organism's genome. Thus, the genome is the blueprint containing the instructions for an organism's development. However, these instructions must be translated into specific functions that allows the formation of a functional organism with the ability to grow, to respond to the environment, and to differentiate specialist cells and tissues. Hence, selecting the right genes at the right time and in the right cells is critical for organisms to respond adequately to the demand of their development and environment. In multicellular organisms, mis-regulation of developmentally or physiologically important genes have dramatic phenotypic effects that can impair the function, location and/or shape of organs (Berleth and Jurgens, 1993; Nüsslein-Volhard and

Wieschaus, 1980; Sessions, 1995) or can be the driving force for morphological innovations during evolution (Sato et al., 2012; Soyk et al., 2017; Wang et al., 1999).

The central dogma of molecular biology tells us that: “DNA makes RNA and RNA makes protein” (Crick 1970). Transcription is the process of making RNA from DNA and is the first step of gene regulation. At the molecular level, transcription can be carried out by one out of four distinct RNA polymerases of which RNA Polymerase II (Pol II) transcribes protein-coding genes. Pol II is an enzyme that reads DNA and transcribes the information into RNA, but it can neither recognise specific DNA sequences (cis- elements) nor initiate transcription at a specific genomic locus. To identify transcriptional start sites, Pol II physically interacts with other proteins called transcription factors. Transcription factors can be general or specific depending on their role in transcriptional regulation. In eukaryotes General Transcription Factors (GTFs) recognise core promoter sequences close to the transcription start site, such as the TATA box, that dictate assembly and orientation of the transcription preinitiation complex (PIC) (Thomas and Chiang, 2006). Several PIC subunits can directly interact with specific transcription factors (Thomas and Chiang, 2006) while others interact with co-factor complexes such as the Mediator complex that can facilitate interaction between specific DNA-binding transcription factors and the general transcription machinery (Wu et al., 2003).

Similar to general transcription factors, specific transcription factors (TFs) bind to DNA-sequences of their target genes. Since transcription of genes involved in developmental programs requires precise temporal and spatial regulation to ensure proper growth and development, the presence of a specific DNA-sequence (cis-element) that allows a stable interaction between the transcription factor’s DNA binding domain is a first step towards achieving specific gene regulation.

In eukaryotes cis-elements are typically 6 bp, which means it could occur every 4,096 bp (4^6) purely by chance and several thousand times depending on the size of the

genome (Lieberman-Lazarovich et al., 2019; Wunderlich and Mirny, 2009). Consequently, this means that any transcription factor will have many unspecific binding sites within the genome that will not lead to transcription initiation. This indicates that gene regulation may require additional levels of DNA-TF recognition. Even though the mechanisms that truly provide target-specificity of transcription factors have not been fully uncovered, there is increasing evidence of multiple strategies that ensure specific binding of transcription factors to their target genes. Cis-elements often occur in repeats or clusters which increases specificity through the requirement for co-operative binding. This leads to higher transcription factor occupancy at these clusters and synergistic events between transcription factors (Olsen et al., 2005; Singh, 1998; Xu et al., 2006). Thus, combinations of different cis-elements in gene regulatory regions bring about another layer of specificity and enable to distinguish between different cis-regulatory clusters. Clustering of regulatory elements increases the complexity implying that transcription factors need to form protein complexes to be able to effectively bind regulatory elements of target genes (Wunderlich and Mirny, 2009). Therefore, protein-protein interactions provide an additional layer that controls specificity in gene regulation. Protein-protein interactions can occur between transcription factors of the same (homo) or of different transcription factor families (hetero). However, such interactions may also occur with other proteins that regulate the activity of the transcription factor as they can interact with proteins that inhibit their activity (Tiwari et al., 2003).

Eukaryotic genomes are organised in chromosomes in which DNA associates with proteins to form chromatin. The main proteins that associate with DNA are the four core histones H2A, H2B, H3 and H4 that form an octameric structure known as a nucleosome, around which DNA is wrapped (Kornberg and Lorch, 1999; Luger et al., 1997). This tight interaction between histones and DNA impedes the accessibility of DNA to other factors. Consequently, the location of histones relative to important

regulatory DNA sequences and the strength of histone-DNA contacts can either hide or expose genes providing yet another layer of gene regulation. In chromatin, both histones and DNA can be chemically modified (Schübeler, 2015; Zhou et al., 2010). Depending on the physical properties of the modification, the chromatin state can either prevent or enhance the transcription of the underlying genes by making them available to the transcriptional machinery only at specific moments or specific cell types. The mechanisms by which post-translational modification of histones is regulated remains widely elusive, however, it is well known that transcription factors can interact with chromatin re-modellers and histone modifying complexes (Kouzarides, 2007; Questa et al., 2016; Wu et al., 2015).

In summary, ensuring that a gene is transcribed in a certain cell at a certain time requires the following: 1) that the local chromatin environment exposes the gene to allow TF binding, 2) the correct combination of proteins must be present to allow binding and 3) the cis-elements must allow stable interaction with the specific transcription factors.

Principles of morphogen signalling in animals and plants

Multicellular development requires tight spatio-temporal control of key regulatory genes to make sure that the correct genes are switched on or off at the right developmental stage. These changes in gene expression are controlled by mobile signals, so called morphogens that co-ordinate cellular decisions in time and space by means of cell–cell communication. Throughout development morphogens form patterns through diffusion, thereby controlling the formation of specific cell types. So called “Reaction-diffusion processes” or “Turing patterns”, describe this kind of morphogen based patterning that is spontaneous and self-regulated (Turing, 1952). During development “Turing patterns” have been shown to regulate the emergence of pigmentation patterns in plants and animals (Bradley et al., 2017; Kondo and Miura, 2010; Nakamasu et al., 2009). Morphogen diffusion also forms concentration

gradients providing spatial information that subdivides a tissue in different domains relative to the source of the morphogen by regulating the expression of a different set of target genes at distinct concentration thresholds. Consequently, cells far from the morphogen source will receive low levels of morphogen and only express target genes that have a low threshold whereas cells close to the source will receive high levels of morphogen and will express both low and high threshold target genes. Distinct cell types differentiate as a result of a different combination of expressed genes across the gradient. This concept of morphogen patterning is called the "French-flag model" (Wolpert, 1969).

Experimentally, morphogen patterning and action is best studied in *Drosophila melanogaster* embryogenesis. During the first thirteen cell divisions early *Drosophila* embryos form a syncytium, a single cell in which numerous nuclei are evenly distributed. In syncytia, homeobox transcription factors such as Bicoid, that plays an important role in anterior-posterior axis formation, can diffuse between nuclei to produce smooth gradients of concentration (Driever and Nüsslein-Volhard, 1988; Johnston and Nüsslein-Volhard, 1992). After cellularisation, membranes have formed between the nuclei of the embryo and morphogen signals can no longer diffuse freely between nuclei. At this stage, morphogens generally encompass secreted signalling peptides or small molecules that bind to extracellular domains of transmembrane receptors (Gurdon and Bourillot, 2001). This mechanism is prevalent in most animal developmental systems including human embryos since these embryos do not form syncytia. Upon ligand binding transmembrane receptors induce a cytoplasmic signalling cascade to communicate the morphogen signal to the nucleus. In the nucleus, morphogen signal cascades usually target transcription factors by modulating their activity towards morphogen responsive target genes in a manner that reflects the morphogen concentration at the cell surface (Gurdon and Bourillot, 2001). A well-studied example for this type of signalling in animals is the wingless/Int-

1(Wnt)/β-catenin signalling pathway. Originally characterised for its segmentation defects in *Drosophila* embryogenesis, Wnt/β-catenin has been demonstrated to control various embryonic processes including body axis patterning, cell differentiation, cell proliferation and cell migration (Cadigan and Nusse, 1997; Nüsslein-Volhard and Wieschaus, 1980). The pathway has also been implemented in various diseases including breast and prostate cancer (Logan and Nusse, 2004). During Wnt/β-catenin signalling, Wnt proteins bind to the Frizzled (Fz) transmembrane receptor inducing a signalling cascade that prevents the ubiquitination and degradation of β-catenin proteins in the cytoplasm. This allows β-catenin to accumulate in the cytoplasm and translocate to the nucleus. Nuclear β-catenin binds transcription factors such as T-Cell Factor (TCF) transcription factors. Interaction between TCF and β-catenin leads to a displacement of co-repressors such as Groucho/TLE (Gro/TLE) that interact with TCF under low Wnt concentrations to repress Wnt-responsive target genes. Binding of β-catenin and displacement of Gro/TLE allows TCF to recruit transcriptional co-activators and chromatin remodelers to subsequently induce target-gene expression (for comprehensive review see Gammons and Bienz 2018).

Plants differ from animals in that their embryos are relatively simple structures consisting of only a few cell types, encompassing the plant stem cells that are organised in meristems at the shoot and root tips. These meristems remain active throughout a plants life span and give rise to all the post-embryonic tissues that make the mature plant (Weigel and Jürgens, 2002). Unlike animal cells, plant cells are surrounded by a rigid cell wall and consequently cannot migrate during development. Hence, oriented cell division and directional expansion plays an important role in morphogenesis during development (Scheres, 2007; Scheres et al., 1994). Despite these differences, the same concepts of morphogen patterning can be applied to both plant and animal development (Abley et al., 2013).

Like animal embryogenesis, plant embryogenesis and postembryonic development requires morphogens to mediate the coordinated acquisition of cell types and the development of new tissues. Plant morphogens, also referred to as phytohormones, comprise a diverse group of structurally unrelated molecules that are important to integrate the plant's developmental program with spatial and temporal information and environmental cues. The molecular diversity of plant hormones, ranging from polypeptides to small organic molecules such as ethylene, is also reflected in the number of different signal transduction mechanisms and the components involved in them.

Peptide morphogens are the predominant type of patterning molecules during animal embryogenesis. In contrast, most plant hormones are small non-peptide molecules. Nonetheless, signalling peptides are involved in the regulation of various developmental processes in plants. A well-known example of a plant peptide regulated developmental process is shoot apical meristem (SAM) size by the plant peptide hormone CLAVATA3 (CLV3) that restricts the expression of *WUSCHEL* (*WUS*), a stem cell-promoting gene (Brand et al., 2000; Clark et al., 1997; Schoof et al., 2000). Action and perception of these peptide hormones is highly similar to animal morphogen action in that it involves peptide ligands binding to transmembrane receptors that induces a cytoplasmic signal transduction cascade mediating the signal to the nucleus where a transcriptional output is generated (Oh et al., 2018). Some non-peptide phytohormones, such as cytokinins and brassinosteroids, also bind to transmembrane receptors. Signal transduction of these hormones appears reminiscent of peptide signal transduction in plants and animals (Kieber and Schaller, 2018; Vukasinovic and Russinova, 2018).

In contrast, most other plant hormones use a fundamentally different signal transduction mechanism. A reoccurring theme in plant-hormone signalling is hormone-induced ubiquitination and proteasome-dependent degradation of

repressive components of the signalling pathway. The ubiquitin–proteasome pathway has evolved in different variations and is the most prevalent among plant hormones (for detailed review see Kelley and Estelle, 2012). Consequently, the signalling pathways of the structurally unrelated hormones auxin, gibberellic acid (GA) and jasmonic acid (JA) resemble each other mechanistically. In all three pathways, the hormone receptor is part of Skp1/Cullin/F-box (SCF) ubiquitin ligase complexes or regulates their activity. When nuclear hormone levels are low, transcription factors that regulate the expression of hormone responsive target genes bind a specific repressor protein (Aux/IAAs for auxin, DELLAs for GA and JAZ for JA). When nuclear hormone levels rise, hormones bind their receptors (TIR1/AFBs for auxin, GID1 for GA and COI1 for JA). Hormone binding to their receptors stabilizes interaction between repressor proteins and receptors. Receptor-bound repressors are ubiquitinated by the SCF complex and degraded by the 26S proteasome. Consequently, repressor degradation enables the previously repressed transcription factors to induce transcription of hormone-responsive target genes (Kelley and Estelle 2012).

Auxin acts like morphogen throughout plant development

In plants, the phytohormone auxin has been established as a key regulator during organ patterning and growth. The most abundant active auxin found naturally in plants is the tryptophan-derived Indole 3-Acetic Acid (IAA) and will be referred to as ‘auxin’ throughout the thesis unless stated otherwise. Throughout plant development auxin has morphogenic action since auxin-concentration gradients provide spatial information that subdivides a tissue in different domains relative to the source of the morphogen by regulating the expression of a different set of target genes at distinct concentration thresholds. Moreover, it appears that auxin is self-regulating through feedback loops (Benjamins and Scheres, 2008). This auxin patterning is crucial for the development of almost all developmental processes in plants including

embryogenesis, vascular development, root growth, lateral root formation, leaf and flower initiation (Vanneste and Friml, 2009). Despite the differences in the ultimate function and processes they are involved in, the initiation of a new growth axis from a specific spot and the differentiation of new specialised tissues are a common theme underlying the development of each of these organs and requires the generation of distinct auxin concentrations such as auxin maxima or minima across plant tissues. Therefore, to achieve pattern formation, auxin needs to be locally produced and redistributed.

Auxin biosynthesis and transport

Auxin biosynthesis from tryptophan occurs in specific cells in a two-step synthesis pathway (Figure 1.1). In the first step tryptophan is converted to indole-3-pyruvate (IPA) by TRYPTOPHAN AMINOTRANSFERASE OF ARABIDOPSIS 1 (TAA1) and its homologs TRYPTOPHAN AMINOTRANSFERASE REALATED 1,2 (TAR1,2) (Stepanova et al., 2008; Tao et al., 2008). In the second step, members of the YUCCA (YUC) family flavin monooxygenases catalyse the oxidative decarboxylation for IPA to produce IAA (Cheng et al., 2006; Mashiguchi et al., 2011; Zhao, 2010). Since auxin is only synthesised by some cells and is unable to exit the cell via passive diffusion, it requires directional transport to form gradients to reach target cells. Auxin efflux carrier proteins of the PIN-FORMED (PIN) family are transmembrane proteins that localise in a polar fashion at the cells plasma membrane to facilitate auxin export from the cell for polar auxin transport. The polar membrane localisation of PIN proteins is the result of a continuous exocytosis/endocytosis cycle (Adamowski and Friml, 2015; Benková et al., 2003; Friml et al., 2002a; Friml et al., 2002b; Müller et al., 1998; Petrášek et al., 2006). Polar auxin transport and its regulation are the main drivers of pattern formation during plant development (Caragea and Berleth, 2016; ten Hove et al., 2015). The serine-threonine kinase, PINOID (PID) and PROTEIN PHOSPHATASE 2A (PP2A) antagonistically regulate the phosphorylation status of PIN proteins (Figure 1.1). Phosphorylation targets PINs to the apical plasma

membrane, while dephosphorylated PINs are targets to the basal plasma membrane (Benjamins et al., 2001; Friml et al., 2004; Michniewicz et al., 2007).

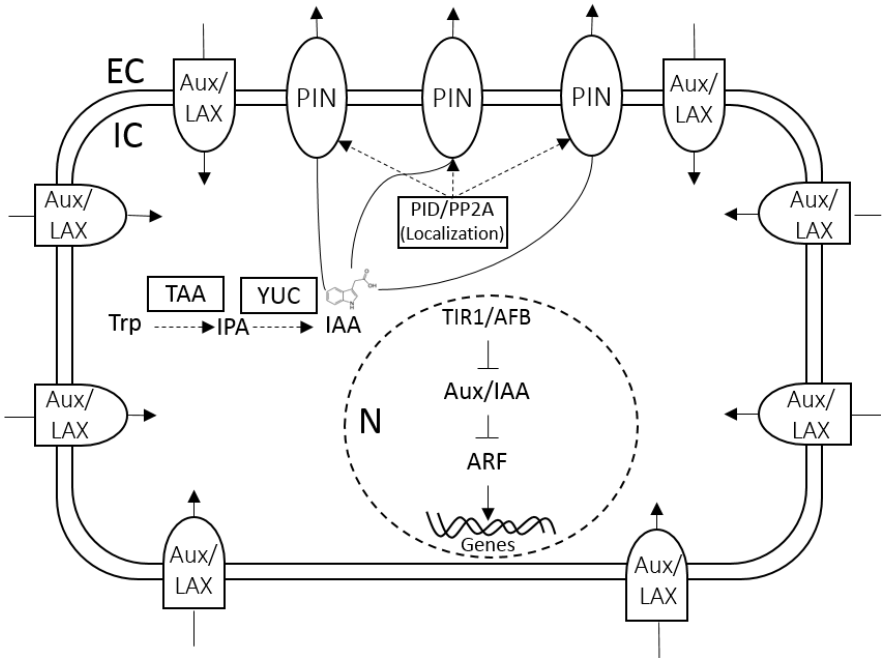

Figure 1. 1: Auxin biosynthesis, transport and signalling pathways. TAA and YUC enzymes synthesise IAA from Tryptophan, intracellular (IC) auxin can either be transported to the extracellular space (EC) or initiate the signalling cascade inside the nucleus (N). Auxin efflux is facilitated by PIN proteins. PID and PP2A regulate the localisation of PINs by phosphorylating and dephosphorylating PINs, respectively. Therefore, PID and PP2A regulate polar auxin transport. In contrast, AUX1/LAX influx carriers, which transport extracellular auxin inside the cell, localise in an apolar fashion.

To trigger a cellular response auxin needs to enter the cell. However, the acidic environment of the apoplast hinders the diffusion of auxin across the plasma membrane (Raven, 1975). AUX1/LAX auxin influx carriers facilitate the major auxin influx into cells (Figure 1.1). Due to their even distribution over the plasma membrane, AUX1/LAX influx carriers are expected to import auxin to the cells in an apolar fashion (Bennett et al., 1996; Péret et al., 2012; Swarup et al., 2008). Auxin accumulation leads to high cellular auxin levels that trigger a cascade of events that will ultimately lead to changes in gene regulation of developmentally important genes in the nuclear auxin-signalling pathway (Figure 1.1 and Figure 1.2).

The nuclear auxin-signalling pathway and its components

After auxin biosynthesis and transport, hormone accumulation triggers transcriptional changes to affect cell division and identity appropriate for the developmental context. The transcriptional output of auxin signalling is mainly determined by three protein families that act as three key components of the signal transduction pathway: AUXIN RESPONSE FACTOR (ARF) transcription factors, AUXIN/INDOLE-3-ACETIC ACID (Aux/IAA) transcriptional co-repressor proteins and TRANSPORT INHIBITOR RESISTANT1/ AUXIN SIGNALING F-BOX (TIR1/AFB) F-box auxin receptor proteins, which are a subunit of the SKP1/CULLIN1/F-BOX (SCF)$^{TIR1/AFB}$. ARFs bind so-called Auxin Responsive Element (AuxRE) cis-regulatory sequences in promoters of their target genes to positively or negatively regulate gene expression (Boer et al., 2014; Lieberman-Lazarovich et al., 2019; Ulmasov et al., 1997a; Ulmasov et al., 1999a; Ulmasov et al., 1999b). In the absence of auxin, Aux/IAA proteins physically interact with ARFs (Tiwari et al., 2003; Ulmasov et al., 1997b). Aux/IAAs inhibit ARF activity towards target genes by recruiting the co-repressor TOPLESS (TPL) to repress auxin-dependent gene expression (Long et al., 2006; Szemenyei et al., 2008). TPL/TPRs mediate their repressive effect by attracting histone deacetylases (HDACs) to promote chromatin condensation (Krogan et al., 2012; Zhu et al., 2010) (Figure 1.2 a).

Auxin binds to both the SCF$^{TIR1/AFB}$ receptor complex and the Aux/IAA protein, increasing the binding affinity between them. Aux/IAAs and TIR1/AFBs form the auxin co-receptor complex together with one of the SCF$^{TIR1/AFB}$ E3 ubiquitin ligases. These ligases can poly-ubiquitinate Aux/IAAs marking them for degradation in the 26S proteasome (Dharmasiri et al., 2005; Gray et al., 2001; Kepinski and Leyser, 2005). Upon degradation of Aux/IAAs, ARFs are released from inhibition to regulate the gene expression of their target genes (Figure 1.2 b).

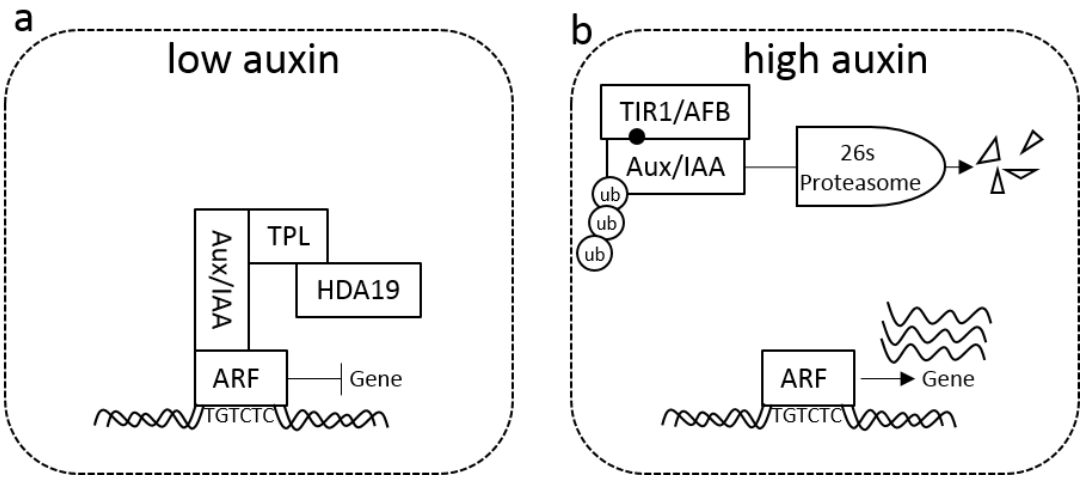

Figure 1. 2: The nuclear auxin-signalling pathway. (a) When auxin levels are low Aux/IAA transcriptional repressors form dimers with Auxin Response Factors (ARFs) and bring about a repressed state at target loci by recruiting TPL and HDA19. (b) In contrast, high auxin levels enhance dimerisation between Aux/IAAs and TIR1/AFB auxin receptors. This leads to Aux/IAA polyubiquitination (ub) and degradation by the 26S proteasome. Thus, ARFs that bind AuxREs (TGTCTC) are relieved from repression and initiate transcription of ARF-targeted loci.

Each of the protein families involved in the nuclear auxin-signalling pathway has multiple members in most land plant species (Mutte et al., 2018). Most ARFs and Aux/IAAs have unique and distinct expression patterns (Rademacher et al., 2011). Additionally, members of the three protein families interact among each other with different affinities (Calderon Villalobos et al., 2012; Vernoux et al., 2011). Together, these properties allow for different combinations of protein complexes in different cells and may contribute to different responses to the same hormonal signal.

Repressor proteins: The Aux/IAA family

The *Arabidopsis thaliana* genome encodes for 29 Aux/IAA proteins that share four distinct domains. The N-terminal domain, also known as domain I, carries an Ethylene-responsive element binding factor-associated Amphiphilic Repression (EAR) motif that mediates the interaction with TPL (Causier et al., 2012; Martin-Arevalillo et al., 2017; Szemenyei et al., 2008). Domain II contains the degron motif that mediates the interaction of Aux/IAAs with the $SCF^{TIR1/AFB}$ receptor complex (Dharmasiri et al., 2005; Kepinski and Leyser, 2005). A subclade of Aux/IAAs containing IAA20, IAA30 and IAA31 lacks the degron domain. The function of these

Aux/IAAs is unclear. However, over expression of the subclade results in auxin-related phenotypes indicating that these Aux/IAAs have function in auxin signalling (Sato and Yamamoto, 2008). Domain III and IV at the C-terminus form a Phox/Bem1 (PB1) domain that is essential for the protein-protein interaction with ARFs (Tiwari et al., 2003).

Interestingly, a recent study has shown that two canonical Aux/IAAs, IAA32 and IAA34, seem to regulate auxin response in an alternative signalling mechanism (Cao et al., 2019). This mechanism involves the extracellular detection of auxin by TRANSMEMBRANE KINASE 1 (TMK1). Auxin detection leads to cleavage of the cytoplasmic C-terminal kinase domain of TMK1 that specifically phosphorylates IAA32 and IAA34. Phosphorylation stabilises IAA32 and IAA34 and prevents their degradation. Hence, auxin-mediated cleavage of the TMK1 kinase domain leads to destabilisation of IAA32 and IAA34 and presumably depression of their target ARFs (Cao et al., 2019). It remains unclear which role this mechanism or other post-translational modifications play for the regulation of auxin response by other Aux/IAAs.

Auxin receptors: the TIR1/AFB family

A family of six F-box proteins called TIR1/AFB are substrate receptors of the $SCF^{TIR1/AFB}$ E3 ligase complex that target Aux/IAAs for ubiquitination (Dharmasiri et al., 2005; Gray et al., 2001; Kepinski and Leyser, 2004; Kepinski and Leyser, 2005). Although all family members act as auxin receptors they differ in their biochemical properties and biological functions (Parry et al., 2009). Recognition of Aux/IAAs by $SCF^{TIR1/AFB}$ complexes only occurs if auxin is directly bound by the TIR1/AFB F-box protein. Structural analysis of TIR1 and the Aux/IAA degron domain revealed that the C-terminal 18 Leucin-Rich-Repeats (LRRs) forms the auxin-binding pocket and mediates the binding of Aux/IAAs (Calderon-Villalobos et al., 2010; Tan et al., 2007). Further analysis has shown that TIR1/AFBs and Aux/IAAs are both required and

sufficient for auxin binding. Given that there are 29 Aux/IAAs and 6 TIR1/AFBs, there are many possible co-receptor pairs (6x29=174 theoretical combinations). Protein-protein interaction assays showed that this is indeed the case. Moreover, biochemical assays suggest that different co-receptor pairs have different auxin affinity (Calderon Villalobos et al., 2012). The formation of TIR1/AFB-auxin-Aux/IAA complexes is critical for Aux/IAA degradation and de-repression of ARFs. Hence, differences among TIR1/AFB-Aux/IAA co-receptors in terms of auxin affinity may therefore be one aspect controlling differential concentration-dependent auxin responses.

Transcription factors: The Auxin Response Factor Family

High levels of auxin trigger the degradation of Aux/IAAs and release the ARFs to regulate gene expression in response to auxin. In *Arabidopsis* there are 23 ARF transcription factors providing in theory 667 (29 Aux/IAAs x 23 ARFs) possible combinations of Aux/IAA-ARF pairs potentially increasing both the diversity and complexity of the auxin-signalling pathway. However, *ARF* genes are expressed in dynamic and different patterns during development and control distinct developmental processes (Rademacher et al., 2012; Rademacher et al., 2011; Weijers et al., 2005; Weijers et al., 2006). Additionally, promoter-swap experiments demonstrated that ARFs cannot compensate for each other (Finet et al., 2013; Rademacher et al., 2011; Weijers et al., 2005) and may even act antagonistically (Rademacher et al., 2012). Thus, differences between ARFs are partly due to differences in protein sequence. Despite years of research, it remains an open question how ARFs achieve target specificity.

ARFs consists of three protein domains, an N-terminal B3 DNA-binding domain (DBD), a Middle Region and C-terminal PB1 domain. Using their B3-DBD, ARFs directly bind to cis regulatory elements, called Auxin Responsive Elements (AuxREs, TGTCTC or TGTCNN), within the regulatory regions of their target genes to positively or negatively regulate gene expression (Boer et al., 2014; Lieberman-Lazarovich et

al., 2019; Ulmasov et al., 1997a; Ulmasov et al., 1999a; Ulmasov et al., 1999b). The DBD is flanked by dimerisation domains, which mediate homo- and hetero-dimerisation among ARFs, and an ancillary domain, which supports the protein structure (Boer et al., 2014). Intuitively, one would expect target specificity of ARFs to be determined by differences in binding affinity or binding preference of ARF DBDs to certain versions of the TGTCNN AuxRE cis-regulatory element. A protein-binding microarray examining the binding preference of two distantly related ARFs, ARF5 and ARF1, found little difference in specificity and intrinsic binding preference between the two (Boer et al., 2014), whilst a cistrome analysis by DAP-seq revealed that ARF5 and ARF2 share only 9% of their binding sites in the genome (O'Malley et al., 2016). Structural analysis of ARF1 and ARF5 DBDs showed the potential of ARFs to form homo- and possibly hetero-dimers. It has been argued that the spacing tolerated between binding sites differs among different ARF-ARF dimers (Boer et al., 2014). However, synthetic auxin-response circuits in yeast using a range of spacings between two AuxREs show that inter-motif spacing cannot sufficiently account for specificity in DNA binding (Pierre-Jerome et al., 2016).

The Middle Region is highly variable between ARFs and has been proposed to determine the transcription factor activity. Based on the composition of the Middle Region (MR), ARFs can be classified into three phylogenetically distinct clades, A, B and C (Finet et al., 2013). Class-A ARFs (ARF5-8,19) contain a glutamine-rich middle region, whilst the MR of class-B (ARF1-4,9,11-15,20-23) and of class-C ARFs (ARF10,16,17) is generally serine-rich (Finet et al., 2013; Mutte et al., 2018). Class-B and class-C ARFs can be distinguished based on their different modes of post-transcriptional regulation. Most class-B ARFs are targeted by the *TAS3* trans-acting siRNA (tasiRNA) (Allen et al., 2005; Axtell et al., 2007; Marin et al., 2010; Tsuzuki et al., 2016) while class-C ARFs can be targeted by the microRNA160 (miR160) (Axtell et al., 2007; Mallory et al., 2005). Both modes of regulation are evolutionarily

conserved and are thought to increase robustness and sensitivity in the auxin response (Plavskin et al., 2016).

Trans-activation assays on an auxin-responsive model gene have demonstrated that class-A ARFs function as transcriptional activators and class-B ARFs as repressors (Ulmasov et al., 1999a). Although not supported experimentally, class C ARFs have traditionally been classified as transcriptional repressors (Finet et al., 2013; Finet et al., 2010; Guilfoyle and Hagen, 2007). However, the role of class C ARFs in auxin response is under debate as recent studies imply that they do not function in auxin-responsive gene regulation (Mutte et al., 2018).

At the C-terminus, most ARFs contain a C-terminal PB1 domain that facilitates the interaction between ARFs and Aux/IAAs (Guilfoyle and Hagen, 2007). It has been proposed that interaction between Aux/IAAs and ARFs through their PB1-domain contributes most to specificity and sensitivity in auxin signalling (Vernoux et al., 2011). Interestingly, three of the 23 ARFs in Arabidopsis (ARF3/ETTIN (ETT), ARF13, ARF17) lack a PB1-domain, and these ARFs are not exceptions, as 30% of the *Zea mays* ARFs and more than 50% of the ARFs in *Medicago trancula* and *Malus domestica* lack the PB1 domain (Chandler, 2016; Guilfoyle and Hagen, 2007). Recently, it has been shown that loss of the PB1 domain has occurred independently several times throughout evolution, mainly among class-B and class-C ARFs (Mutte et al., 2018). Furthermore, several assays demonstrated that class-A ARFs could interact with almost all Aux/IAAs whilst most class-B and class-C ARFs interact with few or no Aux/IAAs (Piya et al., 2014; Vernoux et al., 2011). Intriguingly, these studies indicate that the well-established nuclear auxin-signalling pathway is insufficient to explain auxin-dependent gene regulation through class-B and class-C ARFs. Some of the class-B ARFs contain an EAR motif and have been shown to interact with TPL co-repressors (Causier et al., 2012). It has therefore been argued that class-B and

class-C ARFs are involved in auxin-independent regulation of target genes (Causier et al., 2012; Kato et al., 2018).

Recently, an alternative auxin-signalling mechanism was identified whereby auxin directly affects the activity of a transcription factor (TF) complex towards its downstream targets (Simonini et al., 2017; Simonini et al., 2016). This mechanism involves the class-B ARF ETTIN (ETT/ARF3) as a pivotal component and mediates precise polarity switches during organ initiation and patterning. ETT lacks the PB1 domain (Sessions et al., 1997) and is incapable of interacting with Aux/IAAs (Vernoux et al., 2011). It is therefore likely that ETT mediates auxin signalling via an alternative pathway.

ETT can interact with a diverse set of TFs and these interactions are sensitive to the naturally occurring auxin, indole 3-acetic acid (IAA). The region responsible for auxin-sensitivity is situated within the C-terminal part of ETT, known as the ETT-Specific (ES) domain (Simonini et al., 2016). The sensitivity of ETT-TF interactions to auxin suggests a direct effect of the auxin molecule on the ETT protein. However, the molecular mechanism and biochemical basis of this auxin sensitivity remains elusive. ETT has been implicated in a wide array of developmental processes (Garcia et al., 2006; Kelley et al., 2012; Marin et al., 2010; Pekker et al., 2005), however, the most dramatic phenotypes of *ett* loss-of-function mutants are observed during gynoecium development (Nemhauser et al., 2000; Sessions et al., 1997; Sessions, 1995; Sessions, 1997).

Gynoecium morphology

A gynoecium is made of several distinct tissues that fulfil specialised functions during fruit development, maturation and seed dispersal. Morphologically, the *Arabidopsis* gynoecium is formed by the fusion of two carpels that arise from a single primordium. After fertilisation, the gynoecium develops into a silique-type fruit which dries and

dehisces when mature to release the seeds. Gynoecia - and subsequently the fruit - can be morphologically divided into four different regions: the stigma, style, ovary and gynophore (Figure 1.3) (Bowman et al., 1999; Smyth et al., 1990).

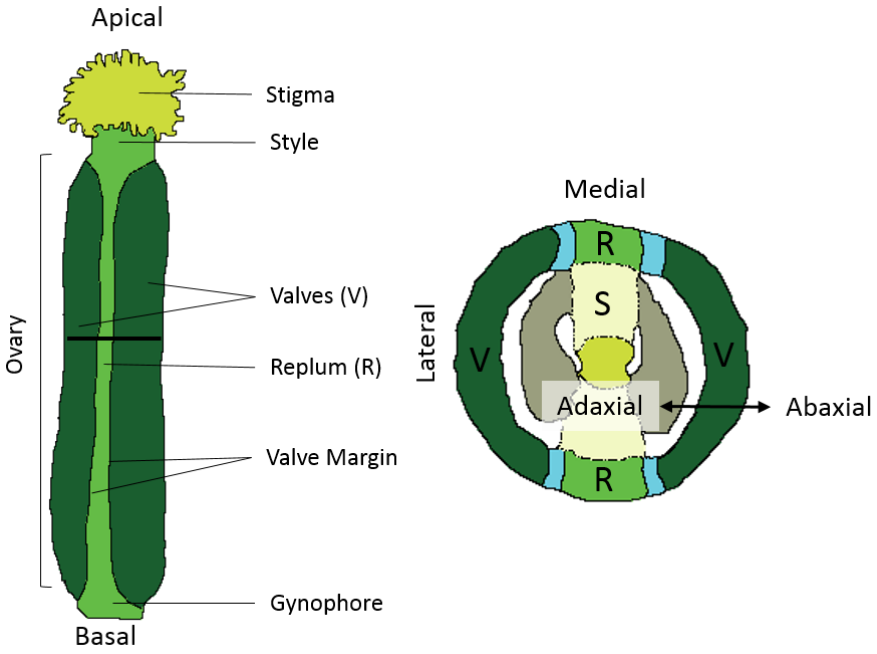

Figure 1. 3: Morphology of the *Arabidopsis* gynoecium. The gynoecium has three axes of polarity: apical-basal, adaxial-abaxial and medio-lateral. Along the apical basal axis, the gynoecium can be divided into stigma, style, ovary and gynophore. A transverse section displays the tissues of the ovary. These tissues exhibit an adaxial-abaxial and medio-lateral polarity. The gynoecium has two lateral valves (V) and two medial repla (R) that are connected by valve margins (blue). Inside the gynoecium, the two repla are connected by a septum (S). The transmitting tract locates at the centre of the gynoecium (yellow). The ovules (grey) connect laterally with the septum. The black bar at the middle of the fruit to the left indicates the approximate location of the transverse section.

Along the apical-basal axis the stigma is located at the apex of the gynoecium. It is formed by a single layer of elongated papilla cells. It plays an important role in pollen collection, germination and mediation of pollen tube growth (Sessions et al., 1997). Basal to the stigma is the style, a cylindrical tissue surrounding the central transmitting tract. Pollen tubes grow through this structure to reach the ovary that is located immediately below the style. The ovary forms the largest part of *Arabidopsis* gynoecia and is formed by several distinct tissues: the valves, replum, valve margins, ovules and the septum. Valves are located at the lateral sides of the ovary protecting the developing seeds. The two repla separate the valves from each other and are located

on the medial sides of the fruit. Inside the ovary, a septum connects the two repla (Figure 1.3). A placenta that gives rise to the ovules is connected to the surface of the septum. Valves and repla are connected by the valve margin, a narrow tissue that when the fruit is mature is important for fruit opening (dehiscence). The base of the fruit is formed by the gynophore a short stalk that connects the fruit with the rest of the plant.

In contrast to wild type gynoecia, in *ett* mutant gynoecia the medial and apical tissues over-proliferate and the gynoecium fails to close. Additionally, the gynophore is enlarged at the expense of ovary size. Interestingly, wild type gynoecia treated with auxin transport inhibitors phenocopy *ett*-mutants highlighting that ETT is an essential integrator of auxin patterns during gynoecium development (Nemhauser et al., 2000; Sessions et al., 1997). Additionally, the sensitivity of the gynoecium to perturbation in auxin dynamics makes it a great model for studying the role of auxin signalling in organogenesis.

Auxin patterns gynoecium development at all stages

Throughout a plant's lifecycle new organs are formed from only a few stem cells within organ primordia. These cells will divide and spatially coordinate the acquisition of different cell identities. Plant hormones pattern this cell growth and differentiation in a spatio-temporal manner, through local hormone production and hormone redistribution. The formation of the gynoecium in flowering plants is no exception to this rule.

All cell and tissue types of the mature fruit are derived from the gynoecium which in turn originates from a few cells within a floral primordium. Flower primordia are formed by the shoot apical meristem (SAM) when the plant commits to flowering. How a flower primordium is specified and how the few cells of a flower primordium define the different floral organs within the four floral whorls has been intensely studied (and

reviewed) for the last decades (Alvarez-Buylla et al., 2010; Bowman et al., 1989; Bowman et al., 2012; Coen and Meyerowitz, 1991). According to developmental events flower and fruit development have been divided into twenty individual stages (Figure 1.4) (Roeder and Yanofsky, 2006; Smyth et al., 1990) most of these stages are under tight hormonal and genetic control, and numerous studies have underlined the importance of auxin patterning in various aspects of the developmental program (Arnaud et al., 2010; Larsson et al., 2013; Larsson et al., 2014; Moubayidin and Ostergaard, 2014; Nemhauser et al., 2000; Sessions et al., 1997; Sorefan et al., 2009).

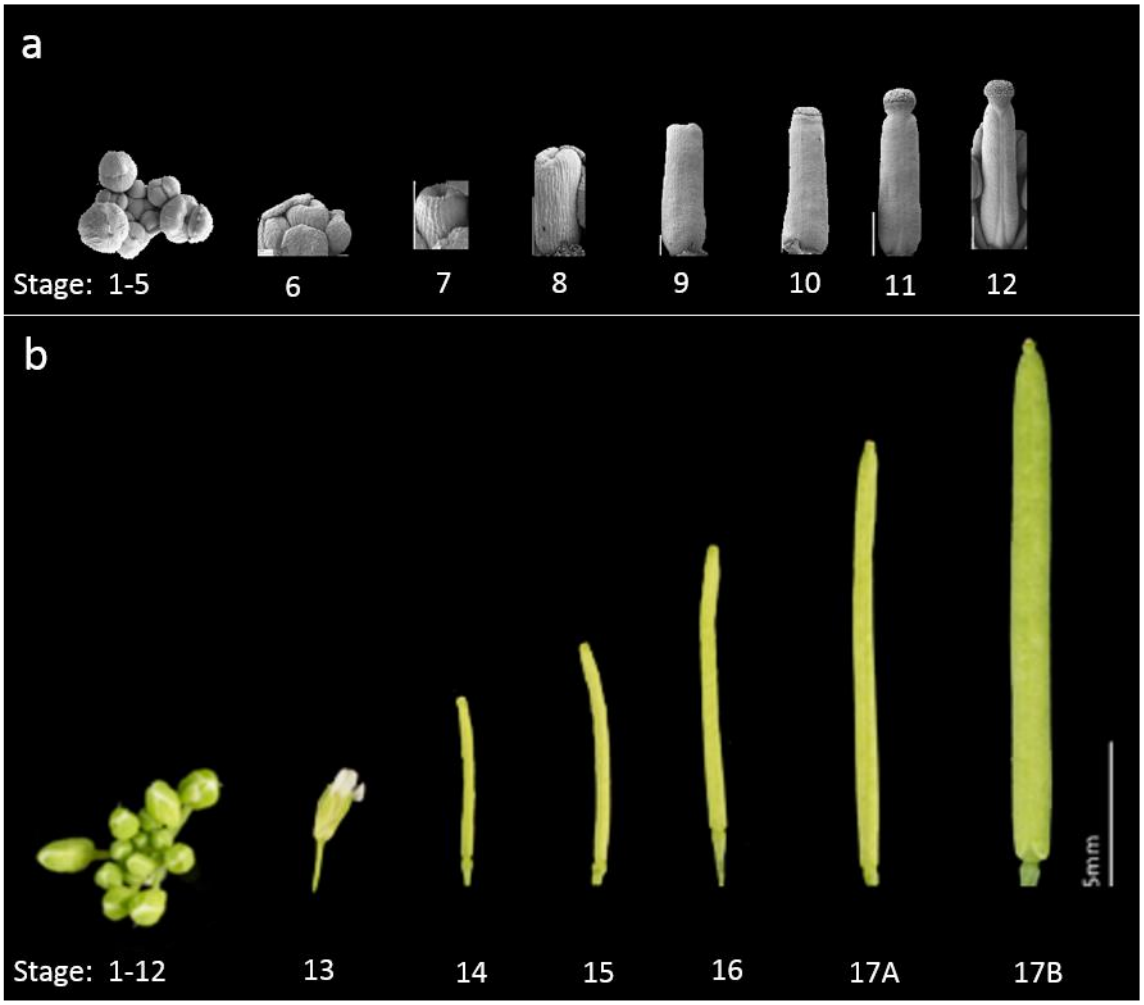

Figure 1. 4: Developmental stages of flower and gynoecium development. (a) Scanning Electron Microscope (SEM) images presenting early developmental stages (scale bar 20 µm). (b) Light microscopy images presenting fruit phenotypes from early developmental stages to full maturity (scalebar 5 mm). The images presented here were kindly provided by Dr. Łukasz Łangowski.

Within the first five stages of flower development (Figure 1.4 a), floral primordia are formed and the outer three floral organs, sepals, petals and stamens, are initiated. In these early stages of gynoecium development, ETT is expressed in flower primordia where it represses the expression of the meristem identify genes *WUS* and *STM* which leads to meristem termination (Chung et al., 2019; Liu et al., 2014).

When sepals enclose the bud in late stage five, the carpel primordia are initiated. At stage six, two fused carpels start to grow as a hollow tube. At stage 7, an auxin maximum appears as two lateral foci at the apex and on the inner surface of gynoecium two medial ridges become visible, which will give rise to the inner tissues, style and stigma at later developmental stages (Reyes-Olalde et al., 2013). At stage 8 and 9, two additional medial auxin foci appear at the apex that fuse with the lateral foci to form an auxin ring at stage 10. The formation of this auxin ring at the apical part of the gynoecium is essential for closure of the gynoecium and subsequently style and stigma development. Two basic helix-loop-helix (bHLH) transcription factors SPATULA (SPT) and INDEHISCENT (IND) regulate the apolar auxin redistribution through direct repression of *PINOID* (*PID*) (Moubayidin and Ostergaard 2014).

As development proceeds (Figure 1.4 a), stigmatic papillae cover the stigma at stage eleven, closing the gynoecium while the style starts to form. The style and transmitting tract differentiate at stage twelve, and the gynoecium becomes ready for pollination. At the same time valves and repla develop and an auxin minimum defines the valve margin (Sorefan et al., 2009).

At stage 13 the flower opens (Figure 1.4 b), anthesis occurs and the gynoecium becomes self-pollinated. After fertilization the gynoecium differentiates into a fruit. In the following stages fruit ripen and the gynoecium elongates as the seeds mature within the ovary (stage 15-17). At stage 17 repla and valves become lignified, and the fruit is mature enough to dry (stage 18-20), dehisce and eventually disperse seed at

stage 20. Further detailed description of each stage with SEM images as well as cross sections can be found in Roeder and Yanofsky (2006).

Regulation of fruit development in *Arabidopsis* and beyond

Fruits are an essential part of the human diet therefore understanding the mechanism that controls the development and maturation of fruits is therefore vital for crop improvement. Fruit types can range from dry dehiscent fruits such as found in rapeseed (*Brassica napus*) to fleshy fruits such as found in tomato (*Solanum lycopersicum*).

In *Arabidopsis*, which has dry dehiscent fruits, a regulatory networks of transcription factors controlling fruit development has been revealed in much detail (Deb et al., 2018; Moubayidin and Ostergaard, 2017) while studies in tomato, a model for fleshy fruits, have mainly focussed on post-fertilization processes controlling fruit ripening and shape (Quinet et al., 2019). Interestingly, the role of the orthologs of *Arabidopsis* genes that are involved in gynoecium patterning are not well understood in other species including tomato.

However, it has become evident that the *CLV-WUS* meristem identity pathway is crucial for the regulation of meristem size in both *Arabidopsis* and tomato (Fletcher et al., 1999; Muños et al., 2011). In both species, mis-regulation of this pathway results in a fasciated stem tissue and an increased number of carpels exhibit an increased number of seed compartments (locules). In tomato, mutations affecting the *CLV-WUS* pathway were key selection targets in the domestication of wild progenitors (Rodríguez et al., 2011; van der Knaap et al., 2014). Two natural mutations in tomato, *fasciated* (*fas*) and *locule number* (*lc*), were mapped to the promoters of *SlCLV3* and *SlWUS* respectively (Muños et al., 2011). *fas* and *lc* synergistically delay the downregulation of *WUS* leading to an increase in fruit size and locule number (Muños et al., 2011; Rodríguez et al., 2011).

In *Arabidopsis* a network of differentially expressed specific transcription factors is required to regulate the establishment of different tissues that make the fruit (see previous section). Valve margin identity is established by *SHATTERPROOF 1* and *2* (*SHP1/2*), two redundantly functioning MADS box transcription factors. *SHP1/2* promote the expression of *IND* and *ALCATRAZ* (*ALC*), a close homolog of *SPT* (Liljegren et al., 2000; Liljegren et al., 2004; Rajani and Sundaresan, 2001). In the ovary, *REPLUMLESS* (*RPL*), a homeodomain protein expressed in the replum and *FRUITFULL* (*FUL*), a MADS box protein expressed in the valves limit *SHP1/2* and *IND* expression to the valve margin (Ferrandiz et al., 2000; Gu et al., 1998).

Upstream of this network, *JAGGED* (*JAG*), *FILAMENTOUS* FLOWER (*FIL*) and *YABBY3* (*YAB3*) (Chen et al., 1999; Ohno et al., 2004; Siegfried et al., 1999; Watanabe and Okada, 2003) genes are expressed in the lateral regions and specify valve and valve margin identity by redundantly promoting the expression of *FUL* and *SHP1/2* (Kumaran et al., 2002). In the replum, *JAG*, *FIL* and *YAB3* are repressed by *RPL*.

Whereas the genetic networks regulating gynoecium and fruit development appears highly conserved among the different Brassicaceae species (Eldridge et al., 2016; Langowski et al., 2016), it remains elusive whether it is the same genetic networks that are responsible for controlling tissue development in fleshy fruits.

Upon fertilisation, the gynoecium grows into a fruit. This growth is controlled by the phytohormones auxin, cytokinin and gibberellin that after fertilization initiate cell division in the growing fruit tissues. After this initial phase of cell division, cells undergo enlargement primarily via elongation (Langowski et al., 2016; Ripoll et al., 2019). In Brassicaceae, the *FUL* gene is pivotal for the regulation of this post-fertilization fruit elongation (Eldridge et al., 2016). Interestingly, the *FUL* homologs in tomato, *SlFUL1* and *SlFUL2*, play a role in controlling the fruit ripening via interactions with another MADS box protein, RIPENING INHIBOTOR (RIN) (Bemer et al., 2012;

Shima et al., 2013). In contrast, a role for FUL in fruit patterning and expansion has not been found in tomato.

Instead, SUN, an IQD family protein that is thought to affect hormone homeostasis impacts fruit shape following fertilisation. Although the mechanism of how SUN controls cell division patterns is unknown, overexpression studies imply a role for auxin (Wu et al., 2011). Notably, a homolog of *SUN* was found to control shape variation in cucumber supporting a role for *SUN*-like genes in fruit shape in other species (Monforte et al., 2014; Pan et al., 2017).

In Arabidopsis, the *CYP450-78A* gene *KLUH* regulates organ size (Anastasiou et al., 2007). Interestingly, in tomato, melon and pepper *KLUH* controls fruit size and ripening whereby the increase in fruit size results from an increased number of cell layers in the pericarp of the developing fruit after fertilization while the delay in ripening may be the result of the extension of the cell proliferation stage (Chakrabarti et al., 2013; Monforte et al., 2014). Remarkably, KLUH has also been found to regulate seed size in maize, wheat and soybean (Ma et al., 2015; Sun et al., 2017; XU et al., 2015; Zhao et al., 2016). The mechanism by which *KLUH* regulates growth has not fully been elucidated, however, it has been hypothesized that *KLUH* generates a mobile growth-promoting signal different from the known phytohormones (Adamski et al., 2009; Anastasiou et al., 2007).

In the developing gynoecium and fruit, transition from the cell division to cell expansion phase and maintenance of cell enlargement is crucial for its proper development. Although some studies suggest that a potential link between auxin and cytokinin signalling may be critical for this transition, the mechanistic aspects of the process are not well understood at the molecular level (Mu et al., 2017).

This thesis aims to elucidate the molecular mechanism underlying non-canonical auxin signalling, rather than post-fertilization fruit growth. Therefore, the *Arabidopsis*

gynoecium is used as a suitable model organ due to ETT's pivotal role in both non-canonical auxin signalling and the regulation of gynoecium development.

Scope of this thesis

The phytohormone auxin is involved in the regulation of almost all aspects of plant development. A signalling pathway and its components (TIR1/AFBs, Aux/IAAs and ARFs) that translate auxin signals into cell-type specific transcriptional outputs has been established more than a decade ago. Recently, an alternative auxin-signalling mechanism was identified whereby auxin directly affects the activity of a transcription factor complex towards its downstream targets. ETT is a pivotal component of this mechanism that mediates precise polarity switches during gynoecium development.

The work presented in this thesis aims to shed light on the molecular mechanism by which this alternative ETT-mediated auxin-signalling pathway perceives and transduces auxin stimuli to generate a transcriptional output.

Chapter 2 addresses to what extent the alternative auxin-signalling pathway is independent of the established TIR/AFB-mediated pathway. The examination of two ETT-target genes *HECATE1* (*HEC1*) and *PINOID* (*PID*) in various auxin receptor mutants demonstrated that the auxin-responsive regulation of both genes in the gynoecium is independent of the canonical TIR1/AFB auxin receptors. Prior studies showed auxin sensitivity of ETT-TF interactions suggesting a direct effect of auxin on the ETT protein. Analysing a potential ETT-auxin interaction using heteronuclear single quantum coherence (HSQC) nuclear magnetic resonance (NMR) and isothermal titration calorimetry (ITC) confirmed that ETT indeed binds auxin directly. This suggests that ETT itself may act as an auxin receptor that exhibits features reminiscent of animal hormonal signalling pathways. Upon hormone binding by the TF, these pathways usually involve extensive chromatin remodelling at their target

loci. Examining the effect of auxin on the local chromatin environment at the *HEC1* and *PID* gene indicates that alternative auxin signalling also involves chromatin remodelling.

To find out which other proteins collaborate with ETT to mediate the effects of auxin on the chromatin, **Chapter 3** reports the result of a yeast-two-hybrid library screen that found potential candidates that link auxin signalling with chromatin regulation. Challenging these interactions with auxin identified a few interactions that were auxin sensitive. Two of these proteins, DEK-DOMAIN CONTAINING PROTEIN 3 (DEK3) and REDUCED VERNALIZATION 2 (VRN2), were evaluated in more detail for their role in gynoecium development. DEK3 has been implemented in various mechanisms involved in chromatin architecture and gene regulation while VRN2 is part of the polycomb complex 2 (PRC2) which is involved in gene silencing. *dek3 dek4* double mutant gynoecia resemble *ett* mutant gynoecia suggesting biological relevance of the ETT-DEK3 interaction. Ectopic expression of the ETT-target gene *PID* in *dek3 dek4* mutants supports this hypothesis. In contrast, *vrn2* mutant gynoecia neither exhibit any developmental defects nor mis-regulation of *PID*. These results imply that the ETT-VRN2 interaction may not play a role in gynoecium development. Finally, the screen identified that the co-repressor TOPLESS (TPL) directly interacts with ETT.

Chapter 4 explores the mechanism by which ETT interacts with TPL and two TPL homologs (TOPLESS RELATED (TPR) 2 and TPR 4) in an auxin-sensitive manner. The results of this chapter show that a conserved repressor motif at the C-terminus of ETT and a conserved region within the WD40 domain of TPL mediates interaction between the two proteins. Testing representative ARFs from each clade shows that TPL can interact with class-B but not with class-A and class-C ARFs. Mutant analysis shows that *tpl tpr2* double mutants show polarity defects at the gynoecium apex indicating a biological role in gynoecium development. TPL/TPRs recruit HISTONE DEACETYLASE 19 (HDA19) to mediate deacetylation of histones and thereby form

a ‘closed’ (repressive) chromatin state at the target genes. Analysis of *hda19* mutants also identified polarity defects at the gynoecium apex. ChIP analysis demonstrated that ETT-TPL and HDA19 cooperatively bind ETT-target loci. In support of such a cooperative role, ETT, TPL and HDA19 binding correlate with both histone acetylation and target gene expression. Collectively, the data presented in this chapter provides molecular insight into the mechanism of the alternative auxin-signalling pathway. This pathway might not be exclusive to the ETT and TPL pair but may play a more general role in class-B ARF-mediated auxin signalling.

While previous chapters address the mechanistic and biochemical basis of complex formation in alternative auxin signalling focusing mainly on the role of trans-factors in gene regulation, **Chapter 5** evaluates the importance of cis-regulatory elements in the regulation of auxin-responsive genes. For this purpose, the *PID* gene was used as a model to investigate the importance of two ETT-binding AuxREs for the gene’s regulation during gynoecium development. Results demonstrate that the regulation of *PID* is robust since even constructs mutated in both AuxREs were able to rescue the fruit phenotype when introduced into the *pid-8* mutant. However, more detailed analysis showed that mutating the AuxREs increases the style length of gynoecia of transformed lines. In agreement with this, the promoter activity in mutant lines was increased. ETT regulates *PID* expression in collaboration with IND in an auxin-sensitive manner. Evaluation of promoter binding *in planta* shows that ETT promoter binding of *PID* is independent of auxin while IND binds the *PID* promoter only in absence of auxin. Collectively, the data suggest that binding of ETT to the *PID* promoter via the two examined AuxREs is important for the fine tuning of *PID* expression during style elongation but not during style establishment. Additionally, it supports previous data that ETT-IND interaction is important to repress *PID* in absence of auxin.

Finally, **Chapter 6,** summarises and discusses all main findings, states the conclusions that can be made from the work presented in this thesis and gives directions for future research.

Chapter 2

Direct ETTIN-auxin interaction regulates chromatin environment at target genes

Introduction

Plants are multicellular organisms that originate from a single cell, a fertilised oocyte, which ultimately differentiates into tissues and organs comprised of numerous cells. The genes involved in these developmental processes are under tight temporal and spatial regulation. Changes in gene expression are often controlled by mobile signals that translate positional information into cell-type specific transcriptional outputs (Hironaka and Morishita, 2012). In plants, this co-ordination can be facilitated by phytohormones, such as auxin, which controls processes throughout plant development (Vanneste and Friml, 2009). Canonical auxin signalling involves binding of the auxin molecule to TIR1/AFB auxin co-receptors stabilising their interaction with Aux/IAA transcriptional repressors (Dharmasiri et al., 2005; Kepinski and Leyser, 2005). TIR1/AFBs are part of the $SCF^{TIR1/AFB}$ ubiquitin-ligase complex. Hence, the auxin mediated enhancement of TIR1-Aux/IAA interaction leads to Aux/IAA polyubiquitination and degradation by the 26S proteasome. Degradation of Aux/IAA proteins relieves the repression of Auxin Response Factors (ARFs), which target auxin-responsive genes. When auxin levels are low, ARFs dimerise with Aux/IAAs, which leads to the recruitment of chromatin-modifying enzymes (Leyser, 2018).

As discussed in the Introduction, ARFs can be classified into three phylogenetically distinct clades, A, B and C (Finet et al., 2013). Class-A ARFs have been shown to act as transcriptional activators and class-B ARFs are repressors of transcription (Ulmasov et al., 1999a). The role of class C ARFs in the auxin response is not clear (Mutte et al., 2018). Interestingly, while all class-A ARFs interact with Aux/IAAs, most class-B ARFs cannot (Piya et al., 2014; Vernoux et al., 2011), which makes it difficult to explain how auxin responsive transcription is regulated by class-B ARFs via the canonical auxin signalling pathway.

Recently, an alternative auxin-signalling mechanism was identified whereby auxin directly affects the activity of a transcription factor (TF) complex towards its

downstream targets (Simonini et al., 2016). This mechanism mediates precise polarity switches during organ initiation and patterning and includes the ARF, ETTIN (ETT/ARF3) as a pivotal component. However, ETT is an unusual ARF which lacks the Aux/IAA-interacting Phox/Bem1 (PB1) domain an essential component of the canonical auxin signalling pathway. It is therefore likely that ETT would mediate auxin signalling via a non-canonical pathway (Simonini et al., 2017; Simonini et al., 2016; Simonini et al., 2018a; Simonini et al., 2018b). ETT interacts with a diverse set of TFs, most of which key regulators of different aspects of gynoecium development. These interactions are sensitive to the naturally occurring auxin, indole 3-acetic acid (IAA) (Simonini et al., 2016). The region responsible for IAA-sensitivity is situated within the C-terminal part of ETT, known as the ETT-Specific (ES) domain (Simonini et al., 2016; Simonini et al., 2018a). Sensitivity of ETT-TF interactions to IAA suggests a direct effect of the IAA molecule on the ETT protein and ETT itself may therefore act as an auxin receptor. Direct transcription factor-hormone binding is common in animal hormonal signalling pathways such as the steroid and thyroid hormone signalling pathways (King et al., 2012; Tsai and O'Malley, 1994). Steroid hormone receptors (SHR) and thyroid hormone receptors (THR) are transcription factors that - depending on their class - localize either to the cytoplasm or the nucleus when hormone levels are low. In the case of cytoplasmic SHRs and THRs, hormone binding triggers translocation to the nucleus where SHRs and THRs bind their target genes. In contrast nuclear SHRs and THRs bind target loci independently of the hormone concentration. When hormone levels are low DNA-bound SHRs and THRs repress their target genes by means of co-repressor recruitment, and thus maintain the chromatin in a repressed state. Upon hormone binding (and DNA-binding), SHRs and THRs undergo conformational changes that enable them to form complexes with co-activators and histone modifiers, leading to extensive chromatin remodelling and activation of gene expression at their target loci (King et al., 2012; Tsai and O'Malley, 1994).

Thus, one could speculate that direct auxin binding by ETT regulates target gene expression in response to auxin using a similar mechanism.

This chapter aims to answer several critical questions regarding non-canonical auxin signalling and the role of ETT as a central component of it. Firstly, prior to this project a genomic approach was taken to identify target genes of the alternative auxin-signalling mechanism during gynoecium development (Simonini et al., 2017). Using this resource, I identified a subset of genes that are robustly auxin-responsive and under direct control of ETT, which will be used as model genes throughout this thesis to further study the non-canonical auxin-signalling pathway.

Secondly, ETT lacks a PB1-domain and is therefore unlikely to mediate auxin signals via the canonical pathway. Through mutant analysis and pharmacological treatments, I elucidate to which extent the alternative auxin signalling pathway is independent of the canonical TIR/AFB-mediated pathway.

Thirdly, the auxin sensitivity of ETT-TF interactions suggests a direct effect of auxin on the ETT protein. Here, I provide biochemical evidence that ETT acts as an auxin receptor that exhibits features reminiscent of components of animal hormonal signalling pathways. Since these pathways typically involve extensive and hormone-dependent chromatin remodelling at their target loci, I examined the effect of auxin on the local chromatin environment at two ETT-target genes.

Results

HEC1 and *PID* are regulated by ETT and auxin responsive

Prior to the start of the project presented in this thesis, a genomic approach was taken to identify which genes are regulated by the ETT-mediated alternative auxin-signalling mechanism during gynoecium development. By combining data from chromatin immunoprecipitation coupled with sequencing (ChIP-seq in a *pETT:ETT-*

GFP line) with analysis of the auxin-responsive transcriptome (RNA-seq) of an *ett* mutant compared to wild type (Simonini et al., 2016), genes under the control of ETT were identified. The results show that ETT can bind cis-elements of several hundred genes, and that a subset of these genes is regulated by ETT in an auxin-responsive manner (Simonini et al., 2017). Here, these genomic resources are used to identify genes that can be used as a model to gain mechanistic insight into how alternative auxin signalling regulates the expression of its target genes. There are several requirements for a gene to be a suitable model to understand this mechanism, 1) the gene must be up-regulated in response to auxin in wild-type gynoecia, 2) the genes must be mis-regulated in *ett*-mutant gynoecia and 3) the gene must be directly regulated by ETT.

By re-analysing the RNA-seq and ChIP-seq data sets, 15 genes were identified that meet these criteria (Figure 2.1 b and Appendix I Table 1). Four genes were selected and their auxin-responsive expression in wild type and *ett-3* mutant gynoecia was validated using quantitative real time PCR (qPCR). The selected genes were *HECATE1* (*HEC1*), *MEMBRANE-ASSOCIATED KINASE REGULATOR 6* (*MAKR6*), *PIN-FORMED 3* (*PIN3*) and *PIN7*. *PINOID* (*PID*), a direct target of ETT identified previously (Simonini et al., 2016), and *Aux/IAA19* (*IAA19*), a gene that is regulated independently of ETT were included in this analysis as a positive and negative control respectively. As expected, the results show that *IAA19* expression is upregulated in response to auxin in wild type and *ett*-mutant gynoecia but is not mis-regulated in untreated *ett*-mutants. Contrary to the results of the RNA-seq, *MAKR6* and *PIN3* follow the same trend as *IAA19* in this experiment, suggesting that they are not under the direct control of ETT, while *PIN7* was unresponsive to auxin in both the wild type and *ett-3* mutant. One explanation for the inconsistencies between the qPCR and RNA-seq data sets is that qPCR was performed on cDNA of dissected gynoecia while the RNA-seq was conducted on tissue from whole inflorescences (Simonini et al.,

2017). However, for *HEC1* and *PID* qPCR confirmed that the expression of both genes is upregulated in gynoecia tissues from the *ett-3* mutant compared to wild type. Moreover, the expression of both genes is induced by auxin, and this effect is abolished in the *ett-3* mutant background (Figure 2.1a).

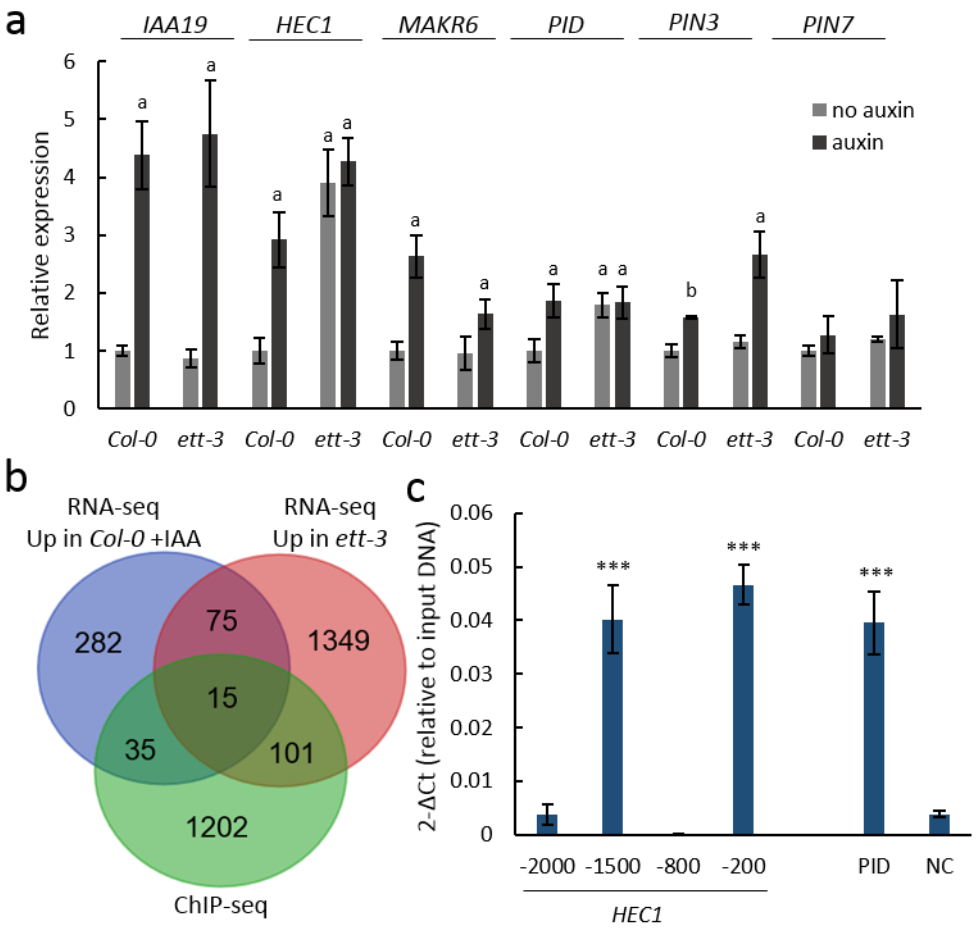

Figure 2. 1: *HEC1* and *PID* can be used as model genes to study non-canonical auxin signalling. (a) expression of candidate genes in gynoecium tissue ± 100 µM IAA treatment; *HEC1* and *PID* are up-regulated by auxin and under direct ETT-control. *IAA19* serves as a negative control, while the results for *MAKR6* and *PIN3* suggest ETT-independent auxin-responsiveness. *PIN7* did not respond to auxin treatment. a $p < 0.001$; b $p < 0.05$; Shown are mean ± standard deviation of three biological replicates. (b) analysis of RNA-seq and ChIP-seq data sets identified 15 candidate genes that are direct targets of ETT and that are up-regulated *ett-3* mutants and in wild type (*Col-0*) after auxin treatment. (c) $ChIP_{qPCR}$ confirmed direct ETT binding to the *HEC1*-promoter, an ETT binding region in the *PID*-promoter was used as a positive control while a region within the *WUS*-promoter was used as a negative control. ***$p < 0.0001$; Shown are mean ± standard deviation of three biological replicates.

While the ETT binding site within the *PID* promoter has previously been identified (Simonini et al., 2016), ChIP-seq identified four distinct binding sites within the *HEC1* promoter. Using the same *pETT:ETT-GFP* line from the ChIP-seq study, ETT binding to two regions (-1500 and -200) of the *HEC1* promoter was confirmed by $ChIP_{qPCR}$ (Figure 2.1c). The well-established ETT binding region within the *PID* promoter was used as a positive control and a region within the WUS promoter was used as a negative control as described previously (Liu et al., 2014; Simonini et al., 2016). The $ChIP_{qPCR}$ results highlight the importance of validating TF binding peaks obtained from ChIP-seq.

Collectively, the data presented here establish and validate that *HEC1* and *PID* are regulated by ETT in an auxin-responsive manner. *HEC1* and *PID* are two genes that play important role in gynoecium development. HEC1, redundantly with its homologs HEC2, HEC3 regulate the synthesis and transport of auxin in the medial tissues through the activation of *YUC4* and *PIN1* and *PIN3 (Gremski et al., 2007; Schuster et al., 2015)*, while PID as regulates polar auxin transport via regulation of PIN localisation and activity (Benjamins et al., 2001; Friml et al., 2004; Michniewicz et al., 2007). Both genes can be considered as suitable models for the characterization of the alternative auxin signalling pathway.

Non-canonical auxin signalling is independent of TIR1/AFB

The data obtained so far suggest that ETT can regulate gene expression of direct target genes in response to auxin, however, it is unclear to what extent this pathway is independent of the established TIR/AFB-mediated pathway. Since ETT lacks the Aux/IAA interacting PB1 domain it is likely that ETT mediates auxin signalling via a TIR1/AFB independent pathway. To test this, the expression and auxin-responsiveness of the ETT-targets *HEC1* and *PID* were examined in gynoecia from *tir1-1 afb2-3,* and *tir1-1 afb2-3 afb3-4* auxin-receptor mutants, while *IAA19* served as a control gene for TIR1/AFB mediated regulation (Figure 2.2 a-c). The results show

that the auxin dependent regulation of ETT targets does not require a functional TIR1/AFB, since the auxin-mediated induction of *PID* and *HEC1* can still be observed in TIR1/AFB higher order mutants, whereas the auxin sensitive induction of *IAA19* is completely abolished in these lines. In support of this, *tir1 afb2 afb3* triple mutant gynoecia where phenotypically examined using scanning electron microscopy (SEM). The auxin receptor triple mutants show no abnormalities in gynoecium development (Figure 2.2 d).

Recently, an engineered auxin-TIR1 system was developed (Uchida et al., 2018) in which the engineered auxin-binding cavity of TIR1 (concave TIR1, ccvTIR1) binds specifically to a modified bulky version of IAA (convex IAA, cvxIAA). By expressing the ccvTIR1 in a *tir1 afb2* mutant background, the canonical pathway will only respond to the addition of cvxIAA and not IAA (Figure 2.2 e). To further assess the TIR1/AFB independence of the ETT-mediated auxin signalling pathway, this synthetic auxin receptor system was exploited. qPCR was performed on cDNA from ccv*TIR1* gynoecia treated ±cvxIAA and ±IAA, as well as on control plants with the same treatments. Like in the previous experiment, *IAA19* served as a control for being under TIR1/AFB mediated regulation and was accordingly upregulated by cvxIAA, but not IAA in the *ccv*TIR1 background. In contrast, *PID* and *HEC1* expression was largely unaffected by cvxIAA, and instead remained responsive to IAA in the *ccv*TIR1 line (Figure 2.2 f). Together, these data demonstrate that ETT-mediated non-canonical auxin signalling occurs independently of the canonical TIR1/AFB signalling machinery.

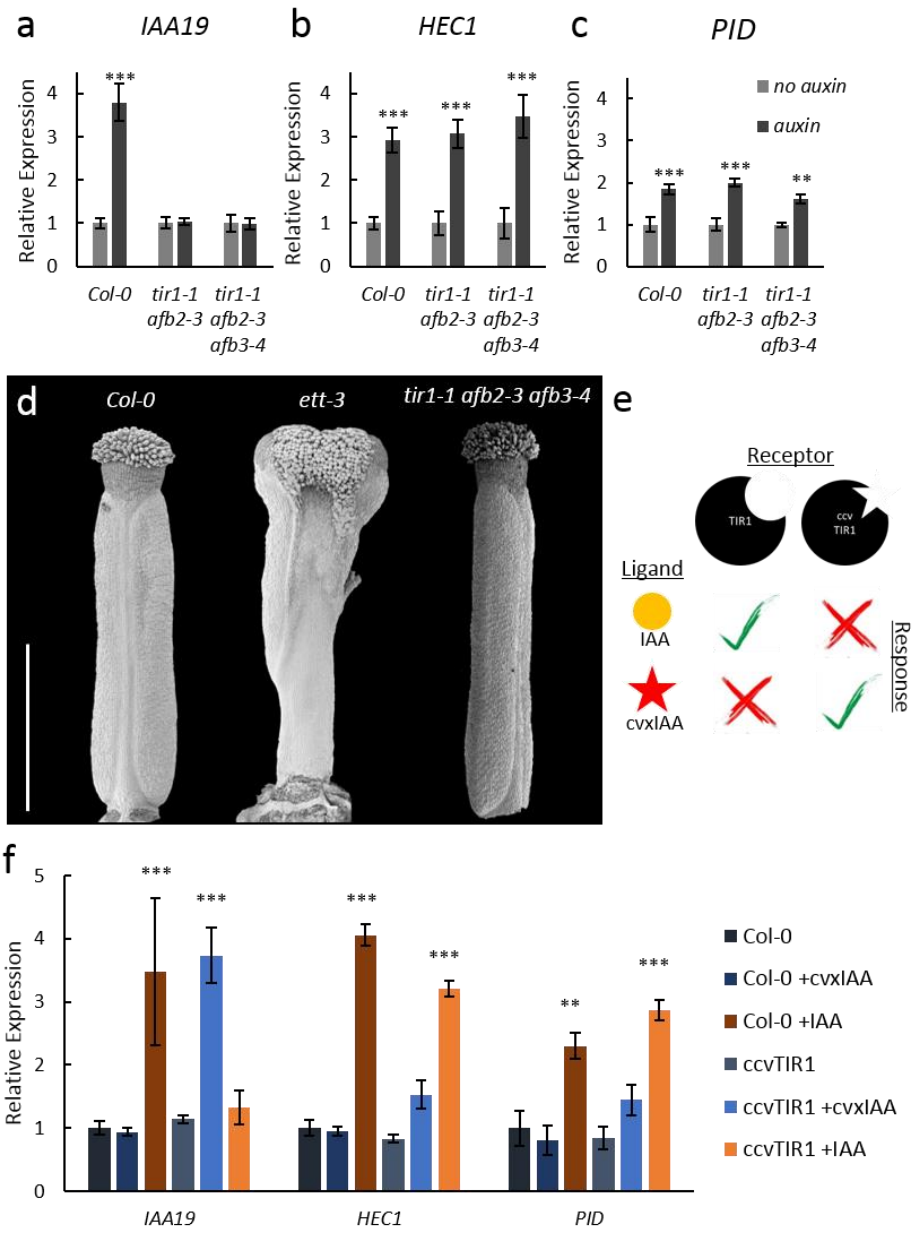

Figure 2. 2: ETT regulates target-gene expression independently of TIR1/AFB auxin receptors. (a-c) Expression of the auxin responsive IAA19 gene (a) and the ETT-target genes *HEC1* (b) and *PID* (c) in mock-treated or 100 µM IAA-treated gynoecia assayed using qPCR. (a) *IAA19* expression is up-regulated in response to auxin in wild type gynoecia (*Col-0*) but not in tir1/afb double and triple mutants. The ETT-target genes *HEC1* and *PID* are up-regulated in response to auxin in both wild type and auxin receptor mutants (b, c). This suggests a TIR1/AFB-independent regulation of these genes. (d) Gynoecium phenotypes of wild type, *ett-3*, *tir1-1 afb2-3 afb3-4*. Scale bar = 100 µm. (e) Schematic visualisation of the principle of the engineered cvxIAA-ccvTIR1 pair. (f) Expression of *IAA19*, *HEC1* and *PID* in response to treatment with 100 µM IAA and 100 µM cvxIAA in wild type (*Col-0*) and *pTIR1:ccvTIR1* gynoecia (ccvTIR1). The data confirm TIR1/AFB independent regulation of *HEC1* and *PID* in the gynoecium. ***p <0.0001; Shown are mean ± standard deviation of three biological replicates.

The ETT-protein can directly bind indole 3-acetic acid (IAA)

ETT can interact with a diverse set of TFs from different families such as INDEHISCENT (IND) and REPLUMLESS (RPL) - two important regulators of gynoecium development - in an auxin-sensitive manner (Girin et al., 2011; Liljegren et al., 2004; Roeder et al., 2003; Simonini et al., 2017; Simonini et al., 2016; Simonini et al., 2018b; Sorefan et al., 2009). The region responsible for auxin-sensitivity is situated within the C-terminal part of ETT, known as the ETT-Specific (ES) domain (Simonini et al., 2016; Simonini et al., 2018a; Figure 2.3 a).

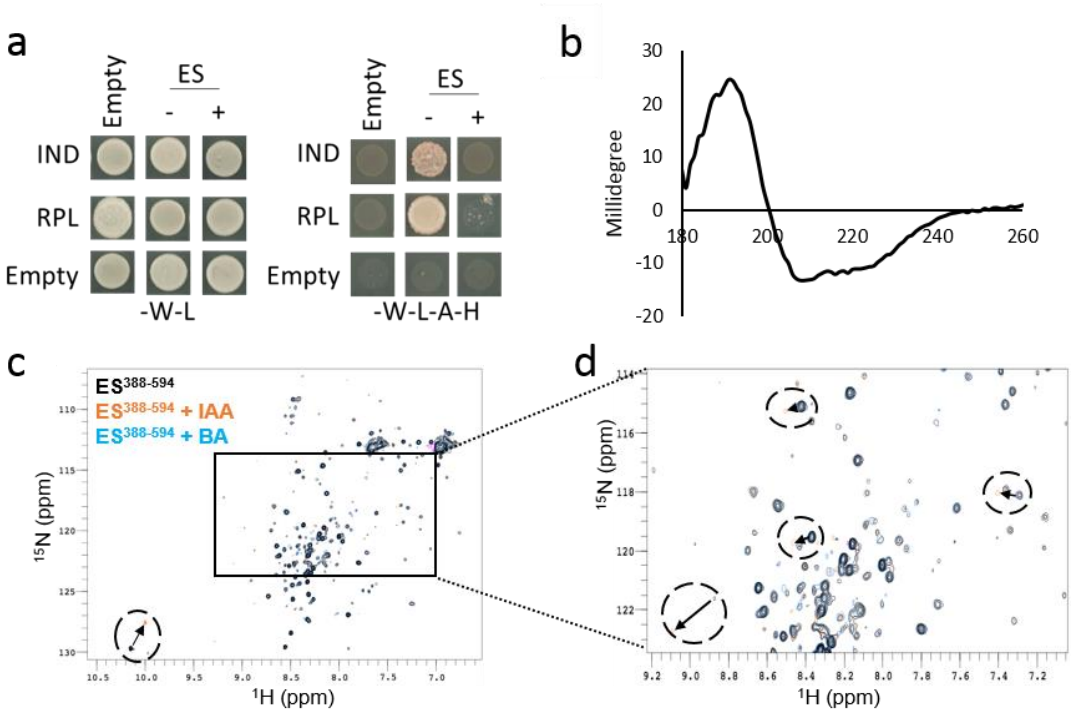

Figure 2. 3: ETT is an intrinsically disordered protein that directly binds auxin (IAA). (a) ETT interacts with IND and RPL in an auxin-sensitive manner. Empty indicates the empty vector control. -W-L indicates that the growth medium lacks Tryptophan (W) and Leucine (L) to select for positive transformation. -W-L-A-H indicates that the growth medium lacks Tryptophan (W), Leucine (L) Adenine (A) and Histidine (H) to test for interaction. – indicates no auxin supplemented to the growth medium, + indicates 100 µM IAA supplemented to the growth medium. The results show that IAA affects the protein-protein interactions but does not inhibit the growth of yeast cells. (b) CD analysis of the ES 388-594 protein showing a characteristic spectrum of an intrinsically disordered protein. (c) HSQC-NMR performed with ES388-594 protein either alone (black), with indole-3-acetic acid (IAA, orange) or benzoic acid (BA, blue). (d) zoom-in of the indicated rectangular region in (c). Changes in chemical shifts are indicated by arrows from control to IAA treatment in panels (c) and (d). The HSQC-NMR experiment shown in (c) and (d) were performed by Dr. Sigurd Ramans Harborough (University of Leeds).

A protein fragment containing 207 amino acids of the ES domain, $ES^{388-594}$, that is sufficient for mediating IAA-sensitivity in ETT-protein interactions, was produced

recombinantly in *Escherichia coli*. Analysis of the protein properties by Circular Dichroism (CD) spectroscopy shows that $ES^{388-594}$ contains some degree of folding but is intrinsically disordered (Figure 2.3 b; Simonini et al., 2018a). To test whether ETT binds IAA a collaboration with Dr. Stefan Kepinski at University of Leeds was established. Together, we conducted heteronuclear single quantum coherence (HSQC) nuclear magnetic resonance (NMR) experiments using nitrogen-15 (^{15}N) isotope-labelled $ES^{388-594}$ protein that was recombinantly produced in *E. coli*. HSQC NMR is a highly sensitive 2D-NMR method that is commonly used in structural biology to study protein structure, protein-protein interactions and protein-ligand binding. The method is based on the transfer of magnetization from a proton to a second atomic nucleus, in this case ^{15}N. After a delay, the magnetization is transferred back to the proton and the signal is recorded. To obtain the HSQC spectrum, a series of experiments is recorded where the time delay is incremented (Meyer and Peters, 2003).

Each residue in the protein has an amide proton attached to a nitrogen atom in the peptide bond. The HSQC correlates between the nitrogen and amide proton, and each amide yields a peak in the HSQC spectrum. Each ^{15}N-labelled residue can therefore produce an observable peak in the spectrum (Meyer and Peters, 2003). In addition to the backbone amide resonances, sidechains with nitrogen-bound protons will also produce peaks. By comparing the HSQC of the free protein with the one bound to the ligand, changes in the chemical shifts of some peaks can be observed, and these peaks are likely to lie on the binding surface.

In our experiment, the HSQC spectrum was recorded at 5˚C and shows a prominent signal-dense region (Figure 2.3 c, d). Consistent with previous observations, the location of this region on the spectrum suggests that the protein is largely intrinsically disordered. Interestingly, the spectrum also shows peaks flanking the signal-dense region, indicating that there is some propensity to form secondary structure,

particularly those with a helical character (Figure 2.3 c). These observations match the data obtained using CD. In addition to an overview of ETT structure, the HSQC NMR probes chemical shifts of protein amide-NH bonds in response to ligand (Meyer and Peters, 2003). We found that a number of residues shifted their position in the spectrum in response to the addition of IAA, whereas the addition of the chemically related Benzoic Acid (BA), which was used as a negative control, had no effect (Figure 2.3 c, d). Due to the low resolution of the HSQC spectrum produced, we were unable to assign specific peaks to the corresponding amino acid within the protein. Thus, we did not identify the exact amino acids that experience chemical shifts, and that are likely to be responsible for ETT-auxin interaction. The exception to this is a tryptophan at position 505 (W505), which is located in the bottom left corner of the ^{15}N spectrum (Figure 2.3 c), which experienced a remarkable shift upon the addition of IAA.

The dissociation constant (K_D) of the ligand-protein interactions can be determined by Water-Ligand Observed via Gradient Spectroscopy (WaterLOGSY) NMR. WaterLOGSY-NMR exploits the intrinsic properties of water in the presence of a ligand and its interactor. Water molecules surrounding free ligand molecules transfer magnetization differently from water molecules surrounding ligand which has formed a complex. Water molecules stabilise protein-ligand interactions due to the hydrogen bonds that form at binding sites between ligand and protein atoms via water. Consequently, the resonances of free ligand tend to be weaker than those of the stabilized ligand (Dalvit et al., 2001).

We determined the K_D of the $ES^{388-594}$-IAA interaction by WaterLOGSY-NMR using a range of different auxin concentration. This gave a K_D of 1.1 mM (Appendix I Figure 1) indicating a low affinity between auxin and the $ES^{388-594}$ domain.

An alternative method to determine the dissociation constant is isothermal titration calorimetry (ITC) (Figure 2.4 a-c). ITC characterises binding affinity of ligands for

proteins by determining the thermodynamic parameters of the interaction. ITC detects the addition of ligand due to temperature increases in the sample cell upon the binding of ligand to its target (in an exothermic reaction) while the temperature in the reference cell stays constant. The power needed to maintain reference and the sample cell at the same temperature is plotted against time, giving the total heat exchanged per injection. The pattern of these heat effects as a function of the molar ratio [ligand]/[protein] can then be analysed to give the thermodynamic parameters of ligand-protein interaction.

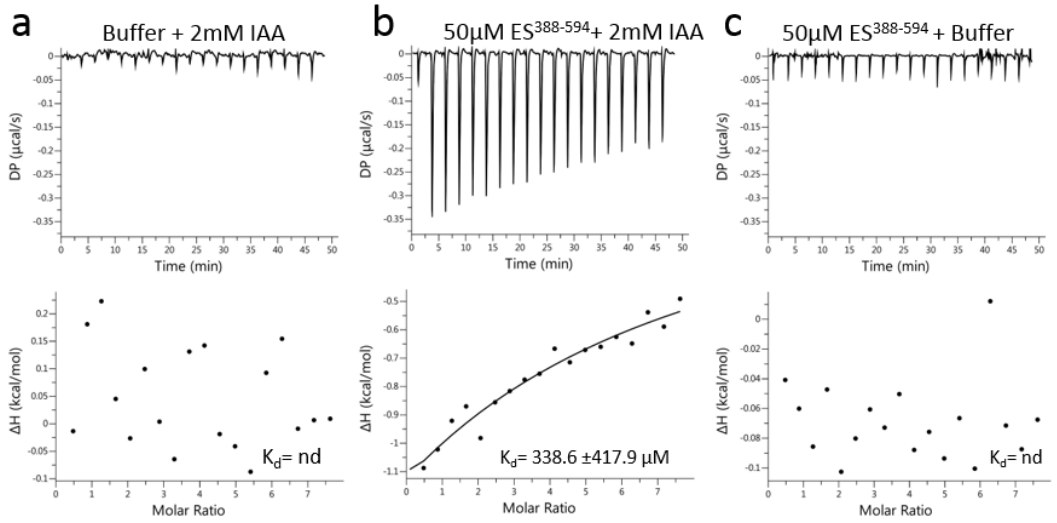

Figure 2. 4: Quantification of binding affinities by ITC assays. (a) negative control; 2mM IAA was titrated into buffer. (b) 2mM IAA was titrated into 50 µM $ES^{388-594}$. (c) negative control; buffer was titrated into 50 µM $ES^{388-594}$. The binding constants (Kd values ± fitting errors) are indicated. ND, no detectable binding.

Analysis of ITC data showed that $ES^{388-594}$ binds to IAA weakly (K_d=338.6 µM), while titrating IAA into buffer alone, or titrating buffer alone into the $ES^{388-594}$ sample clearly showed no heat exchange (*i.e.* no binding of a ligand) (Figure 2.4 a-c). Notably, the findings from the control experiments confirm that the heat exchange observed is due to a real biophysical interaction between $ES^{388-594}$ and auxin, and not due to other buffer components. It remains unclear whether auxin is bound by $ES^{388-594}$ at one or multiple binding sites. I was unable to assess this due to difficulties in determining equivalence points of the titrations, presumably due to the weak ES-IAA interaction.

Likewise, the experiment was not saturated with IAA at the end and was therefore more prone to background noise. It is also possible that ETT forms different species of oligomers some of which may be active, while others may form due to aggregation. At this point it is impossible to make any further prediction about auxin binding sites due to uncertainty about the exact stoichiometry of ETT. Calibrated gel filtration could be used to determine the ability of ETT to form oligomers and may shed light on ETT's stoichiometry. ETT multimers elute earlier from the column than ETT monomers. Once monomers and oligomers are separated, auxin binding could be studied by repeating the ITC experiment as described above using exclusively monomeric ETT. If purified monomers do not aggregate or form oligomers after purification, this experiment will elucidate whether ETT has one or multiple auxin binding sites.

Despite the high dissociation constants (and hence weak interactions) observed by both ITC and WaterLOGSY-NMR, the data demonstrate that ETT can directly bind IAA, which may then affect the interaction between ETT and its TF partners. Together with the TIR1/AFB-independence of the non-canonical auxin signalling pathway, this suggests a direct effect of auxin on the ETT protein and implies that auxin-perception is an intrinsic property of the ETT protein. Direct binding of a (hormone) ligand by a transcription factor is a feature, which is reminiscent of animal hormonal signalling pathways such as the steroid and thyroid hormone and Wnt/ß-catenin pathways. These pathways involve extensive chromatin remodelling at their target loci (Gammons and Bienz, 2018; King et al., 2012; Tsai and O'Malley, 1994).

Chromatin dynamics in response to auxin treatment can be observed at ETT-target loci

Histones can be modified in many ways and, although all histone modifications are thought to regulate the chromatin structure and DNA packing, the effect of most of the modifications on chromatin organisation and gene expression remains elusive. Proving gene regulatory causality of a modification involves showing that the catalytic

activity of the enzyme that mediates the modification is required for the biological response. However, many histone-modifying enzymes occur in big gene families that act redundantly and are often not specific to histones. Thus, implementation of histone modifications in a biological context has mostly been correlative rather than causative (Hon et al., 2009; Kouzarides, 2007). However, some histone modifications have been implemented in the regulation of differential gene expression in numerous developmental contexts in plants and animals (Gammons and Bienz, 2018; Mozgova and Hennig, 2015; Whittaker and Dean, 2017; Xiao and Wagner, 2015). The regulation of gene expression requires the recruitment of chromatin-modifying enzymes to the locus being regulated. Following a developmental or environmental stimulus, transcription factors are recruited to the promoter and this initiates a cascade of chromatin-remodelling events resulting in the promotion or repression of transcription.

Histone modifications can be divided into those that correlate with activation and those that correlate with repression of gene expression. While acetylation of Histone 3 lysine 9 (H3K9ac) and Histone 3 lysine 27 (H3K27ac) and the tri-methylation of Histone 3 lysine 4 (H3K4me3) have been implicated in active transcription, Histone 3 lysine 27 tri-methylation (H3K27me3) is associated with repression. H3K27me3 also plays an important role in epigenetic gene silencing in plants and animals (Mallo and Alonso, 2013; Mozgova and Hennig, 2015; Müller et al., 2002). However, it has become increasingly evident that the role of histone methylation is highly context specific and goes far beyond transcriptional repression. An example is the tri-methylation of Histone 3 lysine 36 (H3K36me3) which promotes transcription when found in gene bodies and represses transcription when it occurs in the promoter (Vakoc et al., 2006; Yang et al., 2017; Yang et al., 2014). Notably, in some epigenetic memory systems H3K27me3 and H3K36me3 antagonise one another and represent two stable states (Berry et al., 2015; Yang et al., 2017; Yang et al., 2014).

The effect of auxin on ETT-TF interactions is reminiscent of hormone signalling pathways in animals that involve chromatin modelling (Gammons and Bienz, 2018; King et al., 2012; Tsai and O'Malley, 1994), and it can therefore be speculated that non-canonical auxin-signalling may regulate gene expression by mediating auxin sensitive chromatin modifications.

To test this hypothesis, the effect of auxin on H3K27me3, H3K36me3 and H3K27ac modification within the local chromatin environment at the *HEC1* and *PID* loci were tested in young gynoecia using $ChIP_{qPCR}$. First, the enrichment of repressive histone H3K27me3 marks were evaluated (Figure 2.5 a, b). H3K27me3 accumulated across the *HEC1* gene body in untreated wild-type gynoecia, peaking at the transcription start site (TSS) while chromatin marks were depleted in *ett-3* mutant gynoecia (Figure 2.5 a). Although only significant at the TSS, H3K27me3 levels were reduced across the whole coding region in wild type gynoecia treated with auxin.

The regulation of the *PID* locus involves *APOLO*; a gene encoding a long non-coding RNA neighbouring the *PID* gene and that modulates *PID* expression upon auxin treatment (Ariel et al., 2014). *APOLO* and *PID* are co-regulated. Under low auxin levels, both *APOLO* and *PID* are repressed whereas auxin induces the expression of both *APOLO* and *PID*. *APOLO* transcript accumulation leads to RNA-directed DNA methylation of the locus and repression of both *APOLO* and *PID* expression. H3K27me3 has been implemented in this pathway since H3K27me3 levels are reduced at *APOLO* and the *PID*-promoter upon auxin treatment (Ariel et al., 2014). The examination of H3K27me3 levels across the *PID* locus show that H3K27me3 accumulates within the promoter region at *APOLO* (-5.5kb from the TSS), within the *PID*-promoter (-3kb from TSS) and towards the end of the last exon of the gene (1.6kb from TSS) in young wild-type gynoecia. A reduction of H3K27me3 levels can be observed in auxin-treated wild type gynoecia (Figure 2.5 b). These data broadly agree with what was previously published (Ariel et al., 2014). In a similar manner to *HEC1*,

H3K27me3 chromatin marks were depleted at the *PID*-locus in *ett*-mutant gynoecia (Figure 2.5 b). Together, the data imply that the H3K27me3 levels of both ETT-target genes are regulated auxin-dependently. Moreover, depletion in *ett*-mutants indicate that H3K27me3 deposition also depends at least partially on ETT.

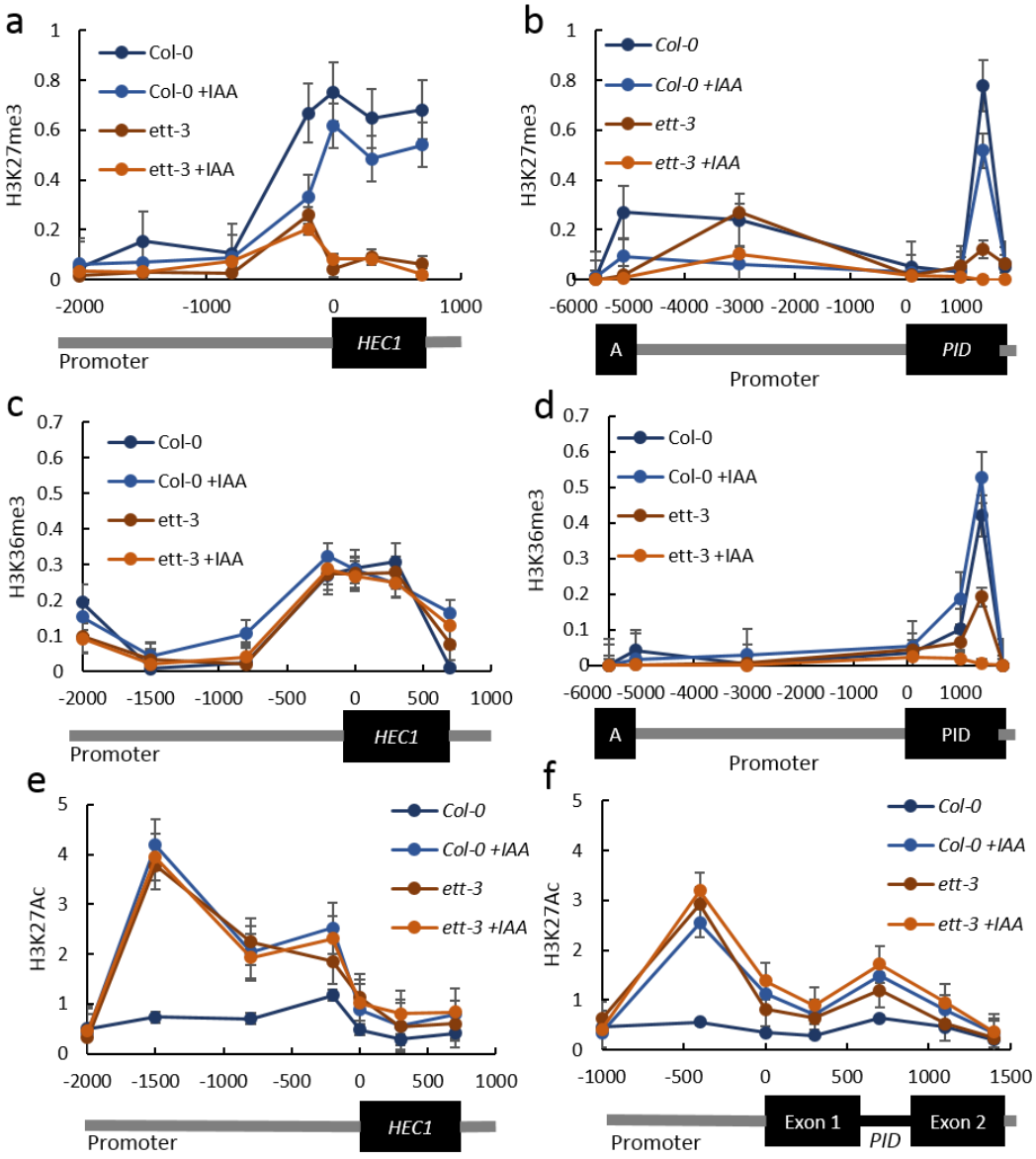

Figure 2. 5: Histone modifications at *HEC1* and *PID* in wild type (*Col-0*) and *ett-3* in response to auxin treatment (100 µM IAA). H3K27me3 (a, b), H3K36me3 (c, d), H3K27Ac (e, f) profiles across the *HEC1* locus (a, c, e) and *PID* locus (b, d, f). *HEC1* or *PID* loci structures are shown schematically at the bottom of the graphs (a-f); A indicates position of the APOLO gene (b, d). Data were presented as the ratio of (*HEC1* or *PID*/H3) to (reference gene/H3). *STM* was used as the reference gene for H3K27me3 and *ACT* was used for H3K36me3 and H3K27Ac.

Accumulation of repressive histone modifications across the gene body, such as those observed at the *HEC1* locus, are a common feature of epigenetically-silenced

genes such as FLOWERING LOCUS C (FLC). FLC is a key regulator of flowering time that is epigenetically silenced in response to cold during vernalisation (Whittaker and Dean, 2017). The silenced chromatin state is epigenetically memorised and inherited through cell division (Angel et al., 2011; Berry et al., 2015). Recently, studies have shown that this epigenetic memory system is bi-stable consisting of two mutually exclusive and self-sustaining states (Berry et al., 2015; Yang et al., 2017; Yang et al., 2014). Whilst the H3K27me3 histone modification represents the repressive state of this bi-stable memory, the active state is characterised by the accumulation of H3K36me3 modifications.

In order to elucidate whether epigenetic silencing and bi-stable memory are features also involved in *HEC1* and *PID* regulation, levels of H3K36me3 modifications were evaluated in these two genes. If epigenetic memory in response to auxin plays a role in the regulation of *HEC1* and *PID*, the profiles of H3K27me3 and H3K36me3 at these loci should exhibit opposite patterns in wild type gynoecia treated with exogenous auxin when compared to those which are untreated. The results show that H3K36me3 levels neither change significantly upon auxin treatment wildtype nor in *ett*-mutant gynoecia at the *HEC1* locus and the *PID* locus (Figure 2.5 c, d) with exception of the last exon of the *PID* gene (1.6kb from TSS). The chromatin modification profiles indicate that local chromatin at *HEC1* and *PID* is not controlled by bi-stable epigenetic memory. Furthermore, the presented results for H3K36me3 suggest that this histone modification is not regulated by auxin and is independent of ETT.

Histone acetylation levels typically enrich across actively transcribed gene loci. In contrast to histone methylation, the working mechanism of acetylation is biophysically well understood. Due to its chemical properties, acetylation neutralises the basic charge of the modified lysine. This unfolds the chromatin and presents the underlying DNA to the transcription machinery (Eberharter and Becker, 2002; Pradeepa et al., 2016; Shogren-Knaak et al., 2006). Here, H3K27 acetylation (H3K27ac) was assayed

at the *HEC1* and *PID* loci. H3K27ac levels at both loci are low in untreated wild type gynoecia but significantly increase across both loci after auxin treatment. Moreover, the level of this histone modification increases in the absence of ETT and upon treatment with auxin. In both cases, upon auxin treatment and in *ett*-mutant gynoecia the increase of histone acetylation is especially strong in the promoter region around the ETT promoter binding sites identified earlier (-1.5kb for *HEC1* and -0.45 kb for *PID*). This suggests a role of ETT in deacetylation of its target genes and hence repression of target-gene expression in the absence of auxin (Figure 5e, f).

Discussion

This chapter provides the groundwork needed to elucidate how auxin levels are translated into changes in gene expression of ETT target genes. I identified and established *HEC1* and *PID* as model genes to study non-canonical auxin signalling in more detail. Intriguingly, plants mis-expressing either *PID* or *HEC1* exhibit strong gynoecium defects (Benjamins et al., 2001; Gremski et al., 2007; Schuster et al., 2015) suggesting that tight regulation of their expression is required for proper gynoecium formation. While the up-regulation of *HEC1* and *PID* by auxin in wild type gynoecia is in agreement with the literature (Simonini et al., 2016, Schuster et al., 2015), the constitutive auxin-independent up-regulation in *ett-3* gynoecia suggests a central role of an ETT-mediated non-canonical auxin signalling mechanism in the regulation of *HEC1* and *PID*. To address to what extent this auxin-signalling pathway is independent of the established TIR1/AFB-mediated pathway, examination of *HEC1* and *PID* expression in various higher order TIR1/AFB auxin receptor mutants and a synthetic auxin receptor line demonstrated that the auxin-responsive regulation of both genes in the gynoecium appears independent of the known auxin receptors. In summary, these genetic and pharmacological experiments suggest a direct effect of auxin on the ETT protein and are supported by prior studies (Simonini et al., 2016).

ETT directly binds auxin

In collaboration with the group of Dr. Stefan Kepinski at the University of Leeds, the auxin binding capabilities of ETT were analysed by HSQC-NMR using a 207 amino acid long ETT fragment ($ES^{388-594}$) that has previously been shown to be responsible for auxin sensitivity (Simonini et al., 2018a). In the HSQC spectra, we found that several residues shifted their position in response to the addition of IAA. ^{15}N HSQC spectra can be used to identify residues that interact with the ligand by assigning each peak to a residue in the protein. However, in case of the spectrum acquired for the ETT-fragment there is a large cluster of overlapped peaks around the middle of the spectrum indicating the presence of intrinsically disordered elements in the protein. In such cases the assignment of resonances in the spectra is unfeasible and requires other experiments such as multi-dimensional NMR methods with ^{15}N and ^{13}C-labelled proteins that provide sequential connectivity between residues, enabling sequential assignment (Meyer and Peters, 2003). Unfortunately, due to time limitations and the requirement for additional expert advice, these experiments have not yet been carried out. Nevertheless, the observed shifts show that certain residues are experiencing a changed chemical environment because of IAA-binding and this may include the conformational change of a structural motif within the ETT protein.

ETT shares no sequence homology with either TIR/AFB receptors nor with AUXIN BINDING PROTEIN 1 (ABP1) (Simonini et al., 2016; Simonini et al., 2018a). ABP1 was the first auxin-binding protein identified and long thought to play an important role as an auxin receptor in various aspects of auxin signalling in plant development (Chen et al., 2014; Napier, 1995; Napier et al., 2002; Robert et al., 2010; Tromas et al., 2013; Xu et al., 2014). Whilst the auxin-binding capacity is firmly established, the role of ABP1 in auxin signalling and plant development is currently highly controversial (Gao et al., 2015; Michalko et al., 2015). The lack of sequence homology does not rule out structural similarity between the auxin binding site in ETT and the binding sites in

ABP1 or TIR1/AFB proteins. However, structural comparisons are not possible until the structure of ETT has been revealed. In the first instance, it will be more feasible to solve the structure of the auxin binding $ES^{388-594}$ by multi-dimensional NMR. As ETT is an intrinsically disordered protein it would be challenging to obtain the structure by x-ray crystallography unless a condition is identified in which the ES domain folds into a defined structure, such as through interaction with a protein partner.

We were unable to elucidate the residues of the ETT protein that are involved in IAA binding from the HSQC-NMR spectrum except for a tryptophan at position 505 (W505) that experienced a strong chemical shift upon the addition of auxin. Interestingly, a tryptophan residue was found to be an integral part of the auxin binding site of ABP1 fulfilling the role of the hydrophobic platform required for the auxin interaction (Napier, 2004; Woo et al., 2002). It would be interesting to mutate the W505 residue in $ES^{388-594}$ to test whether this residue is important for the ETT-auxin interaction.

Using WaterLOGSY-NMR and ITC we obtained values for the dissociation constant (K_D) of the ETT-auxin interaction. The experiments gave a K_D of 1.1 mM in WaterLOGSY-NMR and a K_D of 338.6 µM in ITC. One reason for the difference between the K_D values obtained by the two methods is that the signals obtained from measurements are quite weak, which is not uncommon in studies that analyse protein binding to small ligands. Nonetheless, both experiments agree that the ETT-fragment tested binds IAA with low affinity. Whilst Y2H experiments also required high auxin concentrations to dissociate ETT-TF interactions (Simonini et al., 2016), treatments were generally between 50 µM and 100 µM IAA indicating a tenfold higher affinity of these ETT-TF complexes compared to $ES^{388-594}$-IAA binding. Together this may reflect that other domains in the full-length ETT protein contribute to auxin binding. Alternatively, it is possible that the ETT-auxin interaction is stabilised by additional factors, thereby increasing the affinity. For example, these co-factors could be metal

ions required to stabilise ETT-auxin interaction. Analogously, ABP1 requires zinc ions for efficient auxin binding (Woo et al., 2002; Napier, 2004). Another possibility is that certain proteins interact with ETT to stabilise auxin binding thereby increasing the affinity. Stabilising proteins can be context-specific transcriptional regulators, such as IND or RPL or context-independent proteins such as heat-shock proteins (HSPs). Besides their well-known role as chaperone proteins that support protein folding and their role in stress responses in many biological systems, HSPs play an important role in steroid hormone signalling in mammals (Echeverria and Picard, 2010). For instance, physical interaction of HSP90 proteins with steroid hormone receptors (SHR) stabilises the conformation of the SHR to enable efficient hormone binding (Echeverria and Picard, 2010). Due to their high conservation across kingdoms one could imagine a similar function of HSP90s in plants. The *Arabidopsis* genome encodes seven HSP90-proteins four of which localise to the nucleus. *Arabidopsis* HSP90s have mainly been implemented in stress responses and plant plasticity (Sangster et al., 2007; Sangster and Queitsch, 2005). HSP90 single mutants have a wild type appearance, however, RNA-interference (RNAi) lines targeting all four nuclear HSP90s identified a range of different developmental defects (Sangster and Queitsch, 2005). Although its exact role remains unknown, HSP90 proteins were recently shown to play a role in canonical auxin, gibberellic and jasmonic acid signalling under stress conditions, where they affect receptor protein stability (Wang et al., 2016; Zhang et al., 2015). It would be interesting to test if ETT can physically interact with HSP90s and whether ETT-HSP90 interaction can increase auxin-binding efficiency. This should be done by recombinantly producing both proteins in *E. coli* and assessing auxin-binding affinity using ITC.

Collectively, these data suggest that ETT binds IAA directly thus revealing a key molecular aspect of the alternative auxin-signalling pathway. Direct auxin binding by ETT is a feature that is reminiscent of animal hormonal signalling pathways such as

steroid hormone signalling (King et al., 2012; Tsai and O'Malley, 1994). Upon hormone binding by the TF, these pathways characteristically involve extensive chromatin remodelling at their target loci.

Non-canonical auxin signalling involves chromatin remodelling

Examining the effect of auxin on the local chromatin environment at the *HEC1* and *PID* loci indicates that alternative auxin signalling also involves regulation of at least H3K27me3 and H3K27ac chromatin modification.

Although not conclusive, the results suggest that H3K27me3 levels at *HEC1* and *PID* are at least partially regulated in response to auxin. Furthermore, these data show that the chromatin state is mis-regulated in *ett-3* mutants, and therefore support previous findings that ETT represses *PID* at the gynoecium apex during early stages of development, prior to the formation of the ring-shaped auxin maximum that triggers radialization and leads to style formation (Moubayidin and Ostergaard, 2014; Simonini et al., 2016). Accumulation of repressive histone modifications across the gene body, such as those observed at the *HEC1* locus, are a common feature of epigenetically silenced genes. In animals, epigenetic silencing plays an important role in the regulation of the developmentally important HOX genes (Mallo and Alonso, 2013). In plants, FLOWERING LOCUS C (FLC) is a key regulator of flowering time and the *FLC* locus is epigenetically silenced in response to cold during vernalisation (Whittaker and Dean, 2017). During vernalisation H3K27me3 accumulates locally at a nucleation region within the *FLC* gene and spreads across the gene when the temperature increases, leading to silencing of the locus. After its propagation the silenced chromatin state is epigenetically memorised and inherited through cell division (Angel et al., 2011; Berry et al., 2015).

Recent studies have shown that this epigenetic memory system consists of two stable states that are mutually exclusive and self-sustaining (Berry et al., 2015; Yang et al., 2017; Yang et al., 2014). Whilst the H3K27me3 histone modification represents the

repressive state of this bi-stable memory, the active state is characterised by the accumulation of H3K36me3 modifications. These two histone modifications show antagonising profiles during vernalisation (Yang et al., 2017; Yang et al., 2014). Testing the opposing behaviour of these two chromatin modifications at *HEC1* and *PID* loci showed that that only H3K27me3 levels but not H3K36me3 levels were auxin responsive and ETT dependent.

The deposition of H3K27me3 modifications is mediated by the polycomb repressive complex 2 (PRC2), a protein complex that is highly conserved in eukaryotes, and whose subunits have diverged in plants. The *Arabidopsis* genome encodes three copies of this complex. Although PRC2 is well-known for its role in epigenetic silencing, many PRC2 target genes are under the control of gene regulatory networks, and do not therefore require PRC2-mediated maintenance of epigenetic memory. This raises questions about the role of PRC2 in the regulation of these genes. It has been proposed, that PRC2 proteins collaborate with specific transcription factors in the repression of target genes, rather than being a purely epigenetic regulator (Ringrose, 2007). Furthermore, it has been shown that PRC2 filters transcriptional noise and may therefore act to regulate short-term rather than long-term memory in gene regulatory networks, thereby increasing robustness through this chromatin-based noise filtering (Stoeger et al., 2016).

Recently a model has been proposed that integrates bi-stable cis-acting epigenetic memory and trans-acting gene regulation in a chromatin environment (Berry et al., 2017; Steffen and Ringrose, 2014). The fundamental difference between these two regulatory modes is that the cis-regulation is digital, thus either active or repressive, whereas trans-regulators act in an analogue fashion, where the transcriptional output depends continuously on the concentration of the regulator. Cis-acting regulation includes binding motifs encoded on the DNA, DNA methylation and the chromatin environment, while trans-regulators are proteins e.g. transcription factors or

chromatin-modifying enzymes, such as histone methylases/demethylases or acetylases/deacetylases (Berry et al., 2017).

Based on these models, it was proposed that targets of PRC2 are controlled by the digital chromatin state and can be fine-tuned continuously by the activity of trans-regulators. The extent of gene expression can be influenced depending on trans-regulator activity. Thus, there is an upper threshold of trans-activator activity above which chromatin-based repression cannot be established, a lower threshold below which gene repression is guaranteed, and an intermediate level of trans-regulator activity at which the chromatin state contributes to determining gene expression. Following this model, epigenetically silenced genes such as *FLC* experience low trans-activator activity after vernalisation, and the silenced state is maintained by PRC2 activity (Berry et al., 2017). In contrast, genes regulated by gene regulatory networks are in an intermediate state of trans-activation. This means that activating modifications compete with repressive modifications, like a tug of war, working in *cis*, but can be fine-tuned by local trans-regulator abundance and composition. Together data presented in this chapter suggest that expression of *HEC1* and *PID* and likely most auxin-responsive genes are controlled by gene regulatory networks rather than epigenetic gene silencing. Moreover, it appears that ETT plays an active role in regulation of H3K27me3 status.

Levels of H3K27 acetylation, a histone modification associated with active transcription, increased in wild type gynoecia upon treatment with auxin and were constitutively high in *ett*-mutant gynoecia. This occurred in the regions of the *PID* and *HEC1* promoters where ETT directly associates (as shown in ChIP experiments). This indicates that ETT may mediate histone deacetylation when auxin concentrations are low, and that the deacetylase activity is lost under high auxin conditions. The observation that there were no further increases in acetylation in the *ett-3* mutant upon treatment with auxin implies that histone deacetylation of *HEC1* and *PID*

depends on ETT. Finally, by correlating gene expression data from *PID* and *HEC1* in young wild type and *ett-3* gynoecia with the levels of repressing and activating chromatin modifications, I have shown that both *HEC1* and *PID* are significantly up-regulated by auxin in wild type gynoecia and constitutively up-regulated in *ett-3*, suggesting that chromatin dynamics are translated into transcriptional outputs.

Concluding remarks

The results presented in this chapter support the hypothesis that the non-canonical auxin signalling pathway is fundamentally different from the canonical TIR1/AFB-mediated auxin-signalling pathway as biochemical data show that ETT itself likely acts as an auxin receptor. Thus, non-canonical auxin signalling is independent of the canonical auxin recognition machinery. Direct hormone-ligand binding by a transcription factor is a feature that is reminiscent of animal hormone-signalling pathways such as Steroid/Thyroid Hormone and Wnt/ß-catenin pathways (Gammons and Bienz, 2018; King et al., 2012; Tsai and O'Malley, 1994). Despite identifying auxin binding, due to low resolution it was not possible to determine which residues of ETT interact with auxin using the data obtained in this study.

Future work will focus on understanding different aspects concerning the structural basis of the ETT-auxin interaction. This involves understanding the mechanistic and structural similarities between non-canonical auxin signalling and animal hormone signalling, requires knowledge about the kinetics of the ETT-auxin interaction, and further information on how the conformation of ETT is affected by auxin binding. These aspects will be studied using multi-dimensional NMR and X-ray crystallography to identify the auxin-binding residues and reveal the structural dynamics upon auxin binding. Mutant analysis using HSQC-NMR and ITC will then determine the contribution of each residue to auxin binding.

Additionally, future work should also focus on the potential of additional factors such as interacting transcription factors or chaperone proteins in stabilising the ETT-auxin interaction, and thereby increasing the affinity. ETT-protein interactions and their effect on auxin affinity can be studied initially by ITC or Surface Plasmon Resonance (SPR) and should ultimately provide near-atomic insight using NMR and crystallography.

Due to the limitations described above in terms of the disordered nature of the ETT protein, a more detailed analysis of auxin binding by ETT and the further elucidation of ETT-auxin structural dynamics are beyond the scope of this thesis. In the following chapters I will instead focus on a different aspect of non-canonical auxin signalling. The results presented in this chapter underline a role of ETT in the regulation of auxin-sensitive gene expression through the mediation of chromatin modification. However, it remains unclear how ETT can facilitate these effects since ETT has not been shown to have any direct enzymatic activity to modify histones. In Chapter 3 and Chapter 4, I will evaluate the capacity of ETT to interact with multi-protein complexes to recruit chromatin regulators to its target loci. I will examine the direct effect of these interactions on the expression of *HEC1* and *PID,* and where appropriate the local chromatin environment. Using mutant analysis, I will elucidate whether the interacting proteins have a role in gynoecium development.

In conclusion, the results presented in this chapter are a starting point to gain detailed understanding of non-canonical auxin signalling. While this thesis will focus on elucidating the mechanisms that link chromatin dynamics, auxin signalling, and gene regulation mediated by an alternative auxin-signalling pathway, the results presented here also open the avenue for a detailed structural analysis of ETT's role as a potential auxin receptor.

Materials and Methods

Plant materials, treatments and growth conditions

Seeds were surface sterilised, sown on MS media plates with 0.8% agar and 1% sucrose, and stratified at 4°C in the dark for 2 days. Plants were pre-grown for 7 days under long-day conditions (16h light/8h dark) at 22°C. After 7 days plants were transferred to soil (John Innes Centre in-house compost "Arabidopsis F2 mix with insecticide") and grown in a controlled environment room under long day conditions (16h light/8h dark; 22°C). All mutations were in the *Col-0* background. Mutant alleles and transgenic lines described before include e*tt-3* (Sessions et al., 1997), *pETT:ETT-GFP* in *ett-3* (Simonini et al., 2016), *pTIR1:ccvTIR1* in *tir1-1 afb2-3* (Uchida et al., 2018), *tir1-1 afb2-3* and *tir1-1 afb2-3 afb3-4* (Parry et al., 2009).

For both expression and ChIP analysis, auxin treatments were applied by spraying bolting inflorescences with a solution containing 100 µM IAA (Sigma) or cvxIAA and 0.015% Silwet L-77 (De Sangosse Ltd.). Treated samples were returned to the growth room and incubated for two hours. Prof. Keiko Torii (Department of Biology, University of Washington, USA) and Prof. Shinya Hagihara (Department of Chemistry, Nagoya University, Japan) kindly provided the *pTIR1:ccvTIR1* line and cvxIAA ligand.

RNA extraction and cDNA synthesis

RNA was extracted from 100 mg young gynoecia using the RNeasy plant mini kit (Qiagen) according to the manufacturer's instructions. To remove genomic DNA, the on-column RNase free DNase kit (Qiagen) was used according to the manufacturer's instructions. RNA was eluted in 30 µL RNase-free water. Using the SuperScript™ IV First-Strand Synthesis kit (ThermoFisher), cDNA was synthesised from 1 µg of total RNA according to the manufacturer's instructions.

Quantitative Real Time PCR (qPCR)

Before use all qPCR primers were tested for their efficiency and specificity. The amplification efficiency of primers was tested using a cDNA dilution series (1/4 to 1/65536). The specificity of primers was confirmed by analysing the melting curves (65°C to 95°C). For the quantification of transcript levels, qPCRs were set up in 96-well or 384-well plates and were performed using a CFX96 or LC480 thermal cycler (Bio-Rad). Final reaction volumes were 10 µL (5 µL SYBR Green JumpStart Taq ReadyMix (Sigma) 0.25 µl primer mix (containing 10 µM forward primer and 10 µM reverse primer), 4 µl 1:20 diluted cDNA). The qPCR programs used the following conditions: 95 °C for 2 min followed by 40 cycles at 95°C for 10 s, 60 °C for 10 s and 72 °C for 30 s. Relative expression values were determined using the $2^{-\Delta\Delta Ct}$ method (Livak and Schmittgen, 2001). Data were normalised to *POLYUBIQUITIN 10* (*UBQ10*/AT4G05320) expression. The primers used for qPCR in this chapter can be found in Appendix I Table 2.

Scanning Electron Microscopy

Inflorescences were collected, vacuum infiltrated in fixative (3.7% formaldehyde, 3% acetic acid and 50% ethanol) for 10 min and fixed for 16h at room temperature on a rocking platform. After removing the fixative, tissue was then washed three times for 30 min in 70% ethanol, and subsequently dehydrated using a series of washes in 70%, 80%, 90%, 95% and 100% ethanol, incubating each ethanol concentration for 30 min on a rocking platform. Next, samples were washed three times in 100% dry ethanol and critical point dried using a Leica CPD300. Gynoecia were dissected, coated with gold, using an Agar high resolution sputter coater, and imaged using a Zeiss Supra 55VP Field Emission Scanning Electron Microscope (3kV acceleration voltage).

Yeast two-hybrid interaction assay

The constructs containing the ES (pGBKT7), IND (pGADT7) and RPL (pGADT7) proteins were published previously (Simonini et al., 2016; Simonini et al., 2018a). Using the co-transformation method (Egea-Cortines et al., 1999) the generated constructs were transformed into the AH109 strain (Clontech). Transformations were selected on YSD medium lacking Tryptophan (W) and Leucine (L) at 28°C for 3-4 days. Transformed yeast cells were serially diluted (10^0, 10^1, 10^2 and 10^3) and dotted on YSD medium lacking Tryptophan (W), Leucine (L), Adenine (A) and Histidine (H) to test for interaction. To test for auxin sensitivity, 100 µM was supplemented to the growth medium.

Protein production

The ES domain, $ES^{388-594}$, protein was isotopically labelled in preparation for NMR analysis. The ES domain was expressed as a fusion protein with a 6x Histidine tag (Simonini et al., 2018a) in minimal medium with ^{15}N ammonium chloride. The ^{15}N isotope labelling of the expressed protein involved a 125-fold dilution of cell culture in enriched growth medium into minimal medium with ^{15}N ammonium chloride and grown for 16 hours (37 ˚C / 200 rpm), followed by a further 40-fold dilution into minimal medium for the final period of cell growth and protein expression (induced with L-arabinose 0.2 % w/v / 18 ˚C / 200 rpm and grown for a further 12 hours). Cells were harvested by centrifugation (11,000 g for 20 min at 4 °C) and the pellet frozen at −70 °C. The wet cell pellet was resuspended in lysis buffer (50 mM Tris-HCl, pH 8.0; 10 mM EDTA; 5% (v/v) Glycerol; 1mM DTT; 50 mM NaCl; 1x protease inhibitor (Roche); 0.2% (w/v) Sodium deoxycholate (NaDOC); 200 µg/mL lysozyme) and lysed by sonication (10 microns, 30 seconds on, 30 seconds off, 3 cycles). The sonicated cell suspension was centrifuged (11,000 g for 20 min at 4 °C). The fusion protein was isolated from soluble cell lysate by Co-NTA affinity chromatography with two His-Trap 1 mL TALON Crude columns (GE Healthcare Life Sciences, 28953766).

Chromatography buffers contained sodium phosphate 20 mM pH 8.0, NaCl 500 mM and either no-imidazole (Buffer A) or 500 mM imidazole (Elution Buffer) for wash and elution buffers respectively. Most of the non-specifically bound protein was removed by passing 20 mL of Buffer A through the columns. The protein eluted on a gradient of increasing imidazole concentration of up to 30% Elution Buffer over 20 mL and concentrated to 2mL using Amicon Ultra -15 centrifugal filters with a 10kDa cut-off (Millipore (UK) Ltd.).

For ITC, the fusion protein was purified from inclusion bodies. The $ES^{388-594}$ protein was grown in LB medium, cells harvested and lysed as described above. After centrifugation of the sonicated cell suspension, the pellet was resuspended and washed in Wash Buffer (50 mM Tris-HCl, pH 8.0; 0.1 mM EDTA; 5% (v/v) Glycerol; 0.1 mM DTT; 50 mM NaCl; 2% (w/v) NaDOC) for 1 hour at 4°C followed by centrifugation (11,000 g for 20 min at 4 °C). The resulting pellet was again washed in Wash Buffer and centrifuged as described previously. The pellet was resuspended in 20mL of Solubilisation Buffer (50 mM Tris-HCl, pH 8.0; 0.1 mM EDTA; 5% (v/v) Glycerol; 0.1 mM DTT; 50 mM NaCl; 0.25% Sarkosyl (N-Lauroyl sarcosine) and stirred at 4°C for 1h. Subsequently the resuspension was dialysed overnight in 2L Dialysis Buffer (50 mM Tris-HCl, pH 8.0; 0.1 mM EDTA; 5% (v/v) Glycerol; 0.1 mM DTT; 50 mM NaCl). The Dialysis Buffer was exchanged for fresh Dialysis Buffer after at least 2 hours of dialysis. After dialysis the lysate was centrifuged (11,000 g for 20 min at 4 °C). The resulting supernatant contained the required protein which was concentrated to 2 mL using Amicon Ultra -15 centrifugal filters with a 10kDa cut-off (Millipore (UK) Ltd.) and further purified using size exclusion chromatography. The protein was eluted in Buffer A and concentrated to 2 mL as previously described.

Circular Dichroism Spectroscopy (CD)

CD was carried out on a Chirascan Plus Spectrophotometer (Applied Photophysics) which uses a Xenon light source. The far-UV CD spectrum (from 190 nm to 260 nm)

of the $ES^{388-594}$ protein (10 µM) in a 10 mM Sodium Phosphate buffer was scanned ten times at 20 °C in a 1 mm path-length cuvette for two independent replicates (independent purifications). The baseline was subtracted and the values were plotted (expressed in millidegrees).

NMR methods

NMR experiments were carried out at the NMR facility in the Astbury Centre (Faculty of Biological Sciences, University of Leeds, UK) using the 950 MHz and 600 MHz spectrometers (Bruker Ascend Aeon). The ES domain, $ES^{388-594}$, protein was analysed by NMR at 5°C under reducing conditions (DTT 10 mM), buffered at pH 8.0 (Tris 20 mM). The ^{1}H-^{15}N HSQC and WaterLOGSY (Dalvit et al., 2001) experiments were performed following the parameters described in Table 1. The WaterLOGSY experiment used a 15 ms 5% truncated Gaussian inversion pulse at a mixing time of 1.5 s and was carried out by Dr. Sigurd Ramans Harborough (Kepinski Group, Centre for Plant Sciences, Faculty of Biological Sciences, University of Leeds, Leeds, UK).

Table 2. 1: Parameters for the NMR experiments. HSQC experiments to study the $ES^{388-594}$-auxin interaction were performed at 5˚C and 950 MHz, 3mm TCI probe, Bruker. WaterLOGSY experiments were performed at 5˚C and 600 MHz, QCI-P quadruple resonance probe, Bruker.

Experiment	Recycling Delays (S)	Scans	Nuclei		Spectral width (Hz)		Number of complex points	
			t1	t2	t1	t2	t1	t2
HSQC	1	56	^{15}N	^{1}H	2888.6	15243.9	256	2048
waterLOGSY	2.5	512	^{1}H		9578.544		16384	

Isothermal titration calorimetry (ITC)

ITC was carried out on a MicroCal PEAQ-ITC (Malvern) at 25 °C in a Buffer A (sodium phosphate 20 mM, pH 8.0; NaCl 500 mM). Ligand (2 mM IAA) was injected (19 × 4.0 µl) at 150-s intervals into the stirred (500 rpm) calorimeter cell (volume 270 µl) containing 50 µM $ES^{388-594}$ protein. Titration of Buffer A into 50 µM $ES^{388-594}$ protein

and IAA (2 mM) into Buffer A served as negative controls. Measurements of the binding affinity of all the titration data were analysed using the MicroCal Software (Malvern).

Chromatin Immunoprecipitation (ChIP) qPCR

All ChIP experiments were carried out in triplicate on inflorescence tissue as described previously described (Yang et al., 2014; Questa et al., 2016) with minor modifications:

Inflorescence tissue was vacuum infiltrated in PBS with 1% formaldehyde for 3 times 10 min, to cross-link protein-DNA interactions. Formaldehyde was quenched by adding glycine to a final concentration of 125 mM and vacuum was applied for another 5 min. Plants were then rinsed with water and ground in liquid nitrogen. To extract the nuclei, samples were resuspended in 25 mL Honda Buffer (20 mM HEPES-KOH pH 7.4, 0.44 M sucrose, 1.25% (w/v) Ficoll, 2.5% (w/v) Dextran T40, 10 mM $MgCl_2$, 0.5% Triton X-100, 5 mM DTT, cOmplete protease inhibitor cocktail (Roche)) , filtered through two layers of Miracloth, and centrifuged at 3000 × g for 7 min (4°C) . Nuclear pellets were washed three times with 1 mL of Honda buffer, with a 3 min spin at 3000 x g after each wash.

Nuclear pellets were resuspended in nuclei lysis buffer (50 mM Tris-HCl pH 8.0, 10 mM EDTA, 1.0% SDS, cOmplete protease inhibitor cocktail (Roche)) and sonicated for 3 times 5 min on medium strength using a Bioruptor water bath sonicator (Diagenode) using a 30 sec ON/OFF cycle, to fragment the chromatin. Lysates were cleared by centrifugation at 16 000 x g for 10 minutes (4°C). To reduce the concentration of SDS, the supernatant was diluted 10-fold with ChIP dilution buffer (1.1% Triton X-100, 1.2 mM EDTA, 16.7 mM Tris-HCl pH 8.0, 167 mM NaCl). A 50 µL aliquot of each sample was taken as an input sample.

All following incubations and washes were performed at 4°C on a rotating mixer in 2 mL DNA LoBind tubes (Eppendorf). For IP, the appropriate antibody was conjugated

to pre-washed Pierce Protein G magnetic beads (ThermoFisher, 88847, Lot: SI253639), for 1 hour and antibody-bead complexes were washed for 3 times 5 min in low salt ChIP wash buffer (20 mM Tris-HCl pH 8.0, 2 mM EDTA, 150 mM NaCl, 0.1% (w/v) SDS, 1.0% (w/v) Triton X-100). Samples were then incubated with antibody conjugated beads overnight and then washed sequentially 3 times for 5 min in low salt ChIP wash buffer, 3 times for 5 min high salt ChIP wash buffer (20 mM Tris-HCl pH 8.0, 2 mM EDTA, 500 mM NaCl, 0.1% (w/v) SDS, 1.0% Triton X-100) and 3 times for 5 min TE ChIP wash buffer (10 mM Tris-HCl pH 8.0, 1 mM EDTA, 1.0% NP-40, 1.0% (w/v) sodium deoxycholate).

The final wash was 1 time 5 min in TE buffer (10 mM Tris-HCl pH 8.0, 1 mM EDTA) containing 0.02% Triton X-100. After removing all residual buffer 100 µL of freshly-prepared 10% (w/v) Chelex resin (Bio-Rad) was added to the beads. The cross-linking of protein and DNA was reversed by incubating on shaker (1400rpm) at 65°C for at least 4 hours for all samples (including the input samples). Following reverse cross-linking, proteins were digested with 40 µg of proteinase K (Roche) for 1 hour at 45°C. Proteinase K was inactivated at 95°C for 10 min. Next, DNA was extracted from the samples were extracted using phenol/chloroform/isoamyl alcohol pH 8.0 (25:24:1, Sigma) and ethanol precipitated. DNA pellets were air-dried and resuspended in 100 µL amount of RNase free water (Qiagen).

ChIP performed on the *pETT:ETT:GFP* line using 5 g (fresh weight) of inflorescence tissue. IP was conducted using the anti-GFP antibody (Roche, 11814460001, Lot: 19958500) and Pierce Protein G magnetic beads (ThermoFisher, 88847, Lot: SI253639) were used for IP.

Histone methylation and acetylation ChIP experiments were carried out using 3 g auxin-treated or untreated *Col-0* or *ett-3* inflorescence tissue. The antibodies used for IP were anti-H3K27me3 (Millipore, 07-449, Lot: 2736613, anti-H3K36me3 (Abcam, ab9050, Lot: GR310541-1), anti-H3K27ac antibodies (Abcam, ab4729, Lot:

GR3231937-1) and anti-H3 (Abcam, ab1791, Lot: GR310541-1). All antibodies were validated by the manufacturers.

In all ChIP experiments, DNA enrichment was quantified using quantitative PCR (qPCR) with the appropriate primers (Appendix ITable 2) as described above with minor changes: Final reaction volumes were 10 µL (5 µL SYBR Green JumpStart Taq ReadyMix (Sigma) 0.25 µl primer mix (containing 10 µM forward primer and 10 µM reverse primer), 4 µl 1:20 diluted ChIP-DNA). The qPCR programs used the following conditions: 95 °C for 2 min followed by 60 cycles at 95°C for 10 s, 60 °C for 10 s and 72 °C for 30 s.

For ChIP performed on the *pETT:ETT:GFP* line data were normalised to the input sample as described previously (Schiessl et al., 2014). For histone methylation and acetylation ChIP experiments, the results were presented as described elsewhere (Yang et al., 2014; Questa et al., 2016). In case of H3K27ac and H3K36me3, *ACTIN* was used as an internal control and the data represented as ratio of (H3K27ac or H3K36me3 at *HEC1* or *PID* divided by H3 at *HEC1or PID*) to H3K27ac or H3K36me3 at *ACT* divided by H3 at *ACT*), while in case of H3K27me3, *SHOOT MERISTEMLESS* (*STM*) was used as an internal control and the data represented as ratio of (H3K27me3 at *HEC1* or *PID* divided by H3 at *HEC1or PID*) to H3K27me3 at *STM* divided by H3 at *STM*).

Statistical analyses and replication

In all graphs, error bars represent the standard deviation of the mean for all numerical values. qPCR and ChIP experiments have been carried out at least in triplicate. The data presented here show an average of three replicates. For qPCR data were analysed using one-way ANOVA with post-hoc Tukey multiple comparison test. $ChIP_{qPCR}$ data were analysed using two-way ANOVA with post hoc Bonferroni multiple comparison test. Statistical tests were carried out using GraphPad Prism Version 5.04 (La Jolla California USA, www.graphpad.com).

Chapter 3

The ETT-interactome reveals interaction with chromatin modifying complexes

Introduction

In the previous chapter, I showed that non-canonical auxin signalling involves direct binding of auxin to an Auxin Response Factor, called ETTIN (ETT, ARF3). This pathway, therefore, appears reminiscent of animal hormone signalling in that it affects the activity of the hormone-sensitive unit towards regulation of target genes. While the work presented in Chapter 2 also found that auxin affects the chromatin environment at ETT-target genes and that this depends on ETT, it remains unclear how ETT can facilitate these effects. In this chapter, I will evaluate the capacity of ETT to interact with other proteins to bring chromatin regulators to its target loci.

Throughout an organism's life cycle, the temporal and spatial regulation of gene expression through activation or repression is essential for development, survival and reproduction. Despite tremendous efforts towards understanding how developmental programs are coordinated within cells and across tissues, the exact mechanisms determining spatial and temporal regulation of key developmental genes is yet to be elucidated. This spatial-temporal control of gene expression depends on external cues (e.g. temperature, nutrients, pests), intrinsic signals (e.g. hormones or age) or a combination of several intrinsic and external signals. Gene expression also depends on the local chromatin environment at each locus. Histone modifications shape the chromatin environment at genetic loci. Numerous different histone modifications have been identified but generally the composition of histone modifications determines whether the nucleosome occupancy at a certain locus is high or low. High nucleosome occupancy represses underlying genes by decreasing the accessibility of cis-regulatory elements for transcription factors (Kouzarides, 2007; Li et al., 2007). Although, the essential role of local chromatin environment in gene expression regulation is well-known, a critical question is how the deposition of histone modifications is regulated.

In plants, the composition and regulation of the local chromatin environment has been well-studied for a gene called *FLOWERING LOCUS C* (*FLC*). *FLC* encodes for a regulator of flowering time and has been established as a model gene to understand the mechanisms by which an (environmental) signal can be integrated into a gene expression output. Within the regulatory pathways of flowering, FLC acts as a repressor that regulates the vegetative to floral transition in response to prolonged cold exposure (also called vernalization). Vernalization induces expression of FLC antisense transcripts (called *COOLAIR*), that act as long noncoding RNAs (lncRNAs), and *VERNALIZATION INSENSITIVE 3* (*VIN3*), a plant homeodomain protein. *COOLAIR* facilitates the transcriptional repression of *FLC* while VIN3 associates with Polycomb Repressive Complex 2 (PRC2) to epigenetically silence the *FLC* locus (Angel et al., 2011; Bastow et al., 2004; Csorba et al., 2014; De Lucia et al., 2008). PRC2 silences genes by depositing H3K27me3 histone modifications at the nucleosomes of the target locus (Gendall et al., 2001). In the context of *FLC* silencing, PRC2 is recruited to a region within the first intron of the *FLC* gene, to a so-called nucleation region where H3K27me3 initially accumulates, and subsequently enforces a positive feedback loop to spread H3K27me3 across the whole gene locus (Angel et al., 2011; Yang et al., 2017). The mechanism by which PRC2 is recruited to this nucleation region has recently been elucidated. Central to this mechanism is a pair of RY cis-elements (TGCATG) within the region that facilitates the binding of the B3-transcription factor VIVIPAROUS1/ABI3-LIKE 1 (VAL1). By binding the RY-elements, VAL1 acts as an interaction platform to bring various histone modifying complexes to *FLC*. These complexes include histone deacetylases to shut down transcription and PRC2 to epigenetically silence the locus (Questa et al., 2016). Together, the studies on *FLC* highlight the many layers of regulation that are necessary for the correct integration of signals to produce an appropriate gene expression output. Most importantly, this example shows how the individual components; cis-elements, chromatin regulators, histone modifications and transcription factors; do not act in

isolation but collaborate with each other and affect each other's activity and abundance to regulate target loci.

Analogous to cold, the signal during vernalization, auxin is the signal in almost every aspect of plant development. Like cold affecting chromatin environment at the *FLC* locus, auxin affects the accumulation of the repressing and activating histone modifications (H3K27me3 and H3K27Ac respectively) at the genomic loci of two auxin responsive genes, *HECATE1* (*HEC1*) and *PINOID* (*PID*) (Chapter 2). Previously, these two genes have been identified as direct targets of ETT (Chapter 2; Simonini et al., 2016; Simonini et al., 2017). Since ETT does not have chromatin modifying activity itself, I hypothesise that during auxin responsive regulation ETT may act as an interaction platform to bring the activity of various histone modifying complexes to its target sites. Consequently, it is crucial to evaluate ETT's potential for physical interaction with histone modifying complexes. The post-translational modification of histones is an enzymatic process that in isolation cannot confer spatio-temporal information or locus specificity, yet the chromatin environment is crucial for the proper regulation of gene expression. This spatial-temporal as well as the genome-locus specificity is expected to be provided by transcription factors such as VAL1 at *FLC* during vernalisation. Based on the resemblance of VAL1 and ETT (both B3-type TFs), I therefore hypothesise that there will be a substantial overlap between the chromatin modifying complexes that interact with ETT during auxin responses, and those that interact with VAL1 during vernalization.

Several screens for protein-protein interactions between ARFs and partner proteins have been carried out, however, most studies tried to tackle specific developmental questions and therefore focused on ARF-TF interactions (Oh et al., 2014; Shin et al., 2007; Simonini et al., 2017; Simonini et al., 2016; Varaud et al., 2011). Few protein-protein interaction screens have been carried out to find TFs that interact with chromatin modifiers (Causier et al., 2012; Causier et al., 2014; Efroni et al., 2013; Wu

et al., 2015). Even though ETT was not identified in these screens, several other ARFs have been shown to interact with TOPLESS, a co-repressor that forms complexes with Histone deacetylases (HDACs), and the SWITCH/SUCROSE NONFERMENTING (SWI/SNF) family of chromatin remodellers (Causier et al., 2012; Wu et al., 2015). Moreover, the interaction of MONOPTEROS (MP/ARF5) with SWI/SNF complexes was implemented in flower primordium cell fate acquisition (Wu et al., 2015). Nevertheless, there is a substantial gap in knowledge concerning protein-protein interactions across ARFs in general, and particularly concerning ARF-chromatin modifier interactions.

In this chapter, I aim to overcome this knowledge gap by screening a Yeast-two-Hybrid (Y2H) library that represents the complete *Arabidopsis* inflorescence proteome to identify proteins that interact with ETT (Costa et al., 2013). I have shown that this auxin-sensitivity is independent of the known auxin receptors and that ETT senses auxin through direct auxin-binding. I hypothesise that auxin binding leads to a conformational change of the ETT protein disrupting protein-protein interactions. Therefore, after an initial screen, candidates were short listed based on their known roles in hormone signalling and chromatin regulation. After the validation of interactions by Y2H, their significance for the ETT-mediated non-canonical auxin signalling mechanism was evaluated by systematically testing the auxin sensitivity of each interaction. Using expression and mutant analysis, the candidate's roles in gynoecium development and the regulation of *HEC1* and *PID* was further examined. Here, I present the results of this Y2H library screen and the subsequent evaluation. These results provide a stepping stone for more systematic in-depth analysis of the link between auxin signalling and its effect on the local chromatin environment.

Results

A yeast-two-hybrid library screen revealed that ETT can interact with components of chromatin modifying complexes

ETT contributes to the regulation of chromatin dynamics (Chapter 2). It is therefore likely that ETT recruits' components of chromatin-modifying protein complexes by means of protein-protein interaction to ETT-target genes. To test this, an unbiased Y2H library representing the proteome of *Arabidopsis* inflorescence tissue was screened using ETT as bait (Costa et al., 2013). After selection, 355 colonies representing candidate proteins for ETT interaction were identified by sequencing (Appendix II Table 1). Due to ETT's nuclear localisation as a transcription factor, 60 candidates annotated as nuclear proteins were studied in more detail. After a pre-selection process that involved a literature study identifying proteins involved in chromosome organisation, chromatin modification, gene regulation, transcriptional regulation or hormone signalling, a total of 19 proteins were selected as candidate interactors (Table 3.1). These candidates were cloned from cDNA into pGBKT7, and their interaction with ETT was confirmed by Y2H using co-transformation. It appeared that ten of the pre-selected candidates indeed interact with ETT while five were identified as false positives and four were found to be auto-activating (Figure 3.1). Among confirmed ETT interactors, four proteins were transcription factors while seven proteins were otherwise associated with different aspects of transcriptional regulation.

TEOSINTE BRANCHED, CYCLOIDEA AND PCF 14 (TCP14) and POPCORN (PCN) are two bHLH transcription factors that interact with ETT. Both proteins have previously been described for their role in auxin homeostasis and plant development (Kieffer et al., 2011; Xiang et al., 2011). Another ETT-interacting protein is DWARF AND DELAYED FLOWERING (DDF1), a member of the DREB subfamily A-1 of

ERF/AP2 transcription factor family. DDF1 has been reported to regulate GA biosynthesis in response to abiotic stresses (Magome et al., 2008).

Table 3. 1: Comprehensive summary of candidate ETT interactors and their functions.

Gene	Description
AGO1	ARGONAUTE 1; involved in microRNA and siRNA-mediated DNA-methylation (Baumberger and Baulcombe, 2005)
AGO4	ARGONAUTE 4; involved in siRNA mediated gene silencing (Zilberman et al., 2004)
AP2	APELATA 2; transcription factor; floral homeotic gene (Drews et al., 1991)
BRM	BRAHMA; ATPase subunit of the multiprotein SWI/SNF complex that acts in nucleosome; controls shoot development and flowering. Activates flower homeotic genes (Han et al., 2015)
CKH1	CYTOKININ HYPERSENSITIVE 1; One of two copies of the TBP-associated factor TAF12; Cytokinin hypersensitive (Kubo et al., 2011)
COL5	CONSTANTS LIKE 5;Transcription factor of unknown function involved in flowering time and flower development (Robson et al., 2001)
DDF1	DWARF AND DELAYED FOLWERING 1; transcription factor; involved in GA-biosynthesis and perception (Magome et al., 2008)
DEK3	DEK-DOMAIN CONTAINING PROTEIN 3; binds histones H3 and H4 and contributes to modulation of chromatin structure and function (Waidmann et al., 2014)
HAT3	HOMEOBOX-LEUCINE ZIPPER PROTEIN3; transcription factor; involved in leaf development, modulation of hormone response and shade avoidance (Bou-Torrent et al., 2012)

JAI1	JOASMONATE INSENSITIVE 1; transcription factor; involved in jasmonic acid (JA) signalling in plant development and defence (Dombrecht et al., 2007)
NRPB6B	non-catalytic subunit of nuclear DNA-dependent RNA polymerases II and V (Ream et al., 2009)
PBRP	PLANT-SPECIFIC TFIIB-RELATED PROTEIN; plant-specific homolog of the general transcription factor TFIIB (Cavel et al., 2011)
PCN	POPCORN; transcription factor; involved in auxin signalling and SAM/RAM maintenance (Xiang et al., 2011)
RAP2.12	RELATED TO AP2 12; transcription factor; involved in root development and ethylene signalling, response to hypoxia and auxin (Eysholdt-Derzsó and Sauter, 2017)
SAP18	SIN3 ASSOCIATED PROTEIN 18; part if SIN3 containing complexes, involved in transcriptional repression through recruitment of HDA19 (Zhang et al., 1997)
TAF6	TBP-associated factor TAF6; part of the basal transcription machinery (Lago et al., 2005)
TCP14	TEOSINTE BRANCHED, CYCLOIDEA AND PCF 14; transcription factor; involved in gynoecium development and auxin-cytokinin homeostasis (Kieffer et al., 2011)
TPL	TOPLESS; Together with the TOPLESS-RELATED PROTEINS (TPRs), it is thought to be involved in transcriptional repression (Long et al., 2006)
VRN2	REDUCED VERNALIZATION RESPONSE 2, Histone methyltransferase, member of PRC2 complexes (Gendall et al., 2001)

Since the aim of the Y2H library screen was to identify interactions between ETT and proteins that are associated with chromatin modifying complexes, the transcription-factor interactions were not analysed any further throughout this study.

In contrast, the other six proteins identified were associated with the general transcriptional machinery (TAF6), chromosome architecture (DEK3) or were directly associated with chromatin dynamics and gene expression regulation (BRM, SAP18, TPL and VRN2).

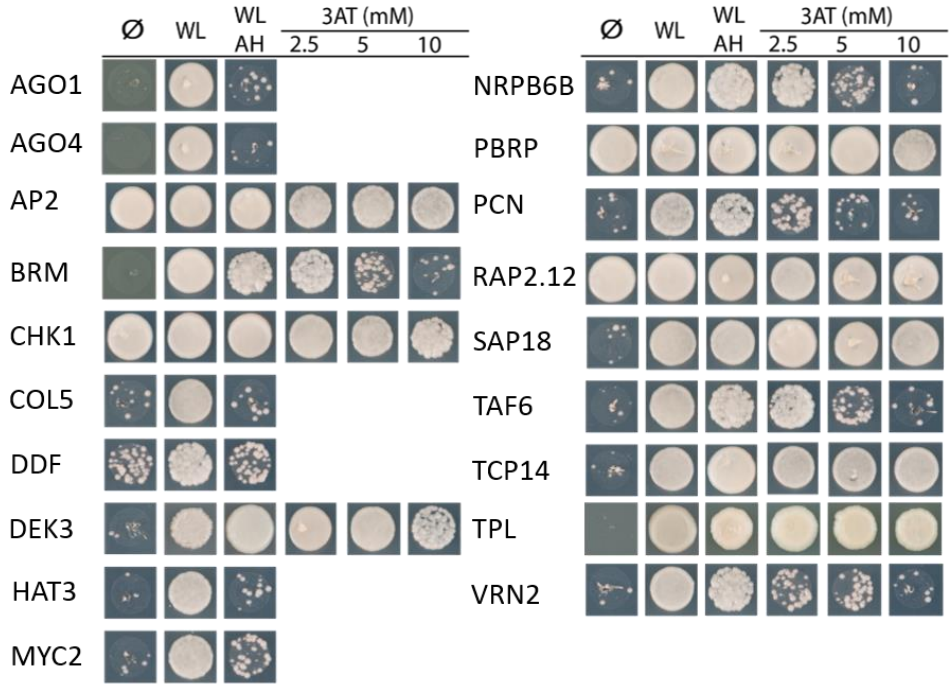

Figure 3. 1: Y2H co-transformation validates interaction of ETT with numerous candidates. Ø indicates the empty vector control (growth on the Ø plates indicates autoactivation). WL indicates that the grow medium lacks Tryptophan (W) and Leucin (L) to select for positive transformation. WLAH indicates that the growth medium lacks Tryptophan (W), Leucine (L) Adenine (A) and Histidine (H) to test for interaction. To examine interaction strength 3-amino-1, 2, 4-triazole (3AT) was added at different concentration to WLAH medium.

BRM is an ATPase subunit of the chromatin remodelling SWITCH/SUCROSE NONFERMENTING (SWI/SNF) complex. SWI/SNF complexes were first discovered in yeast for their capability to alter the positioning of nucleosomes along DNA (Whitehouse et al., 1999) and are evolutionarily conserved from yeast to humans and in plants (Flaus et al., 2006; Han et al., 2015; Kadoch and Crabtree, 2015). studies in plants have been key in understanding the biological roles of chromatin re-modellers

in growth, development and stress responses (Efroni et al., 2013; Vercruyssen et al., 2014; Wu et al., 2012; Wu et al., 2015).

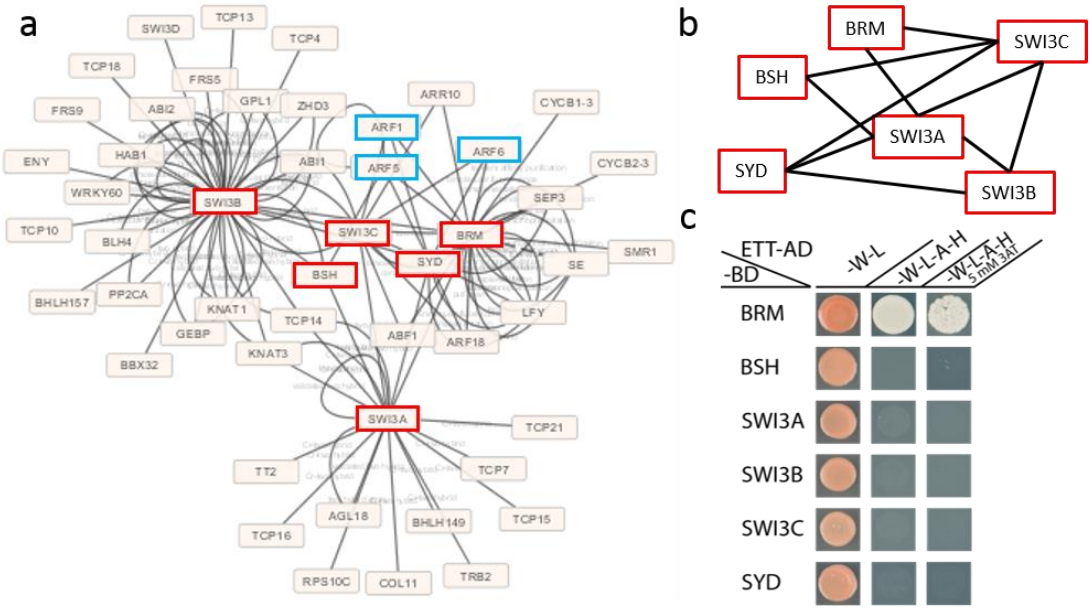

Figure 3. 2: SWI/SNF complexes form interactions with transcription factors including ARFs to shape plant development. (a) Interaction analysis using Cytoscape shows that SWI/SNF family members (red boxes) are chromatin re-modellers that can physically interact with various transcription factors including ARFs (blue boxes). (b) SWI/SNF family members form interaction between each other. BRM and SYD and SWI3B and SWI3C have redundant function. (c) ETT interacts with BRM but not with any other component of SWI/SNF complexes.

SWI/SNF was implemented in the auxin-responsive regulation of homeotic genes during flower primordia initiation (Wu et al., 2015). In this process, MP interacts with several subunits of the SWI/SNF complex to increase accessibility of the DNA for key floral regulators. Besides MP, numerous developmentally important transcription factors, including ARF1, 6 and 18, have been reported to interact with SWI/SNF complexes (Efroni et al., 2013 and Figure 3.2 a). Most identified ARFs can interact with BRM and two other subunits of the complex, BUSHY (BSH) and SPLAYED (SYD). In addition to BRM, BSH and SYD, SWI/SNF complexes have three other subunits called SWITCH/SUCROSE NONFERMENTING 3A (SWI3A), SWI3B and SWI3C. Cooperatively, these subunits form SWI/SNF complexes by interacting with each other in different ways. Hereby, BRM and SYD have redundant functions. Likewise, SWI3B and SWI3C are redundant (Figure 3.2 b). To test, whether ETT can

also interact with several components of the complex, I screened all SWI/SNF subunits for interaction with ETT (Figure 3.2 c). The results show, that ETT interacts exclusively with BRM but not with any other component of SWI/SNF complexes.

Prior studies have shown that ETT can interact with other proteins in an auxin-sensitive manner (Simonini et al., 2017; Simonini et al., 2016; Simonini et al., 2018a; Simonini et al., 2018b). To test the auxin sensitivity of ETT interactions with the identified candidates, auxin (Indole-3-acetic acid or IAA) was added to the yeast selective medium. Colonies co-transformed with ETT and BRM, NRPB6B or SAP18 still grew on the auxin supplemented plates, while yeast colonies transformed with ETT and DEK3, TPL or VRN2 did not grow on auxin-supplemented medium (Figure 3.3 a). Together this suggests that BRM, NRPB6B and SAP18 proteins do not interact with ETT in an auxin-sensitive manner and were not considered for further analysis. In contrast, interactions between ETT and DEK3, TPL or VRN2 were further validated using a quantitative ONPG-assay.

ONPG-assays are Y2H-based assays that are commonly used to determine the strength of interaction between two proteins. This assay makes use of the fact that co-transformed yeast can only produce β-galactosidase when the two introduced proteins interact. β-galactosidase metabolises ONPG to produce a yellow end-product that can be quantified and subsequently used to calculate the galactosidase activity. Here, I used the previously described auxin-sensitive interaction between ETT and IND as a positive control and the established auxin-insensitive interaction between SPT and IND as a negative control. Additionally, the ETT-BRM interaction was assayed as an additional negative control. β-galactosidase activity of yeast expressing ETT -DEK3, ETT-TPL or ETT-VRN2 was significantly reduced when the growth medium was supplemented with auxin, indicating that these interactions are indeed auxin sensitive (Figure 3.3 b).

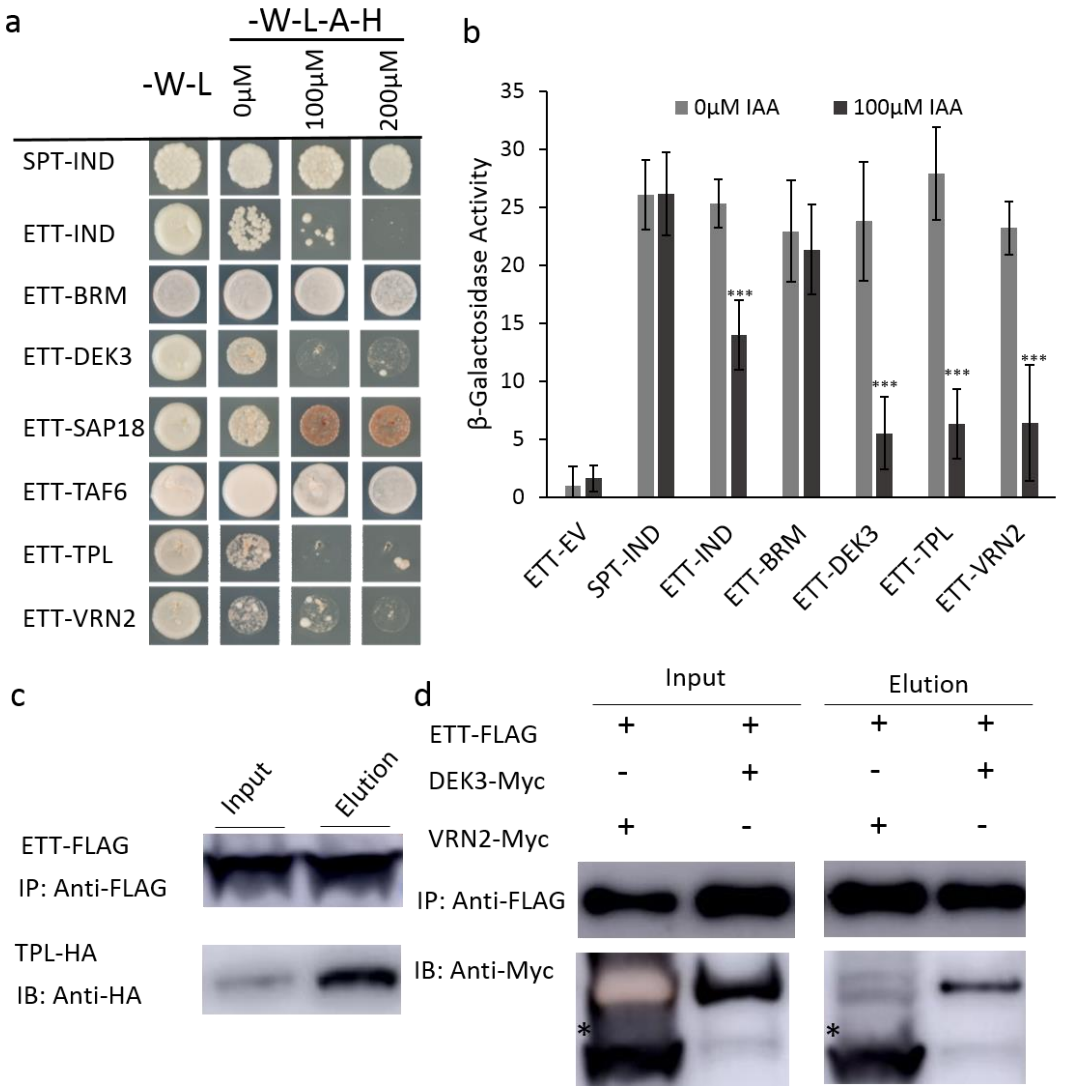

Figure 3. 3: Certain protein-protein interactions can be abolished by auxin. (a) Auxin (0 µM, 100 µM or 200 µM) supplement to the yeast growth medium abolishes the interaction between ETT and DEK3, TPL and VRN2. (b) ONPG-assays confirm the results presented in (a). *** p-values <0.0001. Mean ± standard deviation for three replicates are shown. In both (a) and (b) the SPT-IND interaction was used as a negative control due to its auxin insensitivity, while the ETT-IND interaction was used as a positive control for auxin sensitivity. (c) and (d) Co-IP experiments using transiently expressed protein in N. benthamiana leaves show that ETT can interact with TPL (c), DEK3 and VRN2. (* indicates the specific VRN2 band)

Finally, to assess protein-protein interactions *in planta*, the interacting proteins were transiently expressed in *Nicotiana benthamiana* and interaction assessed using co-immunoprecipitation followed by western blot. The results confirmed interaction of ETT with DEK3, TPL and VRN2 (Figure 3.3 c, d).

In the following sections, the results of detailed analyses of DEK3 and VRN2 are presented while a more systematic study on the auxin sensitivity of the ETT-TPL interaction will be presented in Chapter 4.

ETT interacts with DEK3 – a multifunctional chromatin associated protein that contributes to polarity establishment in gynoecium development

In the previous section, DEK3 was identified as a protein that interacts with ETT in an auxin sensitive manner. Here, I want to understand the importance of this interaction in auxin-mediated gene regulation. ETT is a master regulator controlling polarity and tissue differentiation in gynoecium development. In line with this, I evaluated the role of DEK3 in the tightly controlled process of gynoecium development, aiming to elucidate the biological relevance of the ETT-DEK3 interaction regarding auxin-mediated gene regulation. Furthermore, the identification of a physical interaction between DEK3 and ETT allows us to study how auxin signals can be translated into changes in gene expression through chromatin regulation.

DEK3 is a member of the DEK-containing protein family found in all eukaryotes. Animal genomes generally carry a single gene copy the *DEK* gene, while *DEK* genes in plants form multiple-copy gene families. Four *DEK* genes (*DEK1*, *DEK2*, *DEK3*, *DEK4*) are encoded by the *Arabidopsis* genome (Pendle et al., 2005). The function of *DEK* genes has been studied in much greater detail in animal systems than in plants. In animals, DEK proteins have been implicated in important chromatin-related processes such as heterochromatin integrity (Kappes et al., 2011), DNA-replication (Alexiadis et al., 2000), DNA double-strand break repair (Kavanaugh et al., 2011), mRNA splicing (Le Hir et al., 2001; Le Hir et al., 2000; McGarvey et al., 2000; Soares et al., 2006) and transcriptional regulation (Campillos et al., 2003; Gamble and Fisher, 2007; Kappes et al., 2011; Sammons et al., 2006). Even though, the functions of these DEK plant homologs are less well understood, studies indicate that DEKs have similar functions in plants and animals (del Olmo et al., 2016; Waidmann et al., 2014).

Interaction studies have shown that DEK3 forms homodimers, and heterodimers with DEK4. Therefore, it has been proposed, that DEK3 and DEK4 might have redundant functions. In agreement with that, expression analysis has shown that *DEK3* and *DEK4* but not *DEK1* and *DEK2* are expressed in floral tissues (Waidmann et al., 2014).

Since functional redundancy has been proposed, I tested whether *DEK3* and *DEK4* are both co-expressed with ETT at the style region of the developing gynoecium. I constructed transcriptional reporter lines using 3-kb promoter regions to drive a ß-glucuronidase (GUS) reporter gene. Even though *DEK3* expression is stronger, both genes, *DEK3* and *DEK4*, were exclusively detected within the style and stigmatic tissue where their expression overlaps with ETT (Figure 3.4 a-c). Next, I wondered whether *DEK3* contributes to the establishment of style and stigmatic tissue. Examination of *dek3-2* and *dek4-1* single mutant gynoecia using scanning electron microscopy did not show any style or stigmatic tissue phenotypes (Figure 3.4 d-g). Since the results so far imply redundancy between *DEK3* and *DEK4*, I generated *dek3-2 dek4-1* double mutants. Strikingly, *dek3-2 dek4-1* double mutant gynoecia showed a strong defect in the style region resembling an *ett-3* mutant gynoecium phenotype (Figure 3.4 d-h). The gynoecium phenotype in *ett-3* mutants has been associated with mis-regulation of *PID* (Simonini et al., 2016). Intriguingly, *PID* expression was also significantly up-regulated in *dek3-2 dek4-1* double similarly to the *ett-3* mutant, whilst PID expression in single mutant gynoecia resembled the wild type (Figure 3.4 i).

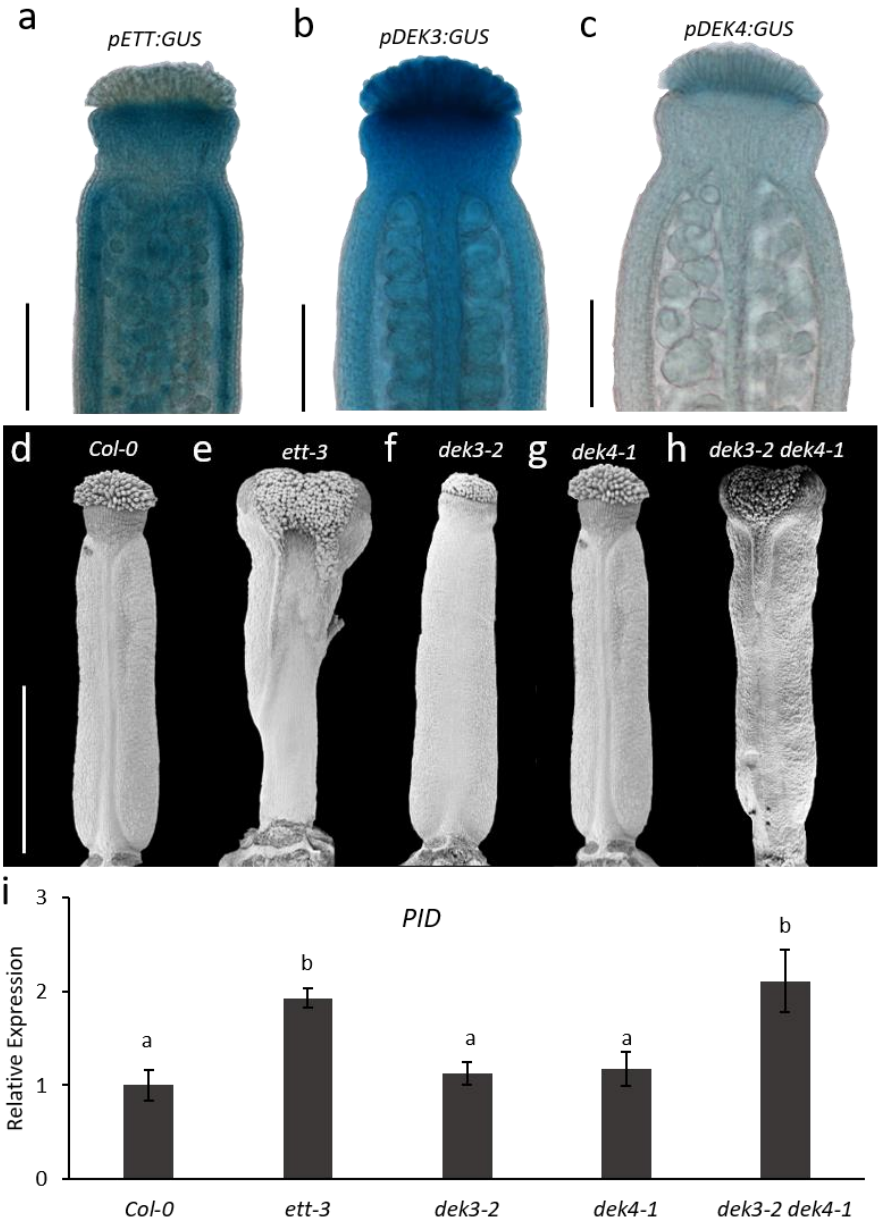

Figure 3. 4: ETT and DEK-proteins co-operatively regulate gene expression to facilitate style development. Promoter GUS expression analysis of *pETT:GUS* (a), *pDEK3:GUS* (b) and *pDEK4:GUS* (c) revealed that *ETT*, *DEK3* and *DEK4* are co-expressed in the Arabidopsis gynoecium. Scale bar = 300 µm. Gynoecium phenotypes of wild type (d), *ett-3* (e) *dek3-2* (f), *dek4-1* (g) and *dek3-2 dek4-1* (h). Scale bar = 1mm. (i) *PID* is constitutively mis-regulated in *ett-3*, and *dek3-2 dek4-1* gynoecia. Mean ± standard deviation of three biological replicates are shown. a and b indicate significance based on one-way ANOVA with TUKEY multiple comparison.

Collectively, these results support the hypothesis of a role for DEK3 in the regulation of gene expression. Moreover, our results suggest that DEK3 and DEK4 are redundantly involved in the auxin-mediated gene regulation at the gynoecium apex

and at least partly (direct or indirectly) through the regulation of the auxin transport regulator *PID*.

ETT interacts with a component of the PRC2 complex

VRN2 was another protein identified as a protein-protein interactor with ETT. VRN2 is part of the VERNALIZATION (VRN) PRC2 and is required for the developmental switch to flowering through epigenetic silencing of the floral repressor FLC. PRC2 was originally identified in *Drosophila melanogaster*, where the complex is involved in the spatial restriction of homeotic selector gene expression. This is a crucial process in *Drosophila* development, and PRC2 covalently modifies Histone 3 (H3) at Lysine 27 (K27) with a trimethyl group (H3K27me3), silencing the expression of the underlying gene (Francis and Kingston, 2001; Lewis, 1978; Mallo and Alonso, 2013). *Drosophila* PRC2 is a complex of four components, Ez, ESC, N55 and Su(z) 12; in Arabidopsis three PRC2 complexes (EMF, VRN, FIS) have been identified and classified based on their Su(z)12 subunit. This subdivision enables each PRC2 complex to repress unique subsets of target genes and to act at different developmental stages (Bemer and Grossniklaus, 2012; Mozgova and Hennig, 2015).

Interestingly, PRC2 activity also plays a role in the modulation of the auxin pathway. Genome-wide studies of H3K27me3 profiles of different tissues revealed that PRC2 complexes directly repress auxin biosynthesis and signalling (He et al., 2014). In line with these findings, PRC2 complexes have been identified to repress lateral root formation by preventing auxin maxima formation through silencing of the auxin transporter *PIN1* (Gu et al., 2014). PRC2 has also been implicated in the auxin sensitive regulation of *PID* in roots (Ariel et al., 2014). Hereby, *APOLO*, a long noncoding RNA neighbouring the *PID* gene, modulates *PID* expression upon auxin treatment. *APOLO* and *PID* are co-regulated. Under low auxin conditions, both *APOLO* and *PID* are repressed via formation of a chromatin loop in the intergenic region between them. Auxin induces the opening of the loop, and the expression of

both *APOLO* and *PID*. *APOLO* transcripts accumulate and are processed by AGONAUTE 4 (AGO4) into siRNAs, leading to DNA methylation across the locus. Additionally, PRC2 restores the chromatin loop leading to a repression of both *APOLO* and *PID* expression (Ariel et al., 2014). However, a direct role for the VRN2-PRC2 complex has not yet been found in any of the described processes other than vernalization.

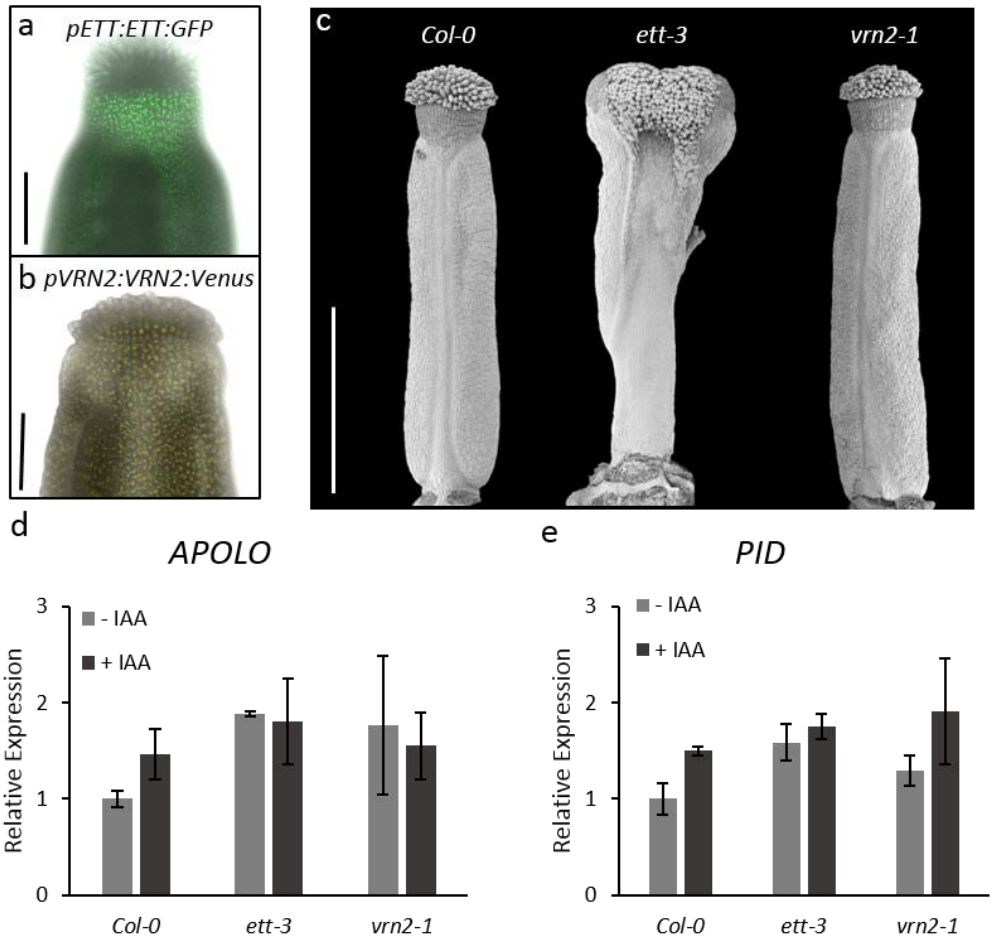

Figure 3. 5 The role of the ETT-VRN2 interaction in gynoecium development remains unclear. (a-b) Examination of *pETT:ETT:GFP* (a) and *pVRN2:VRN2:Venus* (b) revealed that ETT and VRN2 co-localise in the Arabidopsis gynoecium at stage 11. Scale bar = 100 µm. (c), Gynoecium phenotypes at stage 11 of wild type (d), ett-3 and vrn2-1. Scale bar = 1mm. (d-e) *APOLO* (d) and *PID* (e) are constitutively mis-regulated in *ett-3* but unaffected in *vrn2-1* gynoecia. Shown are mean ± standard deviation of three biological replicates. a and b indicate significance base on one-way ANOVA with TUKEY multiple comparison. Treatment with 100 µM IAA. ***p-Values<0.0001; Mean ± standard deviation of three biological replicates are shown.

In Chapter 2, results have shown that auxin affects the dynamics of H3K27me3 histone marks along the *PID*-locus. Although at different scales, the H3K27me3

profiles obtained in gynoecia are in agreement with the published profiles at the same locus in roots (Ariel et al., 2014). Interestingly, we found that H3K27me3 accumulation is altered in *ett-3* mutants suggesting that ETT is a key factor that regulates chromatin dynamics at *PID* in gynoecia. Hence, it is possible that ETT interaction with VRN2 might be meaningful for regulation of these dynamics.

To find out if ETT and VRN2 protein exist in the same tissues within the gynoecium, I examined expression pattern of *pETT:ETT:GFP* and *pVRN2:VRN2:Venus* rescue lines (Simonini et al., 2016). The results show that ETT and VRN2 are indeed expressed in the same tissues (Figure 3.5 a, b). Nevertheless, *vrn2-1* mutant gynoecia did not exhibit any developmental defect when examined using SEM (Figure 3.5 c), which may be due to redundant activities with other PRC2 protein complexes. Next, I tested the expression of *APOLO* and *PID* in wild type, *ett-3* and *vrn2-1*. *APOLO* and *PID* are indeed co-regulated in an auxin-dependent manner as previously described (Ariel et al., 2014). However, in *vrn2-1* mutants, expression of both genes was not significantly different compared to wild type (Figure 3.5 d, e). Based on the presented results, it is evident that VRN2 alone is insufficient to affect the chromatin environment of *PID*. Therefore, I did not assess the H3K27me3 modifications within the *vrn2-1* mutant. In *Arabidopsis*, PRC2 complexes underwent a triplication of the Su(z)12 subunit (*VRN2*, *FIS2* and *EMF2*), thus there is potential redundancy between PRC2-complexes (Mozgova and Hennig, 2015). If VRN2 and its homologs FIS2 and EMF2 indeed act redundantly in the regulation of ETT-target genes it is likely that they also interact with ETT. Therefore, it would be useful to first evaluate these protein-protein interactions using Y2H. Furthermore, examining gynoecia from double and triple mutant combinations of *VRN2*, *FIS2* and *EMF2* would provide further evidence for redundant function during gynoecium development.

Discussion

In the previous chapter, I have shown that the class-B ARF, ETT, regulates its target genes in an auxin-responsive manner. This regulation is independent of the known TIR1/AFB auxin receptors and is likely to involve auxin-responsive chromatin remodelling. I have identified differential accumulation of repressive H3K27me3 and active H3K27ac histone modifications at two ETT-target genes, *HEC1* and *PID*. This differential accumulation of histone modifications is auxin responsive and appears to depend on ETT. In the present chapter, I have attempted to answer the question how ETT mediates these changes in response to auxin. I have used a Y2H approach to identify proteins that can interact with ETT and that have been described in the literature for their association with chromatin. I was able to identify several proteins that met these criteria. Moreover, some of these proteins have been directly associated with the regulation of chromatin dynamics and were studied in more detail.

I propose that there is some degree of analogy between the regulation of *FLC* during vernalization and auxin responsive gene regulation in terms of the protein complexes that directly modify the chromatin environment. Interestingly, it appears that ETT and VAL1 indeed interact with similar proteins and complexes in terms of their function. Both ETT and VAL1 interact with proteins, such as SAP18, DEK3 and TPL, that can bring HDAC activity to the locus and PRC2 that is essential for repression (Prof. C. Dean and Dr. J. Questa, personal communication; Questa et al., 2016). This implies that specific recruitment of these complexes to TF-target loci upon a developmental or environmental signal is not specific to vernalization or auxin signalling but likely a common theme during transcriptional signal integration.

DEK3, one of the ETT-interacting proteins, is one of four DEK-domain containing proteins that are encoded in the *Arabidopsis* genome (Pendle et al., 2005). The role of DEK proteins in plants has not been characterised in detail and therefore remains

elusive. Nevertheless, recent evidence suggests they may play a similar role as animal DEK proteins in chromosome organisation, DNA replication and the regulation of gene expression (del Olmo et al., 2016; Waidmann et al., 2014). DEK3 can physically interact with histone deacetylases (HDACs) and regulatory components of the cohesion complex that is essential for chromosome architecture and chromatin looping. Thus, DEK3 can directly shape the chromatin environment at its target genes (Waidmann et al., 2014). Since DEK proteins do not have DNA-binding activity, they rely on the DNA-binding ability of their interacting partners for target gene recruitment. The physical and auxin-sensitive interaction between DEK3 and ETT demonstrated here suggests that plant DEK proteins might fulfil their task in collaboration with specific transcription factors in higher-order complexes. Moreover, it implies that these complexes can be dissociated by changes in the chemical environment and are therefore conditional. In line with this hypothesis, DEK3 has been implemented in salt-stress tolerance (Waidmann et al., 2014). In the same study, redundancy between DEK3 and its closest homolog DEK4 was suggested. When evaluating gynoecium development, I was unable to detect any developmental defect in *dek3-2* single-mutant gynoecia. However, *dek3-2 dek4-1* double-mutant gynoecia exhibited strong defects reminiscent to the *ett-3* mutant phenotype. This phenotype is partially caused by disturbances of the auxin homeostasis during development presumably caused by mis-regulation of the protein kinase gene, *PID*, which encodes a polar auxin transport regulator (Nemhauser et al., 2000; Simonini et al., 2016). Similarly, I found that *PID* is also mis-regulated in *dek3-2 dek4-1* mutant gynoecia. In plants and animals DEK proteins have been implemented in three-dimensional chromatin organisation, particularly, through their role in the formation and maintenance of chromatin loops (Greenwald et al., 2019; Kadauke and Blobel, 2009; Waidmann et al., 2014; Zheng and Liu, 2019). Intriguingly, a chromatin loop has been implemented in the auxin-responsive regulation of *PID* (Ariel et al., 2014). Taken together, this shows that DEK

proteins indeed have a role in gynoecium development, likely through the regulation of auxin-responsive genes.

In conclusion the experiments described in this chapter show that DEK proteins contribute to auxin-responsive gene regulation on at least two different levels. Firstly, on a global level by regulating auxin-responsive genes by via chromatin structure modulation. DEK-proteins have been implemented in chromatin loop formation and maintenance, which is an important factor in the regulation of *PID*. Secondly, DEK proteins are likely to shape the chromatin environment of their target genes directly through histone deacetylation in response to auxin. In the previous chapter I have found that auxin can influence the histone acetylation of auxin-responsive genes. It is therefore possible that when nuclear auxin concentrations are low, DEK3 interacts with ETT and brings in histone deacetylation at ETT-target loci to repress gene expression. In contrast, high auxin concentrations may instead lead to a disruption of ETT-DEK3-HDAC complexes, leading to a reduction of deacetylation and de-repression of the target locus.

Another interesting protein identified as an ETT-interacting partner is the H3K27 methyltransferase VRN2 which is a Su(z)12 subunit of the POLYCOMB REPRESSIVE COMPLEX 2 (PRC2). The PRC2 complex was first characterised during *Drosophila* development where it has a role in the regulation of HOX genes and other key developmental genes (Francis and Kingston, 2001; Mallo and Alonso, 2013; Simon and Tamkun, 2002).

In plants, PRC2 is best known for its role in flowering-time regulation. Hereby, PRC2 is essential for epigenetic silencing of the flowering repressor *FLC* during the developmental switch to flowering in a process called vernalization. Historically, PRC2 has been associated with epigenetic silencing. However, it has become increasingly evident that PRC2 also controls genes that are under the control of a transcriptional regulatory network rather than gene silencing, and ETT-target genes

appear to be under the control of such a network (Chapter 2; Simonini et al., 2017). PRC2 could have a role integrating chemical and environmental cues in collaboration with specific transcription factors in the repression of target genes, rather than being a purely epigenetic regulator (Ariel et al., 2014; Ringrose, 2007; Steffen and Ringrose, 2014). In the previous chapter, ETT-dependent differences were observed in the accumulation of H3K27me3 at the ETT-target genes, *HEC1* and *PID*, in response to auxin treatment supporting this hypothesis. The data presented here show that VRN2 can interact with ETT in an auxin-sensitive manner. This suggests that ETT can form complexes with PRC2 and can recruit PRC2 activity to its target genes in low auxin concentrations, while high auxin concentrations abolish PRC2 recruitment. Unfortunately, the results presented here are insufficient to reveal the function of PRC2 in the auxin-responsive regulation of ETT-target genes. The most likely reason for this is that there is redundancy between the three PRC2 complexes in *Arabidopsis*. Therefore, to understand the function of PRC2 in the context of auxin-responsive gene regulation, it is critical to evaluate whether the two VRN2 homologs can also interact with ETT. If this is the case, then all further experiments would need to be conducted in higher order mutants to overcome redundancy.

In addition to the candidates that met the criterium of auxin-sensitivity, I found another interesting candidate, BRAHMA (BRM), that interacts with ETT in an auxin-independent manner. BRM is part of the SWI/SNF chromatin remodelling complex. BRM interacts with MP and has previously been identified as a component of auxin-signalling during flower primordium initiation (Wu et al., 2015). The auxin-sensitivity of the MP-BRM interaction was not tested, but it is likely that the MP-BRM interaction is also auxin independent. The study argues that MP interacts with the Aux/IAA BODENLOS (BDL) when auxin levels are low. Under these conditions, BDL blocks the interaction interface required for BRM recruitment, while auxin-mediated degradation of BDL in a high-auxin environment releases MP and enables BRM

recruitment. Similarly, it is possible that ETT interacts with proteins that repress transcription such as VRN2, DEK3 or TPL under low auxin conditions preventing ETT from recruiting BRM. Whereas, under high auxin concentrations ETT binds auxin leading to a disruption of these repressive interactions and enable ETT to recruit BRM.

Remarkably, the BRM homolog in *Drosophila* interacts with UTX, a H3K27-demethylase. The BRM-UTX-containing complex interacts with a histone acetyltransferase that targets H3K27. Thereby, generating an open chromatin environment that counteracts PRC2-mediated silencing (Tie et al., 2012). In *Arabidopsis* an interaction between BRM and the UTX-homolog REF6 has been found recently, suggesting an evolutionary conservation of the underlying gene-regulatory mechanism (Cui et al., 2016; Li et al., 2016). In Chapter 2, I found that auxin induces a reduction in H3K27me3 and an increase in H3K27Ac enrichment at *HEC1* and *PID* loci, implying that this mechanism might also play a role in auxin-responsive gene regulation. Future work will show whether this auxin-induced change in chromatin environment is indeed dependent on BRM.

Concluding remarks

The analysis carried out in this chapter is a stepping stone towards a more detailed understanding of the mechanisms that link chromatin dynamics, auxin signalling, and gene regulation mediated by an alternative auxin-signalling pathway. Several candidate proteins that can act in this pathway in co-operation with ETT have been identified, and an initial evaluation has been carried out. Unfortunately, a more detailed analysis of all candidates and how they work together to mediate the auxin signal is beyond the scope of this thesis. However, in the following section I will present some suggestions for future work that can further our understanding of the candidates' role in auxin-responsive gene regulation.

DEK3 was an interesting candidate identified in the Y2H library screen. The results presented here show that DEK3 can interact with ETT in an auxin-sensitive manner. Mutant analysis has further shown that DEK3 and DEK4 act redundantly during gynoecium development. Future work needs to evaluate this by investigating the ability of DEK4 to interact with ETT. The results presented here imply two hypotheses about how DEK-proteins can affect auxin-responsive gene regulation. Firstly, DEK3 may affect chromatin structure on a global level at auxin-responsive loci through chromatin looping. Secondly, DEK-proteins may shape the chromatin environment of their target genes directly through histone deacetylation in response to auxin. Future analysis using $ChIP_{qPCR}$ will show whether DEK3 co-localises with ETT at binding sites within the *PID* promoter. Examining the expression of target genes and H3Ac dynamics at target sites in *dek3-2 dek4-1* mutants, and in the presence and absence of auxin, will provide insight into the importance of chromatin modifications by DEK3-containing complexes for the transcription of genes in response to auxin.

The second interesting candidate that was identified here is VRN2. Unfortunately, from the results presented in this chapter, the role of VRN2 in the auxin-responsive regulation of ETT target genes remains elusive. The most likely reason for this is redundancy between VRN2 and its homologs FIS2 and EMF2. Consequently, future work first needs to clarify whether FIS2 and EMF2 can also interact with ETT, and whether or not they do so in an auxin-sensitive manner. To fully understand the role of PRC2 in the auxin responsive regulation of ETT target genes, such as *HEC1* and *PID*, the binding of VRN2 and homologs to these loci needs to be evaluated using $ChIP_{qPCR}$. The co-localisation of PCR2 and ARFs at binding sites of auxin responsive loci would indicate that they work together as a complex. Finally, the assessment of H3K27me3 dynamics at the *PID* locus in *VRN2*, *FIS2* and *EMF2* double and triple mutants would provide further evidence to support a role for VRN2 in the auxin-responsive regulation of chromatin dynamics. In summary, data presented here and

by others (Ariel et al., 2014) indicate a role of PRC2 in the regulation of the auxin-responsive gene, *PID*. The suggested experiments will contribute to the general understanding of PRC2 in the regulation of both auxin-responsive genes, and the regulation of genes which are not regulated by epigenetic silencing.

The third promising candidate that I identified in this chapter is the co-repressor protein TOPLESS (TPL). In Chapter 4, I will focus on the role of the ETT-TPL interaction at the molecular level, focussing on its auxin-sensing properties and the effect on chromatin dynamics in more detail.

Materials and Methods

Yeast two-hybrid library screening and candidate gene selection.

To generate the bait construct, the full-length coding sequence of *ETT* was cloned into the pGBKT7 vector using the Gateway method (Thermo Fisher Scientific) and introduced into the α-Y187 strain of yeast. The bait strain was mated with a normalized *Arabidopsis thaliana* total protein library which was generated by cloning *Arabidopsis* total cDNA into the pGADrec vector and introducing it into the α-AH109 yeast strain (Costa et al,. 2013). Transformations were spread on four types of selective media. All media contained Yeast Selection Medium (YSD; Melford Laboratory Ltd., UK) supplemented amino acid dropout (Sigma) lacking either Tryptophan (W), Leucin (L) (-W-L; transformation control), Tryptophan (W), Leucine (L) and Adenine (A) (-W-L-A; weak selection), Tryptophan (W), Leucine (L) and Histidine (H) (-W-L-H; medium selection) or Tryptophan (W), Leucine (L), Adenine (A) and Histidine (H) (-W-L-A-H; strong selection). Positive colonies were selected over a range of 10 days, the pGADrec plasmids were recovered, and cDNA insert s were amplified by PCR using the AK199 and AK200 primers (Table S2). Subsequently, the PCR product was sequenced to identify the underlying putative

candidate genes (Mix-2-seq; Eurofins) using the AK199 primer. Sequences were annotated using the TAIR blast tool (version 2.2.8) on https://www.arabidopsis.org/ (TAIR10).

Yeast two-hybrid interaction assay

For Yeast-two-Hybrid (Y2H) assays coding sequences of putative interactors were cloned into pDONR207 and recombined into the pGBKT7 vector (Clontech), while ETT was cloned into the pGADT7 and pDEST32 vectors. Using the co-transformation method (Egea-Cortines et al., 1999) the generated constructs were transformed into the AH109 strain (Clontech). Transformations were selected on YSD medium lacking Tryptophan (W) and Leucine (L) at 28°C for 3-4 days. Transformed yeast cells were serially diluted (10^0, 10^1, 10^2 and 10^3) and dotted on YSD medium lacking Tryptophan (W), Leucine (L), Adenine (A) and Histidine (H) to test for interaction. To examine interaction strength, 3-Amino-1,2,4-Triazole (3-AT; Sigma) was supplemented to the YSD (-W-L-A-H) medium at different concentrations (0, 5, 10mM). To determine the effects of auxin on the protein-protein interactions, IAA (Sigma) was dissolved in ethanol and added directly to the medium at the desired concentration (100 µM). Pictures were taken after 3 days of growth at 28°C. The Y2H plasmids containing the SWI/SNF family proteins (BRM, BSH, SWI3A, SWI3B, SWI3C and SYD) were in pDEST22 kindly provided by Prof. Doris Wagner (University of Pennsylvania, Philadelphia, USA).

For the β-Galactosidase assay transgenic yeast was grown in liquid YSD (-W-L) medium supplemented with/without 100 µM IAA, to an OD_{600} of 0.5 the cells were then harvested and lysed using 150 µL Buffer Z with β-mercaptoethanol (100 mM Phosphate buffer pH 7, 10 mM KCl, 1mM Mg2SO4, β-mercaptoethanol 50 mM), 50 µL Chloroform and 20 µL of 0.1% SDS. After lysis, the sample was incubated with 700 µL pre-warmed ONPG solution (1mg/mL ONPG (o-Nitrophenyl-β-D-Galactopyranoside, Sigma) prepared in Buffer Z without β-mercaptoethanol at 28°C

until a yellow colour developed in the samples without auxin treatment. After stopping all reactions (using 500 µL Na_2CO_3) the supernatant was collected and OD_{405} determined. The β-Galactosidase activity was calculated as follows: (A405*1000)/(A600*min*mL)

All primers used for cloning can be found in Appendix II Table 2.

Plant material and Growth conditions

Plants were grown as described in Chapter 2. All mutants and reporter lines used in the current chapter were in a *Col-0* background. The *dek3-2* and *dek4-1* mutants were kindly provided by Prof. Claudia Jonack (Austrian Institute of Technology, Vienna, Austria) and the *vrn2-1* mutant was provided by Prof. Caroline Dean (John Innes Centre, Norwich, UK). The *pETT:ETT:GFP* reporter line was previously published (Simonini et al., 2016).

Genotyping of insertion lines

Genomic DNA was extracted form young leaves using a previously described protocol (Edwards et al., 1991) with minor modifications: One leaf per plant was collected in 1.5mL tubes and ground using a pestle. Next, 300 µL of DNA extraction buffer (200 mM Tris HCl pH7.5, 250 mM NaCl, 25 mM EDTA, 0.5% SDS) was added, mixed by inverting the tube and centrifuged at 10,000 x g for 5 minutes. The supernatant (typically 200 µL) was transferred to a fresh 1.5 mL tube and mixed with an equal volume of isopropanol (typically 200 µL), mixed by inverting the tube and incubated for 2 minutes. Following centrifugation at 10,000 xg for 5 minutes, the supernatant was discarded, and the pellet washed in 70% ethanol. After a second round of centrifugation (10,000 xg for 5 minutes), the pellet was air dried and dissolved in 100 µL of water. The extracted DNA samples were immediately used or stored at -20ºC.

For all T-DNA insertion lines, genotyping primers were retrieved from SALK primer design website (http://signal.salk.edu/tdnaprimers.2.html)

For genotyping by PCR, two reactions were set up; one reaction with genotyping primers (LP and RP) within the wild type gene and one reaction with one primer specific to the T-DNA insertion (LBb1.3) and another within the mutated gene (RP). A 25 µL PCR mix was set up containing 0.1 µl GoTaq polymerase (Promega), 5 µL 5 x buffer, 1 µl dNTP mix, 2.4 µL MgCl2, 1 µL forward primer (10 µM,) 1 µL reverse primer (10 µM), 1 µL genomic DNA, and 11.5 µL water. Genotyping PCRs were carried out with the following cycling conditions: 95 °C for 3 min followed by 30 cycles at 95 °C for 30 s, 56 °C for 30 s and 72 °C for 1 min, with a final extension step of 3 min at 72 °C. The PCR product was analysed by gel electrophoresis on a 1 % agarose gel.

Expression analysis

RNA extraction, cDNA synthesis and qPCR were carried out for expression analysis as described in Chapter 2. All primers used can be found in Appendix II Table 2.

Generation of transgenic plants

The pCAMBIA1300 carrying *pVRN2:VRN2-Venus* was kindly provided by Dr. Hongchun Yang (Dean Group, John Innes Centre, Norwich, UK).

All other constructs were generated using the Golden Gate method as described before (Engler et al., 2014) using Golden Gate standard parts obtained from TSL SynBio (http://synbio.tsl.ac.uk/). To design level 0 modules, DNA sequences were retrieved from the TAIR database (www.arabidopsis.org). To design level 0 modules, all DNA-fragments were PCR-amplified from genomic DNA using Q5 High-Fidelity DNA polymerase (New England Biolabs) according to the manufacturer's instructions. PCR-products were analysed by gel electrophoresis on a 1 % agarose gel and purified using the Nucleospin Extract kit (Macherey-Nagel). Level 0 Golden Gate reactions were performed in 15 µL final volume (100 ng L0 backbone plasmid, 100 ng of insert, 1.5 µL 10 x BSA (1 mg/mL), 1.5 µL 10 x T4 buffer, 1 µL BpiI (New England Biolabs), 1 µL T4 DNA ligase (New England Biolabs) and water). For

digestion and ligation of the DNA components were incubated for 25 cycles of 3 min at 37 °C and 4 min at 16°C, followed by 5 min at 50°C. To generate level 1 plasmids Golden Gate reactions were performed in 15 µL final volume (100 ng L1 acceptor backbone plasmid, 100 ng of each L0 plasmid, 1.5 µL 10 x BSA (1 mg/mL), 1.5 µL 10 x T4 buffer, 1 µL BsaI (New England Biolabs), 1 µL T4 DNA ligase (New England Biolabs) and water). For digestion and ligation, the reaction mixes were incubated using the same conditions as for L0 reactions. To generate level 2 vectors, a 15 µL reaction mix was set up (100 ng of each level 1 plasmid, 100 ng of the L2 binary vector, 1.5 µL 10 x BSA (1 mg/mL), 1 µL BpiI (New England Biolabs), 1.5 µL 10 x T4 buffer, 1 µL T4 DNA ligase (New England Biolabs) and water). For digestion and ligation, the reaction mixes were incubated using the same conditions as for L0 reactions

All plasmids were sub-cloned into *E.coli DH5α* (Thermo Fisher Scientific) following the manufacturer's instructions and selected overnight (37 °C) on LB solid medium supplemented with the appropriate antibiotics (Appendix II Table 4). Two surviving colonies per construct were selected and re-grown overnight (37 °C, 250rpm) in liquid LB medium supplemented with the appropriate antibiotics. The plasmids were extracted using the Nucleospin Plasmid kit (Machery-Nagel) and sequenced using the Euronfins Mix2Seq sequencing kit (Eurofins Genomics) according to the manufacturer's instructions.

The final constructs were introduced into *Agrobacterium tumefaciens* strain GV3101 carrying the pSoup plasmid (Rifamipcin and Gentamycin resistance) and grown on plates containing LB medium supplemented with the appropriate antibiotics (Rifampicin at 100 mg/L and Gentamycin at 10 mg/L). Bacteria transformed with pCAMBIA1301 and Golden Gate L2 transcriptional fusions were also supplemented with Kanamycin (50 mg/L) and for Golden Gate L1 Co-IP constructs were supplemented with Carbenicilin (100 mg/L). *Arabidopsis* plants were transformed

using the floral dip method (Clough and Bent, 1998). Plant transformants were selected on plates containing MS medium supplemented with the appropriate herbicide (Hygromycin (40 mg/L) for pCAMBIA1300 and pCAMBIA1301 and Phosphinothricin (PPT/BASTA; 15 mg/L) for all other constructs). Survivors were transferred to soil after 10 days. All primers and plasmids used for cloning can be found in Appendix II Table 3 and Appendix II Table 4, respectively.

GUS histochemical assay

GUS assays were performed using 1mg/mL X-gluc substrate (5-bromo-4-chloro-3-indolyl glucuronide, MELFORD laboratory) dissolved in DMSO. Inflorescences were pre-treated with ice cold acetone for 1h at -20°C and subsequently washed twice for 5 min in 100mM sodium phosphate buffer and washed for 30 min in 100mM sodium phosphate buffer containing 1mM K_3 and K_4 at room temperature. Samples were then stained in staining solution for 2-16 hours at 37°C in the dark. Staining was checked every 2 hours during the first 6 hours. After staining the samples were washed twice with water and incubated in 70% ethanol at room temperature until all chlorophyll was removed from the samples. Finally, gynoecia were dissected, mounted in chloral hydrate solution (Sigma), and imaged using a Leica DM6000 light microscope.

Scanning Electron Microscopy

SEM samples were prepared, and SEM was performed as described in Chapter 2.

Confocal Microscopy

All confocal images were taken in 8-bit format using a Leica SP5 confocal microscope (equipped with an Argon krypton laser and two HyD detectors (Leica Microsystems)) with 20x numerical aperture (NA) water-immersion objective. The pinhole was equivalent to 1x airy disk diameter. GFP was excited at 488nm and Venus at 515nm. GFP emissions were detected between 497 and 551 nm and Venus emissions were detected between 525 and 600nm.

Co-Immunoprecipitation

For co-immunoprecipitation, ETT-FLAG was generated using Golden Gate cloning by recombining a previously described L0 clone for ETT (Simonini et al., 2016) with a 35S promoter (AddGene #50266), a C-terminal 3xFLAG epitope (AddGene #50308) and a Nos-terminator (AddGene #50266) into a L1 vector (AddGene #48000). *DEK3* and *VRN2* coding sequences were clones using the Golden Gate methods into L0 (AddGene #47996) and combined with a 35S promoter (AddGene #50266), a C-terminal 4xMyC epitope (AddGene #50310) and a Nos-terminator (AddGene #50266) into a L1 vector (AddGene #48000). The pGWB14 TPL-HA construct was provided by Prof. Salomé Prat (Centro Nacional de Biotecnología-CSIC, Madrid, Spain). The epitope-tagged proteins were transiently expressed in four-week-old *N. benthamiana* leaves for two days. Co-immunoprecipitation was performed as described previously (Chung et al., 2019). Briefly, 1g of fresh leaf tissue was harvested and ground in liquid nitrogen. The powder was homogenized for 30 min in two volumes of extraction buffer (10% glycerol, 25mM Tris-HCl pH 7.5, 1mM EDTA, 150mM NaCl, 0.15% NP-40, 1mM PMSF, 10mM DTT, 2% Polyvinylpyrrolidone, 1x cOmplete Mini tablets EDTA-free Protease Inhibitor Cocktail (Roche)). The homogenized samples were cleared by centrifugation at 14,000 x g for 10 min, and cleared lysates were incubated for 2 hours with 20 µl anti-FLAG M2 magnetic beads (SIGMA-ALDRICH, M8823; lot: SLB2419). The beads were washed five times with IP buffer (10% glycerol, 25mM Tris-HCl pH 7.5, 1mM EDTA, 150mM NaCl, 0.15% NP-40, 1mM PMSF, 1mM DTT, 1x cOmplete Mini tablets EDTA-free Protease Inhibitor Cocktail (Roche)) and proteins were eluted by adding 80 µl 2x SDS loading buffer followed by an incubation at 95 °C for 10 min. The eluates were analysed by western blot using an anti-FLAG antibody (M2, Abcam, ab49763, Lot: GR3207401-3), an anti-MyC antibody (9E10, Abcam, ab62928, Lot: GR3208762-2) or an anti-HA antibody (Abcam, ab173826, Lot: GR3255539-1). All antibodies were used as 1:10000 dilutions. The antibodies were validated by the manufacturer.

Statistical analyses and replication

In all graphs, error bars represent the standard deviation of the mean for all numerical values. qPCR experiments have been carried out at least in triplicate. The data presented here show an average of three replicates. Data were analysed using one-way ANOVA with post-hoc Tukey multiple comparison test. Statistical tests were carried out using GraphPad Prism Version 5.04 (La Jolla California USA, www.graphpad.com).

Chapter 4

ETTIN regulates transcription via auxin-sensitive interactions with TOPLESS co-repressor complexes

Introduction

In the previous chapters, I have shown that ETT-mediated auxin signalling has a central role in regulating the local chromatin environment (Chapter 2 and Chapter 3). During gynoecium development the specific histone modifications that dictate chromatin state depend on ETT. Seemingly, ETT acts as an interaction platform to bring various chromatin-modifying complexes to its target loci (Chapter 2 and Chapter 3). Chapter 3 identified TPL as an interacting partner of ETT. Moreover, the interaction between ETT and TPL was auxin-sensitive raising several questions about how the two proteins interact and how they co-operatively mediate auxin signalling and modulate the local chromatin environment. This chapter explores the mechanism by which ETT and TPL interact and the consequences of this interaction on the regulation of ETT-target genes. I hypothesise that low levels of auxin maintain ETT associations with TPL at target loci to repress gene expression, whereas, when nuclear auxin levels are high, TPL disassociates from ETT, leading to de-repression of ETT-target genes. The mechanism presented here may not be exclusive to the ETT and TPL pair but may play a more general role in non-canonical auxin signalling.

Differential gene expression is essential for organisms to respond adequately to their surroundings and underpins the accurate execution of developmental programs. It is becoming increasingly evident that most genes are subject to context-dependent regulation and switch between active and repressed states (Kagale and Rozwadowski, 2011; Krogan et al., 2012). Hence, transcriptional repression is a critical mechanism regulating many eukaryotic developmental pathways. To effectively repress transcription at a gene locus, co-repressors, which are incapable of direct DNA binding, are recruited by DNA-binding transcription factors. Numerous eukaryotic co-repressors have been identified including Tup1 in yeast, and Groucho/TLE in *Drosophila* and humans respectively (Buscarlet and Stifani, 2007). The *Arabidopsis* genome encodes several Groucho/TLE-like gene families including

the *TOPLESS*/*TOPLESS RELATED* (*TPL/TPR*) family that consists of *TOPLESS* (*TPL*) and its four homologs *TOPLESS RELATED 1-4* (*TPR1-4*) (Kagale et al., 2010; Kagale and Rozwadowski, 2011). TPL/TPR proteins achieve transcriptional repression of gene expression through complex formation with HISTONE DEACETYLASE 19 (HDA19) (Krogan et al., 2012; Zhu et al., 2010). Across kingdoms Groucho/TLE-like co-repressors have been identified as protein-protein interaction hubs that bring together several proteins to form repressor complexes (Buscarlet and Stifani, 2007; Mosimann et al., 2009). These complexes can contain diverse classes of proteins but the recruitment of histone deacetylases (HDACs) is a common feature for all organisms in which Groucho/TLE-like proteins were studied (Buscarlet and Stifani, 2007; Jennings and Ish-Horowicz, 2008; Kagale and Rozwadowski, 2011; Sekiya and Zaret, 2007). Groucho/TLE homologs in animals act as important regulators of several signalling mechanisms and are best understood for their role in the Wingless/Wnt signalling pathway. Wnt is an essential morphogen in animal embryonic development (Gammons and Bienz, 2018; van Amerongen and Nusse, 2009). Wnt signalling occurs when a Wnt protein ligand binds a plasma-membrane bound receptor. Binding of Wnt to its receptor mediates translocation of the cytosolic ß-catenin protein to the nucleus, where it binds the TCF transcription factor to activate target genes. Binding of ß-catenin to TCF displaces chromatin-repressive factors, including Groucho/TLE. Moreover, the binding of ß-catenin to TCF leads to the activation of chromatin reconfiguring factors that overcome repression (Chodaparambil et al., 2014; Gammons and Bienz, 2018; Mieszczanek et al., 2008; Mosimann et al., 2009; van Tienen et al., 2017).

Despite limited sequence homology, Groucho/TLE co-repressors in all eukaryotes contain shared evolutionarily conserved structural features (Buscarlet and Stifani, 2007; Martin-Arevalillo et al., 2017). Accordingly, the N-terminal Gln-rich (Q) domain and the C-terminal Trp-Asp-repeats (WD40) are present in all eukaryotic

Groucho/TLEs including TPL/TPRs. These domains are essential for interaction with a variety of proteins, including transcription factors and HDACs. Furthermore, the N-terminal Q-rich domain mediates the formation of tetrameric Groucho/TLE complexes, the active form of Groucho/TLE co-repressors (Chambers et al., 2017; Chodaparambil et al., 2014; Jennings and Ish-Horowicz, 2008; Jennings et al., 2006; Jennings et al., 2008; Sekiya and Zaret, 2007). Plant Groucho/TLE-like proteins also share an N-terminal LisH (for Lis1-homologous) domain, as well as a “C-terminal to LisH” (CTLH) domain and a CT11-RanBPM (CRA) domain. These domains promote protein-protein interaction (Cerna and Wilson, 2005; Jennings and Ish-Horowicz, 2008; Martin-Arevalillo et al., 2017).

TPL/TPR co-repressors were originally identified as key factors involved in setting up the apical-basal growth axis during embryo development (Long et al., 2006; Szemenyei et al., 2008). Several studies suggest that the five *Arabidopsis* TPL/TPRs are redundantly involved in the repression genes in nearly all plant hormone signalling pathways, and consequently have roles throughout plant development (Akiko et al., 2012; Causier et al., 2012; Espinosa-Ruiz et al., 2017; Krogan et al., 2012; Kwon et al., 2012; Long et al., 2006; Pauwels et al., 2010; Pi et al., 2015; Szemenyei et al., 2008; Zhu et al., 2010). Recent crystallization studies have identified that the Ethylene-responsive element binding factor-associated Amphiphilic Repression (EAR) motif (LxLxL), present in many transcriptional regulators physically interacts with the N-terminal CTLH domain of TPL (Ke et al., 2015; Martin-Arevalillo et al., 2017).

It is well established that Aux/IAA transcriptional repressors form complexes with TPL/TPR co-repressors through their N-terminal EAR-motif (Ke et al., 2015; Martin-Arevalillo et al., 2017). Aux/IAA proteins are central components of canonical auxin signalling, and act as transcriptional repressors of auxin responsive genes by binding to Auxin Response Factors (ARFs) when auxin levels are low (Kato et al., 2018;

Kelley and Estelle, 2012; Leyser, 2018). Increasing levels of auxin enhance the interaction of Aux/IAA proteins with TIR1/AFB auxin co-receptors. Interaction with TIR1/AFB-proteins leads to Aux/IAA ubiquitination and subsequent degradation, thus relieving the repression of ARF-target loci (Kelley and Estelle, 2012). Interestingly, some ARFs can interact with TPL/TPR proteins directly through EAR-motifs within their protein sequence, suggesting that TPL/TPRs can modulate auxin response repression in two distinct manners. It was suggested that direct TPL/TPR-ARF interactions can attenuate auxin signalling independently of auxin levels (Causier et al., 2012; Choi et al., 2018). However, this is speculative since the effect of auxin on TPL/TPR-ARF interactions has not yet been evaluated, and the capacity of ARFs to interact directly with TPL/TPR-co-repressors remains to be determined systematically.

In the previous chapter, I found that the non-canonical ARF, ETT, can interact with TPL directly. Moreover, the application of auxin disrupts the TPL-ETT interaction. It is not yet known if ETT can interact with other members of the TPL/TPR family, and the residues responsible for ETT-TPL/TPR interactions remain elusive. ETT is not among the list of ARFs which are known to contain an EAR-motif, and therefore ETT possibly interacts with TPL via an alternative peptide motif. Since the mechanism of interaction remains unknown, it would be interesting to evaluate which region of the TPL protein mediates the ETT-TPL interaction. Chapter 2 found that auxin increases histone acetylation at the *HEC1* and *PID* loci, which correlates with the up-regulation of these genes. Since TPL/TPRs have been implemented in histone deacetylation and transcriptional repression, the auxin-sensitive interaction of ETT with TPL suggests that these two proteins are key components of the non-canonical auxin signalling pathway. This leads to the hypothesis that low levels of auxin maintain ETT associations with TPL at target loci to repress gene expression via histone deacetylation. As auxin levels increase, TPL disassociates from ETT and histone

deacetylase activity is lost, leading to de-repression of ETT-target genes. In such a mechanism ETT and TPL would act as an auxin co-receptor pair mechanistically reminiscent to the components of Wnt signalling.

This chapter attempts to test this hypothesis, and to shed light on how ETT and TPL function as key components of the non-canonical auxin signalling pathway to regulate auxin responsive gene expression in the context of gynoecium development.

Results

ETT interacts with several TPL/TPR family members via a C-terminal repressive motif

Using the Geneious software, a phylogenetic analysis of ETT protein sequences across the angiosperm phylum was carried out to understand how ETT interacts with TPL/TPRs. This analysis identified several regions that are highly conserved (Figure 4.1 a). Unsurprisingly, the N-terminal DNA-binding domain characteristic of B3-type TFs, such as ARF proteins, was conserved in ETT across all species. Towards the C terminus of the ES domain an RLFGF-motif with a particularly high level of conservation was identified (Figure 4.1 a). RLFGF-motifs have been described as repressive motifs that - like EAR-motifs - can facilitate interactions with co-repressors such as TPL (Causier et al., 2012). The classical EAR-motif (LxLxL) can be found in Aux/IAAs and some ARFs (e.g. ARF2; Causier et al., 2012; Choi et al., 2018). Interactions between Aux/IAAs and members of the TOPLESS and TOPLESS-RELATED (TPL/TPR) family of co-repressors occurs via this motif (Szemenyei et al., 2008). TPL/TPRs mediate their repressive effect by attracting histone deacetylases (HDACs; Krogan and Long, 2012).

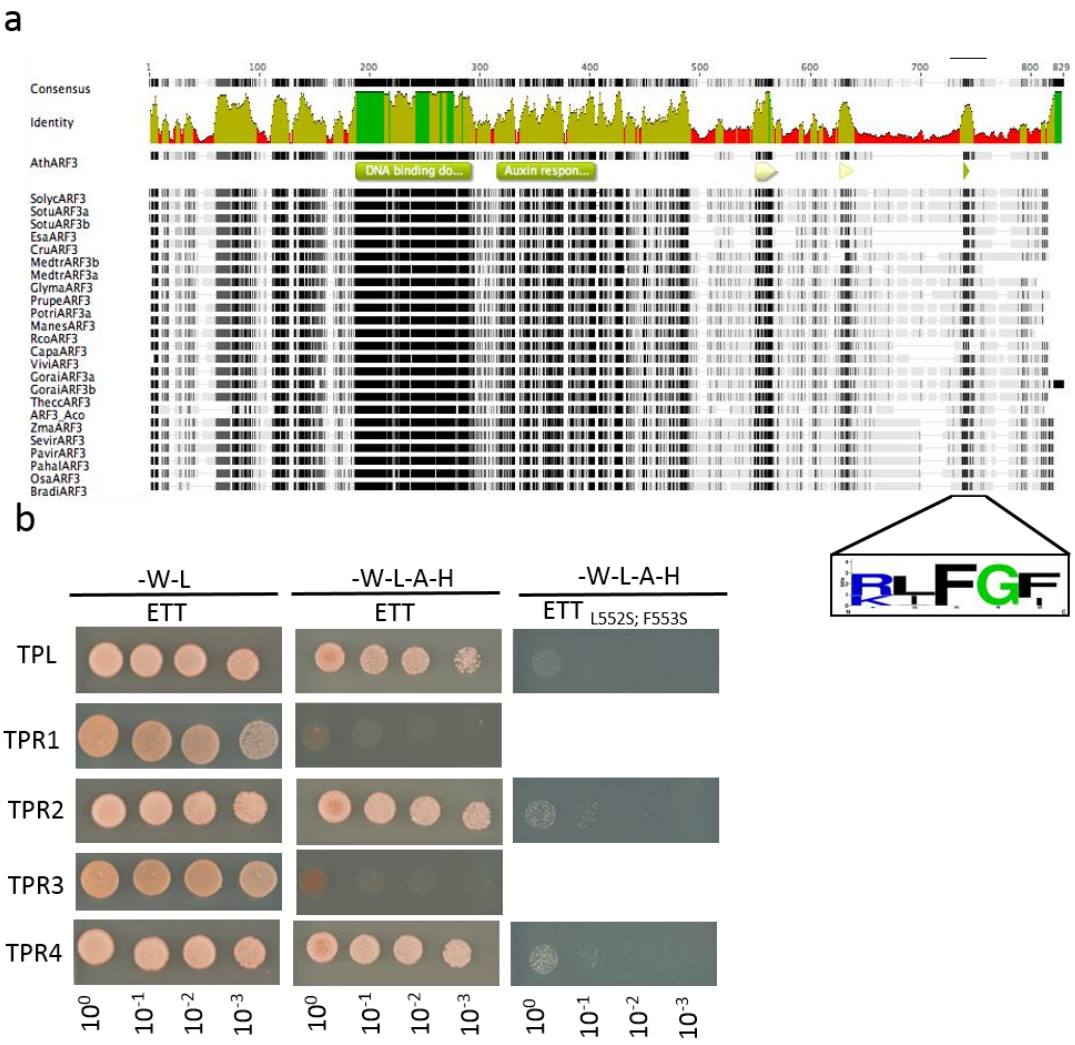

Figure 4. 1: ETT interacts with members of the TPL/TPR co-repressor family via a conserved repressive motif. (a) Alignment of ETT protein sequences of 22 species identified a conserved repressive motif (RLFGF) at its C-terminal domain. (b) ETT interacts with several members of the TPL/TPR co-repressor family in Y2H. The repressive motif mediates the interaction as mutating the motif disrupts complex formation (negative controls can be found in Appendix III Figure 1).

Since ETT functions independently of the canonical auxin signalling pathway, it is possible that its effect on the local chromatin environment occurs via direct interaction with TPL/TPRs via the RLFGF-motif. The previous chapter found that ETT interacts with TPL in an auxin sensitive manner. It is well-known that the five members of TPL/TPR family act redundantly. To test whether ETT also interacts with other family members, I carried out Yeast 2-Hybrid (Y2H) assays screening for interaction between ETT and all five TPL/TPRs. In this screen ETT was found to interact with TPL, TPR2 and TPR4 (Fig. 4.1 b). Next, two highly conserved residues within the

repressive motif were mutated (RLFGF to RSSGF). Mutating these residues abolished the interactions demonstrating its requirement for the ETT-TPL/TPR interaction (Figure 4.1 b and Appendix III Figure 1).

The repressive motif and the capability to interact with TPL/TPR family members is conserved across class B ARFs but not class A and C ARFs

ETT interacts with TPL/TPR co-repressors via an RLFGF motif that is conserved among ETT proteins across the angiosperm phylum. An interesting question is whether this RLFGF motif is specific to ETT or whether it is a general feature of ARF proteins.

Phylogenetically, ARF proteins are classified into three distinct clades, A, B and C (Finet et al., 2013; Finet et al., 2010; Mutte et al., 2018). Transactivation assays have demonstrated that class A and class B ARFs may function as transcriptional activators and repressors, respectively (Ulmasov et al., 1999a). Although not supported experimentally, class C ARFs have traditionally been classified as transcriptional repressors. However, the role of class C ARFs in auxin response is under debate as recent studies imply that they do not function in auxin responsive gene regulation (Mutte et al., 2018). In canonical auxin signalling, ARFs interact with Aux/IAA repressor proteins which in turn recruit TPL/TPRs to carry out the repressive function under low nuclear auxin concentrations. Thus, this pathway relies on the physical interactions of AUX/IAAs with ARFs through the PB1 domain to recruit TPL-containing repressive complexes to ARF target sites. However, interaction studies showed that not all ARFs can interact with Aux/IAAs. Moreover, it is mainly the class A ARFs that can interact with almost all Aux/IAAs while class B ARFs interact with none or a limited number of Aux/IAAs (Piya et al., 2014; Vernoux et al., 2011). Some ARFs have been shown to directly interact with TPL without the aid of Aux/IAAs (Causier et al., 2012; Causier et al., 2014). Whilst some ARFs contain an EAR-motif that facilitates the interaction with TPL (Causier et al., 2012; Choi et al., 2018), the

mode of interaction for other ARFs is yet to be understood. To evaluate how common the RLFGF-motif that is required for interaction between ETT and TPL is among ARFs, I compared all 23 ARFs in *Arabidopsis* by protein sequence alignment generated using the MEGA 7 software. The alignment was used to generate the ARF gene tree. As expected, class A, B and C ARFs formed three distinct clades (Figure 4.2 a). While an LFG-core motif was conserved among almost all ARFs, the flanking amino acids differed considerably. The full RLFGF-motif was only found in several class B ARFs. Interestingly, some class B ARFs have variants of this motif in which the first Arginine (R) was substituted with a Lysine (K), or the Phenylalanine (F) at the fifth position was substituted for a Valine (V) or Isoleucine (I). To test whether the LFG-core motif is sufficient for ARF-TPL interaction, representative ARFs (ETT/ARF3, ARF4, MONOPTEROS (MP)/ARF5, ARF6 and ARF16) that vary in the amino acids flanking the core LFG were screened by Y2H against the TPL/TPR family. Remarkably, only the class B ARFs ETT (RLFGF) and ARF4 (KLFGV) were able to interact with TPL/TPR family proteins (TPL, TPR2, TPR4) while neither class A ARFs, MP (CLFGN), ARF6 (LLFGV) nor the class C ARF, ARF16 (VLFGK) showed interaction (Figure 4.2 b). The ARFs tested all share the LFG-core motif but vary in their amino acid composition at the first and fifth position of the motif. Variation on the fifth position is shared between the three classes, making it impossible to distinguish between them at this position. In contrast, class B ARFs have a positively charged amino acid at the first position while positively charged residues are not present in the corresponding position of other ARFs. This leads to the hypothesis that a positively charged amino acid in position one of the motif, such as the Arginine (R) or Lysine (K) found in class B ARFs, is required for TPL/TPR interaction. To test this, the Arginine (R) in ETT was mutated to a Leucine (L) and the mutated version was screened for interaction with TPL/TPRs by Y2H (Figure 4.2 c and Appendix III Figure 2). Surprisingly, the interaction between TPL/TPRs and the mutated ETT version was not abolished, but strongly reduced, suggesting that a positively charged amino acid

at the first position of the motif stabilises the interaction but is not required for it. Moreover, the results suggest that in addition to the R/KLFGF/V/I-motif other residues in the protein may support or interfere with ARF-TPL complex formation.

Together, the results imply that interaction with TPL/TPR is not specific to ETT but a general feature of class B ARFs that might be important for auxin responsive gene regulation.

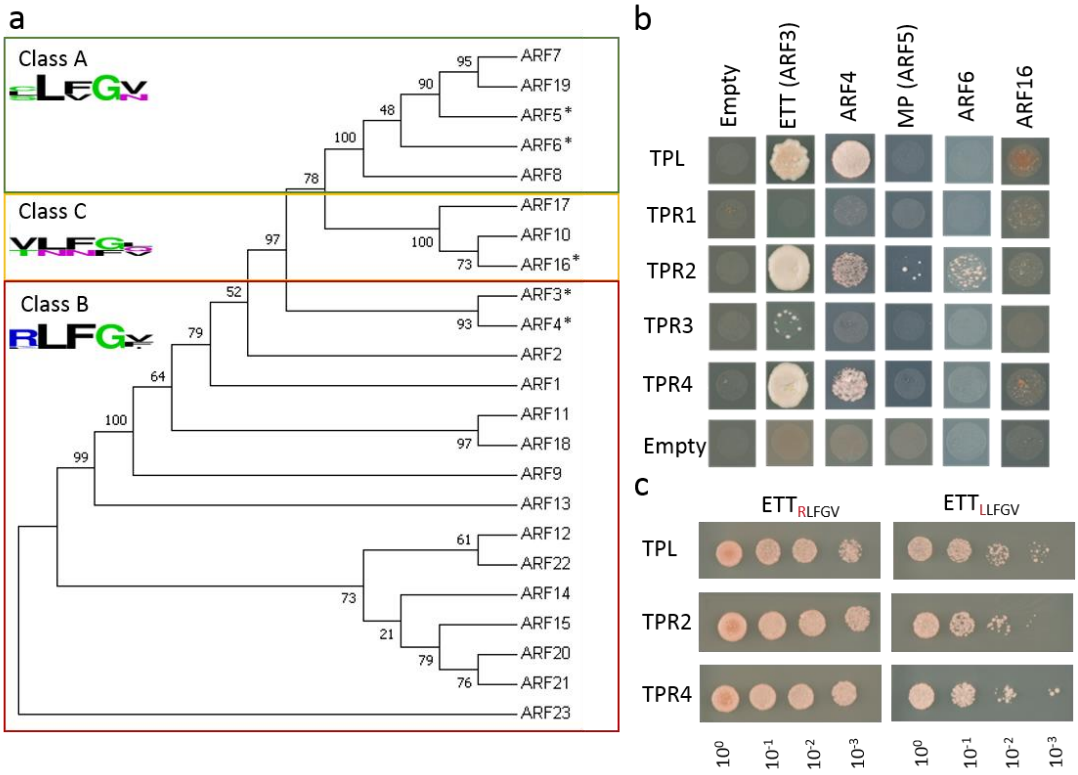

Figure 4. 2: Only Class B ARFs interact with members of the TPL/TPR co-repressor family via a conserved repressive motif. (a) the phylogenetic tree of all 23 Arabidopsis ARF protein sequences identified that the core of the repressive motif (LFG) is conserved among all ARF classes. However, the complete motif is only present in class B ARFs. Motifs are highlighted with sequence logos. (b) Representative ARFs of each class (indicated by * in a) were tested for interaction with members of the TPL/TPR co-repressor family in Y2H. Only class B ARFs can interact with several TPL/TPR family members. (c) a positively charged amino acid at the first position of the motif contributes to interaction strength. Mutating this position, however, does not disrupt the interaction but reduces interaction strength (supporting panels can be found in Appendix III Figure 2).

TPL interacts with the RLFGF-motif via its C-terminal region

In the previous sections, ETT was found to interact with TPL, TPR2 and TPR4. Moreover, mutating residues in the evolutionarily conserved RLFGF-motif abolished the interactions, demonstrating its requirement for the ETT-TPL/TPR interaction.

Several studies have established that the N-terminal CTLH domain of TPL/TPR proteins (Figure 4.3 a) is responsible for interaction with the EAR-motif (Ke et al., 2015; Martin-Arevalillo et al., 2017). By contrast, no domain mapping has been carried out for interaction with RLFGF-motifs. Given the structural differences between the LxLxL (EAR) motif and the RLFGF motif, I hypothesise that they may interact with different regions of TPL. To test this hypothesis, TPL was truncated into three different regions, two for the N-terminal part and one for the C-terminal part, and the ability of the fragments to interact with full length ETT, the ES domain alone, or the ES domain carrying the mutated RLFGF motif ($ES_{L->S;\ F->S}$) was tested using Y2H. The N-terminal truncations, TPL_{1-185} and TPL_{1-202} are identical to the TPL fragments that were previously used to solve the crystallographic structure of the *Arabidopsis* TPL N-terminal region (Martin-Arevalillo et al., 2017). This region contains the LisH and CTLH domains which are important for TPL tetramerization and interaction with EAR-motifs respectively. The third fragment includes the entire C-terminal region of TPL ($TPL_{185-1131}$). As expected, ETT and the wildtype ES domain were able to interact with the full length TPL, whilst $ES_{L->S;\ F->S}$ could not (Figure 4.3 b). In contrast, ETT and the wildtype ES domain did not interact with the two N-terminal TPL fragments but could interact with the C-terminal $TPL_{185-1131}$ region, whilst $ES_{L->S;\ F->S}$ did not interact with any TPL fragments, indicating that interaction between the TPL C-terminal fragment and ETT is mediated by the RLFGF motif (Figure 4.3 b).

The C-terminal region of TPL consists of 15 WD40 repeats. To further fine-map the RLFGF-interaction domain a series of truncations of the TPL C-terminal region were generated. Each construct encoded 6 WD40 repeats in such a way that constructs overlapped one another by at least one WD40 repeat ($TPL_{185-634}$, $TPL_{595-914}$, $TPL_{874-1131}$). Testing the interaction between the C-terminal fragments and the three ETT fragments showed that only $TPL_{185-634}$ can interact with ETT and ES, but not with ES_{L-}

$_{>S;\ F->S}$. This suggests that the $TPL_{185-634}$ region is responsible for RLFGF-motif binding in TPL-ETT interactions (Figure 4.3 b).

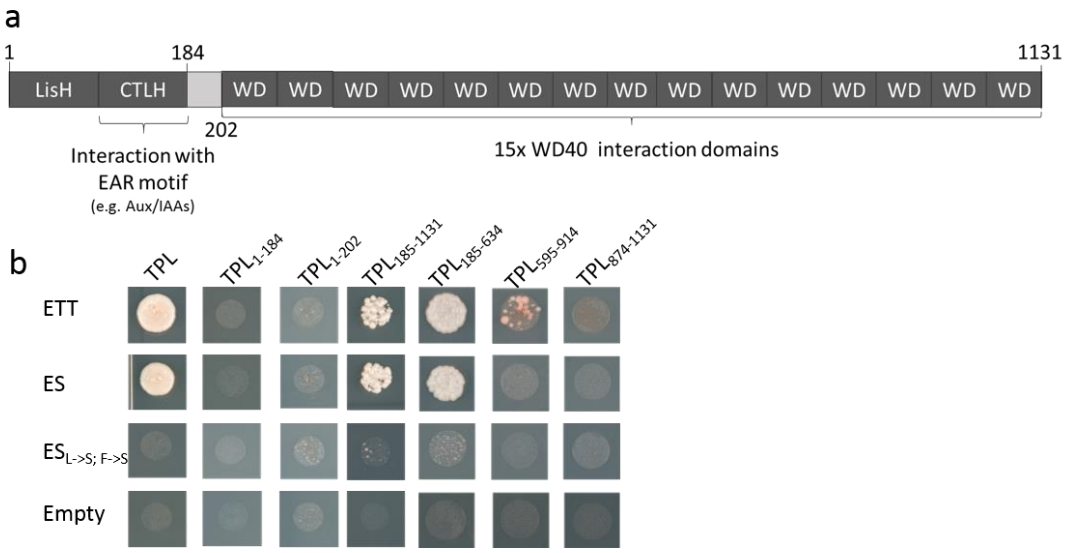

Figure 4. 3: ETT interacts with TPL via a region in the C-terminal part of the protein. (a) Schematic representation of the TPL protein highlighting the proteins domains and their position. (b) TPL interacts with ETT via a C-terminal region $TPL_{185-634}$ but not with the previously described CTLH domain that mediates interaction with EAR-motifs. ETT interacts with the C-terminal region of TPL via a RLFGF-motif within the ETTIN specific (ES) domain.

Remarkably, the results presented here for TPL binding to the RLFGF motif of ETT are in agreement with the results of a study that characterised the interaction of REL2 (Liu et al., 2019). REL2 is a member of the TOPLESS family in maize (*Zea mays*) that interacts with RLFGV- and DLN-type motifs (Gallavotti et al., 2010; Liu et al., 2019). Like the RLFGF-TPL interaction in *Arabidopsis*, RLFGV- and DLN-type motifs in maize interact with the C-terminal WD40 domain of REL2 rather than the N terminus. By screening the *REL2* mutant germplasm Liu and co-workers were able to identify an allele that carried a Glycine (G) to Aspartate (D) substitution at position 368 (G368D). Y2H and Co-IP showed that the mutation of this G368 residue was sufficient to abolish REL2-RLFGV and REL2-DLN interaction. Interestingly, the G368 residue is highly conserved between *Zm*REL2 and *At*TPL/TPRs (Appendix III Figure 3). Structural homology modelling showed that the loop region containing the G368 residue lies in the β-propeller 1 region of Groucho/TLE co-repressors which most

commonly mediate protein interactions in WD40 proteins (Buscarlet and Stifani, 2007; Jennings and Ish-Horowicz, 2008; Liu et al., 2019).

Altogether, the finding that TPL interacts with the RLFGF-motif in ETT via its C-terminal WD40 domains is analogous to the binding of its homolog in maize REL2 to RLFGV-motifs. Moreover, it is highly analogous to the TF motif binding by the WD40 domain of Groucho/TLE corepressors in animals, implying an even deeper level of mechanistic convergence (Buscarlet and Stifani, 2007; Jennings and Ish-Horowicz, 2008; Liu et al., 2019).

ETT-TPL/TPR interactions are specifically sensitive to IAA and not to other auxins

Chapter 3 showed that ETT-TPL interactions are sensitive to IAA in Y2H. This auxin-sensitivity has previously been described for other ETT-protein interactions as specific to the naturally occurring auxin, Indole-3-acetic acid (IAA) (Simonini et al., 2016). To test whether this is also the case for the ETT-TPL interaction, the effect of three auxinic compounds, IAA, 1-Naphthaleneacetic acid (NAA), and 2,4-Dichlorophenoxyacetic acid (2,4-D) were tested. Benzoic acid (BA), which is chemically related to auxin was used as a negative control. Y2H assays showed that 2,4-D and BA did not affect the interaction, while IAA completely abolished it (Figure 4.4 a). Interestingly, NAA appeared to reduce the interaction to an intermediate level. However, testing IAA and NAA in ONPG assays showed that only the effect of IAA, but not of NAA, was significant compared to a mock treatment (Figure 4.4 a, b). Thus, in agreement with previous results for other ETT-protein interactions, the sensitivity of the ETT-TPL interaction was specific to IAA as other auxinic compounds tested did not show this effect. Henceforth, ‘auxin’ will refer to IAA unless stated otherwise.

Supplementing yeast medium with 100 µM auxin completely abolishes the interaction between ETT and TPL. However, it is not clear whether lower auxin concentrations affect the interaction. To evaluate this, the ETT-TPL interaction was treated with auxin

concentrations ranging from 0 µM to 100 µM in Y2H assays. Unsurprisingly, the ETT-TPL interaction was completely abolished at 100 µM auxin but interestingly, a mild reduction was already observed at 25 µM IAA (Figure 4.4 c). Generally, interactions were reduced with increasing IAA concentrations. Even though supplementing auxin to the yeast growth medium is a suitable method to quickly screen the effects of auxin on an interaction, it does not reflect the *in planta* situation and has two main issues. Firstly, it is unclear how much auxin is taken up by the yeast cell. Secondly, yeast needs to be incubated at 28°C for several days to observe growth and it is unknown how much active auxin is still present in the growth medium after days of incubation due to chemical decay. Both issues may lead to an overestimation of the auxin concentration needed to disrupt auxin-sensitive interactions. To overcome these problems, co-immunoprecipitation (Co-IP) experiments, like those described in Chapter 3, were carried out with the addition of auxin to the IP and washing buffers in concentrations ranging from 0- 50 µM. Strikingly, the ETT-TPL interaction was reduced with increasing IAA concentrations, and is almost completely abolished at 25 µM auxin, and higher auxin concentrations have no further effect (Figure 4.4 d). To ensure that the dissociation was due to the addition of IAA, a similar experiment using NAA was performed as a negative control. As expected, none of the NAA concentrations tested affected the ETT-TPL interaction (Figure 4.4 e).

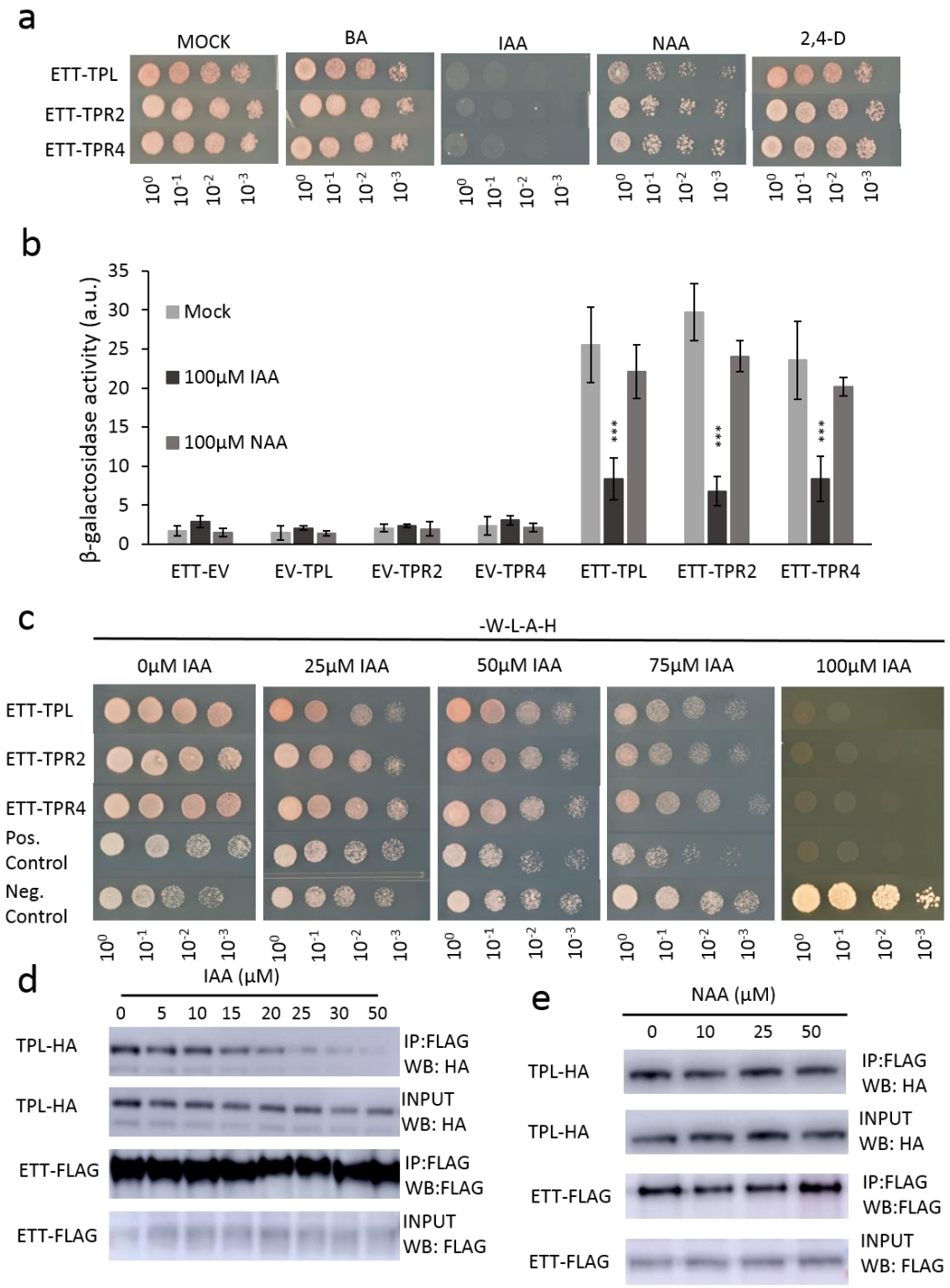

Figure 4. 4: Interaction between ETT and TPL, TPR2 and TPR4 is auxin-sensitive and specific to IAA. (a) Y2H to test specificity of auxin-sensitivity using BA, IAA, NAA, and 2,4D in a yeast growth assay. The data suggest that the auxin-sensitivity observed is IAA-specific. (b) Y2H based ONPG assay measuring the β-galactosidase activity as a measure of interaction strength showing that the interaction between ETT and TPL is insensitive to NAA. ***p <0.0001; Shown are mean ± standard deviation of three biological replicates. (c) In Y2H increasing concentrations of IAA lead to reduction of yeast growth abolishing the interaction between ETT and its partners. The interactions are, therefore, auxin-sensitive. (d) Co-IP revealed that ETT interacts with TPL in an auxin-sensitive manner. Increasing concentrations of IAA weaken the interaction. (e) Co-IP confirms that NAA has no effect in the ETT-TPL interaction strength.

In summary, like other ETT-protein interactions, the auxin-sensitivity of ETT-TPL interactions is specific to IAA as other auxinic compounds did not affect the interaction. In both Y2H and in Co-IP experiments, the interactions were reduced with increasing IAA concentrations (Figure 4.4). These results indicate that in conditions with low auxin levels, ETT can interact with TPL/TPR proteins to repress the expression of target genes. An increase in cellular auxin levels causes ETT to bind auxin (as described in Chapter 2) thereby undergoing a conformational change that abolishes interaction with TPL/TPR co-repressors.

ETT and TPL co-operatively recruit HDA19 to regulate gene expression during gynoecium development

TPL was originally identified as a key factor involved in setting up the apical-basal growth axis during embryo development (Long et al., 2006; Smith and Long, 2010). Large-scale interaction studies suggest that the five *Arabidopsis* TPL/TPRs have roles throughout plant development (Causier et al., 2012; Krogan et al., 2012). Whilst ETT has been implicated in a wide array of developmental processes (Garcia et al., 2006; Kelley et al., 2012; Marin et al., 2010; Pekker et al., 2005), the most dramatic phenotypes of *ett* loss-of-function mutants are observed during gynoecium development (Nemhauser et al., 2000; Sessions et al., 1997; Sessions, 1995). In support of this, *ETT* is highly expressed in the gynoecium (Figure 4.4 a). To test if their expression domains overlap with *ETT* expression in the gynoecium, reporter lines of *TPL*, *TPR2* and *TPR4* promoters fused to the *GUS* reporter gene were generated. Both *pTPL:GUS* and *pTPR2:GUS* exhibited strong expression in the apical part of the gynoecium where *ETT* is also expressed, while no *pTPR4:GUS* expression was observed (Figure 4.5 a-d). Next, expression of all *TPL/TPR* family members was examined using qPCR to confirm their expression. The result showed that *TPL* and *TPR2* but not *TPR1*, *TPR3* and *TPR4* are indeed expressed in the gynoecium (Figure 4.5 e).

This indicates that TPL and TPR2 are the primary members of the TPL/TPR2 family present during gynoecium development. A loss-of-function analysis would shed more light on this, and T-DNA insertion lines in the *TPL* and *TPR2* genes were obtained and genotyped (Alonso et al., 2003). The SALK 034518 line carried a homozygous T-DNA insertion in the twelfth exon of the *TPL* gene and will be referred to as the *tpl* mutant. T-DNA insertion lines that were received for insertion within the *TPR2* turned out not to contain any insertions and were therefore not suitable for analysis.

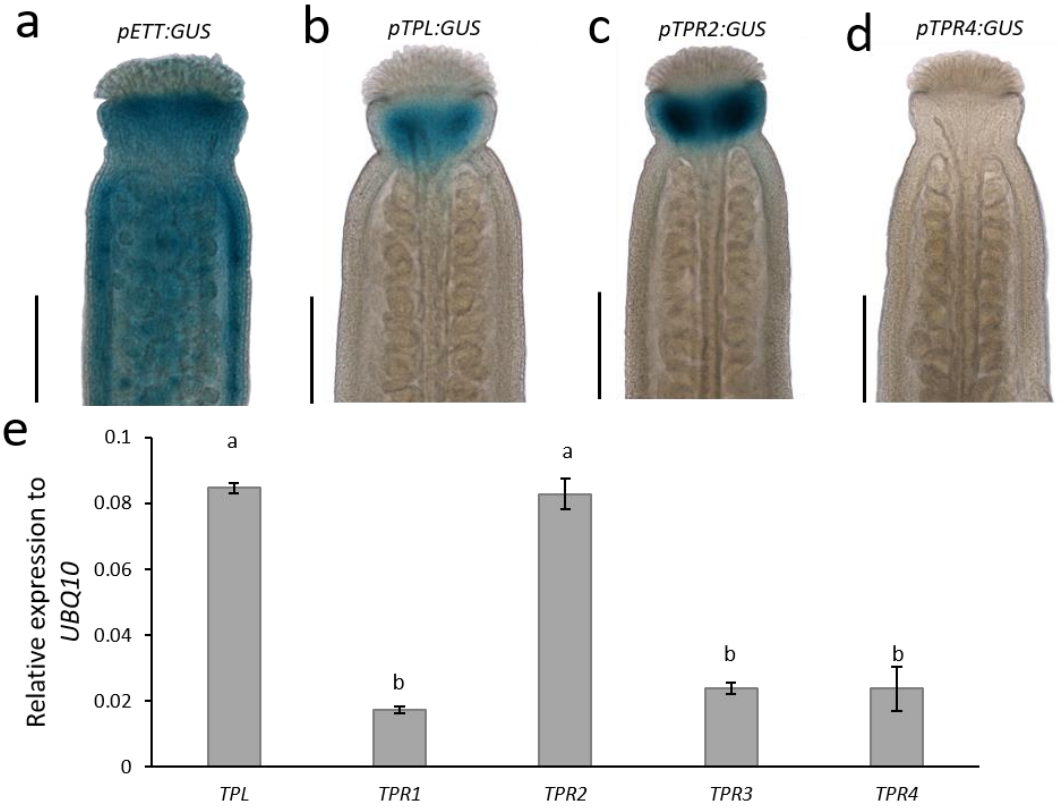

Figure 4. 5: *ETT*, *TPL* and *TPR2* but not *TPR4* are expressed in the style of the developing gynoecium. (a-d) Expression analysis of *pETT:GUS* (a), *pTPL:GUS* (b), *pTPR2:GUS* (c) and *pTPR4:GUS* (d) revealed that *ETT*, *TPL* and *TPR2* but not *TPR4* are expressed in the *Arabidopsis* style. Scale bar = 300 µm. (e) Expression analysis using qPCR in wild type gynoecia revealed that TPL and TPR2 are more strongly expressed than TPR1, 3 and 4. In panel e, a and b indicate significant difference p-Value <0.0001; Shown are mean ± standard deviation of three biological replicates.

To obtain a *tpr2* mutant allele, I decided to use CRISPR/cas9 genome editing in *Col-0* and *tpl* backgrounds to obtain single and double mutants. As a result, one single and one double mutant allele was produced (Figure 4.6 a, b). The mutant alleles were

named *tpr2*$^{GE-1}$ and *tpr2*$^{GE-2}$, where “GE” stands for “genome edited”. The *tpr2*$^{GE-1}$ allele contains a 611 bp deletion leading to a premature stop codon after 160 amino acids (Figure 4.6 a).

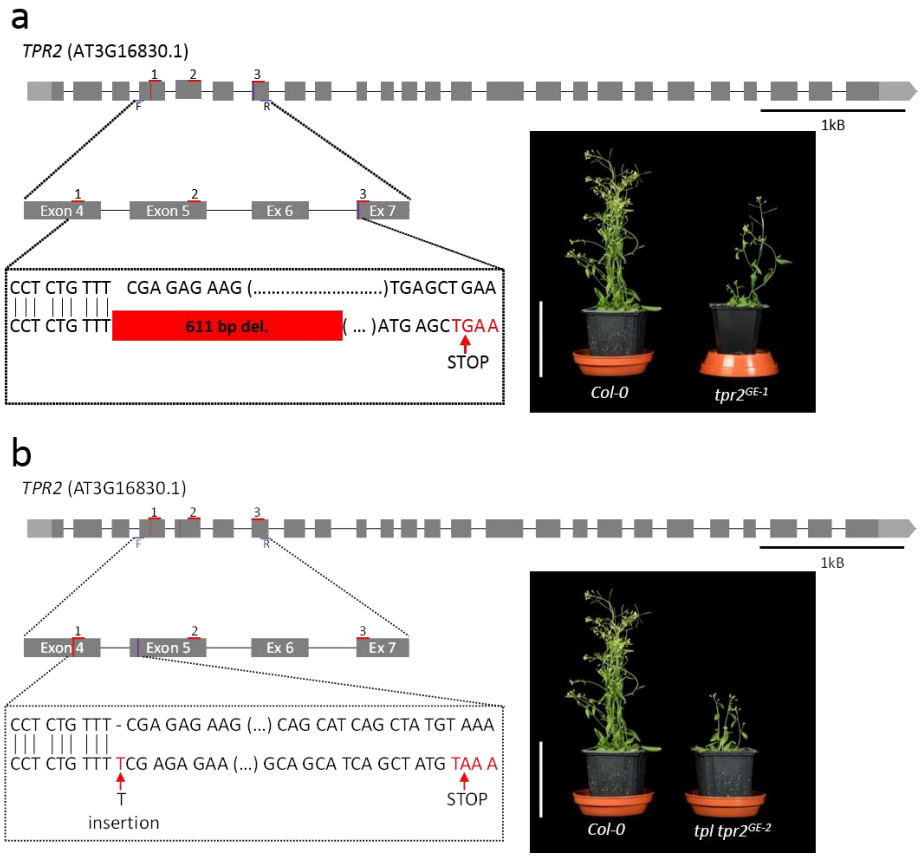

Figure 4. 6: *TPR2* mutant alleles generated using CRISPR/Cas9 in wild type and tpl background. (a) the *tpr2*$^{GE-1}$ allele shows a 611 bp deletion spanning across exon 5 and 6 generating a premature stop codon at the beginning of exon 7 (purple). The location of the guideRNAs within the *TPR2* gene are indicated in red. *tpr2*$^{GE-1}$ shows reduced plant height when compared to wild type (*Col-0*). Scale bar = 10 cm. (b) the *tpr2*$^{GE-2}$ allele shows a 1 bp insertion in exon 5 generating a premature stop codon in the same exon (purple). The location of the guideRNAs within the *TPR2* gene are indicated in red. *tpl tpr2*$^{GE-2}$ shows reduced plant height when compared to wild type (*Col-0*). Scale bar = 10 cm.

In contrast, *tpr2*$^{GE-2}$ was generated in the *tpl* background and is a *tpl tpr2* double mutant. The *tpr2*$^{GE-2}$ allele has a single bp insertion in exon 5 that leads to a frame shift and subsequently to a premature stop codon after 186 amino acids (Figure 4.6 b). The location of the premature stop codon makes both mutant alleles especially useful for studying their role in gynoecium development because they only encode

the N-terminal LisH and CTLH domains but not the C-terminal region that is essential for interaction with ETT.

Phenotypically, *tpr2*$^{GE-1}$ and *tpl tpr2*$^{GE-2}$ exhibit reduced plant height compared to wild type indicating that TPL/TPR proteins may not be fully redundant but might have specific functions in certain developmental contexts (Figure 4.7).

Despite having a slightly reduced plant height when compared to wildtype or *ett* mutant (Figure 4.7 a), single loss-of-function mutants in *TPL* and *TPR2* do not show any abnormal phenotypes during gynoecium development (Figure 4.7 b-d). However, the *tpl tpr2*$^{GE-2}$ double mutant has defects in the development of the apical gynoecium similar to *ett* mutants (Figure 4.7 e, f).

TPL and homologs have been shown to recruit the histone deacetylase, HDA19, during early *Arabidopsis* flower development to keep chromatin in a repressed state (Krogan et al., 2012). HDA19 is seemingly also required for gynoecium development as the *hda19-4* mutant has strong style defects (Figure 4.7 g). In agreement with this, the *HDA19* gene was highly expressed in gynoecium tissue, whereas another member of the *HDA* gene family that has previously been implemented in flower development, *HDA6*, was not expressed (Figure 4.7 h). HDA19 recruitment likely involves *ETT*, since expression of the ETT target genes, *PID* and *HEC1*, are increased in *ett-3*, *tpl tpr2*$^{GE-2}$ and *hda19-4* mutants compared to wildtype, with auxin treatment failing to further induce expression in these mutants (Figure 4.7 i, j). Together with the protein interaction data, these observations suggest that ETT, TPL/TPR2 and HDA19 function cooperatively to promote gynoecium development.

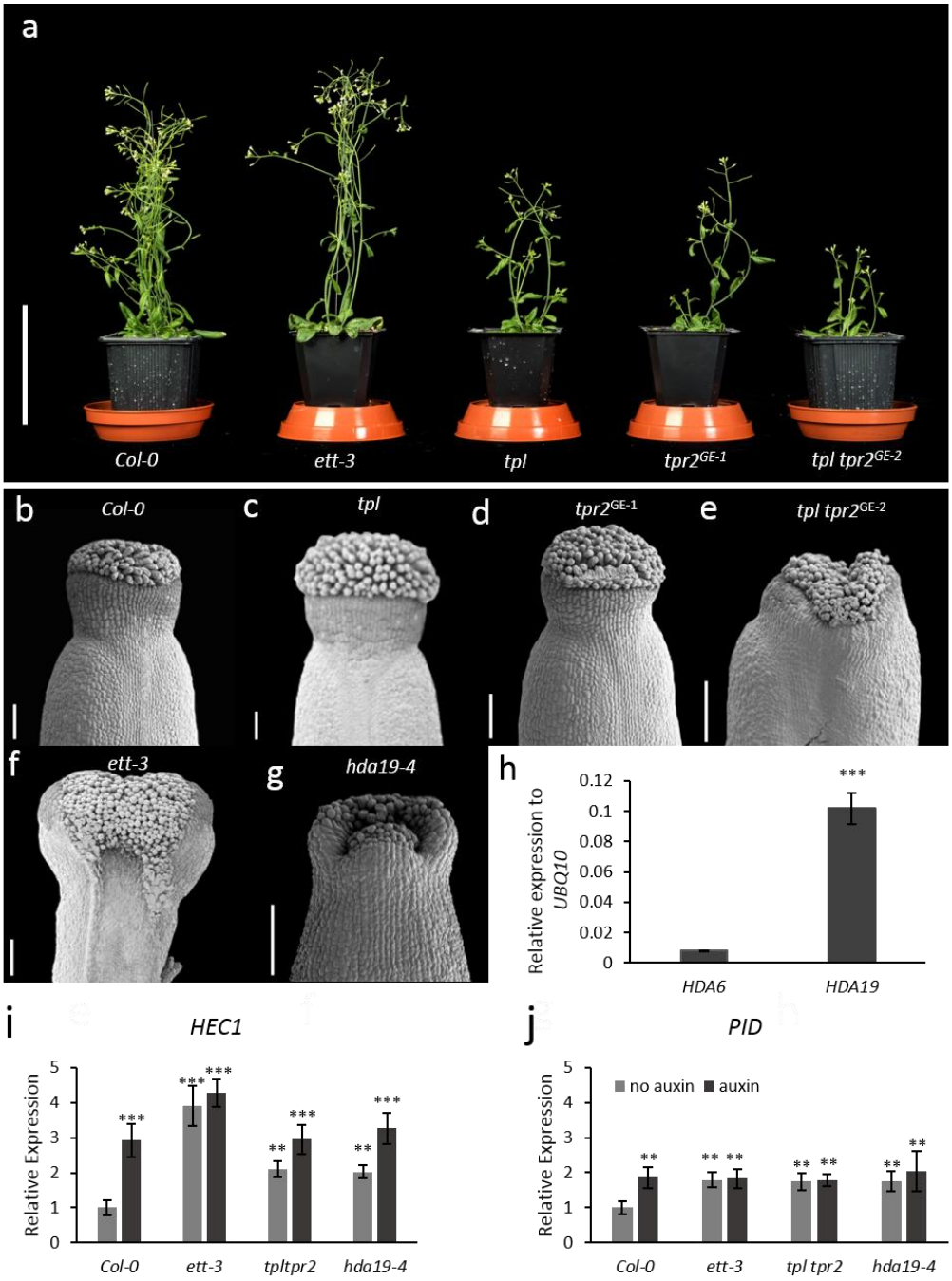

Figure 4. 7: ETT, TPL/TPR2 and HDA19 co-operatively regulate gene expression to facilitate gynoecium development. (a) *tpl, tpr2*$^{GE-1}$ and *tpl tpr2*$^{GE-2}$ show reduced plant height when compared to wild type (*Col-0*) and *ett-3*. Scale bar = 10 cm. (b-g) Gynoecium phenotypes of wild type (b), *tpl* (c) *tpr2*$^{GE-1}$ (d), *tpl tpr2*$^{GE-2}$ (e), *ett-3* (f) and *hda19-4* (g). Scale bar = 100 µm. (h) Expression analysis using qPCR in wild-type gynoecia showed that HDA19 exhibits higher expression compared to *HDA6*. (i-j) *HEC1* (i) and *PID* (j) are constitutively mis-regulated in *ett-3*, *tpl tpr2*$^{GE-}$ and *hda19-4* gynoecia. This mis-regulation is unaffected by treatment with 100 µM IAA. **p-Values<0.01; ***p-Values<0.0001 ; Shown are mean ± standard deviation of three biological replicates.

To test the direct interaction of ETT, TPL and HDA19 on chromatin, GFP-tagged translational reporter lines were obtained for all three proteins. Protein enrichment at

ETT binding sites within the *HEC1* and *PID* loci was evaluated using Chromatin-Immunoprecipitation (ChIP).

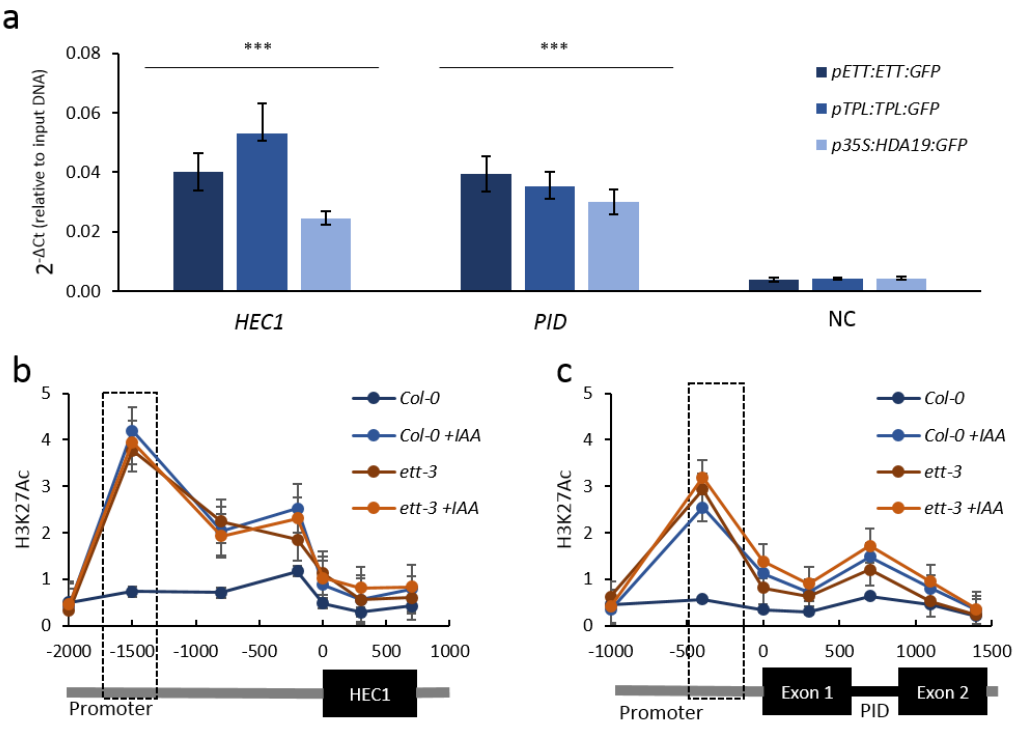

Figure 4. 8: ETT, TPL and HDA19 co-operatively regulate *HEC1* and *PID* by modulation of chromatin acetylation. (a) Chromatin immunoprecipitation (ChIP) shows ETT, TPL and HDA19 binding to conserved regions of *HEC1* and *PID* loci. *WUSCHEL* served as negative control (NC). (b, c) H3K27ac accumulation (from ChIP analysis) along the *HEC1* (b) and *PID* (c) loci in wild type (Col-0) and ett-3 plants ± treatment with 100 µM IAA. Numbers on the x axes indicate distance to the Transcription Start Site (TSS). The schematics of the loci are shown below each panel. Dashed boxes represent ETT binding regions (identical with regions presented in (a). The data presented in (b and c) have also been presented in Chapter 2 Figure 2.5 (e, f) and are shown here for convenience.

Although only ETT has a DNA-binding domain (DBD) and is, therefore, the only protein expected to bind DNA, $ChIP_{qPCR}$ revealed that all three proteins associate with DNA elements (Fig. 4.8 a). Moreover, they associate to the same regions of the promoters of *PID* and *HEC1* that have been identified as ETT binding regions previously (Chapter 2; Simonini et al., 2017; Simonini et al., 2016). This result supports a model in which ETT recruits TPL/TPR2 and HDA19 to ETT target loci to keep chromatin in a condensed state through histone deacetylation. When auxin levels increase, the ETT-TPL/TPR2 interaction dissociates, presumably preventing HDA19 recruitment leading to local loss of histone deacetylation. In Chapter 2, I

assayed H3K27 acetylation at *HEC1* and *PID*. The results show an increase in this histone modification in the *ett*-mutant and upon treatment with auxin. Remarkably, if comparing ETT, TPL and HDA19 occupancy with H3K27 acetylation across the examined loci it becomes apparent that the strongest increase of H3K27 acetylation occurred in the same regions of the *PID* and *HEC1* promoters where the proteins were otherwise found to associate (Figure 4.8 b, c). There was no further increase of acetylation in the *ett-3* mutant upon treatment with auxin (Figure 4.8 b, c and Chapter 2 Figure 2.5 e, f) supporting the hypothesis that ETT is mediating the association of TPL/TPR and HDA19 with these regions.

Discussion

The data presented in this chapter provide molecular insights into how TPL and ETT interact to co-operatively transduce auxin signals into changes in the local chromatin environment, and subsequently regulate the expression of ETT target genes.

ETT interacts with TPL/TPR via a conserved repressive domain

The Yeast 2-Hybrid (Y2H) library screen presented in Chapter 3 identified TPL as a protein that can interact with ETT in an auxin-sensitive manner. In *Arabidopsis*, the TPL/TPR family has five members of which three members, TPL, TPR2 and TPR4 can interact with ETT. To find out how ETT interacts with TPL/TPR proteins a phylogenetic analysis of ETT protein sequences across the angiosperm phylum was carried out identifying a RLFGF motif at the C-terminus of the ES domain with a high level of conservation. Similar to EAR-motifs, RLFGF sequences are repressive motifs, which are common in plant transcription regulators. EAR motifs are also found in Aux/IAA proteins and interactions between Aux/IAAs and members of the TOPLESS and TOPLESS-RELATED (TPL/TPR) family of co-repressors occur via this motif (Martin-Arevalillo et al., 2017). Mutating residues at the second and third position (L to S; F to S) in the RLFGF motif of ETT abolished the interactions with TPL/TPRs

demonstrating its requirement for this interaction. A phylogenetic analysis revealed that ETT, which is an atypical ARF lacking the PB1-domain, appears after the divergence of gymnosperms and angiosperms. ETT is therefore a specific ARF in flowering plants (Finet et al., 2013). In agreement with this, the most dramatic phenotypes of *ett* loss-of-function mutants are observed during gynoecium development. To test if TPL-ARF interactions through the RLFGF-motif is specific to ETT or could be a general feature of ARFs, all 23 *Arabidopsis* ARF protein sequences were compared. Interestingly, a core LFG-motif was conserved in most ARFs, however, class A and class C ARFs differed considerably in the flanking amino acids, whilst the RLFGF motif was completely conserved in most class B ARFs with minor synonymous amino acid changes. Y2H assays testing representative ARFs of each class that differ in their LFG-containing motifs found that only class B ARFs interact with TPL/TPRs. In this class of ARFs, a positively charged amino acid (R or K) is conserved at the first position of the motif and is found in neither class A nor class C ARFs. Rather than abolishing the interactions, mutation of the R/K residue only reduced the strength of the interactions, suggesting a role for this amino acid in the stabilization of ARF-TPL complexes. Finally, testing the auxin-sensitivity of ETT-TPL/TPR interactions showed that interactions were reduced with increasing IAA concentrations. Moreover, as described previously for other ETT-protein interactions, the sensitivity was specific to IAA as opposed to other auxinic compounds, which did not show this effect when tested.

ETT interacts with a region of the C-terminal WD40 domain in TPL

Canonical auxin signalling relies on binding of the auxin molecule to F-box proteins of the TIR1/AFB family (Dharmasiri et al., 2005; Kepinski and Leyser, 2005). This facilitates interaction with Aux/IAA transcriptional repressors, which become ubiquitinylated and subsequently degraded by the 26S proteasome (Leyser, 2018). When auxin levels are low, Aux/IAAs dimerise with ARFs to repress expression of

ARF target genes via the recruitment of chromatin-modifying enzymes (Kelley and Estelle, 2012; Leyser, 2018). Increased auxin levels therefore lead to the de-repression of ARF-targeted loci by mediating the degradation of the Aux/IAA repressors (Leyser, 2018). While this mechanism makes sense for activating ARFs belonging to class A, it is not clear why repression would be required for repressive ARFs. It cannot be assumed that repression of a repressor leads to activation since the co-repressor proteins such as TPL that are recruited by Aux/IAAs have a repressive effect in the local chromatin. Indeed, it is becoming increasingly evident, that protein-protein interactions between ARFs and Aux/IAAs are limited to class-A ARFs (Piya et al., 2014; Vernoux et al., 2011). Moreover, in class B ARFs the PB1 domain has been lost independently in various species during evolution of land plants (Chandler, 2016). ARF proteins lacking a PB1 domain presumably act independent from Aux/IAA repressors. Truncated versions of the class A ARFs MP, ARF7 and ARF19 that artificially lack the PB1 domain were shown to confer gain-of-function phenotypes and de-repressed auxin responsive genes, leading to the hypothesis that ARFs that cannot interact with Aux/IAA regulate downstream genes in an auxin-independent manner (Cho et al., 2013; Krogan et al., 2012). However, the ARFs used in these studies are not capable of interacting with TPL/TPRs directly. In contrast to that, class B ARFs, despite their inability to interact with Aux/IAAs, have been shown to regulate genes in an auxin responsive manner (Chung et al., 2019; Finet et al., 2013; Mutte et al., 2018; Simonini et al., 2017; Simonini et al., 2016). Consequently, the canonical auxin signalling pathway fails to explain how these ARFs regulate their downstream targets in response to auxin. Direct auxin-sensitive interactions between class B ARFs and TPL/TPR-type co-repressors support the existence of a non-canonical, Aux/IAA and TIR1/AFB independent auxin signalling pathway.

While several studies have established that the N-terminal CTLH domain of TPL/TPR proteins mediates interaction with EAR peptides (Ke et al., 2015; Ma et al., 2017;

Martin- Arevalillo et al., 2017), little is known about the domain required for interaction with RLFG-motifs. A series of truncated TPL fragments were tested for interaction with ETT. The results identified a region C-terminal of the EAR-interacting CTLH domain that was sufficient to mediate interaction with the RLFG-motif. Interestingly, the discovered region shows high conservation with a region that has recently been characterised as an RLFG-interacting domain in REL2 (the TPL orthologue in Maize) (Liu et al., 2019). In this study, Liu et al. identified a glycine residue (G368) that is responsible for the interaction with RLFG-motifs. REL2 and TPL/TPRs belong to a group of evolutionarily conserved Groucho/TLE co-repressors. Intriguingly, the G368 residue lies in the WD40 domain that forms the β-propeller 1 structure of Groucho/TLE co-repressors, which is often found to mediate protein interactions and, which is highly conserved among eukaryotes (Buscarlet and Stifani, 2007; Jennings et al., 2008; Liu et al., 2019). Collectively, the several lines of evidence, presented here and by others, indicate that TPL and homologs bind RLFG-motifs via a C-terminal WD40 domain. This mode of interaction is highly analogous to the binding of LxIxIL-motifs by WD40 domains of Groucho/TLE co-repressors in animals (Jennings and Ish-Horowicz, 2008; Jennings et al., 2008) revealing a deeper level of mechanistic convergence. Finally, the identification of an interaction domain at the C-terminal region in addition to the known CTLH and LisH domains provides further evidence to support the hypothesis that Groucho/TLE co-repressors provide a hub for interaction with numerous proteins to form large protein complexes.

TPL/TPR and HDA19 are required for gynoecium development

Interaction between several members of the TPL/TPR family and ETT suggests a role for these proteins in gynoecium development. Both *pTPL:GUS* and *pTPR2:GUS* exhibited strong expression in the apical part of the gynoecium where ETT is also expressed. Presumably due to redundancy, single loss-of-function mutants in *TPL* and *TPR2* did not show any obvious abnormal phenotypes during gynoecium

development. However, the *tpl tpr2* double mutant has defects in the development of the apical gynoecium similar to *ett* mutants. GROUCHO/TLE co-repressors recruit histone deacetylases and regulate the local chromatin environment of target genes across all kingdoms. TPL interacts with HDA19 which has previously been shown to keep chromatin in a repressed state during early *Arabidopsis* flower development (Krogan et al., 2012). Seemingly, HDA19 is also required for gynoecium development as the *hda19-4* mutant has strong style defects. Together with the protein interaction data, these observations suggest that ETT, TPL/TPR2 and HDA19 function cooperatively to promote gynoecium development.

TPL and HDA19 interact with *PID* and *HEC1* loci at same locations as ETT

ChIP followed by qPCR revealed that TPL and HDA19 associate with DNA elements in the same regions of the *PID* and *HEC1* promoters that are bound by ETT. This observation supports a model in which ETT recruits TPL/TPR2 and HDA19 to its target loci to keep chromatin in a condensed state through histone deacetylation when auxin levels are low. When auxin levels increase, the ETT-TPL/TPR2 interaction is lost, presumably preventing HDA19 from deacetylating histones (Figure 9). In Chapter 2, H3K27 acetylation, which is a substrate for HDA19, was assayed at the *HEC1* and *PID* locus. H3K27 acetylation increased in the absence of ETT and upon treatment with auxin. The strongest increase occurred in the same regions of the *PID* and *HEC1* promoters where the proteins were otherwise found to associate. In agreement with ETT mediating the association of TPL/TPR and HDA19 at these regions, there was no further increase of acetylation in the *ett-3* mutant upon treatment with auxin.

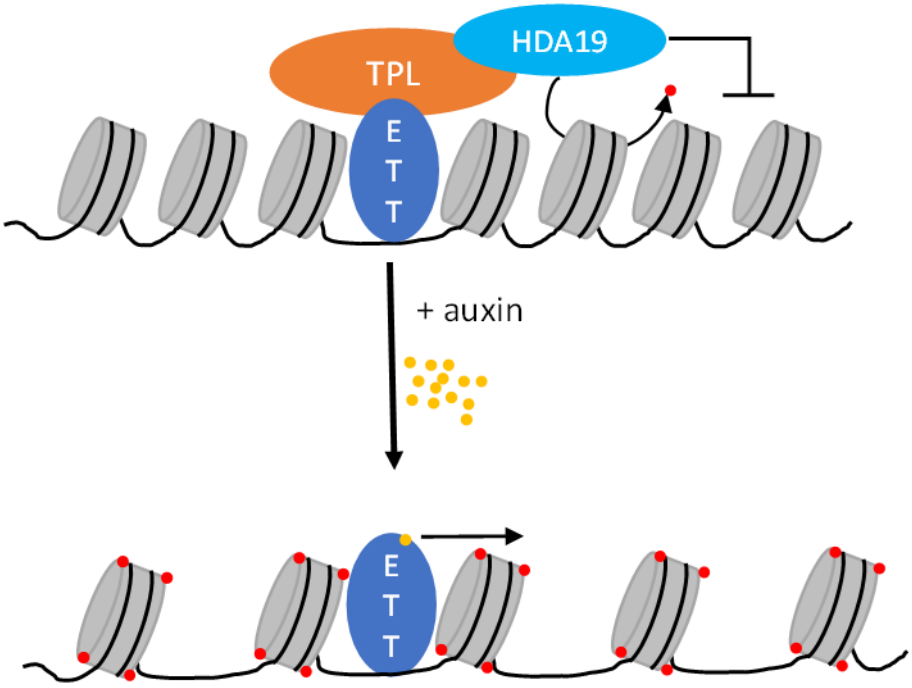

Figure 4. 9: Schematic model illustrating non-canonical auxin signalling. Under low auxin conditions an ETT-TPL-HDA19 complex binds to ETT-target genes keeping their chromatin environments repressed, through de-acetylation. High nuclear auxin concentrations abolish the ETT-TPL-HDA19 complex through direct ETT auxin interaction. This leads to an accumulation of histone acetylation and up-regulation of ETT-target genes.

Collectively, these data provide molecular insights into how auxin levels are translated into changes in gene expression at ETT target loci. The model depicted in Figure 4.9 agrees with previous data showing auxin dynamics at the gynoecium apex, where *PID* expression is repressed during the early stages of gynoecium development to mediate radialization of the style, and subsequently de-repressed as auxin levels rise to facilitate polar auxin transport (Moubayidin and Ostergaard, 2014; Simonini et al., 2016). Finally, the results in this chapter also support a role for co-repressors in the recruitment of HDA19 during the repression of *STM* by ETT and ARF4, a hypothesis which was suggested in a recent study (Chung et al., 2019).

Concluding remarks

The direct effect of auxin on ETT-TPL/TPR interactions is central to the non-canonical auxin signalling pathway. This pathway is fundamentally different from the canonical TIR1/AFB-mediated auxin signalling pathway as it does not require the degradation

of its core components. Moreover, the auxin molecule does not affect whether ETT is bound to DNA (Simonini et al., 2016). The effect of auxin is therefore instantly reversible, making it possible to switch between activating and repressive states immediately in response to changes in auxin levels. This feature is reminiscent of animal hormonal signalling pathways such as the Thyroid Hormone and Wnt/ß-catenin pathways (Gammons and Bienz, 2018; Tsai and O'Malley, 1994) and may be particularly important in controlling changes in tissue polarity during plant organogenesis. It is possible that auxin functions like the Thyroid Hormone and ß-catenin in Wnt signalling (see Introduction) by inducing a conformational change in the ETT protein, which then triggers the dissociation of ETT-TPL/TPR complexes and mediates a repression-to-activation switch of the ETT-containing regulatory complex at ETT target genes.

Future work will focus on understanding different aspects concerning the structural basis of the ETT and TPL interaction. This involves understanding the mechanistic and structural similarities between non-canonical auxin signalling and animal signalling and requires knowledge about the kinetics of the ETT-TPL interaction and how this interaction is affected by auxin. The identification of the region within the TPL protein that is responsible for interaction with the RLFGF-motif in ETT, and a version of ETT that cannot bind to auxin will be crucial to experimentally answer the questions raised above. Both the ETT-TPL interaction and the effect of auxin on the interaction can be initially studied by Isothermal Titration Calorimetry (ITC) or Surface Plasmon Resonance (SPR) and should ultimately provide near-atomic insight using Nuclear Magnetic Resonance (NMR) and crystallography. Furthermore, future work evaluating the auxin sensitivity of the interaction between TPL and other class B ARFs will show whether non-canonical auxin signalling is specific to ETT or a common alternative pathway of auxin signalling among class B ARFs.

Finally, the identification of the auxin-sensitive interaction between ETT and Groucho/TLE-type co-repressors in plants could help to explain how those ARFs which cannot interact with components of the canonical pathway integrate auxin signals in diverse processes throughout plant development. Furthermore, it suggests that other transcription factors may also bind auxin and that the direct regulation of transcription factor interactions by hormones and other small molecular regulators could be a more general feature of plant biology.

Materials and Methods

Plant materials and treatments

Plants were grown as described in Chapter 2. All mutations were in the Col-0 background. For both expression and ChIP analysis, auxin treatments were applied by spraying, as described in Chapter 2. Mutant alleles described before include *ett-3* (Sessions, 1995; Simonini et al., 2016), *hda19-4* (SALK_139443) (Kim et al., 2008), *pETT:ETT-GFP in ett-3* (Simonini et al., 2016), *pTPL:TPL:GFP* (Pi et al., 2015) and *p35S:HDA19:GFP* (Pi et al., 2015).The *tpl* mutant (SALK_034518C) was obtained from the Nottingham Arabidopsis Stock Centre (NASC). The *hda19-4* mutant was kindly provided by Dr. Julia Questa (Dean Group, John Innes Centre, Norwich, UK) and the *pTPL:TPL:GFP* and *p35S:HDA19:GFP* seeds were kindly shared by Prof. Thomas Laux (BIOSS Centre for Biological Signalling Studies/Universität Freiburg, Freiburg im Breisgau, Germany).

Genotyping of insertion lines

All plant lines were genotyped as described in Chapter 3 using the appropriate primers (Appendix III Table 1).

ETT protein analysis by alignment

Published *ETT* sequences of 22 angiosperm species were retrieved from Phytozome version 12 (Rokhsar et al., 2011). Nucleotide sequences were translated and aligned using MUSCLE in Geneious version 6.1.8 (Kearse et al., 2012). The RLFG-domain was extracted as a sequence logo.

For the protein sequence analysis of the 23 Arabidopsis ARFs, sequences were retrieved from TAIR (https://www.arabidopsis.org/) and aligned using MUSCLE in MEGA version 7.0 (Kumar et al., 2016). The gene tree was generated in MEGA using the Maximum Likelihood method.

Protein interaction

Yeast 2-Hybrid (Y2H) and co-immunoprecipitation cloning and assays were carried out as described in Chapter 3. All primers used for cloning can be found in Appendix III Table 1.

Co-IP experiments were carried out as described in Chapter 3. To examine auxin sensitivity by Co-IP, 4 g of fresh leaf tissue was collected, ground in liquid nitrogen and protein was extracted. The lysate was then divided according to the number of treatments. The desired concentration of IAA or NAA was added to each of the cleared lysates prior to the addition of the anti-FLAG M2 magnetic beads. IAA or NAA at the desired concentration was also supplemented to the IP buffer during the washes. The eluates were analysed by western blot as described in Chapter 3.

***TPL*, *TPR2* and *TPR4* reporter lines**

For the construction of the promoter:GUS reporter plasmids of *TPL*, *TPR2* and *TPR4*, 2.5 kb of promoter sequences were isolated from genomic DNA and inserted upstream of the ß-glucoronidase gene of pCambia1301 vectors using the In-Fusion Cloning Recombinase kit (Clontech) following the manufacturer's instructions. The constructs were transformed into *Agrobacterium tumefaciens* strain GV3101 by

electroporation, followed by plant transformation by floral dip as described in Chapter 3. GUS histochemical assays were also performed as described in Chapter 3.

Phenotypic analysis

Photos of whole plants were taken by Phil Robinson (Bioimaging, John Innes Centre, Norwich, UK) and Scanning Electron Microscopy was carried out as described in Chapter 2.

Expression analysis

RNA was extracted from 100mg dissected stage 12-14 gynoecia as described in Chapter 2. cDNA synthesis and qPCR were carried out for expression analysis as described in Chapter 2 using the appropriate primers (Appendix III Table 1).

Generation of the *tpl tpr2* CRISPR mutant

The *tpr2*$^{GE-1}$and *tpl tpr2*$^{GE-2}$ mutant was generated using CRISPR/Cas9 technology by a method previously described (Castel et al., 2019). Briefly, for the construction of the RNA-guided genome-editing plasmid, DNA sequences encoding the gRNA adjacent to the PAM sequences were designed to target two specific sites in *TPR2* (AT3G16830). DNA-oligonucleotides (Appendix III Table S1) containing the specific gRNA sequence were synthesised and used to amplify the full gRNA from a template plasmid (AddGene #46966). Using Golden Gate cloning (see Chapter 3; Engler et al., 2014) each gRNA was then recombined in an L1 vector downstream of the U6 promoter (Castel et al., 2019). Finally, the resulting gRNA plasmids were then recombined with a L1 construct containing *pYAO:Cas9_3:E9t* (kindly provided by Prof. Jonathan Jones, The Sainsbury Laboratory, Norwich, UK) and a L1 construct containing Fast-Red selection marker (AddGene #117499) into a L2 binary vector (AddGene #112207).

The construct was transformed into *Agrobacterium tumefaciens* strain GV3101 by electroporation, followed by plant transformation by floral dip into the *tpl* single mutant

(Clough and Bent, 1998). Transgenic T0 seeds appear red under UV light and were selected under a Leica M205FA stereo microscope. T0 plants were genotyped using PCR (as described above) and the *TPR2* locus sequenced using the Euronfins Mix2Seq sequencing Kit (Eurofins Genomics) according to the manufacturer's instructions (Primers: Appendix III Table 1). Genome-edited plants were selected, and the next generation grown (T1). Seeds of this generation were segregating in a 3:1 ratio for the transgene. Transgene negative plants were selected and grown on soil. To find homozygous mutations T1 plants were genotyped again. The T2 generation was re-checked for the absence of the transgene by selecting for seeds that do not appear red under UV light and were selected under a Leica M205FA stereo microscope.

Chromatin Immunoprecipitation (ChIP) qPCR

ChIP was performed in triplicate on the *pETT:ETT:GFP*, *pTPL:TPL:GFP* and *p35S:HDA19-GFP* lines using 5 g (fresh weight) inflorescence tissue as described in Chapter 2. Histone acetylation ChIP data for *Col-0* ±auxin treatment and untreated *ett-3* have previously been presented in Chapter 2. H3K27 acetylation ChIP for treated *ett-3* was carried out analysed using the same protocol.

In all ChIP experiments, DNA enrichment was quantified using quantitative PCR (qPCR) with the appropriate primers (Table S1) and the data were analysed as described in Chapter 2.

Statistical analyses and replication

In all graphs, error bars represent the standard deviation of the mean for all numerical values. qPCR and ChIP experiments have been carried out at least in triplicate. The data presented here show an average of three replicates. For qPCR data were analysed using one-way ANOVA with post-hoc Tukey multiple comparison test. $ChIP_{qPCR}$ data were analysed using two-way ANOVA with post hoc Bonferroni multiple

comparison test. Statistical tests were carried out using GraphPad Prism Version 5.04 (La Jolla California USA, www.graphpad.com).

Chapter 5

Two cis-regulatory elements fine-tune *PINOID* expression during gynoecium development

Introduction

In previous chapters I explored the mechanistic and biochemical basis of complex formation in alternative auxin signalling. While these chapters focussed mainly on the role of trans-factors in gene regulation, Chapter 5 will focus on the importance of cis-regulatory elements in the regulation of auxin responsive genes. To do this, I investigated the importance of cis-regulatory elements in gynoecium development using the *PINOID* (*PID*) gene as model.

Great efforts have been made in understanding how eukaryotic transcription factors can specifically recognize the genes that they are regulating (Furey, 2012; Godoy et al., 2011; Jolma et al., 2010). Eukaryotic transcription factors recognise small specific DNA sequences present in regulatory regions of their target genes. These regulatory DNA sequences are called cis-regulatory elements. Loss or mutation of these cis-regulatory elements can dramatically impact an organism's lifestyle and development (Questa et al., 2016; Yamaguchi et al., 2013). Thus, the first element that provides specificity to transcription factor- DNA interactions is the DNA sequence itself. Specific binding to these sequences depends on protein sequence and structure of the transcription factor and the range of biophysical interactions that the transcription factor properties permit (Boer et al., 2014). In many cases members of transcription factor families, such as the ARF family, share affinity for the same DNA motif, yet regulate different genes (Boer et al., 2014; Franco-Zorrilla et al., 2014; Merika and Orkin, 1993). The mechanisms that truly provide target-specificity in these transcription factor families are widely unknown. Since a typical cis-element is 6 bp, a specific DNA sequence would occur 1,000s of times in most eukaryotic genomes purely by chance (1 in 4,096bp for a 6-bp element). This indicates that specific DNA binding may require additional levels of control to ensure regulation of target genes complies with developmental needs. As discussed previously in Chapter 2, chromatin structure and DNA accessibility can be considered as another element specifying

gene regulation and DNA binding by transcription factors. The third element to further fine-tune specific DNA binding is the ability of the transcription factor to interact and cooperate with other DNA binding proteins. In this thesis, complex formation has been discussed in more detail in Chapter 3 and Chapter 4. Regardless of whether a transcription factor complex is homo- or heterotypic the conformation of the complex increases the number of cis-regulatory elements needed for specific binding. In the case that a transcription factor complex is heterotypic and thus consists of transcription factors from different families the number as well as the sequence of cis elements matters for binding specificity (Olsen et al., 2005; Singh, 1998; Wunderlich and Mirny, 2009; Xu et al., 2006).

Auxin Response Factors (ARFs) are transcription factors that are responsible for regulating numerous developmental processes during a plant's lifespan in response to the plant hormone auxin (indole-3-acetic acid or IAA). Impaired response to auxin can lead to severe flower defects and low fertility, as in case of *arf6/8* and *arf3* (*ett*) mutants or even plant death, as in case of the *arf5* mutants, which cannot form a root (Berleth and Jurgens, 1993; Sessions et al., 1997; Tabata et al., 2009). Through their B3 DNA-binding domain (DBD), ARF proteins bind to cis-regulatory elements composed of six base pairs that are called Auxin Responsive Elements (AuxREs). The AuxRE motif has the sequence TGTCNN and was first discovered and characterised in the late 1990's in the promoter of the soybean GH3 auxin responsive gene (Ulmasov et al., 1997a). Since then it has been characterised in more detail concerning its biophysical and regulatory properties (Boer et al., 2014; Liao et al., 2015; O'Malley et al., 2016; Omelyanchuk et al., 2017; Stigliani et al., 2018; Ulmasov et al., 1999a; Ulmasov et al., 1999b). Systematically mutating AuxREs in the auxin-responsive gene *LEAFY* confirmed the physiological importance of AuxREs for auxin response (Boer et al., 2014; Yamaguchi et al., 2013).

In recent years structural and genetic studies have identified two different modes of ARF-ARF complex formation each of which is expected to impact upon the DNA binding specificity (Boer et al., 2014). Firstly, it was shown that the C-terminal PB1 domain found in most ARFs can mediate head-to-tail multimerization (Korasick et al., 2014). Secondly, ARFs appear to dimerise through their DBD that would facilitate high-affinity binding to inverted repeat AuxREs (Boer et al.,2014, Heather McLaughlin personal communication). Intriguingly, in a natural variant of *Brassica rapa* with abnormal seed size, the effect was shown to be caused by a mutation that affected ARF18 DBD dimerization, which suggests that this property may be generally important for ARF function (Liu et al., 2015). Finally, there is increasing evidence that ARF DNA-binding specificity depends on orientation and spacing between AuxRE repeats. It seems that different ARFs prefer different binding site arrangements and that such arrangements rather than AuxRE sequence determine ARF-binding specificity (O'Malley et al., 2016; Stigliani et al., 2018). Despite these studies, complex DNA-binding sites and transcription factor-DNA binding have not been studied systematically for the ARF family. The main reason for that is the lack of high-quality data on validated target sites (e.g. through ChIP-seq) and protein-protein interaction studies (e.g. through IP MS/MS). This may be due to a low abundance of ARF proteins and rapid protein turn-over that make studies increasingly difficult.

The ETT protein is an ARF that has been implemented in several key developmental processes including gynoecium and fruit development (Sessions et al., 1997). Recent studies on protein-protein interactions identified a diverse range of proteins that directly interacts with ETT (Simonini et al., 2016; Simonini et al., 2017; this thesis). These proteins include several transcription factors from different families (Simonini et al., 2017; Simonini et al., 2016). One of the identified interacting partners of ETT is the bHLH transcription factor INDEHISCENT (IND). IND is required for the formation of the valve margins; a tissue that allows the Arabidopsis fruit to open and disperse

the seeds upon maturation (Liljegren et al., 2004). Additionally, IND was implemented in the control of polarity and symmetry transition at the apex of the gynoecium during development. Hereby, IND cooperates with the bHLH transcription factor SPATULA (SPT, Girin et al., 2011; Moubayidin and Ostergaard 2014). In both processes, IND mediates its function at least in part by controlling auxin distribution (Girin et al., 2011; Moubayidin and Ostergaard, 2014; Sorefan et al., 2009). IND coordinates directional auxin flux by direct repression of the *PINOID* (*PID*) gene, which encodes a serine–threonine kinase that is fundamental for proper symmetry establishment (Moubayidin and Ostergaard, 2014; Sorefan et al., 2009). PID phosphorylates PIN-FORMED (PIN) auxin efflux carriers their localisation and activity and thereby mediates polar auxin transport (Benjamins et al., 2001; Friml et al., 2004; Lee and Cho, 2006).

Detailed characterisation of the ETT-IND interaction has shown that these two proteins control polarity at the gynoecium apex by direct regulation of *PID* gene expression. Two AuxREs in position -429 and -447 with respect to the start codon were identified as ETT-binding sites using chromatin immunoprecipitation (ChIP) using an ETT-GFP transgenic line and an antibody against GFP (Simonini et al., 2016). This inverted AuxRE repeat lies firstly, within a region that is evolutionarily conserved among *PID* promoters in the *Brassicaceae* family (Figure 5.1 a), secondly, in close proximity of two G-Boxes and one an E-Box which are putative SPT and IND binding sites, respectively (Figure 5.1 b). Together, this makes the locus a complex regulatory patch within the *PID* promoter. Prior experiments showed that the loss of either ETT or both ETT and IND function leads to mis-regulation of *PID*. In addition, *in vitro* studies using yeast-one-hybrid (Y1H) experiments showed that mutating the identified AuxRE inverted repeat leads to loss of ETT binding (Simonini et al., 2016). Together, this suggests an important role for the two AuxREs *in planta*. SPT and IND binding to the G- and E-boxes close to the AuxRE repeat have only been studied by Y1H (Sorefan et al., 2009; Girin et al., 2011). This prior knowledge on the regulation

of the *PID* locus makes it a suitable model for *in planta* studies of cis-regulatory elements and their biological relevance in the context of complex regulatory regions within promoters.

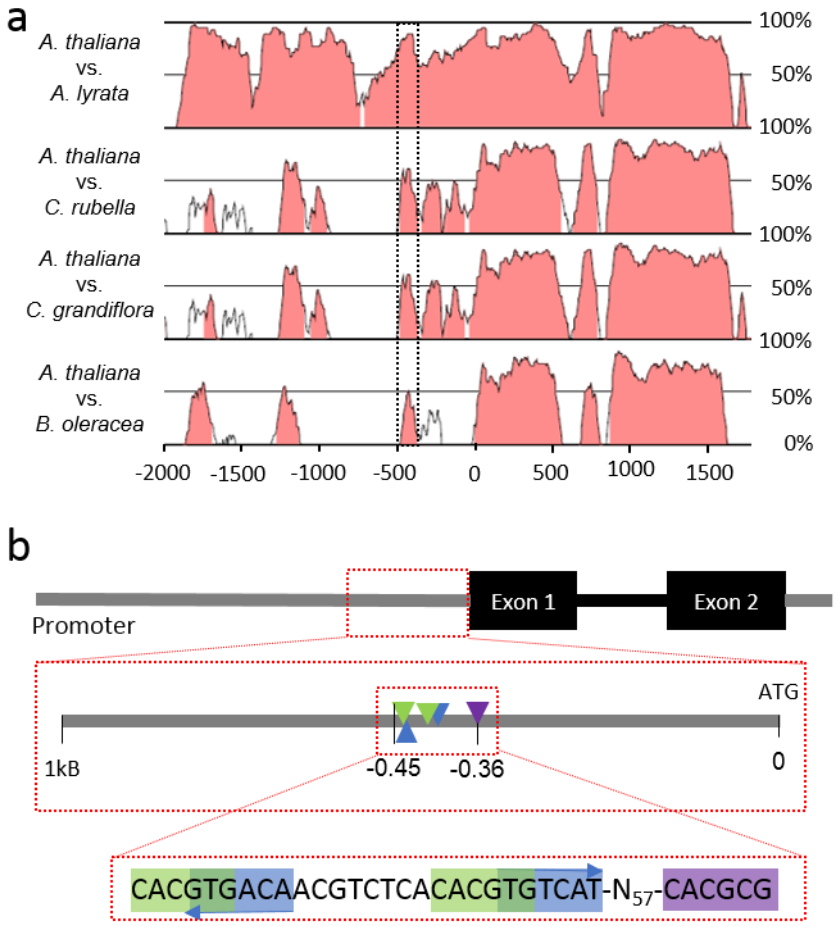

Figure 5. 1: Several different cis-regulatory elements can be found within a conserved region of the *PID* promoter. (a) Phylogenetic shadowing using mVISTA of the *PID* locus with pairwise alignments of *Arabidopsis thaliana* with *Arabidopsis lyrata*, *Capsella rubella*, *Capsella grandiflora* and *Brassica oleracea*. The box highlights the complex regulatory region. (b) Schematic representation of the arrangement of AuxREs, G-boxes and E-box (purple) within the complex regulatory region. Notice the G-boxes (green) overlap with the AuxREs (blue).

In this chapter, I address the biological importance of these two specific AuxREs for the regulation of the *PID* gene *in vivo*. Furthermore, I address the question whether IND can bind the previously identified E-box within the *PID* promoter *in planta*. Together, I aim to examine the requirement of complex AuxREs for the regulation of ARF target genes using the *PID* promoter as a model.

Results

Mutation of cis-regulatory AuxREs within the *PID* promoter affects style length

To elucidate the relevance of the identified two AuxRE sites for the regulation of *PID* different constructs were generated and introduced into the *pid-8* mutant. Each of these constructs carries 5 kb of the *PID* promoter region upstream of the *PID* genomic sequence fused to GFP. The 5-kb promoter region either carries a wild-type form of the two previously discussed AuxREs or mutated versions of this region. Hereby, the G at the second positions of the AuxRE was mutated into a T to prevent ARF promoter binding as previously described (Boer et al., 2014, Simonini et al., 2016). Using this approach, single mutants in the first (-434) and second (-447) AuxRE as well as a double mutant for both sites were generated (named 1M, 2M and 1+2M, respectively). In addition, the construct also carries a nuclear-localised mCherry gene under control of a constitutive *ACTIN2* (*ACT2*) promoter. This part of the construct enables quantitative studies of gene expression because it can be used to normalise expression for genome localisation of the integrated construct.

The *pid-8* mutant phenotype shows a dramatic reduction in fruit size and a reduction of the valves (Moubayidin and Ostergaard, 2014). Interestingly, all four constructs could rescue the *pid-8* phenotype regarding the defects in valve development and silique length (Figure 5.2 a-c). However, it seemed that the style of the fruits was enlarged in different mutants. Therefore, we measured the style length and compared it to wild-type (*Col-0*). Over ten independent lines we measured five styles per line in all four promoter mutants and the wild type (*Col-0*) and found that indeed style length differs between them (Figure 5.2 d & e).

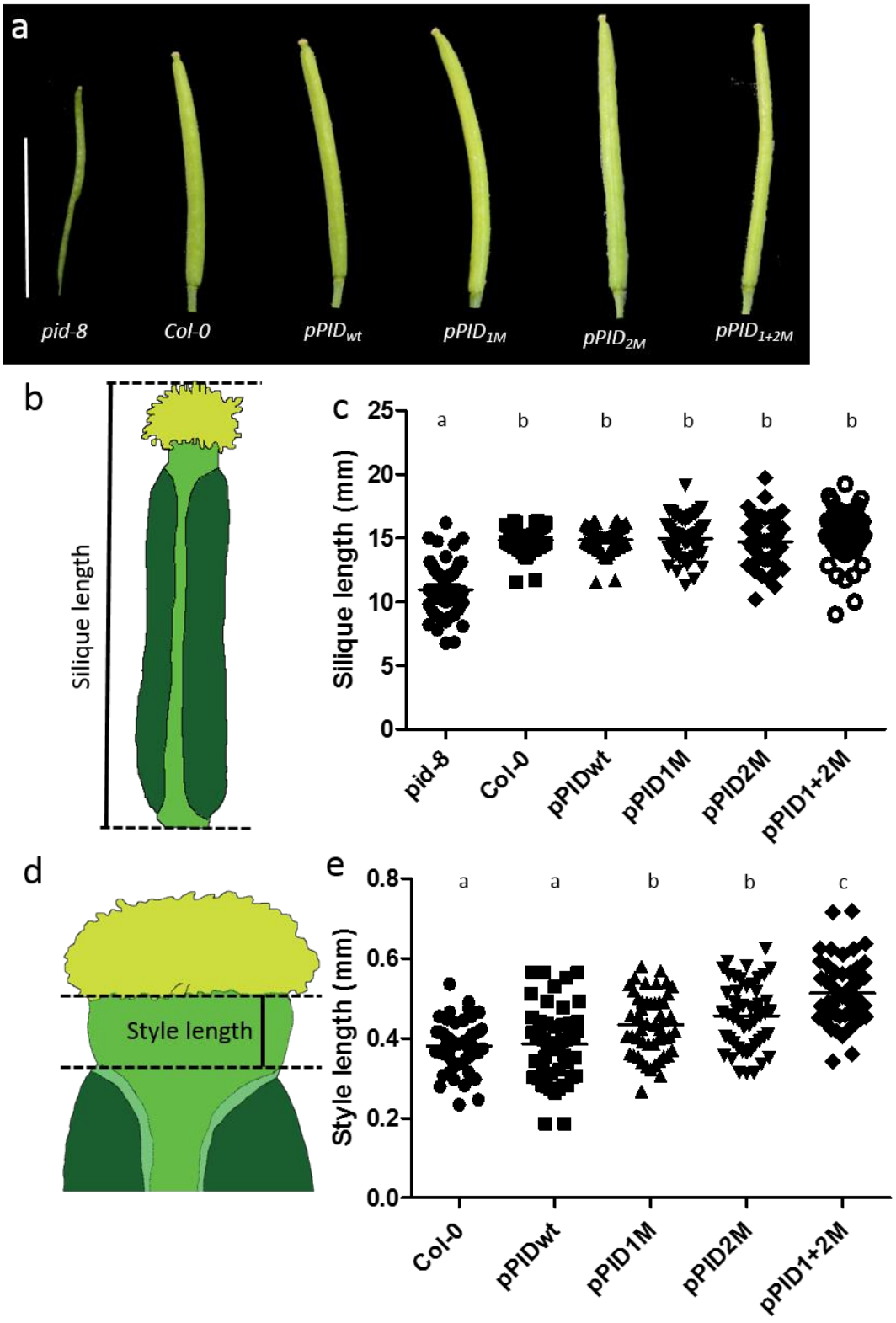

Figure 5. 2: All four promoter variants can rescue the *pid-8* fruit phenotype. However, rescue lines differ significantly in style length. Scale bar = 10mm (a) Representative siliques for each promoter variant construct. (b) Silique length describes the length of the fruit from the lower edge of the valves to the tip of the stigmatic tissue. (c) Silique length measurements show that all promoter variants can rescue the *pid-8* fruit length phenotype and none of the rescue lines differs significantly from the wild-type (N=50). (d) Style length describes the length of the style from the upper edge of the valves to the tip of the stigmatic tissue. (e) Style length

measurements show that styles of rescue lines carrying a mutation in either of the two AuxREs differ significantly from the wild type style (N=50).

The result showed that the construct carrying the wild type promoter allele is sufficient to fully rescue the *pid-8* phenotype regarding both silique length and style length. There is no significant difference between fruits of $pPID_{wt}$-lines and wild type (*Col-0*) fruits. Interestingly, while mutating the first AuxRE (-434) in the *PID* promoter did not change the silique length significantly it had a moderate yet significant effect on the style length. In these lines the style is generally longer, and the increase in length is significant when compared to *Col-0* or mutants rescued with the wild type promoter construct. Mutating the second AuxRE (-447) again leads to an increase of style length. Like $pPID_{1M}$, $pPID_{2M}$-styles are significantly longer compared to *Col-0* and lines rescued with the wild type promoter. However, $pPID_{2M}$ styles length is not significantly changed compared to $pPID_{1M}$ lines. The longest style was found in the double AuxRE mutant the style length of these lines was significantly longer than *Col-0* and mutants rescued with the wild type promoter. Moreover, $pPID_{1+2M}$ rescue lines had significantly longer styles then $pPID_{1M}$ and $pPID_{2M}$ lines. This indicates that both AuxRE in the examined region affect style length in an additive manner. The data also suggest that the second AuxRE may have a higher but not significant contribution to style length in contrast to the first AuxRE. Finally, the results imply that the two AuxRE are indeed biologically important for the correct regulation of *PID* gene expression during style development.

Higher PID protein abundance at the style apex during gynoecium development correlates with increase in style length

Next, I decided to examine the expression and the localization of the PID protein in the rescue lines. As expected PID localized to the plasma membrane at the tip of the developing gynoecium in all examined lines (Figure 5.3 a-h). The PID protein localises to the membranes in an apolar fashion as described previously (Michniewicz et al., 2007).

It was hypothesised that changes in the transcription factor binding site lead to changes in gene expression. Subsequently, this would also most likely be reflected in protein abundance. Following this logic, I quantified and compared the PID-GFP abundance at the plasma membrane between the four different constructs. This was done by determining the corrected total cell fluorescence (CTCF) of individual cells within the gynoecium. To rule out that the measurements are affected by the genomic insertion position of the construct I normalised the CTCF values obtained for PID-GFP with the ones obtained for the nuclear localised mCherry control (ratio $CTCF_{GFP}/CTCF_{mCherry}$) (Figure 5.3 i-k). Measurements were taken from gynoecia apices of stage 9 and stage 12 gynoecia.

Stage 9 and stage 12 represent two important developmental stages in style establishment and elongation. During gynoecium development, style formation is tightly controlled by the distribution of auxin in a spatial and temporal fashion. At stage 7, auxin accumulates in two lateral foci at the apex of developing gynoecia. At stage 8, two medial auxin foci emerge. These foci fuse to form an apical auxin ring at stage 9/10 that triggers a bilateral-to-radial symmetry switch establishing the development of the radial style (Moubayidin and Ostergaard, 2014). The generation of this apical auxin accumulation pattern relies on transcriptional repression of *PID*. After the bilateral-to-radial symmetry switch, *PID* becomes up-regulated and the apical auxin maximum disappears at stage 12 and is absent throughout style elongation (Moubayidin and Ostergaard, 2014; Simonini et al., 2016).

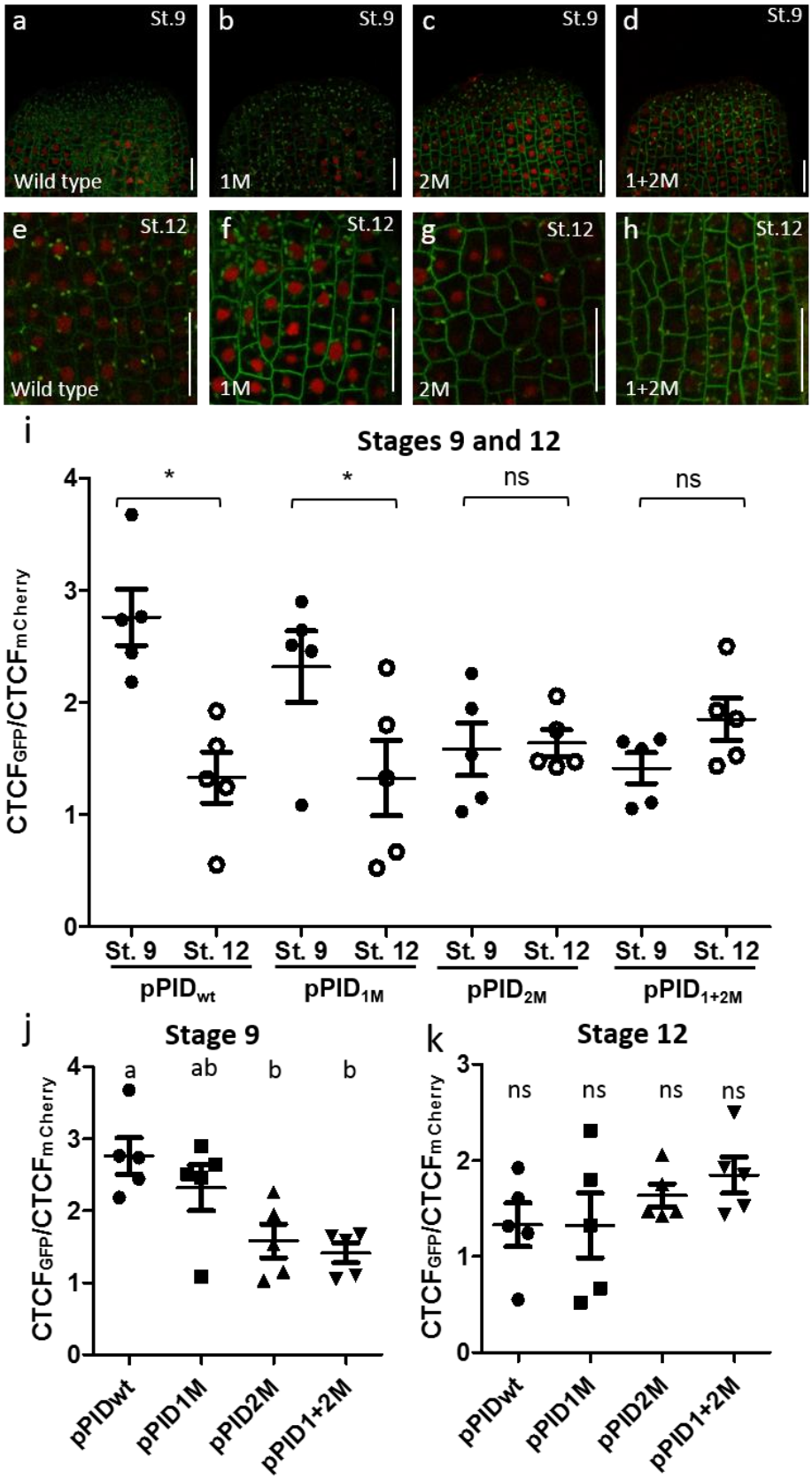

Figure 5. 3: All four promoter variants express functional PID-GFP that localises to the plasma membrane. (a-d) Representative confocal images of stage 9 gynoecia and (e-h) the style region of stage 12 for the respective promoter variant rescue lines Scale bars = 20 µM. (a &

e) unmutated wild-type rescue line, (b & f) rescue line with the first AuxRE mutated, (c & g) rescue line with the second AuxRE mutated and (d & h) rescue line with both AuxRE mutated. (i) Fluorescence quantification shows that only pPIDwt and pPID1M have significantly higher PID abundance at stage 9 compared to stage 12 (N=5 lines). *p-Values<0.05. (j) Fluorescence quantification shows that pPIDwt and pPID1M recue lines have significantly higher PID abundance at stage 9 when compared to pPID2M and pPID1+2M rescue lines (N=5 lines). (k) Fluorescence quantification shows that no significant differences can be detected between the promoter variants in stage 12 (N=5 lines). a; ab; b indicate significant differences according to multiple comparison. ns means not significant.

In line with these previous observations, I would expect to observe significant differences when comparing the two different stages. Moreover, I would expect to see higher PID abundance in stage 12 styles compared to stage 9 styles. Examining the PID-GFP abundance, I observed significant differences in PID abundance between the two examined developmental stages for $pPID_{wt}$ and $pPID_{1M}$ lines while $pPID_{2M}$ and $pPID_{1+2M}$ lines exhibited no significant differences (Figure 5.3 i). Surprisingly, it seems that the PID-GFP abundance was slightly higher at stage 9 than stage 12 in all lines tested and for $pPID_{wt}$ and $pPID_{1M}$ lines in particular. This might be due to a well-known artefact of the quantification method used. Values taken from a small cell appear higher than values taken from a large cell due to its smaller size concentrating the staining in a smaller space when in reality both cells have a similar level of fluorescence (Burgess et al., 2010; McCloy et al., 2014). Additionally, a low signal to noise ratio that may have been caused by normalising the GFP signal at the plasma membrane with the mCherry signal in the nucleus. An approach like that may lead to highly variable and faulty measurements that make the result hard to interpret. To improve the data, one could substitute the nuclear mCherry marker with a plasma membrane marker such as PIP2A, BOR1 or NIP5;1 (Liao and Weijers, 2018).

Next, I compared the PID-GFP abundance within the examined stages to answer the question about the importance of the two conserved AuxREs within the *PID* promoter and how mutating them affects PID abundance. In stage 9 gynoecia there was higher abundance of PID-GFP in $pPID_{wt}$ and $pPID_{1M}$ lines compared to $pPID_{2M}$ and $pPID_{1+2M}$ lines (Figure 5.3 j). The difference in normalised GFP intensity was only significantly different between $pPID_{wt}$ and $pPID_{2M}$ and $pPID_{1+2M}$ but not $pPID_{1M}$. Interestingly,

$pPID_{1M}$ values appear as an intermediate between $pPID_{wt}$ and $pPID_{2M}$, $pPID_{1+2M}$. Observed values for $pPID_{1M}$ lines are neither significantly different from $pPID_{wt}$ nor $pPID_{2M}$ and $pPID_{1+2M}$ lines. This suggests that mutating any of the two AuxRE triggers repression of the *PID* gene at stage 9. By contrast no significant differences in PID-GFP abundance between any of the four promoter variants was observed in examined stage 12 gynoecia (Figure 5.3 k). However, it seems that the average PID-GFP abundance is strongest in $pPID_{1+2M}$ lines and weakest in $pPID_{wt}$ lines with $pPID_{1M}$ and $pPID_{2M}$ lines exhibiting intermediate levels of abundance. As mentioned before, normalising the GFP signal at the plasma membrane with the mCherry signal in the nucleus may have caused a low signal to noise ratio. That makes it difficult to pick up subtle changes in PID-GFP abundance. Nevertheless, the PID-GFP intensity data follow at least generally, the trend observed in the phenotypic analysis of the style length. Despite high noise I was able to identify significantly higher PID-GFP abundance in $pPID_{wt}$ compare to the other three promoter variants.

Altogether, the results showed that rescue lines that are mutated in any of the two AuxREs have a decreased normalised PID-GFP signal when compared to wild type promoter rescue lines. This observation negatively correlates with the increase in style length observed in these lines previously (Appendix IV Figure 1 a, R^2=0.868). Interestingly, mutating the first AuxRE (-434) only has a mild effect on PID-GFP abundance at stage 9 while mutating the second AuxRE (-447) has a strong effect on both style length and PID-GFP abundance. This implies that mutating the second but to a lesser extent the first AuxRE (-434) might trigger early repression and mis-regulation of the *PID* gene at stage 9. Moreover, this indicates that ectopic repression of *PID* at stage 9 at least partially leads to an increase in style length. At stage 12, no significant differences between any of the four promoter variants implying that the examined AuxREs do not affect PID abundance at this stage. Even though no

significance was found, a weak positive correlation between PID abundance and style length was identified (Appendix IV Figure 1 b, R^2=0.834).

Mutating ETT-binding AuxRE positively affects *PID* promoter activity at stage 12

Phenotypic analysis of style length suggests an additive effect of the two AuxRE sites for gene regulation while measuring the protein abundance at the plasma membranes suggests that *PID* is mainly regulated through the second AuxRE at stage 9 of gynoecium development. Moreover, the data imply that the two examined AuxRE do not affect *PID* regulation in stage 12. However, the previously used approach might have generated a low signal to noise ratio by normalising a GFP signal at the plasma membrane with a nuclear mCherry signal. Therefore, subtle changes in PID abundance might have been missed. Next, I decided to evaluate the regulation of *PID* in the style region of elongating stage 12 gynoecia. Loss of function mutants of ETT show ectopic up-regulation of *PID* at stage 12 of gynoecium development (Chapter 2; Simonini et al., 2016). Therefore, I hypothesise that *PID* will be de-repressed in lines in which either one or both AuxREs are mutated.

This hypothesis could be tested by quantitative PCR or *in situ* hybridisation. However, since I am interested in differential expression between the lines and promoter variants in the style region this would require handling many samples at a time. In case of qPCR it would require isolating the style region of developing gynoecia.

Dissecting the style region from the rest of the gynoecium would require methods such as fluorescence activated cell sorting (FACS) or isolation of nuclei tagged in specific cell types (INTACT) that are technically very difficult and require the generation of style-specific promoter reporter lines.

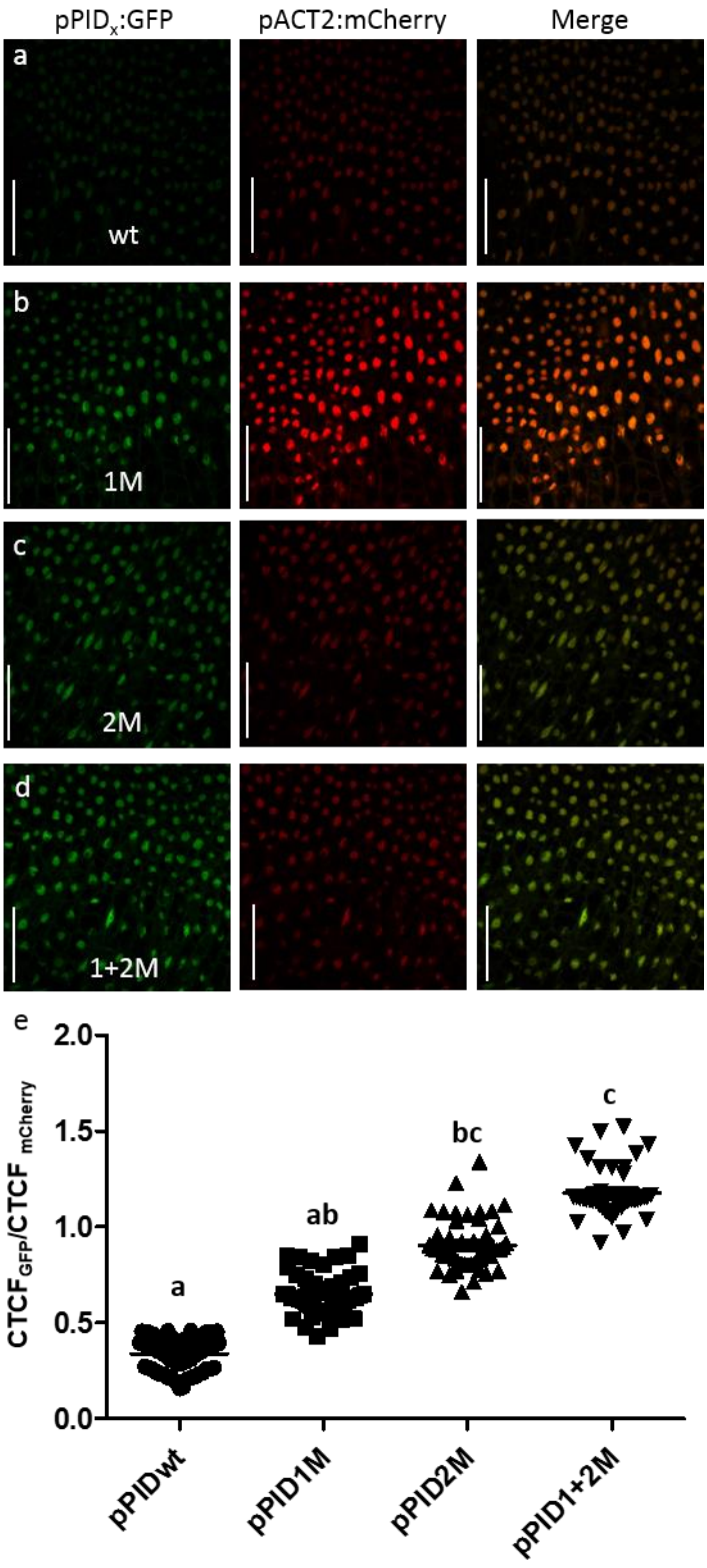

Figure 5. 4: Mutating AuxREs affects the *PID*-promoter activity in the style region. (a-d) Representative confocal images of the style region of stage 12 for the respective promoter variant reporter lines. Scale bars = 50 µM (e) Fluorescence quantification shows that mutating AuxREs leads to a gradual de-repression of the *PID* gene. The data indicate that the two AuxREs have an additive effect (N=40). a,b,c indicate significant differences according to multiple comparison.

To overcome these constrains, I chose to generate a different set of reporter constructs. Like the rescue lines these constructs carried the 5-kb *PID* promoter containing the same mutations as described previously. However, in these lines the promoter variants are controlling the expression of a nuclear GFP. Additionally, these constructs carry a nuclear mCherry controlled by a constitutive *ACTIN2* (*ACT2*) promoter. The constructs were transformed into *Col-0* plants. Using these reporter lines, the promoter activity of the different variants was examined in stage 12 gynoecia (Figure 5.4 a-d) as described in the previous section of this chapter. Consequently, the ratio of CTCF of GFP and mCherry can be used as a measure of promoter activity and gene expression. Expressing a nuclear localised GFP under control of the four promoter variants helped to overcome the problem of high variability that previously made the data hard to interpret.

The results show significant differences between lines of different promoter variants (Figure 5.4 e). Normalised GFP-fluorescence ($CTCF_{GFP}/CTCF_{mCherry}$) was weakest in lines carrying the wild type promoter variant while fluorescence in lines with the promoter mutated in the first AuxRE were moderately but not significantly stronger. Like fluorescence in the rescue lines, GFP fluorescence in lines mutated in the second AuxRE was significantly increased compared to wild type but not compared to the single mutant in the first AuxRE. The highest fluorescence was quantified for the double mutated promoter lines. For these lines the expression was significantly higher compared to all other lines.

In contrast to the previous results, these data suggest that both the first and the second AuxRE affect *PID* promoter activity. Even though, activity $pPID_{1M}$ lines do not differ significantly from wild type promoter or $pPID_{2M}$ promoter activity and appears as intermediate between the two it seems that combining mutations in the first and the second AuxRE has an additive effect on PID promoter activity. This suggests that both AuxRE are regulatory elements important for the repression of the *PID* gene.

Comparing the *PID* promoter activity with the phenotypic style-length data it becomes evident that high promoter activity at stage 12 correlates positively with longer styles (Appendix IV Figure 1 c, R^2=0.978). This implies that higher *PID* expression promotes style elongation at this stage.

Complex transcription factor interactions regulate *PID* expression during style development

The presented data indicate that the two examined AuxREs affect *PID* promoter activity during style formation in two fashions. Firstly, mutations of the second AuxRE affects promoter activity in a temporal manner because *PID* is ectopically repressed at gynoecium apices at stage 9 in $pPID_{2M}$ and $pPID_{1+2M}$ mutated lines. Secondly, mutations in both AuxREs affect promoter activity in a dosage-dependent manner because mutating any of the AuxREs increases the promoter activity significantly at stage 12. Besides ETT, two other transcription factors, SPT and IND, are crucial for regulating *PID* during style formation (Girin et al., 2011; Moubayidin and Ostergaard, 2014). Like ETT, SPT physically interacts with IND and *PID* is ectopically expressed in mutants and double mutants in combination with IND (Moubayidin and Ostergaard, 2014). However, in contrast to the ETT-IND interaction, SPT-IND interactions cannot be disrupted by auxin (Chapter 2; Chapter 3; Chapter 4; Simonini et al., 2016). Intriguingly, two repeated G-boxes which are putative SPT binding sites partially overlap with the examined ETT-binding AuxRE repeat. Additionally, a putative IND binding E-box lays 57bp downstream of the AuxRE-G-box patch (Figure 5.5 a). Previous *in vitro* protein-DNA binding studies suggest that SPT and IND can bind these identified cis-elements *in planta* (Girin et al., 2011; Sorefan et al., 2009). To evaluate whether this is indeed the case I decided to examine *in planta* binding in the gynoecium by means $ChIP_{qPCR}$.

$ChIP_{qPCR}$ was carried out in collaboration with Billy Tasker-Brown using reporter mutant rescue lines (*pIND:IND:YFP*) in the presence and absence of an auxin

treatment. A previous study has shown that ETT AuxRE binding at the examined region is insensitive to auxin. This means that ETT can bind its binding site under both high and low auxin conditions (Simonini et al., 2016). We repeated this experiment and found our data in agreement with the literature (Figure 5.5 b). Evaluation of binding profiles showed that IND enriches within the examined described regulatory patch around 0.4-kb up-stream of the transcription start site (TSS) (Figure 5.5 c). Strikingly, we were able to observe a significant reduction in IND enrichment after auxin treatment. This implies that IND binds its target DNA sequence in an auxin-sensitive manner.

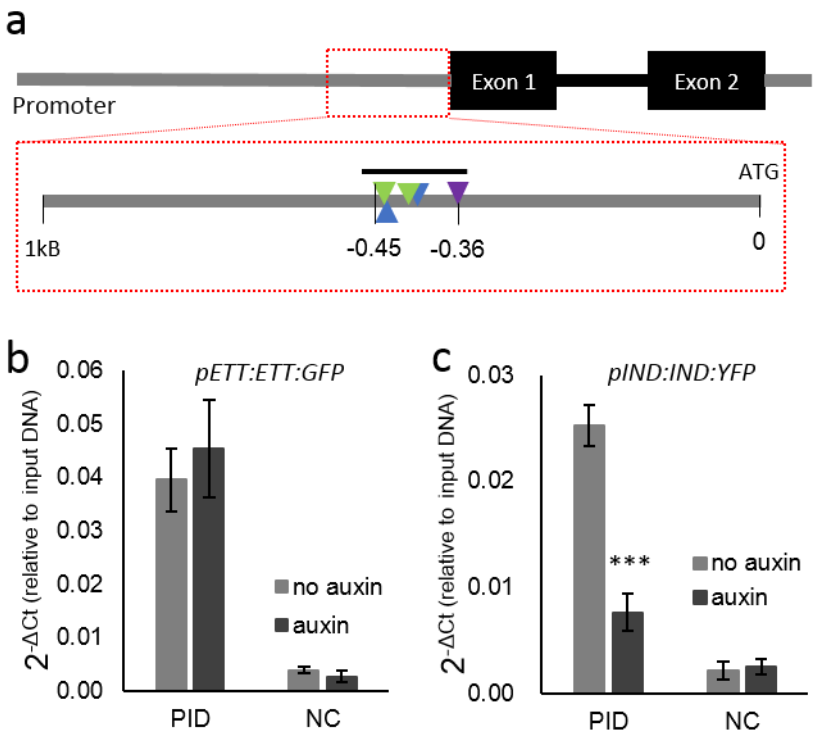

Figure 5. 5: The transcription factors ETT and IND can bind to the complex regulatory patch within the *PID*-promoter. (a) Schematic representation of the regulatory region. The black bar above the zoomed region indicates the amplicon used in qPCR reactions. (b) ETT can bind to the regulatory patch. Its binding is unaffected by auxin. (c) IND can bind to the regulatory patch. Auxin reduces IND binding to *PID*-promoter. ***p-Values<0.0001; Shown are mean ± standard deviation of three biological replicates.

The auxin-sensitive E-box binding behaviour of IND at the *PID* promoter adds an additional layer of complexity to the regulation of the *PID* gene. Even though, in the ChIP experiment plants have been treated with auxin by spraying high auxin

concentrations, it is likely that a similar binding behaviour can be observed during development in cells that naturally accumulate high auxin. During gynoecium development such a situation can be found at the gynoecium apex at stage 9 (Moubayidin and Ostergaard, 2014). It can therefore be assumed that in cells of these high auxin domains, IND is unable to bind the E-box within the *PID* promoter whilst binding occurs under low auxin conditions (e.g. before stage 9 and after stage 11).

Discussion

Spatial and temporal control of gene expression is key for the regulation of most developmental processes. However, key regulatory genes are often subject to complex regulation that involves multiple transcription factors forming various protein complexes interacting with various cis-regulatory elements at a complex regulatory region. Often the composition of these complexes and their mode of action depends on the biological context and can differ within the same cell in different developmental stages or under different environmental conditions. For this reason, there is still little known about the contribution of specific cis-regulatory elements to the regulation of a gene in a specific developmental context.

This study has attempted to uncover the importance of two previously characterised ETT-binding AuxRE sites within the promoter for *PID* gene expression during gynoecium development. *PID* has been identified as a main driver of this apical auxin accumulation due to its role in directing auxin transport by regulating PIN activity and localisation. By doing so, *PID* has been implemented as a main regulator of auxin dynamics during style establishment and elongation (Moubayidin and Ostergaard, 2014). During style establishment *PID* is repressed at early stages (stage 7-10). This leads to auxin accumulation at the gynoecium apex triggering a bilateral-to-radial symmetry switch to establish the radial style. At later stages, during style elongation, auxin levels decrease and *PID* is expressed (*e.g.* stage 12).

The presented data show that both examined AuxREs play a role in the regulation of the *PID* promoter activity during style establishment and elongation. Phenotypic analysis showed that the *PID* gene under control of any of the four examined promoter variants was able rescue the *pid-8* fruit length and valve phenotype. This suggests that the examined AuxREs do not play a major role in development of this phenotype. Further phenotypic examination, however, showed significant differences in style length between different promoter variants indicating a role of the two AuxREs in the regulation of style length. Remarkably, examining promoter activity in two developmentally important stages (stage 9 and stage 12) showed two different modes *cis*-element regulation of *PID*. Firstly, mutating of the second AuxRE leads to a stronger repression of promoter activity at stage 9 gynoecium apices indicating that this AuxRE temporally controls *PID* expression. Secondly, mutations in both AuxREs increases the promoter activity significantly at stage 12 in a dosage dependent manner. Hereby, the second AuxRE appears to have the major contribution while the first AuxRE enhances repression. Hence mutating the AuxREs leads to a de-repression of *PID* at developmental stage 12.

It is well-established that, besides ETT, two bHLH transcription factors SPT and IND are essential regulators for *PID* expression during gynoecium development (Moubayidin and Ostergaard 2014). *SPT* single mutants fail to develop a radial style and the gynoecium apex remains unfused (Heisler et al., 2001). In *spt ind* double mutants this phenotype is exaggerated (Moubayidin and Ostergaard 2014). In *spt* mutants, the *PID* gene was ectopically expressed at the apex of developing gynoecia in early stages indicating that SPT acts as a repressor of *PID* expression. Similarly, *PID* is also ectopically expressed in *ETT* mutant gynoecia. In *ett ind* double mutants this ectopic expression is enhanced (Simonini et al., 2016) indicating that ETT and IND can also repress *PID* expression. Interestingly, while *spt* and *spt ind* mutants exhibit severe split style phenotypes styles in *ett* and *ett ind* show less strong style

phenotypes (Moubayidin and Ostergaard, 2014; Simonini et al., 2016). Sequence analysis has identified the presence of a putative IND-binding E-box and two SPT-binding G-boxes in close proximity to the evaluated AuxREs. Moreover, the G-boxes appear as a repeat and overlap partially with the examined AuxRE repeat. Additionally, previous studies have identified that both ETT and SPT can form complexes with IND (Girin et al., 2011). However, while high auxin concentrations can disrupt ETT-IND interactions this is not the case for SPT-IND interactions.

Evaluation of *in planta* promoter binding of IND to a previously identified *cis*-regulatory E-box showed that IND can bind the *PID* promoter. Intriguingly, auxin treatment leads to a disruption of this TF-DNA interaction. The mechanism by which auxin affects IND binding to its cis-element is not yet understood. Nonetheless, such a binding behaviour might have biological relevance for the regulation of *PID*. The binding of SPT to the identified G-boxes was not evaluated *in planta*. *ETT* and *IND* are expressed at the gynoecium apex and style from early stages throughout development (Simonini et al., 2016; Sorefan et al., 2009; Girin et al., 2011) while SPT is predominantly expressed until stage 11 but absent from stage 12 (Girin et al., 2011; Schuster et al., 2015). Therefore, one might not expect SPT to play a role in regulating *PID* at this stage.

The presented results suggest the following model for regulating *PID* expression during style establishment and elongation (Figure 5.6): During early stages (stage 7/8) of style establishment low concentrations of auxin are present at the gynoecium apex. Under these conditions, IND binds its corresponding *cis*-element within the *PID* promoter and can physically interact with both SPT and ETT. Ectopic *PID* expression occurs when either *ett* or *spt* mutants are combined with *ind* mutants implying that ETT and SPT alone might be less efficient in binding to the *PID* promoter. Thus, it is possible that in this situation IND is actively recruiting ETT and SPT through protein-protein interaction to the *PID* locus. It remains unclear whether IND can interact with

SPT and ETT at the same time or whether it can only interact with either protein at a time. Using a Y3H experiment this could be addressed in the future. Either way, SPT and ETT binding leads to the repression of *PID* expression. Consequently, it initiates apolar localisation of PIN auxin transporter and an increase in auxin concentration at the gynoecium apex.

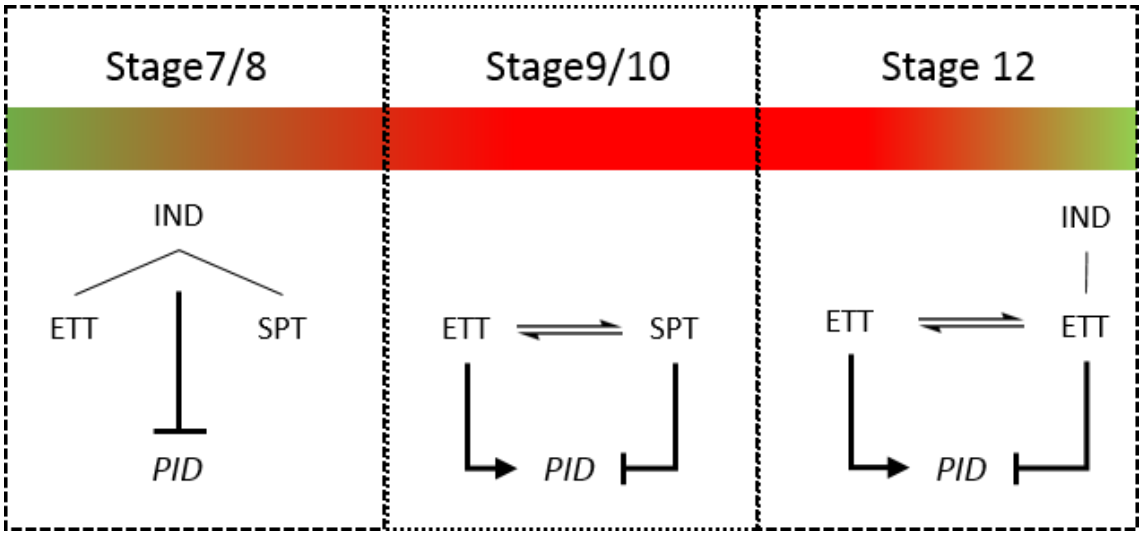

Figure 5. 6: Model describing the regulation of *PID* during style development. The colour bar indicates the auxin concentration throughout development; green indicates low auxin while red indicates high auxin concentrations.

Once the auxin concentrations are high enough (stage 9/10), IND is unable to bind its promoter element through a mechanism that is not yet understood. One could imagine a role of ETT in this process since the interaction between ETT and IND can be disrupted by auxin (Figure 5.6). Likewise, high auxin concentrations lead to an activity switch of the ETT protein from repression to activation. The role of SPT at this stage is not clear and requires further investigation. However, one could imagine at least two different possibilities. Firstly, the SPT-IND interaction is not affected by auxin. Therefore, it is possible that the release of IND from its binding site leads to a destabilisation of SPT promoter binding. This would subsequently release SPT from its G-boxes, thereby releasing repression. In the second possibility SPT promoter binding is unaffected by auxin and the release of IND from the *PID*-locus. In this scenario SPT will still act as a repressor as there is no evidence for an auxin-induced

activity switch. At the *PID* promoter, SPT-binding G-boxes overlap with ETT-binding AuxREs. Overlapping or neighbouring transcription factor binding sites suggests either co-operative binding or competition for binding. Since it is well-known that SPT and ETT cannot physically interact (Simonini et al., 2016) and the fact that SPT and ETT have opposing modes of action in high auxin concentrations, this makes co-operative DNA binding of SPT and ETT unlikely. Therefore, one could imagine a situation in which these two transcription factors compete for available G-boxes or AuxRE respectively in high auxin conditions. This would lead to a tug-of-war situation balancing activation and repression of *PID* expression. Strikingly, the experimental data show that mutating the second AuxRE (-447) or the first and the second AuxRE (-434 and -447) lead to lower PID-GFP abundance and therefore a down-regulation of *PID* at stage 9 when compared to lines carrying the wild-type promoter. This indicates that in these lines the equilibrium has been shifted towards repression supporting the tug-of-war hypothesis. The hypothesis could further be tested by systematically mutating the G-boxes in the same way as I have demonstrated for the AuxREs here. An alternative method could involve *in vitro* transactivation assays using systematically mutated promoter elements. These assays use transient protein expression and will also allow evaluation of differences in proteins abundancies. Together this will increase our understanding of their role in *PID* regulation.

Recently, it has been shown that *SPT* expression within the developing style decreases from stage 10 and disappears from the style at stage 12 (Girin et al., 2011; Schuster et al., 2015). Following the logic of the tug-of-war hypothesis decreasing levels of SPT lead to a decrease of repression and therefore shifts the balance towards gene activation. Remarkably, an increase in *PID* expression has indeed been described at these stages of gynoecium development further supporting the hypothesis (Girin et al., 2011; Simonini et al., 2016; Sorefan et al., 2009).

Nevertheless, the actual dynamics of SPT-promoter binding and the effect of auxin on it will need to be addressed in the future for instance using $ChIP_{qPCR}$.

At stage 12, the style identity has fully been established and will continue to elongate. *SPT* is not expressed anymore (Schuster et al., 2015). Furthermore, in previous stages, *PID* has been up-regulated through a negative auxin-induced feedback loop (Girin et al., 2011; Simonini et al., 2016) leading to decreasing auxin levels in the style at this stage. It is expected that both decreasing auxin levels and the absence of SPT will have immediate consequences for the regulation of *PID* expression. Firstly, decreasing auxin concentrations enable IND to restore binding to the *PID* promoter and its interaction with ETT. Secondly, auxin concentrations under a yet unknown threshold also affect ETT's mode-of-action so that ETT protein will be predominantly in a repressive state. In the experiment, I observed that mutations in both AuxREs lead to de-repression of the *PID* promoter. Moreover, this seems to happen in a dosage-dependent manner because mutating both AuxREs had a larger effect than mutating them individually. One AuxRE has a bigger effect on promoter de-repression than the other. Intriguingly, the AuxRE that has the minor contribution is in closer proximity to the IND-binding site (at position -434). To date, not much is known about dynamic DNA-protein interactions and their kinetics in developmental processes due to their complexity. Therefore, interpretation of the presented data remains largely speculative. It has been proposed that TF-TF interactions can provide robustness to their *cis*-binding properties (Jolma et al., 2015). If IND is required to recruit ETT to the *PID* locus, one could speculate that this recruitment might affect ETT binding specificity and allow mis-matches in the ETT-AuxRE interaction. Thus, in $pPID_{1M}$ and $pPID_{1+2M}$ a small proportion of ETT might still be able to bind the mutated *cis*-element with reduced affinity and thereby milden the de-repression effect on *PID* expression. By contrast, in the case of mutations in the second AuxRE this softening does not occur. A possible reason for this could be that this cis-element requires a clearer

sequence presentation. ETT can form dimers with itself and other ARFs (Heather McLaughlin personal communication). Therefore, ETT binding the second AuxRE might recruit ETT binding to the first AuxRE or vice versa. It is also possible that other transcription factors affect the regulation of *PID* as well as the binding kinetics of the examined transcription factors adding another layer of regulatory binding complexity. Nevertheless, *PID* promoter activity at stage 12 correlates strongly and positively with increased style length suggesting a dependency between style elongation and *PID* expression.

Organ growth can occur either through cell elongation or cell proliferation or a combination of both processes. In the presented experiments I have not addressed whether the increase in style length is the result of cell proliferation or cell division. However, in the future this could be addressed by determining the cell number and cell length within styles of the four promoter rescue lines using scanning electron microscopy. Both processes, cell division and cell elongation are under tight hormonal control predominantly through antagonistic action of auxin and cytokinins. Both hormones have a crucial role controlling the balance between cell elongation and cell division. While auxin generally inhibits cell proliferation, cytokinins promote cell proliferation in the shoot (Kieber and Schaller, 2018). Homeostasis between auxin and cytokinins plays an important role for the regulation of gynoecium development and organ growth. Pharmacological studies showed that disturbing this homeostasis by allocating high concentrations of cytokinin triggers ectopic cell proliferation throughout the length of the gynoecium (Marsch-Martinez et al., 2012; Schuster et al., 2015). Local application of moderate cytokinin concentrations trigger an increased placenta length (Cucinotta et al., 2016). The role of auxin-cytokinin homeostasis in the context of style elongation has not yet been addressed. However, one could imagine a mechanism in which disturbing the balance by shifting the equilibrium towards cytokinin might also trigger an increase in style length similarly to what has

been observed for placenta length. The presented data show that mutating *PID*-regulating AuxREs leads to ectopic up-regulation of *PID* in stage 12. This mis-regulation correlates highly with increase in style length (R^2=0.978). An increase in *PID* expression would increase polar auxin transport for the style, thereby, reducing local auxin concentrations. One could speculate that this leads to a higher cytokinin to auxin ratio that promotes cell proliferation. In the future, the role of cytokinin in style elongation could be assessed by overexpression of cytokinin biosynthesis and degradation genes specifically in the style region. If high cytokinin promotes style length this should be measurable. One would expect longer styles when biosynthesis genes are overexpressed while overexpression of degradation genes would lead to shorter styles.

Concluding remarks

In this chapter I present an approach to test the contribution of two ETT-binding AuxREs in the promoter of an auxin responsive gene (*PID*) in the developmental context of gynoecium development. This work shows that targeted mutations of cis-regulatory elements can be used to dissect the importance of cis-regulation within complex regulatory regions *in planta*. However, it also shows the challenges as gene regulation is highly robust and mutations within gene regulatory regions may display subtle phenotypes. To conclude, this study provides a starting point for a more in-depth study understanding cis-regulation of auxin responsive genes as the data still do not permit full elucidation of the mechanism by which ETT regulates *PID* expression. For example, it remains an open question how ETT is recruited to its cis-binding sites and whether ETT binds as a monomer, homo- or heterodimer. In line with this, it is yet to be addressed whether IND is indeed required to recruit other TFs to the *PID*-locus and also the role of SPT is yet to be elucidated. Nonetheless, this work indicates that cis-elements are likely to affect the complex formation at target loci as well as their regulation. Furthermore, it shows the benefits of studying cis-

regulation *in planta* using a specific developmental process. Finally, this work opens the avenue for more comprehensive studies systematically dissecting the role of cis-elements in the regulation of developmentally important genes.

Materials and Methods

Plant materials and treatments

Plants were grown as described in Chapter 2. All transgenic plant lines and the pid-8 were in Columbia (*Col-0*) background. The *pETT:ETT:GFP* and *pIND:IND:YFP* lines were previously published (Simonini et al., 2016).

Generation of transgenic lines

The transgenic rescue and reporter lines were generated using the Golden Gate method (Engler et al., 2014) and transformed into *Arabidopis* as described in Chapter 3. Rescue constructs were transformed into *pid-8* mutants while reporter lines were transformed into *Col-0*. Transgenic lines were generated together with Bethany Runciman as part of her MSc project. Primers and plasmids used for cloning can be found in Appendix IV Table 1 and Appendix IV Table 2.

Phenotypic analysis

For the silique and style length measurements siliques were sampled from plants when they were mature. For wild-type ten siliques from five plants (n=50 siliques) were collected while for transgenics ten siliques from five independent lines per construct were collected and photographed. Silique and style length were then measured using ImageJ 1.48 (Schneider et al., 2012). The results were statistically analysed by one-way ANOVA followed by Tukey's multiple comparison test using GraphPad Prism Version 5.04 (La Jolla California USA, www.graphpad.com).

Confocal microscopy and corrected total cell fluorescence quantification

Confocal images were taken from stage 9 and stage 12 gynoecium using a Leica SP5 (HyD detector) confocal microscope (Laser 20%, Smart Gain 30%, 200hz, 8x Line

Average and a pinhole equivalent to 1.0x the Airy disk diameter) using a 40X oil emersion lens. Excitation and detection of fluorophores were configured as follows: GFP was excited at 488 nm and detected at 498–530 nm; mCherry was excited at 561 nm and detected at 571–630 nm. For comparability the acquisition settings were set on the brightest sample and kept constant. All confocal images of the rescue lines were taken by Bethany Runciman as part of her MSc project. Analysis was conducted in ImageJ 1.48 (Schneider et al., 2012) using the corrected total cell fluorescence method (McCloy et al., 2014) to quantify GFP and mCherry expression at the gynoecium apex. $CTCF_{GFP}$-to-$CTCF_{mCherry}$ ratios were calculated and statistically analysed using two-tailed t-test to compare between stages or using one-way ANOVA followed by Tukey's multiple comparison test using GraphPad Prism Version 5.04 (La Jolla California USA, www.graphpad.com).

Chromatin Immunoprecipitation (ChIP) qPCR

$ChIP_{qPCR}$ was performed using *pETT:ETT:GFP* and *pIND:IND:YFP* plants as described in Chapter 2. ChIP experiments using *pIND:IND:YFP* plants were performed together with Billy Tasker-Brown. $ChIP_{qPCR}$ data were analysed using one-way ANOVA followed by Tukey's multiple comparison test using GraphPad Prism Version 5.04 (La Jolla California USA, www.graphpad.com).

Chapter 6

General Discussion

Understanding how developmental programmes coordinate morphogenesis of complex organisms has been a fascinating and longstanding question in developmental biology. Through studies on model organisms such as *Drosophila melanogaster* and *Arabidopsis thaliana*, it has become evident that morphogen patterning and signalling is a fundamental requirement for the coordination of organ development (Cadigan and Nusse, 1997; Gurdon and Bourillot, 2001; Kondo and Miura, 2010; Sablowski, 2015). In plants, the phytohormone auxin, a chemically simple tryptophan-derived molecule, fulfils a primary morphogenic role in almost every aspect of plant development (Vanneste and Friml, 2009). Although it remains unclear how auxin can regulate so many different responses, it has become apparent that the specificity of hormone action between organs is not an intrinsic property of the hormone itself but depends on the proteins responding to it in the different cells. As discussed in the Introduction, a mechanism by which an auxin signal can generate a transcriptional output, referred to as the “nuclear auxin signalling pathway” or “canonical auxin signalling pathway”, has been discovered. Like many other phytohormone signalling pathways, the canonical auxin signalling pathway includes the hormone induced degradation of a repressor protein by the ubiquitin-proteasome pathway, thereby, releasing the repression of auxin responsive target genes.

Prior to the start of this project, an alternative/non-canonical auxin-signalling mechanism whereby auxin directly affects the activity of a transcription factor (TF) complex towards its downstream targets (Simonini et al., 2016; Simonini et al., 2017; Simonini et al., 2018a; Simonini et al., 2018b), was discovered. This mechanism mediates precise polarity switches during gynoecium development and includes the class-B ARF ETTIN (ETT/ARF3) as a pivotal component. However, the exact molecular mechanism remains elusive. The aim of this thesis is to shed light onto the molecular mechanism by which this non-canonical auxin-signalling pathway perceives and transduces auxin stimuli to generate a transcriptional output.

Non-canonical auxin signalling is independent of TIR1/AFB auxin receptors

ETT is an unusual ARF lacking the Aux/IAA-interacting Phox/Bem1 (PB1) domain (Sessions et al., 1997; Simonini et al., 2016). Consequently, ETT cannot interact with Aux/IAAs which are a central component of canonical auxin signalling mechanism. It was therefore proposed that ETT might transduce the auxin signal through an alternative auxin-signalling pathway, however, it is unclear to what extent this pathway is independent of the established TIR/AFB-mediated pathway. Expression analysis of *HEC1* and *PID*, two auxin-responsive genes under direct control of ETT in both higher order *tir1/afb* receptor mutants and a recently-developed synthetic auxin-TIR1 pair (Uchida et al., 2018) revealed that the ETT-dependent regulation of *HEC1* and *PID* does not require a functional TIR1/AFB machinery and is therefore TIR1/AFB independent (Chapter 2). Nevertheless, one cannot exclude the possibility that this TIR1/AFB independent pathway interacts with the canonical auxin signalling pathway in some instances. Such crosstalk between the two pathways could occur at gene loci where ETT and class A ARF dimerise via their DBD domains. Although the ARF heterodimerisation and the potential crosstalk between canonical and non-canonical auxin signalling pathways has not yet been studied, future work will focus on elucidating the importance of these two aspects for the regulation of auxin responsive gene expression.

ETT is an auxin binding protein and may act as an auxin receptor

ETT interacts with a diverse set of TFs an auxin-sensitive manner through the C-terminal part of ETT, known as the ETT-Specific (ES) domain (Simonini et al., 2016). Systematic truncation of the ETT-protein found a fragment containing 207 amino acids of the ES domain, $ES^{388-594}$, that appears to be sufficient to mediate auxin-sensitivity in ETT-protein interactions (Simonini et al., 2018a). The sensitivity of ETT-TF interactions to IAA suggests a direct effect of the auxin molecule on the ETT protein. An obvious question became whether ETT could act as an auxin receptor by direct auxin binding. The biochemical and biophysical examination of the auxin

binding potential of the $ES^{388-594}$ protein presented in Chapter 2, shows that ETT binds naturally occurring auxin (IAA) directly.

However, the interactions observed were weak, which may reflect that other domains in the full-length ETT protein contribute to auxin binding. Alternatively, it is possible that the ETT-auxin interaction needs to be stabilised by additional factors, thereby increasing the affinity. For instance, metal ions are common co-factors that stabilise interactions between proteins and their ligands. Analogously, ABP1 requires zinc ions for efficient auxin binding (Woo et al., 2002; Napier, 2004). Another possibility is that certain proteins interact with ETT to stabilise auxin binding thereby increasing the affinity *in planta*. Stabilising proteins can be context-specific transcriptional regulators, such as IND, RPL or TPL, or context-independent proteins such as heat-shock proteins (HSPs). Besides their well-known role as chaperone proteins that support protein folding and their role in stress responses in many biological systems, HSP90s play an important role in steroid hormone signalling in mammals where they physically interact with the receptor and are required for efficient hormone binding (Echeverria and Picard, 2010). It would be intriguing to see whether HSP90s play a similar role in non-canonical auxin signalling.

Unfortunately, it was not possible to determine which residues of ETT interact with auxin using the data obtained in this study. Therefore, future work should focus on understanding different aspects concerning the structural basis of the ETT-auxin interaction. This involves understanding the mechanistic and structural similarities between non-canonical auxin signalling and animal hormone signalling, requires knowledge about the kinetics of the ETT-auxin interaction, further information on which ETT-residues bind auxin and how the conformation of ETT is affected by auxin binding. These aspects will be studied using multi-dimensional NMR and X-ray crystallography to identify the auxin-binding residues and reveal the structural

dynamics upon auxin binding. Mutant analysis using HSQC-NMR and ITC will then determine the contribution of each residue to auxin binding.

Nevertheless, the results suggest that ETT binds IAA directly thus revealing a key molecular aspect of the non-canonical auxin-signalling pathway that suggests that this pathway is fundamentally different to canonical auxin signalling. Moreover, direct binding of a small hormone such as auxin by a transcription factor is an uncommon phenomenon in plant signalling since most phytohormone pathways use either signal transduction cascades using extracellular receptors (e.g. BR and peptide signalling) or the ubiquitin-proteasome pathway (e.g. canonical auxin signalling or GA signalling) (Kelley and Estelle, 2012; Oh et al., 2018; Vukasinovic and Russinova, 2018).

In contrast, signalling pathways in animals often involve either direct binding of a hormone-ligand (steroid and thyroid signalling) or an effector protein (Wnt/β-catenin signalling) by a transcription factor (Gammons and Bienz, 2018; King et al., 2012; Tsai and O'Malley, 1994). Nuclear SHRs, THRs and TCF bind target loci independently of the ligand concentration, a DNA-binding behaviour that can also be observed for ETT (Chapter 5; Simonini et al., 2016). Despite the differences in the ligands and the proteins involved in their perception, all three animal signalling pathways use analogous mechanisms involve direct ligand-binding and an activity switch of the transcription factor, both of which are features that are reminiscent of auxin binding by ETT.

Non-canonical auxin signalling affects the local chromatin environment of its target genes

Upon hormone binding by the receptor, animal hormone-signalling pathways involve extensive chromatin remodelling at their target loci (Gammons and Benz, 2018; King et al., 2012; Tsai and O'Malley, 1994). Due to its reminiscence with these pathways in terms of direct hormone binding, a critical question to answer is whether non-

canonical auxin signalling affects the chromatin environment at its target genes in response to auxin.

The effect of auxin treatment on three distinct histone modifications (H3K27me3, H3K27Ac and H3K36me3) at *HEC1* and *PID* loci revealed that repressive H3K27me3 and activating H3K27ac marks indeed respond to auxin treatment in wild type gynoecia, while H3K36me3 levels appears neither to be auxin-responsive nor dependent on ETT at the loci examined. The levels of repressive (H3K27me3) and activating (H3K27Ac) histone modifications correlated with the level of *HEC1* and *PID* expression. Similar to the gene expression response, the effect of auxin on histone modifications was lost in the *ett*-mutant, suggesting that ETT plays an essential role in regulating the expression of *HEC1* and *PID* by modulating the levels of activating and repressive histone modifications.

Although it has been shown that ARFs can control the local chromatin environment of their target genes, those observations are based on experiments in *arf* mutants or histone-modifying enzyme mutants, rather than on wild type plants with auxin treatments (Chung et al., 2019; Weiste and Droege-Laser, 2014; Wu et al., 2015). Thus, results from these studies show that chromatin state and gene expression data correlate with protein-protein interactions between components of the canonical auxin signalling machinery and protein complexes that regulate the chromatin environment but not changes in auxin levels itself. In contrast, the experiments presented in Chapter 2 assay changes in chromatin state upon auxin treatment in both wild type and *ett-3* mutant. The combination of wild type and mutant data allows to draw conclusions about the requirement of both auxin and ETT for the auxin-effect on the chromatin environment and the auxin responsive regulation of its target genes. In the future it would be interesting to see whether such direct causality can also be found for other ARFs. Furthermore, it would be interesting to assay the effect of auxin on the chromatin environment on a whole genome scale. Combining these with the RNA-

seq and ChIP-seq data sets for ETT would elucidate which genes are under control of ETT in an auxin responsive manner. Moreover, these data may help to obtain insight into the many different ways in which chromatin is involve in gene regulation.

ETT recruits chromatin-modifiers to mediate auxin dependent chromatin remodelling

ETT does not have chromatin-modifying activity itself but interacts with proteins that mediate histone modifications (Chapter 3). Some of these proteins, including DEK3, TPL and VRN2, interact with ETT in an auxin-sensitive manner. These three interactions were analysed in further detail to find out how they can modulate the local chromatin environment at ETT-target genes in response to auxin and in cooperation with ETT.

The results lead to two hypotheses about how DEK-proteins can affect auxin-responsive gene regulation:

Firstly, DEK3 may affect chromatin structure on a global level at auxin-responsive loci through chromatin looping, which is supported by mutant analysis, which has further shown that DEK3 and its close homolog, DEK4, redundantly regulate the polar auxin transport regulator *PID* during gynoecium development (Chapter 3). In plants and animals DEK proteins have been implemented in three-dimensional chromatin organisation, particularly, through their role in the formation and maintenance of chromatin loops (Greenwald et al., 2019; Kadauke and Blobel, 2009; Waidmann et al., 2014; Zheng and Liu, 2019). In agreement with this, a chromatin loop has been implemented in the auxin-responsive regulation of *PID* (Ariel et al., 2014). Future work will evaluate this by investigating the ability of DEK4 to interact with ETT.

Secondly, DEK3 can directly interact with histone deacetylases (Waidmann et al., 2014). Consequently, DEK proteins may shape the chromatin environment of their target genes directly through histone deacetylation in response to auxin. This

hypothesis agrees with the auxin effect on histone acetylation of auxin-responsive genes presented in Chapter 2. It is therefore possible that when nuclear auxin concentrations are low, DEK3 interacts with ETT and brings in histone deacetylation at ETT-target loci to repress gene expression. In contrast, high auxin concentrations may instead lead to a disruption of ETT-DEK3-HDAC complexes, leading to a reduction of deacetylation and de-repression of the target locus. Future analysis using $ChIP_{qPCR}$ will show whether DEK3 co-localises with ETT at binding sites within the *PID* promoter. Examining the expression of target genes and H3K27Ac dynamics at target sites in *dek3-2 dek4-1* mutants, and in the presence and absence of auxin, will provide insight into the importance of chromatin modifications by DEK3-containing complexes for the transcription of genes in response to auxin.

The second ETT-interacting protein examined in more detail was VRN2, which is a Su(z)12 subunit of the POLYCOMB REPRESSIVE COMPLEX 2 (PRC2). Although PRC2 is most prominent for its role in epigenetic silencing and memory through H3K27me3 deposition at its target genes, PRC2 has also been implemented in the regulation of genes subjected to regulation by gene regulatory networks (Ringrose, 2007). In plants, the antagonistic action of H3K27me3 and H3K36me3 appears characteristic for epigenetic silencing and memory (Berry et al., 2015; Berry et al., 2017; Yang et al., 2014; Yang et al., 2017). The examination H3K27me3 and H3K36me3 levels suggest that *HEC1* and *PID* (and likely, most ETT-target genes) are not regulated through epigenetic memory but rather by gene regulatory networks (Chapter 2).

The further examination of VRN2 remained inconclusive concerning its role in the auxin-responsive regulation of ETT-target genes, which may be due to redundancy between VRN2 and its homologs FIS2 and EMF2. Since it appears that ETT plays an active role in regulation of H3K27me3 status, one could speculate that ETT directly recruits PRC2 action to its target genes. Therefore, future work first needs to clarify

whether FIS2 and EMF2 can also interact with ETT, and whether they do so in an auxin-sensitive manner. To fully understand the role of PRC2 in the auxin responsive regulation of ETT target genes, such as *HEC1* and *PID*, the binding of VRN2 and homologs to these loci needs to be evaluated using $ChIP_{qPCR}$. The co-localisation of PCR2 and ARFs at binding sites of auxin-responsive loci would indicate that they work together as a complex. Finally, the assessment of H3K27me3 dynamics at the *PID* locus in *VRN2*, *FIS2* and *EMF2* double and triple mutants would provide further evidence to support a role for VRN2 in the auxin-responsive regulation of chromatin dynamics. Nevertheless, results presented in Chapter 2, Chapter 3 and by others (Ariel et al., 2014) indicate a role of PRC2 in the regulation of the auxin-responsive gene, *PID* and possibly also *HEC1*. The suggested experiments will contribute to the general understanding of PRC2 in the regulation of both auxin-responsive genes, and the regulation of genes which are not regulated by epigenetic silencing.

The third ETT-interacting candidate that was identified in Chapter 3 is the Groucho/TLE-type co-repressor protein TOPLESS (TPL). The interaction between ETT and TPL was auxin sensitive raising several questions about how the two proteins interact and how they co-operatively mediate auxin signalling and modulate the local chromatin environment. Chapter 4 explores the mechanism by which ETT and TPL interact and the consequences of this interaction on the regulation of ETT-target genes. The results show that ETT interacts with several TPL/TPR family members in an auxin-sensitive manner through a conserved motif (RLFGF) in its C-terminal ES domain. Further analysis showed that a core LFG-motif is conserved among all ARFs. However, only class-B ARFs encode for the full motif and can interact with TPL/TPRs (Chapter 4; Causier et al., 2012; Liu et al., 2019). Since most class-B ARFs cannot interact with Aux/IAA proteins and regulation of their target genes can therefore not be explained through the canonical auxin-signalling pathway (Vernoux et al., 2011), it would be intriguing for future investigation to examine

whether non-canonical auxin signalling is a general feature of class-B ARFs rather than an ETT-specific phenomenon. This would suggest that class-B ARFs can directly recruit TPL to ARF-target genes instead of the indirect Aux/IAA-mediated recruitment of TPL by class-A ARFs. It would also imply a much wider significance of non-canonical auxin signalling in plant development. Phylogenetically, ETT has diverged relatively recently and can only be found in angiosperms (Finet et al., 2013; Mutte et al., 2018). In order to elucidate whether non-canonical auxin signalling is a recent ETT-specific innovation or whether it has evolved in parallel to canonical auxin signalling, it would be interesting to assay auxin-sensitivity of other class-B ARF-TPL interactions. Ideally, this would be done within *Arabidopsis* and other model plant species (e.g. *Marchantia polymorpha* (liverwort), *Physcomitrella patens* (moss)). Covering the whole evolutionary linage of land plants, could reveal the origin of non-canonical auxin signalling.

In agreement with what was recently shown for REL2, a homolog of TPL in maize (Liu et al., 2019), I show that interaction between ETT and TPL is mediated through the C-terminal region of TPL containing two WD40 repeats rather than through the N-terminal CTLH domain that facilitates interaction with the EAR-motif (LxLxL) of Aux/IAA proteins (Ke et al., 2015; Martin-Arevalillo et al., 2017). Interestingly, Groucho/TLE co-repressors interact with TFs through their WD40 domains in animals, suggesting an even deeper level of mechanistic convergence (Buscarlet and Stifani, 2007; Jennings and Ish-Horowicz, 2008; Liu et al., 2019).

Across kingdoms, Groucho/TLE-type co-repressors recruit histone deacetylases and regulate the local chromatin environment of target genes (Buscarlet and Stifani, 2007). In agreement with this, TPL interacts with HDA19 to repress target genes during flower development (Krogan et al., 2012). The results presented in Chapter 4 revealed that this is also the case in gynoecium development. Moreover, I found that ETT directly recruits TPL and HDA19 to its target loci. All three proteins associate

with DNA elements in the same regions of the promoters of *PID* and *HEC1* supporting a model in which ETT recruits TPL/TPR2 and HDA19 to ETT target loci. In Chapter 2, I show H3K27 acetylation increased in the absence of ETT and upon treatment with auxin. In the *ett-3* mutant there was no further increase of acetylation upon treatment with auxin suggesting that ETT mediates the association of TPL/TPR and HDA19 with these loci. This leads to a model in which low levels of auxin maintain ETT associations with TPL/TPR2 to repress gene expression via H3K27 deacetylation, whereas increasing auxin levels, disassociate TPL/TPR2 (and hence HDA19) from ETT, promoting H3K27 acetylation. Analogously to the auxin effect on the ETT-TPL-HDA19 interaction, ß-catenin-induced dissociation of the TCF-Groucho/TLE interaction and target locus acetylation is pivotal to Wnt/ß-catenin signalling during animal development (Gammons and Bienz, 2018).

Moreover, the proposed model agrees with previous data showing auxin dynamics at the gynoecium apex where *PID* expression is repressed at early stages of development to mediate radialization, but subsequently de-repressed as auxin levels rise to facilitate polar auxin transport (Simonini et al., 2016; Moubayidin and Ostergaard 2014). These data also support a hypothesis raised in a recent study in which a role for co-repressors in the recruitment of HDA19 during the repression of *STM* by ETT and ARF4 was suggested (Chung et al., 2019).

Low auxin binding affinity of ETT could be functionally relevant

The auxin concentrations required to dissociate the ETT-TPL interaction are relatively high compared to the auxin concentrations that promote Aux/IAA-TIR1/AFB interactions in the canonical pathway (Calderon Villalobos et al., 2012; Kepinski and Leyser, 2005). It can be speculated that the relatively high concentrations of auxin required for the auxin-effect in non-canonical pathway, are functionally relevant in a model in which the non-canonical pathway crosstalks with the canonical pathway (Figure 6.1).

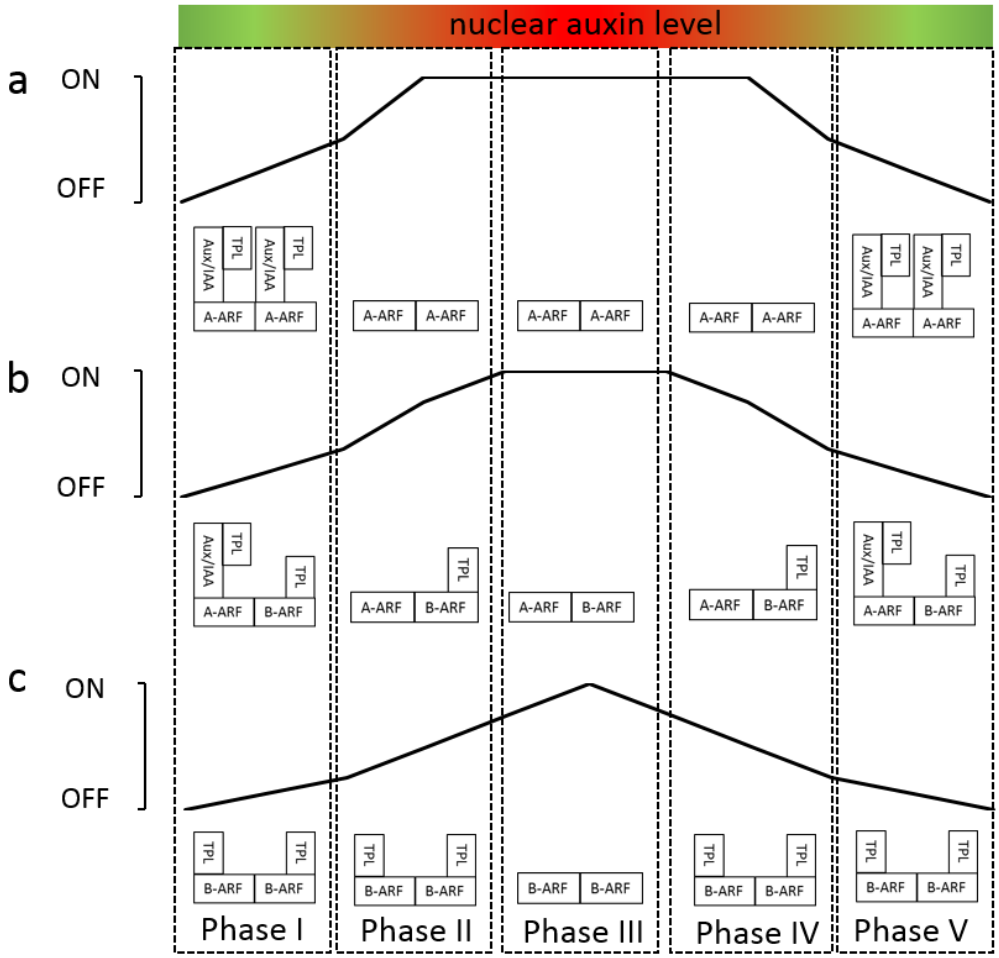

Figure 6. 1: Model describing potential crosstalk between canonical and non-canonical auxin signalling pathways. Canonically regulated class-A ARFs (A-ARF) are quickly relieved from repression due to the high auxin binding affinity of the TIR1/AFB receptors (a, b), while non-canonically regulated class-B ARFs (B-ARF) are de-repressed slowly at under high auxin levels (b, c). In contrast, non-canonically regulated ARFs can be repressed under higher auxin levels (b,c) then canonically regulated ARFs (a, b). If a gene is regulated by several canonical and non-canonical ARFs, then the ratio between the two types of ARF determines the auxin concentration threshold at which the gene is transcribed (b). ON indicates the full upregulation of the target gene while of indicates full repression of the target gene; green indicates low auxin while red indicates high auxin concentrations

In this model promoter bound canonically regulated class-A ARFs (i.e. Aux/IAA binding ARFs) are quickly relieved from repression when auxin levels increase due to the relatively high affinity of TIR1/AFBs to auxin (Figure 6.1 a, b). In contrast, promoter bound non-canonically regulated class-B ARFs (i.e. auxin binding ARFs such as ETT) are de-repressed at higher auxin levels due to the low auxin binding affinity of class-B ARFs (Figure 6.1 b, c). However, when auxin levels decrease, repression of non-canonically regulated ARFs could be restored at higher residual

auxin concentration, because their mode of regulation allows direct switching independent of the abundance of Aux/IAAs (Figure 6.1 b, c). Consequently, in such model non-canonically regulated ARFs act as a break on transcription due to their slow de-repression and fast repression. If a gene is regulated by several canonical and non-canonical ARFs, then the ratio between the two types of ARF determines the auxin concentration threshold at which the gene is transcribed (Figure 6.1 b). Since physical ARF-ARF interactions are likely, and AuxREs are often arranged as repeats it would be interesting to investigate such a mode of ARF-target gene regulation in more detail (Boer et al., 2014; Cherenkov et al., 2018; Korasick et al., 2014).

Two ETT-binding cis-regulatory elements within the *PID*-promoter are required for *PID* regulation during style development.

Throughout this thesis it is evident that auxin controls plant development through the gene-regulatory properties of Auxin Response Factors (ARFs). It is well-established that ARFs bind cis-regulatory elements, so-called Auxin Responsive Elements (AuxREs) in regulatory regions of their target genes (Boer et al., 2014; O'Malley et al., 2016). However, because all ARFs bind to this element, it is remains unclear how target-gene specificity of ARFs is achieved. A common hypothesis is that ARFs interact and cooperate with other transcription factors (TFs) to bind to complex DNA-binding sites harbouring cis-elements for several TFs (Kato et al., 2018; O'Malley et al., 2016; Weiste and Droege-Laser, 2014). Complex DNA-binding sites have not been studied systematically for ARF-target genes. In Chapter 5, I evaluate the importance of cis-regulatory elements in the regulation of auxin-responsive genes using *PID* as a model. *PID* is a gene involved in regulating polar auxin transport throughout plant development and also plays an important role during gynoecium apical development (style development). *PID* expression is directly regulated by ETT and its interacting partner INDEHISCENT (IND). In addition, *PID* is also directly

regulated by SPT, another TF that can interact with IND. Within the *PID*-promoter, ETT, IND and SPT binding sites are located close to each other forming a complex regulatory patch (Chapter 5; Girin et al., 2011; Simonini et al., 2016; Sorefan et al., 2009). To address the question of how relevant ETT binding to *PID* is for the regulation of gynoecium development, I mutated two ETT-binding AuxREs within the regulatory patch and observed increased style length in gynoecia of plants carrying mutated promoter variants. Furthermore, mutating the AuxREs led to ectopic repression of *PID* in one developmental context while leading to ectopically up-regulated *PID* expression at another stage. The data also show that IND associates with the *PID* promoter in an auxin-sensitive manner, while ETT binding to the promoter is insensitive to auxin. Altogether, the results demonstrate that targeted mutations of cis-regulatory elements can be used to dissect the importance of single cis-regulatory elements within complex regulatory regions, supporting the importance of the ETT-IND interaction for *PID* regulation. Although supporting the hypothesis that ARFs cooperate with other TFs to regulate target genes, this work also highlights the challenges of such studies as gene regulation is highly robust and mutations within gene regulatory regions may display subtle phenotypes.

Conclusion

The proper development of fruits is not only crucial for the successful completion of a plants life cycle. Fruits and the seeds enclosed in them are also a major source of nutrition for animals including humans and livestock. Over the last two decades, the hormonal and genetic basis of gynoecium development has been studied in detail in the model species *Arabidopsis thaliana*. It became evident that the phytohormone auxin has an essential role in gynoecium initiation and patterning throughout its development (Deb et al., 2018; Moubayidin and Østergaard, 2017). Moreover, ETT was found to be critical in orchestrating the developmental programs during the formation of gynoecia via the translation of auxin signals into differential gene

expression via an alternative auxin-signalling pathway in which auxin affects the activity of ETT-containing transcription factor complexes towards their target genes (Simonini et al., 2016; Simonini et al., 2017; Simonini et al., 2018b).

The work described in this thesis is aimed at elucidating this molecular mechanism and reveal how the ETT-mediated auxin-signalling pathway perceives and transduces auxin stimuli to generate a transcriptional output. I found that non-canonical auxin signalling is fundamentally different from and independent of the canonical TIR1/AFB-mediated auxin signalling pathway as it does not require protein degradation of its core components. Moreover, auxin has a direct effect on ETT suggesting that ETT acts as an auxin receptor. Direct auxin binding to ETT is a feature which is reminiscent of animal hormone-signalling pathways such as the Steroid/Thyroid Hormone and Wnt/ß-catenin signalling pathways. Moreover, auxin does not affect whether ETT is bound to DNA, which is another parallel to animal signalling mechanisms. These observations together with the lack of protein degradation makes the non-canonical auxin-signalling pathway instantly reversible, which could make it particularly suitable for controlling changes in tissue polarity during organogenesis.

In this study, I provide evidence that regulation of target genes through modification of local chromatin environment is a central aspect of the non-canonical auxin signalling. In agreement with that, ETT directly interacts with proteins that are parts of chromatin-modifying complexes under low auxin levels while high auxin levels dissociate these interactions. The work presented in this thesis shows that co-repressors of the TPL/TPR family as well as the HDA19 histone deacetylase are required for proper gynoecium development and molecular data suggest that ETT recruits these factors to its target genes under low auxin levels to mediate formation of a repressive chromatin state. My results and those of others have shown that other class-B ARFs can also interact directly with TPL, raising the possibility that this

mechanism may not be exclusive to ETT but may also play a role in controlling auxin-responsive gene expression through other class-B ARFs. This could suggest a much deeper significance of non-canonical auxin signalling in plant development (Chapter 2; Causier et al., 2012; Liu et al., 2019). Remarkably, the direct and ligand-dependent dissociation of a Groucho/TPL-HDAC module by transcription factors seems to be highly conserved in signalling mechanisms across eukaryotes (Buscarlet and Stifani, 2007; Chambers et al., 2017; Turki-Judeh and Courey, 2012).

In conclusion, this thesis describes the efforts taken to shed light onto the mechanism behind non-canonical auxin signalling. The identification of ETT as an auxin receptor which adds an additional layer of complexity to auxin biology, could help to explain how auxin imparts its effect on highly diverse processes throughout plant development. Furthermore, it raises the possibility that other transcription factors may also bind auxin and raises the exciting possibility that direct regulation of transcription factor interactions by other hormones and small molecules is a more general feature in plant biology.

Appendix

Appendix I - Supplemental Figures and Tables for Chapter 2

Appendix I Table 1: List of ETT regulated target genes based on re-analysing the results published in Simonini et al., 2017.

Gene ID	Name	log2 (fold change) *Col-0* +IAA	log2 (fold change) *ett-3*
AT5G67060	*HEC1*	1.6278	1.65224
AT5G52900	*MAKR6*	1.49142	1.37113
AT4G34760	*SAUR50*	1.19271	0.69973
AT1G70940	*PIN3*	0.94715	0.526049
AT2G36430	*DUF247*	0.65153	0.602134
AT2G21210	*SAUR6*	0.6336	0.560865
AT1G19050	*ARR7*	0.55704	0.432073
AT1G69780	*ATHB13*	0.36989	0.332443
AT2G45310	*GAE4*	0.36469	0.286333
AT2G30520	*RPT2*	0.36183	0.25828
AT3G60400	*SHOT1*	0.35908	0.407656
AT4G26540	*RGI3*	0.35812	0.391366
AT1G23080	*PIN7*	0.33233	0.319203
AT5G23280	*TCP7*	0.24671	0.573688
AT3G23050	*IAA7*	0.20174	0.427759

Appendix I Table 2: Oligonucleotides used in Chapter 2.

ID	Orientation	Amplico*n*	Sequence	Purpose
AK203	Sense	*UBQ10*	AGAACTCTTGCTGACTACAATATCCAG	qPCR
AK204	Antisense	*UBQ10*	ATAGTTTTCCCAGTCAACGTCTTAAC	qPCR
AK205	Sense	*PID*	ATTTACACTCTCTCCGTCATAGACAAC	qPCR
AK206	Antisense	*PID*	ACATGTGTAGATATTCTAACGCCACTA	qPCR
AK295	Sense	*IAA19*	GAGCATGGATGGTGTGCCTTAT	qPCR
AK296	Antisense	*IAA19*	TTCGCAGTTGTCACCATCTTTC	qPCR
AK348	Sense	*HEC1*	TGCATCAGATGGAGAAGCTTC	qPCR
AK349	Antisense	*HEC1*	ACCTGGTTCGTTGGTCATTG	qPCR
AK287	Sense	*PIN3*	GCGTCAATAAAAACCCGAAAG	qPCR
AK288	Antisense	*PIN3*	GAAGCTCCTTGGCGTCATG	qPCR
AK289	Sense	*PIN7*	TATTGGATTACGTGGAGACCTATTG	qPCR
AK290	Antisense	*PIN7*	CAAGATTGCGGGATGAACATTATAC	qPCR
AK291	Sense	*MAKR6*	CCATTGTGTAAGAGATTAAGGAGATGTAGA	qPCR
AK292	Antisense	*MAKR6*	GTCACAAGACCTTCTCCAATAATAATCA	qPCR
AK356	Sense	*HEC1 -2000*	ACAGTGAGAGCTTGTGGTGT	ChIP

AK357	Antisense	*HEC1 -2000*	ACCGTAAACAAGAAGCAGCA	ChIP
AK358	Sense	*HEC1 -1500*	TATCGGGTTGTCAGATGCAG	ChIP
AK359	Antisense	*HEC1 -1500*	ACTGACTTTCCTTCTGGCGA	ChIP
AK360	Sense	*HEC1 -800*	TGTTGTGCTTGTGAGACGAC	ChIP
AK361	Antisense	*HEC1 -800*	CGCATTTATCGACCGTCCAG	ChIP
AK362	Sense	*HEC1 -200*	CCGAATGACCGAATGCATGT	ChIP
AK363	Antisense	*HEC1 -200*	ATAGCAACTTGTGGCCCATC	ChIP
AK348	Sense	*HEC1 0*	TGCATCAGATGGAGAAGCTTC	ChIP
AK349	Antisense	*HEC1 0*	ACCTGGTTCGTTGGTCATTG	ChIP
AK350	Sense	*HEC1 300*	ACGGTTCCGGTTTACTCACT	ChIP
AK351	Antisense	*HEC1 300*	CTGCCATGTTCGTGCCATTA	ChIP
AK354	Sense	*HEC1 700*	ACTCATCAGATGGTGGGCAA	ChIP
AK355	Antisense	*HEC1 700*	cttggcttccctctccagaa	ChIP
AK096	Sense	*PID*	ACTAAACGTCGCCGATTTCA	ChIP
AK097	Antisense	*PID*	ACTAAAAGACTTGGGTCACG	ChIP
AK098	Sense	*PID*	TGGTTCTAAAGTCTGAACCT	ChIP
AK099	Antisense	*PID*	CTCTCTCTATGCTCCGACTC	ChIP
AK100	Sense	*PID*	GTCAATGCATGTAACTATAA	ChIP
AK101	Antisense	*PID*	CCCTCTCTTCCGCCAGGTAA	ChIP
AK102	Sense	*PID*	TGAGGCGAAAATCTCGGAAG	ChIP
AK103	Antisense	*PID*	TCAGCCGGTTATCATTCGAC	ChIP
AK104	Sense	*PID*	CTAGAGAACTCATGGTCACGG	ChIP
AK105	Antisense	*PID*	ATATAGGTTGGGTCCCTTCCAG	ChIP
AK106	Sense	*PID*	TTTACGTGGCTCCACTCCAC	ChIP
AK107	Antisense	*PID*	TGACCGAACCAATTCTAGCA	ChIP
AK108	Sense	*PID*	GTGGCTTCCATAGCGCCGGA	ChIP
AK109	Antisense	*PID*	CTAGCAACAGAGACCAACCC	ChIP
AK110	Sense	*PID*	GAACTCTTCTATGTAAGGTA	ChIP
AK111	Antisense	*PID*	TTTTAAACACAACATCTCGT	ChIP
AK112	Sense	*PID*	GTGGTAAACCCTATAACGGT	ChIP
AK113	Antisense	*PID*	CTACATGATGCGCCAAAGAT	ChIP
AK114	Sense	*PID*	TTCATTCCGTTTATCCGCTT	ChIP
AK115	Antisense	*PID*	GAAATTTTGTGTTTCTTCCG	ChIP
AK116	Sense	*PID*	AATTAGAAATATTCATCTCA	ChIP
AK117	Antisense	*PID*	TTGTTTTCAACATAAAAATC	ChIP
AK104	Sense	*PID*	CTAGAGAACTCATGGTCACGG	ChIP
AK105	Antisense	*PID*	ATATAGGTTGGGTCCCTTCCAG	ChIP
AK377	Sense	*PID*	gaatcactagtccaatatttctcc	ChIP
AK378	Antisense	*PID*	cagtaaaaagacgttacagagacc	ChIP
AK215	Sense	*PID*	TCTCACCGTCTGATTCTCGT	ChIP
AK216	Antisense	*PID*	ccctgtcctgtttcatctctg	ChIP
AK213	Sense	*PID*	CTCAGCGTAAAGAGTCGGC	ChIP

AK214	Antisense	*PID*	GGAGACGAAGAAGAGAGCCG	ChIP
AK211	Sense	*PID*	ACTAGAACTTCGGCGGCATA	ChIP
AK212	Antisense	*PID*	tcatgtcggtcttttccagttc	ChIP
AK098	Sense	*PID*	TGGTTCTAAAGTCTGAACCT	ChIP
AK099	Antisense	*PID*	CTCTCTCTATGCTCCGACTC	ChIP
AK207	Sense	*PID*	tgttcccaagttccgaagagt	ChIP
AK208	Antisense	*PID*	tattccctcgaagctgtcct	ChIP
AK217	Sense	*ACT*	GATATTCAGCCACTTGTCTGTG	ChIP
AK218	Antisense	*ACT*	CTTACACATGTACAACAAAGAAGG	ChIP
AK219	Sense	*STM*	GCCCATCATGACATCACATC	ChIP
AK220	Antisense	*STM*	GGGAACTACTTTGTTGGTGGTG	ChIP

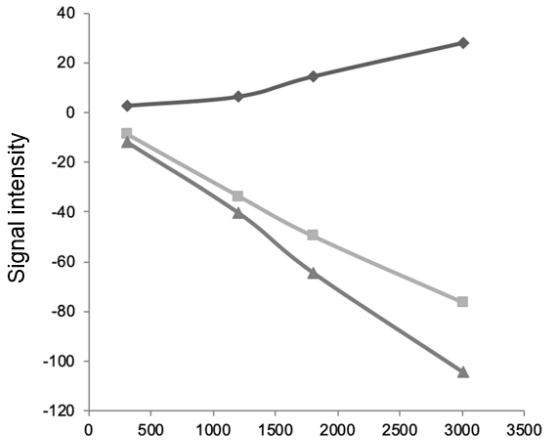

$K_D = L(I_{max} - x)/x = 1.1$ mM

where $x = I + aL$

WaterLOGSY values: L = 1,800 µM IAA;

$I_{max} = 2810547.75$; $I = 1467317.25$; $a = 3462.8$

Appendix I Figure 1: WaterLOGSY NMR showing the binding of IAA to ES388-594 protein. Signal intensity for IAA was recorded over a concentration range (x-axis) in the presence (square) and absence (triangle) of $ES^{388-594}$ protein. These values were compared to give the difference in signal intensity and binding curve (diamond). The K_D was calculated using the formula and values indicated. The WaterLOGSY NMR experiment was performed by Dr. Sigurd Ramans Harborough (University of Leeds).

Appendix II - Supplemental Figures and Tables for Chapter 3

Appendix II Table 1: List of candidates identified by Y2H library screen

Gene ID	Gene name	Localization	Condition
AT1G01550	BPS1, BYPASS 1	Chloroplast, plasma membrane	WLH
AT1G02140	HAP1, HAPLESS 1, MAGO, MAGO NASHI,	Chloroplast	WLAH
AT1G02205	CER1, CER22, ECERIFERUM 1, ECERIFERUM 22	ER	WLA
AT1G03900	ABCI18, ATNAP4	Cytosol	WLAH
AT1G04420	NAD(P)-linked oxidoreductase superfamily protein	Chloroplast	WLA
AT1G04950	ATTAF6	Nucleus	WLH
AT1G06040	B-BOX DOMAIN PROTEIN 24, BBX24	Nucleus	WLA
AT1G06680	OE23, OEE2, OXYGEN EVOLVING COMPLEX SUBUNIT 23 KDA	Chloroplast	WLAH
AT1G06760	winged-helix DNA-binding transcription factor family protein	Nucleus	WLH
AT1G07080	Thioredoxin superfamily protein	Vacuole	WLA
AT1G08190	ATVAM2, ATVPS41	Vacuole	WLH
AT1G09590	Translation protein SH3-like family protein	Cytosol	WLAH
AT1G09970	LRR XI-23, RECEPTOR-LIKE KINASE 7, RLK7	plasma membrane	WLA
AT1G10350	DNAJ heat shock family protein	Cytoplasm	WLAH
AT1G12050	FUMARYLACETOACETATE HYDROLASE	Cytosol	WLA
AT1G12610	DWARF AND DELAYED FLOWERING 1, DDF1	Nucleus	WLH
AT1G13210	ACA.L, AUTOINHIBITED CA2+/ATPASE II	Golgi	WLA
AT1G15125	S-adenosyl-L-methionine-dependent methyltransferases	Nucleus	WLA
AT1G15500	ATNTT2	Chloroplast	WLH
AT1G15730	unknown protein	Chloroplast	WLA
AT1G15750	TOPLESS, TPL	Nucleus	WLAH
AT1G15820	CP24, LHCB6, LIGHT HARVESTING COMPLEX PHOTOSYSTEM II SUBUNIT 6	Chloroplast	WLA
AT1G16250	Galactose oxidase/kelch repeat superfamily protein	Cytosol	WLH
AT1G17440	CKH1, CYTOKININ-HYPERSENSITIVE 1	Nucleus	WLAH
AT1G18330	EARLY-PHYTOCHROME-RESPONSIVE1, EPR1, REVEILLE 7, RVE7	Nucleus	WLA
AT1G20020	ATLFNR2, FERREDOXIN-NADP(+)-OXIDOREDUCTASE 2	Chloroplast	WLH
AT1G20340	DNA-DAMAGE-REPAIR/TOLERATION PROTEIN 112, DRT112	Nucleus	WLH
AT1G20620	ATCAT3, CAT3, CATALASE 3	Apoplast	WLH
AT1G25230	Calcineurin-like metallo-phosphoesterase superfamily protein	Apoplast	WLA
AT1G25550	myb-like transcription factor family protein	Nucleus	WLH
AT1G27400	Ribosomal protein L22p/L17e family protein	Cytosol	WLA

AT1G29310	SecY protein transport family protein	Chloroplast	WLA
AT1G29930	AB140, CAB1, CAB140, CHLOROPHYLL A/B BINDING PROTEIN 1	Chloroplast	WLA
AT1G30360	EARLY-RESPONSIVE TO DEHYDRATION 4, ERD4	Chloroplast	WLA
AT1G30400	ABCC1	plasma membrane	WLH
AT1G30520	AAE14, ACYL-ACTIVATING ENZYME 14	Chloroplast	WLA
AT1G31330	PHOTOSYSTEM I SUBUNIT F, PSAF	Chloroplast	WLH
AT1G31350	KAR-UP F-BOX 1, KUF1	Nucleus	WLA
AT1G32130	ARABIDOPSIS THALIANA IWS1 (FROM YEAST INTERACTS WITH SPT6)	Nucleus	WLA
AT1G32640	ATMYC2, JAI1, JASMONATE INSENSITIVE 1	Nucleus	WLH
AT1G32930	GALT31A, GLYCOSYLTRANSFERASE OF CAZY FAMILY GT31A	Golgi	WLAH
AT1G33055	unknown protein	Mitochondrion	WLH
AT1G43170	ARP1, EMB2207, EMBRYO DEFECTIVE 2207, RIBOSOMAL PROTEIN 1, RP1, RPL3A	Ribosome	WLA
AT1G43890	ARABIDOPSIS RAB GTPASE HOMOLOG B18, ARABIDOPSIS RAB GTPASE HOMOLOG C1,	Cell Membrane	WLH
AT1G48410	AGO1, ARGONAUTE 1, ATAGO1, ICU9	Nucleus	WLAH
AT1G48598	CONSERVED PEPTIDE UPSTREAM OPEN READING FRAME 31		WLA
AT1G49970	CLP PROTEASE PROTEOLYTIC SUBUNIT 1, CLPR1	Chloroplast	WLH
AT1G50970	Membrane trafficking VPS53 family protein	Golgi	WLA
AT1G51590	ALPHA-MANNOSIDASE 1, ALPHA-MANNOSIDASE IB, MANIB, MNS1	golgi	WLH
AT1G52400	A. THALIANA BETA-GLUCOSIDASE 1, ATBG1	ER	WLH
AT1G53000	ATCKS, CKS, CMP-KDO SYNTHETASE, KDSB	Mitochondrion	WLAH
AT1G53910	RAP2.12, RELATED TO AP2 12	Nucleus	WLH
AT1G54080	OLIGOURIDYLATE-BINDING PROTEIN 1A, UBP1A	Nucleus	WLA
AT1G61120	TPS4	Chloroplast	WLH
AT1G61790	OLIGOSACCHARYLTRANSFERASE SUBUNIT 3/6, OST3/6	Chloroplast	WLH
AT1G65900	unknown protein		WLAH
AT1G65930	CICDH	Apoplast	WLA
AT1G67090	RBCS1A, RIBULOSE BISPHOSPHATE CARBOXYLASE SMALL CHAIN 1A	Apoplast	WLH
AT1G67360	Rubber elongation factor protein	Cytoplasm	WLH
AT1G67630	DNA POLYMERASE ALPHA 2, EMB2814, EMBRYO DEFECTIVE 2814, POLA2	Mitochondrion	WLH
AT1G67750	Pectate lyase	Cytosol	WLA
AT1G68560	ALPHA-XYLOSIDASE 1, ALTERED XYLOGLUCAN 3, ATXYL1	Apoplast	WLH
AT1G69040	ACR4, ACT DOMAIN REPEAT 4	Cytosol	WLAH
AT1G70160	unknown protein	Nucleus	WLAH
AT1G70370	PG2, POLYGALACTURONASE 2	Apoplast	WLA

AT1G71695	Peroxidase superfamily	Cell Wall	WLH
AT1G72440	EDA25, EMBRYO SAC DEVELOPMENT ARREST 25, SLOW WALKER2, SWA2	Nucleus	WLH
AT1G72520	ARABIDOPSIS THALIANA LIPOXYGENASE 4, ATLOX4, LIPOXYGENASE 4, LOX4	Chloroplast	WLH
AT1G73885	unknown protein		WLA
AT1G74040	2-ISOPROPYLMALATE SYNTHASE 1	Chloroplast	WLAH
AT1G74470	multifunctional protein with geranylgeranyl reductase activity	Chloroplast	WLH
AT1G74790	unknown protein		WLA
AT1G75940	BETA GLUCOSIDASE 20	ER	WLH
AT1G76160	SKS5, SKU5 SIMILAR 5	Apoplast	WLH
AT1G76810	eIF2, EUKARYOTIC TRANSLATION INITIATION FACTOR 2	Cytosol	WLA
AT1G79380	RGLG4, RING DOMAIN LIGASE 4	Cell Membrane	WLA
AT1G80070	ABNORMAL SUSPENSOR 2, SUS2	Nucleus	WLA
AT2G01010	18SrRNA	Ribosome	WLH
AT2G01600	ENTH/ANTH/VHS superfamily protein	Golgi	WLA
AT2G01630	O-Glycosyl hydrolases family 17 protein	Plasmamembrane	WLH
AT2G02148	unknown protein		WLA
AT2G02870	Galactose oxidase/kelch repeat superfamily protein	Chloroplast	WLAH
AT2G04630	NRPB6B, NRPE6B	Nucleus	WLH
AT2G05520	GLYCINE RICH PROTEIN 3, ATGRP-3, ATGRP3	Cell Wall	WLH
AT2G06950	Retrotransposon		WLH
AT2G07706	unknown protein	Chloroplast	WLH
AT2G15580	RING/U-box superfamily protein	Mitochondrion	WLA
AT2G16600	ROC3	Golgi	WLA
AT2G17990	unknown protein		WLH
AT2G20790	clathrin adaptor complexes medium subunit family protein	Nucleus	WLH
AT2G21270	UBIQUITIN FUSION DEGRADATION 1, UFD1	Chloroplast	WLAH
AT2G21660	"COLD, CIRCADIAN RHYTHM, AND RNA BINDING 2", ATGRP7, CCR2,	Apoplast	WLA
AT2G23450	Protein kinase superfamily protein	Golgi	WLH
AT2G24500	FZF, REI1-LIKE 2, REIL2	Cytosol	WLA
AT2G26770	SCAB1, STOMATAL CLOSURE-RELATED ACTIN BINDING PROTEIN 1	Cytoplasm	WLAH
AT2G27600	ATSKD1, SKD1, SUPPRESSOR OF K+ TRANSPORT GROWTH DEFECT1, VACUOLAR PROTEIN SORTING 4, VPS4	Cytoplasm	WLAH
AT2G28830	ATPUB12, PLANT U-BOX 12, PUB12	Nucleus	WLA
AT2G30040	MAPKKK14, MITOGEN-ACTIVATED PROTEIN KINASE 14	Cytoplasm	WLH
AT2G30570	PHOTOSYSTEM II REACTION CENTER W, PSBW	Chloroplast	WLH
AT2G30870	ARABIDOPSIS THALIANA GLUTATHIONE S-TRANSFERASE PHI 10, ATGSTF10, ATGSTF4	Apoplast	WLA
AT2G35020	GLCNA.UT2, GLCNAC1PUT2, N-ACETYLGLUCOSAMINE-1-PHOSPHATE URIDYLYLTRANSFERASE 2	Cytosol	WLA

AT2G36170	60S RIBOSOMAL PROTEIN L40 A, RPL40A, UBIQUITIN EXTENSION PROTEIN 2, UBQ2	ribosome	WLA
AT2G36460	FBA6, FRUCTOSE-BISPHOSPHATE ALDOLASE6	Cytoplasm	WLAH
AT2G37520	Acyl-CoA N-acyltransferase with RING/FYVE/PHD-type zinc finger domain	Nucleus	WLA
AT2G38700	ATMVD1, MEVALONATE DIPHOSPHATE DECARBOXYLASE 1, MVD1	Cytosol	WLA
AT2G39700	ATEXP4, ATEXPA4, ATHEXP ALPHA 1.6, EXPA4, EXPANSIN A4	Cytosol	WLA
AT2G41340	"RNA POLYMERASE II FIFTH LARGEST SUBUNIT, D", RPB5D	Nucleus	WLH
AT2G42500	PP2A-3, PROTEIN PHOSPHATASE 2A-3	Cytosol	WLH
AT2G42840	PDF1, PROTODERMAL FACTOR 1	Apoplast	WLH
AT2G44200	CBF1-interacting co-repressor CIR	Nucleus	WLH
AT2G46020	BRAHMA, BRM, CHROMATIN REMODELING 2	Nucleus	WLAH
AT2G47490	NAD+ TRANSPORTER	Chloroplast	WLH
AT2G47940	DEG2 Protease	Chloroplast	WLAH
AT3G01500	ATBCA1, ATSABP3	Chloroplast	WLH
AT3G03630	Cysteine synthase 26	Chloroplast	WLA
AT3G05280	Integral membrane Yip1 family protein	Cell Membrane	WLA
AT3G05350	Metallopeptidase M24 family protein	Chloroplast	WLA
AT3G06483	PYRUVATE DEHYDROGENASE KINASE	Mitochondrion	WLA
AT3G08580	mitochondrial ADP/ATP carrier	Golgi	WLA
AT3G09030	BTB/POZ domain-containing protein	Cell Membrane	WLA
AT3G09200	Ribosomal protein L10 family protein	Apoplast	WLAH
AT3G09300	ORP3B	Cytosol	WLA
AT3G10360	APUM4, PUM4, PUMILIO 4	Cytoplasm	WLH
AT3G11800	unknown protein		WLA
AT3G11830	TCP-1/cpn60 chaperonin	Cytosol	WLA
AT3G12120	ATFAD2, FAD2, FATTY ACID DESATURASE 2	ER	WLH
AT3G12270	ARABIDOPSIS THALIANA PROTEIN ARGININE METHYLTRANSFERASE 3, ATPRMT3	Cytoplasm	WLAH
AT3G12760	unknown protein	Nucleus	WLA
AT3G13060	ECT5, EVOLUTIONARILY CONSERVED C-TERMINAL REGION 5	Cytoplasm	WLAH
AT3G14100	RNA-binding (RRM/RBD/RNP motifs) family protein	Nucleus	WLA
AT3G15730	PHOSPHOLIPASE D ALPHA 1, PLD	Chloroplast	WLAH
AT3G15950	NAI2	ER	WLH
AT3G16950	LIPOAMIDE DEHYDROGENASE 1, LPD1, PTLPD1	Cytosol	WLAH
AT3G17680	Kinase interacting (KIP1-like) family protein		WLAH
AT3G17900	unknown protein	Chloroplast	WLH
AT3G19860	BASIC HELIX-LOOP-HELIX 121, BHLH121	Nucleus	WLAH
AT3G21070	ATNADK-1, NAD KINASE 1, NADK1	Cytosol	WLAH
AT3G22440	FRIGIDA-like protein	Nucleus	WLA

AT3G23410	ARABIDOPSIS FATTY ALCOHOL OXIDASE 3, ATFAO3, FAO3, FATTY ALCOHOL OXIDASE 3	Cell Membrane	WLA
AT3G24530	AAA-type ATPase family protein / ankyrin repeat family protein	Chloroplast	WLAH
AT3G26085	CAAX amino terminal protease	Chloroplast	WLA
AT3G27350	unknown protein	Nucleus	WLH
AT3G41768	18SrRNA	Cytoplasm	WLH
AT3G47290	ATPLC8, PHOSPHATIDYLINOSITOL-SPECIWC PHOSPHOLIPASE C8, PLC8	plasma membrane	WLA
AT3G47620	ATTCP14, TCP14, TEOSINTE BRANCHED, CYCLOIDEA AND PCF (TCP) 14	Nucleus	WLH
AT3G48000	ALDEHYDE DEHYDROGENASE 2	Chloroplast	WLAH
AT3G48560	ACETOHYDROXY ACID SYNTHASE, ACETOLACTATE SYNTHASE, AHAS	Chloroplast	WLA
AT3G49010	40S RIBOSOMAL PROTEIN, ATBBC1, BBC1, BREAST BASIC CONSERVED 1, RSU2	Golgi	WLH
AT3G50820	OEC33, OXYGEN EVOLVING COMPLEX SUBUNIT 33 KDA, PHOTOSYSTEM II SUBUNIT O-2, PSBO-2, PSBO2	Chloroplast	WLAH
AT3G51550	FER, FERONIA	Apoplast	WLA
AT3G51580	unknown protein	golgi	WLA
AT3G51740	IMK2, INFLORESCENCE MERISTEM RECEPTOR-LIKE KINASE 2	Cell Wall	WLH
AT3G52590	UBIQUITIN EXTENSION PROTEIN 1, UBQ1	Nucleus	WLA
AT3G53120	VPS37-1	Nucleus	WLH
AT3G54100	O-fucosyltransferase family protein	Golgi	WLH
AT3G54890	LHCA1, PHOTOSYSTEM I LIGHT HARVESTING COMPLEX GENE 1	Chloroplast	WLAH
AT3G55110	ABCG18, ATP-BINDING CASSETTE G18	plasma membrane	WLH
AT3G55330	PPL1, PSBP-LIKE PROTEIN 1	Chloroplast	WLAH
AT3G55710	UDP-Glycosyltransferase superfamily protein	Golgi	WLAH
AT3G55980	ATSZF1, SALT-INDUCIBLE ZINC FINGER 1, SZF1	Nucleus	WLH
AT3G57550	AGK2, GK-2, GUANYLATE KINAS 2, GUANYLATE KINASE	Cytoplasm	WLA
AT3G57870	SCE1, SCE1A, SUMO CONJUGATING ENZYME 1A, SUMO CONJUGATION ENZYME 1	Cytosol	WLA
AT3G58600	Adaptin ear-binding coat-associated protein 1	Cytoplasm	WLA
AT3G60340	alpha/beta-Hydrolases superfamily protein	Vacuole	WLA
AT3G60390	HAT3, HOMEOBOX-LEUCINE ZIPPER PROTEIN 3	Nucleus	WLA
AT3G61010	Ferritin/ribonucleotide reductase	Chloroplast	WLAH
AT3G61240	DEA(D/H)-box RNA helicase	Cytoplasm	WLA
AT3G61440	ARATH;BSAS3;1, ATCYSC1, BETA-SUBSTITUTED ALA SYNTHASE 3;1, CYSC1, CYSTEINE SYNTHASE C1	Mitochondrion	WLAH
AT3G62300	ABAP1-I NTERACTING PROTEIN 1, AIP1, ATDUF7, DOMAIN OF UNKNOWN FUNCTION 724 7, DUF7	Nucleus	WLH

AT3G62580	Late embryogenesis abundant protein (LEA) family protein	Chloroplast	WLH
AT4G00100	ATRPS13A	Chloroplast	WLA
AT4G00238	DNA-binding storekeeper protein-related transcriptional regulator	Nucleus	WLH
AT4G01850	ATSAM2, MAT2, S-ADENOSYLMETHIONINE SYNTHETASE 2, SAM-2, SAM2	Cytosol	WLA
AT4G02330	ATPME41, ATPMEPCRB, PECTIN METHYLESTERASE 41, PME41	Cell Wall	WLA
AT4G02940	oxidoreductase, 2OG-Fe(II) oxygenase family protein		WLH
AT4G04970	ATGSL01, ATGSL1, GLUCAN SYNTHASE LIKE 1, GLUCAN SYNTHASE LIKE-1, GLUCAN SYNTHASE-LIKE 1, GSL01, GSL1	Cell Wall	WLA
AT4G07410	PCN, POPCORN	Nucleus	WLH
AT4G08870	ARGAH2, ARGININE AMIDOHYDROLASE 2	Mitochondrion	WLA
AT4G11420	ATEIF3A-1, ATTIF3A1, EIF3A, EIF3A-1, EUKARYOTIC TRANSLATION INITIATION FACTOR 3A, TIF3A1	Cytosol	WLH
AT4G12800	PHOTOSYSTEM I SUBUNIT L, PSAL	Chloroplast	WLH
AT4G13285	unknown protein		WLAH
AT4G13850	ATGRP2, GLYCINE RICH PROTEIN 2	Mitochondrion	WLAH
AT4G16590	ATCSLA01, ATCSLA1, CELLULOSE SYNTHASE-LIKE A01, CELLULOSE SYNTHASE-LIKE A1, CSLA01	Golgi	WLA
AT4G16770	2-oxoglutarate (2OG) and Fe(II)-dependent oxygenase superfamily protein	Cytoplasm	WLA
AT4G16845	REDUCED VERNALIZATION RESPONSE 2, VRN2	Nucleus	WLA
AT4G16870	copia-like retrotransposon family		WLA
AT4G18440	L-Aspartase-like family protein	Chloroplast	WLA
AT4G20670	Domain of unknown function (DUF26)	Apoplast	WLAH
AT4G21960	PRXR1	Cell Wall	WLH
AT4G22310	unknown protein	Mitochondrion	WLH
AT4G25550	Cleavage/polyadenylation specificity factor	Nucleus	WLA
AT4G26630	DEK-DOMAIN CONTAINING PROTEIN 3, DEK3	Nucleus	WLA
AT4G26690	GDPDL3, GLYCEROPHOSPHODIESTER PHOSPHODIESTERASE (GDPD) LIKE 3	Cell Wall	WLAH
AT4G27020	unknown protein		WLAH
AT4G27520	ATENODL2, EARLY NODULIN-LIKE PROTEIN 2, ENODL2	Chloroplast	WLAH
AT4G30190	AHA2, H(+)-ATPASE 2, HA2, PLASMA MEMBRANE PROTON ATPASE 2, PMA2	golgi	WLH
AT4G30950	FAD6	Chloroplast	WLH
AT4G31700	RPS6	ribosome	WLA
AT4G32260	PDE334, PIGMENT DEFECTIVE 334	Chloroplast	WLH
AT4G32410	ANISOTROPY1	Golgi	WLH
AT4G33680	ABERRANT GROWTH AND DEATH 2, AGD2	Cytosol	WLAH
AT4G34890	ATXDH1, XANTHINE DEHYDROGENASE 1, XDH1	Cytosol	WLH

AT4G35090	CAT2, CATALASE 2	Chloroplast	WLA
AT4G35310	ATCPK5, CALMODULIN-DOMAIN PROTEIN KINASE 5, CPK5	Cytosol	WLA
AT4G35420	DIHYDROFLAVONOL 4-REDUCTASE-LIKE1, DRL1, TETRAKETIDE ALPHA-PYRONE REDUCTASE 1, TKPR1	ER	WLA
AT4G35630	PHOSPHOSERINE AMINOTRANSFERASE 1, PSAT1	Chloroplast	WLH
AT4G35780	ACT-like protein tyrosine kinase	Cytosol	WLH
AT4G36105	unknown protein	Nucleus	WLA
AT4G36650	ATPBRP, PBRP, PLANT-SPECIFIC TFIIB-RELATED PROTEIN	Nucleus	WLH
AT4G36920	AP2, APETALA 2, ATAP2, FL1, FLO2, FLORAL MUTANT 2, FLOWER 1	Nucleus	WLH
AT4G39280	phenylalanyl-tRNA synthetase	Cytosol	WLH
AT4G39550	Galactose oxidase/kelch repeat superfamily protein	Nucleus	WLA
AT4G40040	H3.3, HISTONE 3.3	Nucleus	WLA
AT5G01650	Tautomerase/MIF superfamily protein	Chloroplast	WLA
AT5G02500	ARABIDOPSIS THALIANA HEAT SHOCK COGNATE PROTEIN 70-1, AT-HSC70-1, ATHSP70-1	Cytoplasm	WLAH
AT5G02970	alpha/beta-Hydrolases superfamily protein	Cytoplasm	WLH
AT5G03520	ARABIDOPSIS RAB HOMOLOG E1D, ATRAB-E1D	Golgi	WLA
AT5G03850	Nucleic acid-binding, OB-fold-like protein	Golgi, Cytosol	WLH
AT5G04060	-adenosyl-L-methionine-dependent methyltransferases superfamily protein	Golgi	WLA
AT5G07030	aspartyl protease family protein	Cell Wall	WLA
AT5G08640	ATFLS1, FLAVONOL SYNTHASE, FLAVONOL SYNTHASE 1, FLS, FLS1	Cytoplasm	WLH
AT5G08680	mitochondrial ATP synthase	Mitochondrion	WLA
AT5G08770	unknown protein		WLH
AT5G09760	Plant invertase/pectin methylesterase inhibitor superfamily	Cell Wall	WLH
AT5G09810	ACT7, ACTIN 7, ATACT7	Cytoplasm	WLA
AT5G11170	HOMOLOG OF HUMAN UAP56 A	Nucleus	WLA
AT5G11490	adaptin family protein	Golgi	WLA
AT5G11720	Glycosyl hydrolases family	Cytosol	WLA
AT5G13450	ATP5, DELTA SUBUNIT OF MT ATP SYNTHASE	Mitochondrion	WLH
AT5G13530	KEG	Cytosol	WLA
AT5G13630	ABA-BINDING PROTEIN, ABAR	Chloroplast	WLH
AT5G13650	SUPPRESSOR OF VARIEGATION 3, SVR3	Chloroplast	WLH
AT5G14040	MITOCHONDRIAL PHOSPHATE TRANSPORTER 3	Mitochondrion	WLAH
AT5G14420	RGLG2, RING DOMAIN LIGASE2	Nucleus	WLAH
AT5G14540	unknown protein		WLH
AT5G14590	Isocitrate/isopropylmalate dehydrogenase family protein	Chloroplast	WLA
AT5G16715	EMB2247, EMBRYO DEFECTIVE 2247	Chloroplast	WLAH
AT5G17230	PHYTOENE SYNTHASE, PSY	Chloroplast	WLA

AT5G17920	ATCIMS, ATMETS, ATMS1, COBALAMIN-INDEPENDENT METHIONINE SYNTHASE, METHIONINE SYNTHESIS 1	Apoplast	WLAH
AT5G18040	HEAT-INDUCED TAS1 TARGET 2, HTT2	Mitochondrion	WLA
AT5G18570	ATOBGC, ATOBGL, CHLOROPLASTIC SAR1	Chloroplast	WLH
AT5G20300	TOC90	Chloroplast	WLAH
AT5G21326	CALCINEURIN B-LIKE PROTEIN (CBL)-INTERACTING PROTEIN KINASE 26, CIPK26	Cytosol	WLH
AT5G23090	NUCLEAR FACTOR Y, SUBUNIT B13	Nucleus	WLAH
AT5G24490	30S ribosomal protein	ribosome	WLA
AT5G24620	Pathogenesis-related thaumatin superfamily protein	Apoplast	WLAH
AT5G24770	ATVSP2, VEGETATIVE STORAGE PROTEIN 2, VSP2	Chloroplast	WLAH
AT5G25980	BETA GLUCOSIDASE 37, BGLU37, GLUCOSIDE GLUCOHYDROLASE 2, TGG2	Apoplast	WLA
AT5G27380	ATGSH2, GLUTATHIONE SYNTHETASE 2, GSH2, GSHB	Chloroplast	WLAH
AT5G27520	ATPNC2, PEROXISOMAL ADENINE NUCLEOTIDE CARRIER 2, PNC2	Mitochondrion	WLH
AT5G27560	Domain of unknown function DUF1995	Chloroplast	WLH
AT5G27630	ACBP5, ACYL-COA BINDING PROTEIN 5, ATACBP5	Cytoplasm	WLAH
AT5G35670	IQ-DOMAIN 33, IQD33	Nucleus	WLAH
AT5G35790	G6PD1, GLUCOSE-6-PHOSPHATE DEHYDROGENASE 1	Chloroplast	WLAH
AT5G38170	Bifunctional inhibitor/lipid-transfer protein/seed storage 2S albumin superfamily protein	Cell Wall	WLAH
AT5G38410	RBCS3B, RUBISCO SMALL SUBUNIT 3B	Apoplast	WLA
AT5G38420	RBCS2B, RUBISCO SMALL SUBUNIT 2B	Apoplast	WLAH
AT5G40580	20S PROTEASOME BETA SUBUNIT PBB2, PBB2	Cytoplasm, Nucleus	WLH
AT5G44060	unknown protein	Mitochondrion	WLA
AT5G44070	ARA8, ARABIDOPSIS THALIANA PHYTOCHELATIN SYNTHASE 1	Chloroplast	WLA
AT5G47200	ARABIDOPSIS RAB GTPASE HOMOLOG D2B, ATRAB1A, ATRABD2B, RAB GTPASE HOMOLOG 1A, RAB1A	Cytosol	WLH
AT5G47480	MAG5, MAIGO 5	Golgi	WLA
AT5G48485	DEFECTIVE IN INDUCED RESISTANCE 1, DIR1	Apoplast, ER	WLH
AT5G49030	OVA2, OVULE ABORTION 2	Chloroplast	WLA
AT5G49510	PFD3, PREFOLDIN 3	Cytosol	WLA
AT5G50180	Protein kinase superfamily protein		WLA
AT5G50920	HEAT SHOCK PROTEIN 93-V, HSP93-V	Chloroplast	WLH
AT5G52970	thylakoid lumen 15.0 kDa protein	Chloroplast	WLH
AT5G54310	ARF-GAP DOMAIN 5	Cytosol	WLH
AT5G54600	PLASTID RIBOSOMAL PROTEIN L24, RPL24, SUPPRESSOR OF VARIEGATION 8, SVR8	Chloroplast	WLH

AT5G54770	THI1, THI4, THIAMINE4, THIAZOLE REQUIRING, TZ	Chloroplast	WLA
AT5G55250	ATIAMT1, IAA CARBOXYLMETHYLTRANSFERASE 1, IAMT1	Nucleus	WLA
AT5G56010	ATHSP90-3, ATHSP90.3, HEAT SHOCK PROTEIN 81-3	Golgi	WLA
AT5G56290	PEROXIN 5	Peroxisome	WLH
AT5G56670	Ribosomal protein S30 family protein	ribosome	WLAH
AT5G57660	ATCOL5, B-BOX DOMAIN PROTEIN 6, BBX6, COL5, CONSTANS-LIKE 5	Nucleus	WLH
AT5G57800	CER3, ECERIFERUM 3, FACELESS POLLEN 1, FLP1, WAX2, YRE	ER	WLAH
AT5G58330	NADP-DEPENDENT MALATE DEHYDROGENASE, NADP-MDH	Apoplast	WLAH
AT5G58340	myb-like HTH transcriptional regulator family protein	Nucleus	WLA
AT5G58590	RAN BINDING PROTEIN 1, RANBP1	Nucleus	WLA
AT5G60390	GTP binding Elongation factor Tu family protein	Golgi	WLH
AT5G62530	ALDEHYDE DEHYDROGENASE 12A1, ALDH12A1	Chloroplast	WLAH
AT5G64070	PHOSPHATIDYLINOSITOL 4-OH KINASE BETA1, PI-4KBETA1, PI4KBETA1	Golgi	WLH
AT5G64350	FK506-BINDING PROTEIN 12, FKBP12, FKP12	Chloroplast	WLA
AT5G64740	CELLULOSE SYNTHASE 6, CESA6, E112, ISOXABEN RESISTANT 2, IXR2, PRC1, PROCUSTE 1	Golgi	WLH
AT5G64816	unknown protein		WLH
AT5G65760	Serine carboxypeptidase S28 family protein	Chloroplast	WLAH
ATCG00780	RIBOSOMAL PROTEIN L14, RPL14	Chloroplast	WLH

Appendix II Table 2: List of primers used Y2H (Gateway cloning)

ID	Description	Sequence 5'-3'
AK199	Library Screen	CTGGTTGGACGGACCAAACTG
AK200	Library Screen	GATCAGAGGTTACATGGCCAAG
AK035	AGO1 F	GGGGACAAGTTTGTACAAAAAAGCAGGCTTTATGGTGAGAAAGAGAAGAACG
AK036	AGO1 R	GGGGACCACTTTGTACAGAAAGCTGGGTATCAGCAGTAGAACATGACACG
AK118	AGO4 F	GGGGACAAGTTTGTACAAAAAAGCAGGCTTTATGGATTCAACAAATGGTAACGG
AK119	AGO4 R	GGGGACCACTTTGTACAGAAAGCTGGGTATTAACAGAAGAACATGGAGTTGGC
AK031	AP2 F	GGGGACAAGTTTGTACAAAAAAGCAGGCTTTATGTGGGATCTAAACGACGCAC
AK032	AP2 R	GGGGACCACTTTGTACAGAAAGCTGGGTATCAAGAAGGTCTCATGAGAGGAG
AK120	BRM F	GGGGACAAGTTTGTACAAAAAAGCAGGCTTTATGCAATCTGGAGGCAGTGG
AK121	BRM R	GGGGACCACTTTGTACAGAAAGCTGGGTACTATAAATGGCTAGGCCGTC
AK025	CKH1 F	GGGGACAAGTTTGTACAAAAAAGCAGGCTTTATGGCGGAACCGATTCCCTCATC
AK026	CKH1 R	GGGGACCACTTTGTACAGAAAGCTGGGTATTAGTATCGTGTCATGTGTTGTAATATG
AK070	COL5 F	GGGGACAAGTTTGTACAAAAAAGCAGGCTTTATGGGATTCGGCTTAGAGAG
AK071	COL5 R	GGGGACCACTTTGTACAGAAAGCTGGGTATCAGAACGTTGGTACGACAC
AK068	DDF1 F	GGGGACAAGTTTGTACAAAAAAGCAGGCTTTATGAATAATGATGATATTATTCTGG
AK069	DDF1 R	GGGGACCACTTTGTACAGAAAGCTGGGTATTAATATCTGTAACTCCACAATG

AK029	DEK3 F	GGGGACAAGTTTGTACAAAAAAGCAGGCTTTATGGGGGAAGATACAAAGGC
AK030	DEK3 R	GGGGACCACTTTGTACAGAAAGCTGGGTATTAGGCTTTCACCTCCTCACC
AK062	HAT3 F	GGGGACAAGTTTGTACAAAAAAGCAGGCTTTATGAGTGAAAGAGATGATGGATTG
AK063	HAT3 R	GGGGACCACTTTGTACAGAAAGCTGGGTACTAATGAGAACCAGCAGCAGG
AK076	MYC2 F	GGGGACAAGTTTGTACAAAAAAGCAGGCTTTATGACTGATTACCGGCTACAAC
AK077	MYC2 R	GGGGACCACTTTGTACAGAAAGCTGGGTATTAACCGATTTTTGAAATCAAAC
AK122	NRPB6B F	GGGGACAAGTTTGTACAAAAAAGCAGGCTTTATGGCTGACGACGATTACAATG
AK123	NRPB6B R	GGGGACCACTTTGTACAGAAAGCTGGGTATCAATCACCACCGACTTGACG
AK078	PBRP F	GGGGACAAGTTTGTACAAAAAAGCAGGCTTTATGAAGTGTCCGTACTGTTCATCG
AK079	PBRP R	GGGGACCACTTTGTACAGAAAGCTGGGTACTAGAAGTCTCCATGGGGATTATC
AK037	PCN F	GGGGACAAGTTTGTACAAAAAAGCAGGCTTTATGCTCGAGTACCGTTGCAGC
AK038	PCN R	GGGGACCACTTTGTACAGAAAGCTGGGTATCAAGTTCCAAAAATATGTCTGTC
AK066	RAP2.12 F	GGGGACAAGTTTGTACAAAAAAGCAGGCTTTATGTGTGGAGGAGCTATAATATCC
AK067	RAP2.12 R	GGGGACCACTTTGTACAGAAAGCTGGGTATCAGAAGACTCCTCCAATCATG
AK151	SAP18 F	GGGGACAAGTTTGTACAAAAAAGCAGGCTTTATGGCTGAAGCAGCGAGAAG
AK152	SAP18 R	GGGGACCACTTTGTACAGAAAGCTGGGTACTAGTAAATTGCCACATCCA
AK027	TAF6 F	GGGGACAAGTTTGTACAAAAAAGCAGGCTTTATGAGCATTGTACCTAAGGAAAC
AK028	TAF6 R	GGGGACCACTTTGTACAGAAAGCTGGGTATTAGAGGAATACTGACATCTCTG
AK041	TCP14 F	GGGGACAAGTTTGTACAAAAAAGCAGGCTTTATGCAAAAGCCAACATCAAG
AK042	TCP14 R	GGGGACCACTTTGTACAGAAAGCTGGGTACTAATCTTGCTGATCCTCCTC
AK153	TPL F	GGGGACAAGTTTGTACAAAAAAGCAGGCTTTATGTCTTCTCTTAGTAGAGAGCTCG
AK154	TPL R	GGGGACCACTTTGTACAGAAAGCTGGGTATCATCTCTGAGGCTGATCAGAT
AK023	VRN2 F	GGGGACAAGTTTGTACAAAAAAGCAGGCTTTATGTGTAGGCAGAATTGTCGCGC
AK024	VRN2 R	GGGGACCACTTTGTACAGAAAGCTGGGTATTACTTGTCTCTGCTGTTATTGTCC

Appendix II Table 3: List of primers used for cloning and genotyping

ID	Description	Sequence 5'-3'	Purpose
AK230	DEK3 promoter part1 F	TGAAGACTTGGAGACGGTACTTAAGCTACGTGGTC	Cloning Gus-line
AK231	DEK3 promoter part1 R	TGAAGACTTCGATTCTTCGGAATCTCACCTC	Cloning Gus-line
AK232	DEK3 promoter part2 F	TGAAGACTTATCGTGCTTTAGAACCCTGTGG	Cloning Gus-line
AK233	DEK3 promoter part2 R	TGAAGACTTCATTATTACAAACCAGTTCAGTAGATCC	Cloning Gus-line
AK236	DEK4 promoter part1 F	TGAAGACTTGGAGTCCGAGCATACCCCAAACTC	Cloning Gus-line
AK237	DEK4 promoter part1 R	TGAAGACTTCGATTCTTTGGAATCTCACCTTC	Cloning Gus-line
AK238	DEK4 promoter part2 F	TGAAGACTTATCGTCCTTTCGAGTCTCTTTGTAC	Cloning Gus-line
AK239	DEK4 promoter part2 R	TGAAGACTTCATTTGCTCACACCCAATGTTCAG	Cloning Gus-line
AK157	SALK_112581.46.05.x (*dek3-2*) F	CGTAGCCTGCAGAAGAACAAC	Genotyping
AK158	SALK_112581.46.05.x (*dek3-2*) R	ACTGTCCATCACTGGTCAACC	Genotyping
AK261	SALK_102885.16.70.x (*dek4-1*) F	CGTTGCTACTGAGGAAGATGC	Genotyping
AK262	SALK_102885.16.70.x (*dek4-1*) R	ACTTCAAAGCCATGGGAATTC	Genotyping
AK195	SALK_047055.43.00.x (*vrn2-1*) F	ACAATCAACAACGTCCAGAGC	Genotyping

AK196	SALK_047055.43.00.x (*vrn2-1*) R	TCCTGTGAGTTTCAGCTAGCC	Genotyping
AK203	UBQ10 F	AGAACTCTTGCTGACTACAATATCCAG	qPCR
AK204	UBQ10 R	ATAGTTTTCCCAGTCAACGTCTTAAC	qPCR
AK205	PID F	ATTTACACTCTCTCCGTCATAGACAAC	qPCR
AK206	PID R	ACATGTGTAGATATTCTAACGCCACTA	qPCR
AK108	APOLO F	GTGGCTTCCATAGCGCCGGA	qPCR
AK109	APOLO R	CTAGCAACAGAGACCAACCC	qPCR

Appendix II Table 4: List of plasmids used for cloning of Gus-reporter lines. The Plasmids are available from TSL Synbio (http://synbio.tsl.ac.uk/)

ID	Level	Description	AddGene	Selection
pICH41295	L0	Acceptor for Pro+5U modules	AddGene #47997	Spectinomycin
pICH75111	L0	Gus gene	AddGene #50327	Spectinomycin
pAGM5331	L0	Simian Virus 40 nuclear localisation signal	AddGene #50294	Spectinomycin
pICH41421	L0	Nos (nopaline synthase) terminator	AddGene #50339	Spectinomycin
pICSL11017	L1	Position1 BASTA resistance cassette	-	Ampicilin
pICH47742	L1	Position 2	AddGene #48001	Ampicilin
pICH41744	L1	End-linker 2 for level 2 construction	AddGene #48017	Spectinomycin
pAGM4723	L2	Binary vector	-	Kanamycin

Appendix III - Supplemental Figures and Tables for Chapter 4

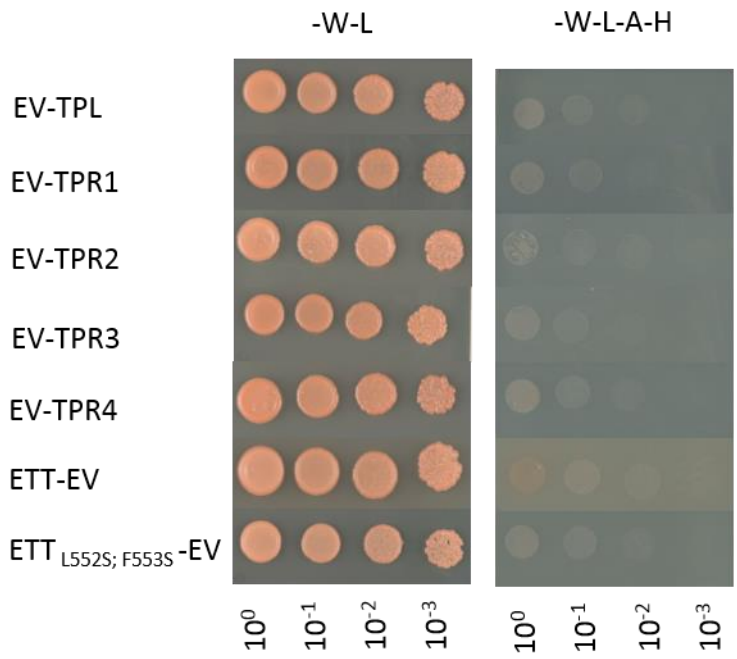

Appendix III Figure 1: Negative controls for Y2H Figure 4.1b.

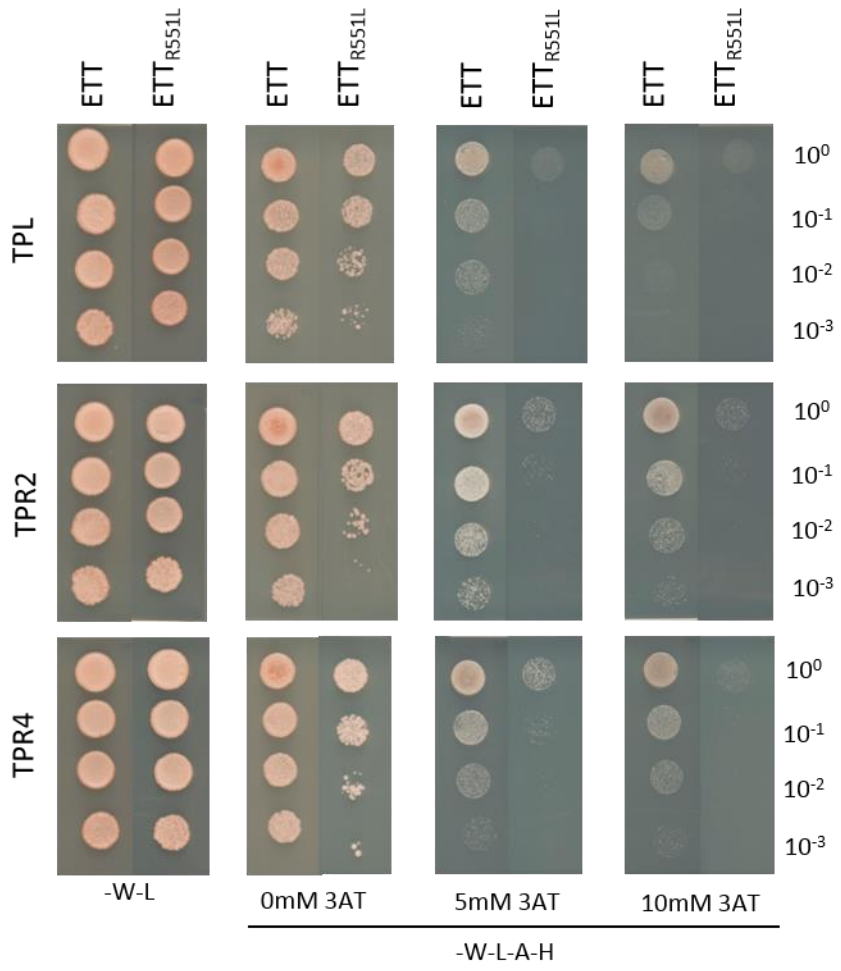

Appendix III Figure 2: Additional panels supporting Figure 4.2.

```
REL2     MSSLSRELVFLILQFLDEEKFKETVHKLEQESGFYFNMKHFEDLVQGGEWDEVEKYLSGF   60
TPL      MSSLSRELVFLILQFLDEEKFKETVHKLEQESGFFFNMKYFEDEVHNGNWDEVEKYLSGF   60
         ************************************:****:*** *:.*:***********

REL2     TKVEDNRYSMKIFFEIRKQKYLEALDRHDRAKAVEILVKDLKVFASFNEELFKEITQLLT  120
TPL      TKVDDNRYSMKIFFEIRKQKYLEALDKHDRPKAVDILVKDLKVFSTFNEELFKEITQLLT  120
         ***:**********************:*** ***:*********::**************

REL2     LENFRQNEQLSKYGDTKSARNIMLLELKKLIEANPLFRDKLNFPPFKASRLRTLINQSLN  180
TPL      LENFRENEQLSKYGDTKSARAIMLVELKKLIEANPLFRDKLQFPTLRNSRLRTLINQSLN  180
         *****:*************** ***:*****************:** :: ************

REL2     WQHQLCKNPRPNPDIKTLFTDHSCAAPTNGARAPPPA-NGPLGSIPKSAGFPPMGAHAPF  239
TPL      WQHQLCKNPRPNPDIKTLFVDHSCGPPN-GARAPSPVNNPLLGGIPKAGGFPPLGAHGPF  239
         ******************.****. *. ***** *. *  **.***:.****:***.**

REL2     QPVVSPSPNAIAGWMTNANPSLPHAAVAQGPPGLVQAPNTAAFLKHPRTPTSAPGIDYQS  299
TPL      QPTASPVPTPLAGWMSSPS-SVPHPAVSAGAIA-LGGPSIPAALKHPRTPPTNASLDYPS  297
         **..** *. :****:. . *:** **: *  . : .*.  * ******* :  .:** *

REL2     ADSEHLMKRMRV-GQPDEV---------SFSGA--SHPANMYTQEDLPKQVSRTLNQGSN  347
TPL      ADSEHVSKRTRPMGISDEVNLGVNMLPMSFSGQAHGHSPAFKAPDDLPKTVARTLSQGSS  357
         *****: ** *  *  ***         ****   .*   : : :**** *:***.***.

REL2     VMSLDFHPVQQTILLVGTNVGDIAVWEVGSRERIAHKTFKVWDIGSCTLPLQASLMKDAA  407
TPL      PMSMDFHPIKQTLLLVGTNVGDIGLWEVGSRERLVQKTFKVWDLSKCSMPLQAALVKEPV  417
          **:****::**:*******R**.:********:.:*******:..*::****:*:*: .

REL2     VSVNRCLWSPDGTILGVAFSKHIVQTYTFVPNGDLRQQAEIDAHIGGVNDIAFSHPNKTL  467
TPL      VSVNRVIWSPDGSLFGVAYSRHIVQLYSYHGGEDMRQHLEIDAHVGGVNDISFSTPNKQL  477
         ***** :*****:::***:*:**** *::  . *:**: *****:******:** *** *

REL2     SIITCGDDKLIKVWDAQTGQKQYTFEGHEAPVYSVCPHYKESIQFIFSTAIDGKIKAWLY  527
TPL      CVITCGDDKTIKVWDAATGVKRHTFEGHEAPVYSVCPHYKENIQFIFSTALDGKIKAWLY  537
         .:******* ****** ** *::******************.********:*********

REL2     DCLGSRVDYDAPGHWCTTMAYSADGTRLFSCGTSKEGDSHLVEWNETEGAIKRTYNGFRK  587
TPL      DNMGSRVDYDAPGRWCTTMAYSADGTRLFSCGTSKDGESFIVEWNESEGAVKRTYQGFHK  597
         * :**********:**********************:*:*.:*****:***:****:**:*

REL2     RSLGVVQFDTTRNRFLAAGDEFLVKFWDMDNNNILTTTDCDGGLPASPRLRFNREGSLLA  647
TPL      RSLGVVQFDTTKNRYLAAGDDFSIKFWDMDAVQLLTAIDGDGGLQASPRIRFNKEGSLLA  657
         ***********:**:*****:* :******  ::**: * **** ****:***:******

REL2     VTTSDNGIKILANTDGQRLLRMLESRAFEGSRGPPQQINTKPPIVALGPVSNVSSPIAVN  707
TPL      VSGNENVIKIMANSDGLRLLHTFENISSESSKPAINSIAA---------AA---AAAATS  705
         *: .:* ***:**:** ***: :*. : *.*:   :.* :         .:   :  *..

REL2     AERPDRILPAVSTSGLAPMDASRTPDVKPRITDE-SEKVKTWKLADIVDNGHLRALHLTD  766
TPL      AGHADRSANVVSIQGMN-GDSRNMVDVKPVITEESNDKSKIWKLTEVSEPSQCRSLRLPE  764
         * : **   .** .*:   *: .  **** **:* .:* * ***::: : .: *:*:* :

REL2     TDTNPSKIVRLLYTNNGVALLALGSNAVHKLWKWQRSDRNPSGKSTASVAPHLWQPANGI  826
TPL      N-LRVAKISRLIFTNSGNAILALASNAIHLLWKWQRNERNATGKATASLPPQQWQPASGI  823
         .  . :** **::**.* *:***.***:* ******.:** :**:***: *: ****.**

REL2     LMTNDTNDGNPEEATACIALSKNDSYVMSASGGKVSLFNMMTFKVMTTFMAPPPAATFLA  886
TPL      LMTNDVAETNPEEAVPCFALSKNDSYVMSASGGKISLFNMMTFKTMATFMPPPPAATFLA  883
         *****. : *****. *:****************:*********.*:*** *********
```

Appendix III Figure 3: Alignment indicating the high degree of conservation between *AtTPL* and *ZmREL2*. The G368 residue that is essential for interaction is highlighted in red.

Appendix III Table 1: Oligonucleotides used in Chapter 4

ID	Orientation	Amplicon	Sequence	Purpose
AK420	Sense	*ETT*	GGGGACAAGTTTGTACAAAAAAGCAGGCTTTATGGGTGGTTTAATCGATCTGAACG	Gateway Cloning
AK340	Antisense	*ETT*	GGGGACCACTTTGTACAAGAAAGCTGGGTACTAGAGAGCAATGTCTAGCAACATG	Gateway Cloning
AK330	Sense	$ETT_{L552S;\ F553S}$	ATGCAGGTCTTCTGGTTTCC	Gateway Cloning
AK331	Antisense	$ETT_{L552S;\ F553S}$	GGAAACCAGAAGACCTGCAT	Gateway Cloning
AK418	Sense	$ETT_{R->L}$	ATGCCTGCTGTTTGGTTTC	Gateway Cloning
AK419	Antisense	$ETT_{R->L}$	GAAACCAAACAGCAGGCAT	Gateway Cloning
AK281	Sense	*TPL*	GGGGACAAGTTTGTACAAAAAAGCAGGCTTTATGTCTTCTCTTAGTAGAGAGCTCG	Gateway Cloning
AK282	Antisense	*TPL*	GGGGACCACTTTGTACAGAAAGCTGGGTATCATCTCTGAGGCTGATCAGAT	Gateway Cloning
AK379	Sense	$TPL^{1-184/202}$	GGGGACAAGTTTGTACAAAAAAGCAGGCTTTATGTCTTCTCTTAGTAGAGAG	Gateway Cloning
AK380	Antisense	TPL^{1-202}	GGGGACCACTTTGTACAAGAAAGCTGGGTACTAGTGATCCACAAAAAGAGTC	Gateway Cloning
AK381	Antisense	TPL^{1-184}	GGGGACCACTTTGTACAAGAAAGCTGGGTACTACTGGTGTTGCCAATTTAAG	Gateway Cloning
AK401	Sense	$TPL^{\ 185-END}$	GGGGACAAGTTTGTACAAAAAAGCAGGCTTTCTTTGTAAAAATCCAAGGC	Gateway Cloning
AK402	Antisense	$TPL^{\ 185\ -634}$	GGGGACCACTTTGTACAAGAAAGCTGGGTACTAATGGCAGTTAAAAGCTGTACA	Gateway Cloning
AK403	Sense	TPL WD6 - WD11	GGGGACAAGTTTGTACAAAAAAGCAGGCTTTCACAAGCGTTCTCTAGGTGT	Gateway Cloning
AK404	Antisense	TPL WD6-WD11	GGGGACCACTTTGTACAAGAAAGCTGGGTACTAAGCTTACTCTTCACCTCAT	Gateway Cloning
AK405	Sense	TPL WD11-WD15	GGGGACAAGTTTGTACAAAAAAGCAGGCTTTCCACCACCGGCTGCTACTT	Gateway Cloning
AK406	Antisense	TPL -END	GGGGACCACTTTGTACAAGAAAGCTGGGTACTATCTCTGAGGCTGATCAGAT	Gateway Cloning
AK383	Sense	CRISPR TPR2 Guide 1	agGGAAAATGAGCAACTGTCG	Genotyping

AK384	Antisense	CRISPR TPR2 Guide 2	TCTTGCTCACCATCAAACGG	Genotyping
AK385	Sense	CRISPR TPR2 Guide 3	TTGGATGTTTGTGCAGACCG	Genotyping
AK386	Antisense	CRISPR TPR2 Guide 4	TCGAGGTGTTGACGTAGGTC	Genotyping
AK255	Sense	SALK_034518C	GCTATGCTGTTTATTGCAGGC	Genotyping
AK256	Antisense	SALK_034518C	GTTCTGAATTGCAGGAGTTGC	Genotyping
AK325	Sense	SALK_139443	ACTCTCTTCCTTGTCTGCGTG	Genotyping
AK326	Antisense	SALK_139443	ACCAGACAATGAATCAGCACC	Genotyping
AK364	Sense	CRISPR *TPR2* Guide 1	TGTGGTCTCAATTGGCTAGCTTCTCTCGAAACAGGTTTAAGAGCTATGCTGGAA	GoldenGate
AK365	Sense	CRISPR *TPR2* Guide 2	TGTGGTCTCAATTGGACTCCACCATGCACTCCAAGGTTTAAGAGCTATGCTGGAA	GoldenGate
AK366	Sense	CRISPR *TPR2* Guide 3	TGTGGTCTCAATTGGAGAGAGTTAGACGGTGCCCGGTTTAAGAGCTATGCTGGAA	GoldenGate
AK367	Sense	CRISPR *TPR2* Guide 4	TGTGGTCTCAATTGGCTCCATGCTACACGAGTGAGTTTAAGAGCTATGCTGGAA	GoldenGate
AK299	Sense	*pTPL*	CCTCTAGAGTCGACCTGCAGAAATGGTTTGAACGCTTCGT	infusion cloning
AK300	Antisense	*pTPL*	CTCAGATCTACCATGGGTTTTCTCTCACTTCCTTAAAAGAC	infusion cloning
AK301	Sense	*pTPR2*	CCTCTAGAGTCGACCTGCAGCGGTGGTATGCAACAGAAAA	infusion cloning
AK302	Antisense	*pTPR2*	CTCAGATCTACCATGGTTTTTCCTAAAACTCTCAGAAGAAG	infusion cloning
AK303	Sense	*pTPR4*	CCTCTAGAGTCGACCTGCAGACGCTTTGTCTGGAGAAGGT	infusion cloning
AK304	Antisense	*pTPR4*	CTCAGATCTACCATGGATCCTCTTCTTATTGCTCGCTC	infusion cloning
AK399	Sense	*HDA19*	CGCTCACTACGGTCTCCTTC	qPCR
AK400	Antisense	*HDA19*	GGTAATGCTGCGGAGAAAAG	qPCR
AK397	Sense	*HDA6*	ATTCGCCGGAGTATGTTGAC	qPCR
AK398	Antisense	*HDA6*	AAGGATCGCCCATAGATTCC	qPCR
AK348	Sense	*HEC1*	TGCATCAGATGGAGAAGCTTC	qPCR

AK349	Antisense	*HEC1*	ACCTGGTTCGTTGGTCATTG	qPCR
AK205	Sense	*PID*	ATTTACACTCTCTCCGTCATAGACAAC	qPCR
AK206	Antisense	*PID*	ACATGTGTAGATATTCTAACGCCACTA	qPCR
AK387	Sense	*TPL*	CTCGAGGCTTTGGATAAGCATG	qPCR
AK388	Antisense	*TPL*	ACACTTTCAAATCCTTCACTAGTATATCCAC	qPCR
AK389	Sense	*TPR1*	ATTGGCATCAAATGCTATTCATCTG	qPCR
AK390	Antisense	*TPR1*	AGTTGCATTACGGTCATTTCGC	qPCR
AK391	Sense	*TPR2*	CAGCTGCTTACTCTGGAGAATTTTAGG	qPCR
AK392	Antisense	*TPR2*	AGATTTAGTATCACCATATTTCGACAGTTG	qPCR
AK393	Sense	*TPR3*	ACTCTATTCACAGACCACACTTGCAC	qPCR
AK394	Antisense	*TPR3*	AACAGGCTGATTGACTGCTGAAG	qPCR
AK395	Sense	*TPR4*	TGATACACGTGAGGGAAACAAAGAG	qPCR
AK396	Antisense	*TPR4*	TGACATAAGAATCATTTTTTGAGAGTGC	qPCR
AK203	Sense	*UBQ10*	AGAACTCTTGCTGACTACAATATCCAG	qPCR
AK204	Antisense	*UBQ10*	ATAGTTTTCCCAGTCAACGTCTTAAC	qPCR

Appendix IV - Supplemental Figures and Tables for Chapter 5

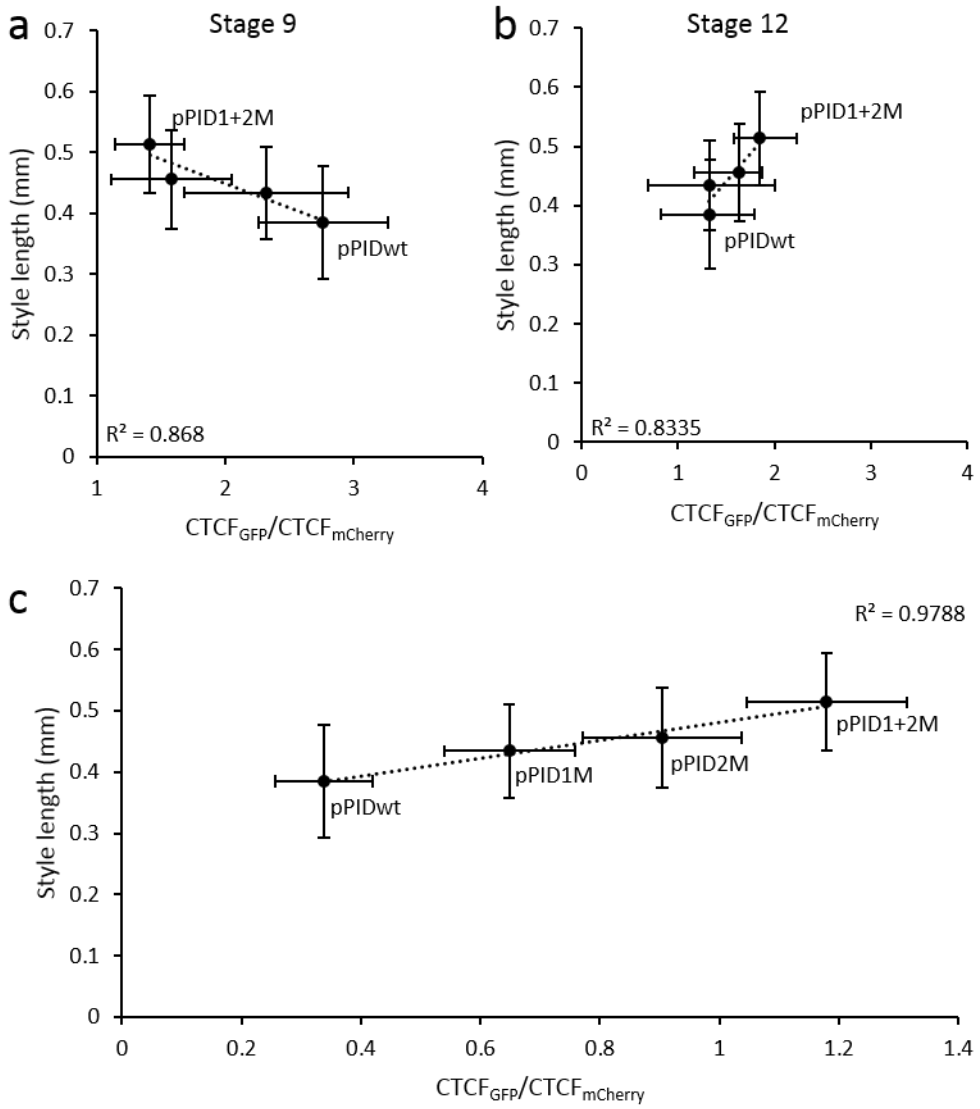

Appendix IV Figure 1: Correlation between style length and PID-GFP abundance in stage 9 (a) and stage 12 (b) and correlation between *PID* promoter activity and style length (c) in different AuxRE mutant lines. Shown are means ± standard deviation

Appendix IV Table 1: Oligonucleotides used in Chapter 5.

ID	Orientation	Description	Sequence 5'-3'
AK173	Sense	Promoter	TGAAGACTTGGAGCGTGTAGACCAAATCCAGGGT
AK174	Antisense	Promoter	TGAAGACTTCATTCGCCGGGAAAATCGAAGTTA
AK175	Antisense	Promoter 1M	TGAAGACTTTGAGACGTTATCACGTGCCTGAAA
AK176	Sense	Promoter 2M	TGAAGACTTCTCACACGTGTCATATATCTTACG
AK177	Sense	Promoter 1M	TGAAGACTTCTCACACGTATCATATATCTTACG
AK178	Antisense	Promoter 2M	TGAAGACTTTGAGACGTTGTCACGTGCCTGAAA
AK179	Sense	Gene part1	TGAAGACTTAATGTTACGAGAATCAGACGGTGAGA

AK180	Antisense	Gene part1	TGAAGACTTGCCTCCTGATCTCTGCGTAAGCGA
AK181	Sense	Gene part2	TGAAGACTTAGGCGAAAAAAACAAGGCCTAACC
AK182	Antisense	Gene part2	TGAAGACTTATGACGAGGAAGATTCAACGGCTG
AK183	Sense	Gene part3	TGAAGACTTTCATCGCCGGAGAATCAACAACTC
AK184	Antisense	Gene part3	TGAAGACTTCGAAGATCCAAAGTAATCGAACGCC G

Appendix IV Table 2: List of plasmids used for cloning. The Plasmids are available from TSL Synbio (http://synbio.tsl.ac.uk/)

ID	Level	Description	AddGene	Selection
pICH41295	L0	Acceptor for Pro+5U modules	AddGene #47997	Spectinomycin
opICSL01005	L0	Acceptor for CDS no stop (ns) modules	AddGene #47996	Spectinomycin
pICSL50008	L0	Green Fluorescent Protein (GFP) for C-terminal fusion	AddGene #50314	Spectinomycin
pICSL80013	L0	GFP with Simian Virus 40 nuclear localisation signal	-	Spectinomycin
pICH50581	L0	ACTIN 2 Constitutive promoter – plants	AddGene #50256	Spectinomycin
pAGM5331	L0	Simian Virus 40 nuclear localisation signal	AddGene #50294	Spectinomycin
pICSL80007	L0	mCherry Fluorescent protein	AddGene #50321	Spectinomycin
pICH41421	L0	Nos (nopaline synthase) terminator	AddGene #50339	Spectinomycin
pICSL11017	L1	Position1 BASTA resistance cassette	-	Ampicilin
pICH47742	L1	Position 2	AddGene #48001	Ampicilin
pICH47751	L1	Position 3	AddGene #48002	Ampicilin
pICH41766	L1	End-linker 3 for level 2 construction	AddGene #48018	Ampicilin
pAGM4723	L2	Binary vector	-	Kanamycin

List of Abbreviations

Abbreviation	Full Name
^{13}C	carbon-13 isotope
^{15}N	nitrogen-15 isotope
2,4-D	2,4-Dichlorophenoxyacetic acid
3AT	3-Amino-1,2,4-triazole
2D	2 Dimensional
ABP1	AUXIN BINDING PROTEIN 1
ACT2	ACTIN2
AGO4	AGONAUTE 4
ALC	ALCATRAZ
ANOVA	Analysis of variance
APOLO	AUXIN REGULATED PROMOTER LOOP RNA
ARF	Auxin Response Factor
At	*Arabidopsis thaliana*
Aux/IAA	AUXIN/INDOLE-3-ACETIC ACID
Aux/LAX	AUXIN RESISTANT 1/ LIKE AUXIN RESISTENT 1
AuxRE	Auxin Responsive Element
BA	Benzoic Acid
BDL	BODENLOS; INDOLE-3-ACETIC ACID INDUCIBLE 12 (IAA12)
bHLH	helix-loop-helix
BP	BREVIPEDICELLUS
bp	base pairs
BRM	BRAHMA
BSH	BUSHY
ccvTIR1	concave TIR1
CD	Circular Dichroism Spectroscopy
cDNA	complementary DNA
$ChIP_{qPCR}$	chromatin immunoprecipitation followed by qPCR
ChIP-seq	chromatin immunoprecipitation followed by sequencing
CK	cytokinin
CLV3	CLAVATA 3
COI1	CORONATINE INSENSITIVE 1
Col-0	Columbia-0
CRISPR	Clustered Regularly Interspaced Short Palindromic Repeats
CTCF	corrected total cell fluorescence
C-terminal	carboxy-terminal
CTLH	C-terminal to LisH
cvxIAA	convex IAA
DBD	DNA binding domain
DDF1	DWARD AND DELAYED FLOWERING
DEK3	DEK-DOMAIN CONTAINING PROTEIN 3
DNA	deoxyribonucleic acid
E. coli	Escherichia coli

EAR motif	Ethylene-responsive element binding factor-associated Amphiphilic Repression motif
EC	extracellular space
EMF	EMBRYONIC FLOWER
ES domain	ETT-Specific domain
ETT	ETTIN
FACS	fluorescence activated cell sorting
FIS	FERTILIZATION INDEPENDENT SEED
FLC	FOWERING LOCUS C
Fz	Frizzled
GA	Gibberelic Acid
GE	genome edited
GFP	Green Fluorescent Protein
GID1	GA RECEPTOR RING E3 UBIQUITIN LIGASE
Gro/TLE	Groucho/T
GTF	general transcription factor
GUS	ß-glucoronidase
H2A	Histone 2A
H2B	Histone 2B
H3	Histone 3
H3K27ac	Histone 3 lysine 27 Acetylation
H3K27me3	Histone 3 lysine 27 tri-methylation
H3K36me3	Histone 3 lysine 36 tri-methylation
H3K4me3	Histone 3 lysine 4 tri-methylation
H3K9ac	Histone 3 lysine 9 Acetylation
H4	Histone 4
HDA19	HISTONE DEACETYLASE 19
HDACs	histone deacetylases
HD-Zip	homeodomain-leucin zipper
HEC1, 2, 3	HECTATE1, 2, 3
HOX genes	Homeobox genes
HSP	heat-shock protein
HSQC	heteronuclear single quantum coherence
IAA	Indole 3-Acetic Acid
IC	intracellular space
IND	INDEHISCENT
INTACT	isolation of nuclei tagged in specific cell types
IP MS/MS	Immunoprecipitation Mass Spectormetry
IPA	indole-3-pyruvate
ITC	isothermal titration calorimetry
JA	Jasmonic Acid
JAZ	JASMONATE ZIM-DOMAIN PROTEIN
K_D	dissociation constant
LB medium	Lysogeny broth medium
LisH	Lis1-homologous
lncRNA	noncoding RNA
LRR	Leucin-Rich-Repeat
MAKR6	MEMBRANE-ASSOCIATED KINASE REGULATOR 6

MP	MONOPTEROS/ARF5
MS medium	Murashige and Skoog medium
NAA	1-Naphthaleneacetic acid
NMR	nuclear magnetic resonance
NPA	N-1-naphthylphthalamic acid
N-terminal	amino-terminal
ONPG	o-Nitrophenyl-β-D-Galactopyranoside
PB1 domain	Phox and Bem1 domain
PCN	POPCORN
PCR	Polymerase chain reaction
PIC	preinitiation complex
PID	PID
PIN	PIN-FORMED
Pol II	RNA Polymerase II
PP2A	PROTEIN PHOSPHATASE 2A
PPT/BASTA	Phosphinothricin
PRC2	Polycomb Repressive Complex 2
qPCR	quantitative real time PCR
REF6	RELATIVE OF EARLY FLOWERING 6
REL2	RAMOSA 1 ENHANCER LOCUS 2
RNA	ribonucleic acid
RNAi	RNA-interference
RNA-seq	RNA-sequencing
RPL	REPLUMLESS
SAM	Shoot Apical Meristem
SAP18	SIN3-ASSOCIATED PROTEIN 18
SCF	Skp1/Cullin/F-box
SEM	scanning electron microscopy
SHR	steroid hormone receptors
SPR	Surface Plasmon Resonance
SPT	SPATULA
STM	SHOOT MERISTEMLESS
SWI/SNF	SWITCH/SUCROSE NONFERMENTING
SWI3A, B, C	SWITCH/SUCROSE NONFERMENTING 3A, B, C
SYD	SPLAYED
TAA1	TRYPTOPHAN AMINOTRANSFERASE OF ARABIDOPSIS 1
TAR	TRYPTOPHAN AMINOTRANSFERASE REALATED
TCF	T-Cell Factor
TCP14	TEOSINTE BRANCHED, CYCLOIDEA AND PCF 14
TF	transcription factor
THR	thyroid hormone receptors
TIR1/AFB	TRANSPORT INHIBITOR RESPONSE 1/AUXIN SIGNALING F-BOX
TMK1	TRANSMEMBRANE KINASE 1
TPL	TOPLESS
TPR	TOPLESS RELATED
TSS	transcription start site
UBQ10	POLYUBIQUITIN 10

VAL1	VIVIPAROUS1/ABI3-LIKE 1
VIN3	VERNALIZATION INSENSITIVE 3
VRN2	REDUCED VERNALIZATION 2
WaterLOGSY	Water-Ligand Observed via Gradient SpectroscopY
WD40	Tryptophane-Aspartic acid-repeats
Wnt	wingless/Int-1
WT	Wild type
WUS	WUSCHEL
X-gluc	5-bromo-4-chloro-3-indolyl glucuronide
Y1H	Yeast-one-Hybrid
Y2H	Yeast-two-Hybrid
Y3H	Yeast-three-Hybrid
YFP	Yellow Fluorescent Protein
Zm	*Zea maize*

References

Abley, K., De Reuille, P.B., Strutt, D., Bangham, A., Prusinkiewicz, P., Marée, A.F.M., Grieneisen, V.A., and Coen, E. (2013). An intracellular partitioning-based framework for tissue cell polarity in plants and animals. Development *140*, 2061-2074.

Adamowski, M., and Friml, J. (2015). PIN-Dependent Auxin Transport: Action, Regulation, and Evolution. Plant Cell *27*, 20-32.

Adamski, N.M., Anastasiou, E., Eriksson, S., O'Neill, C.M., and Lenhard, M. (2009). Local maternal control of seed size by KLUH/CYP78A5-dependent growth signaling. Proceedings of the National Academy of Sciences *106*, 20115-20120.

Akiko, Y., Yoshihiro, O., Hidemi, K., Fumio, T.-S., and Hiro-Yuki, H. (2012). ABERRANT SPIKELET AND PANICLE1, encoding a TOPLESS-related transcriptional co-repressor, is involved in the regulation of meristem fate in rice. The Plant Journal *70*, 327-339.

Alexiadis, V., Waldmann, T., Andersen, J., Mann, M., Knippers, R., and Gruss, C. (2000). The protein encoded by the proto-oncogene DEK changes the topology of chromatin and reduces the efficiency of DNA replication in a chromatin-specific manner. Genes & Development *14*, 1308-1312.

Allen, E., Xie, Z.X., Gustafson, A.M., and Carrington, J.C. (2005). microRNA-directed phasing during trans-acting siRNA biogenesis in plants. Cell *121*, 207-221.

Alonso, J.M., Stepanova, A.N., Leisse, T.J., Kim, C.J., Chen, H., Shinn, P., Stevenson, D.K., Zimmerman, J., Barajas, P., Cheuk, R.*, et al.* (2003). Genome-Wide Insertional Mutagenesis of Arabidopsis thaliana>. Science *301*, 653-657.

Alvarez-Buylla, E.R., Benitez, M., Corvera-Poire, A., Chaos Cador, A., de Folter, S., Gamboa de Buen, A., Garay-Arroyo, A., Garcia-Ponce, B., Jaimes-Miranda, F., Perez-Ruiz, R.V.*, et al.* (2010). Flower development. The Arabidopsis book / American Society of Plant Biologists *8*, e0127-e0127.

Anastasiou, E., Kenz, S., Gerstung, M., MacLean, D., Timmer, J., Fleck, C., and Lenhard, M. (2007). Control of Plant Organ Size by KLUH/CYP78A5-Dependent Intercellular Signaling. Developmental Cell *13*, 843-856.

Angel, A., Song, J., Dean, C., and Howard, M. (2011). A Polycomb-based switch underlying quantitative epigenetic memory. Nature *476*, 105-+.

Ariel, F., Jegu, T., Latrasse, D., Romero-Barrios, N., Christ, A., Benhamed, M., and Crespi, M. (2014). Noncoding Transcription by Alternative RNA Polymerases Dynamically Regulates an Auxin-Driven Chromatin Loop. Molecular Cell *55*, 383-396.

Arnaud, N., Girin, T., Sorefan, K., Fuentes, S., Wood, T.A., Lawrenson, T., Sablowski, R., and Ostergaard, L. (2010). Gibberellins control fruit patterning in Arabidopsis thaliana. Genes & Development *24*, 2127-2132.

Avery, O.T., MacLeod, C.M., and McCarty, M. (1944). STUDIES ON THE CHEMICAL NATURE OF THE SUBSTANCE INDUCING TRANSFORMATION OF PNEUMOCOCCAL TYPES. Journal of Experimental Medicine *79*, 137-158.

Axtell, M.J., Snyder, J.A., and Bartel, D.P. (2007). Common Functions for Diverse Small RNAs of Land Plants. The Plant Cell *19*, 1750-1769.

Bastow, R., Mylne, J.S., Lister, C., Lippman, Z., Martienssen, R.A., and Dean, C. (2004). Vernalization requires epigenetic silencing of FLC by histone methylation. Nature *427*, 164-167.

Bateson, W. (1903). Mendel's Principles of Heredity in Mice. Nature *68*, 33-34.

Baumberger, N., and Baulcombe, D.C. (2005). Arabidopsis ARGONAUTE1 is an RNA Slicer that selectively recruits microRNAs and short interfering RNAs. Proceedings of the National Academy of Sciences of the United States of America *102*, 11928-11933.

Bemer, M., and Grossniklaus, U. (2012). Dynamic regulation of Polycomb group activity during plant development. Current Opinion in Plant Biology *15*, 523-529.

Bemer, M., Karlova, R., Ballester, A.R., Tikunov, Y.M., Bovy, A.G., Wolters-Arts, M., Rossetto, P.d.B., Angenent, G.C., and de Maagd, R.A. (2012). The Tomato FRUITFULL Homologs TDR4/FUL1 and MBP7/FUL2 Regulate Ethylene-Independent Aspects of Fruit Ripening. The Plant Cell *24*, 4437-4451.

Benjamins, R., Quint, A., Weijers, D., Hooykaas, P., and Offringa, R. (2001). The PINOID protein kinase regulates organ development in Arabidopsis by enhancing polar auxin transport. Development *128*, 4057-4067.

Benjamins, R., and Scheres, B. (2008). Auxin: The Looping Star in Plant Development. Annual Review of Plant Biology *59*, 443-465.

Benková, E., Michniewicz, M., Sauer, M., Teichmann, T., Seifertová, D., Jürgens, G., and Friml, J. (2003). Local, Efflux-Dependent Auxin Gradients as a Common Module for Plant Organ Formation. Cell *115*, 591-602.

Bennett, M.J., Marchant, A., Green, H.G., May, S.T., Ward, S.P., Millner, P.A., Walker, A.R., Schulz, B., and Feldmann, K.A. (1996). Arabidopsis AUX1 Gene: A Permease-Like Regulator of Root Gravitropism. Science *273*, 948-950.

Berleth, T., and Jurgens, G. (1993). The role of the monopteros gene in organising the basal body region of the Arabidopsis embryo. Development *118*, 575-587.

Berry, S., Dean, C., and Howard, M. (2017). Slow Chromatin Dynamics Allow Polycomb Target Genes to Filter Fluctuations in Transcription Factor Activity. Cell Systems *4*, 445-+.

Berry, S., Hartley, M., Olsson, T.S., Dean, C., and Howard, M. (2015). Local chromatin environment of a Polycomb target gene instructs its own epigenetic inheritance. Elife *4*.

Boer, R., Freire-Rios, A., van den Berg, W.A.M., Saaki, T., Manfield, I.W., Kepinski, S., Lopez-Vidrieo, I., Manuel Franco-Zorrilla, J., de Vries, S.C., Solano, R.*, et al.*

(2014). Structural Basis for DNA Binding Specificity by the Auxin-Dependent ARF Transcription Factors. Cell *156*, 577-589.

Borlaug, N.E. (1983). Contributions of Conventional Plant Breeding to Food Production. Science *219*, 689-693.

Bou-Torrent, J., Salla-Martret, M., Brandt, R., Musielak, T., Palauqui, J.-C., Martínez-García, J.F., and Wenkel, S. (2012). ATHB4 and HAT3, two class II HD-ZIP transcription factors, control leaf development in Arabidopsis. Plant Signaling & Behavior *7*, 1382-1387.

Bowman, J.L., Baum, S.F., Eshed, Y., Putterill, J., and Alvarez, J. (1999). Molecular genetics of gynoecium development in Arabidopsis. Current Topics in Developmental Biology, Vol 45 *45*, 155-205.

Bowman, J.L., Smyth, D.R., and Meyerowitz, E.M. (1989). GENES DIRECTING FLOWER DEVELOPMENT IN ARABIDOPSIS. Plant Cell *1*, 37-52.

Bowman, J.L., Smyth, D.R., and Meyerowitz, E.M. (2012). The ABC model of flower development: then and now. Development *139*, 4095-4098.

Bradley, D., Xu, P., Mohorianu, I.-I., Whibley, A., Field, D., Tavares, H., Couchman, M., Copsey, L., Carpenter, R., Li, M.*, et al.* (2017). Evolution of flower color pattern through selection on regulatory small RNAs. Science *358*, 925-928.

Brand, U., Fletcher, J.C., Hobe, M., Meyerowitz, E.M., and Simon, R. (2000). Dependence of Stem Cell Fate in Arabidopsis on a Feedback Loop Regulated by CLV3 Activity. Science *289*, 617-619.

Brummer, E.C., Barber, W.T., Collier, S.M., Cox, T.S., Johnson, R., Murray, S.C., Olsen, R.T., Pratt, R.C., and Thro, A.M. (2011). Plant breeding for harmony between agriculture and the environment. Frontiers in Ecology and the Environment *9*, 561-568.

Burgess, A., Vigneron, S., Brioudes, E., Labbé, J.-C., Lorca, T., and Castro, A. (2010). Loss of human Greatwall results in G2 arrest and multiple mitotic defects due to deregulation of the cyclin B-Cdc2/PP2A balance. Proceedings of the National Academy of Sciences *107*, 12564-12569.

Buscarlet, M., and Stifani, S. (2007). The 'Marx' of Groucho on development and disease. Trends in Cell Biology *17*, 353-361.

Cabrera-Bosquet, L., Crossa, J., von Zitzewitz, J., Serret, M.D., and Luis Araus, J. (2012). High-throughput Phenotyping and Genomic Selection: The Frontiers of Crop Breeding ConvergeF. Journal of Integrative Plant Biology *54*, 312-320.

Cadigan, K.M., and Nusse, R. (1997). Wnt signaling: a common theme in animal development. Genes & Development *11*, 3286-3305.

Calderon-Villalobos, L.I., Tan, X., Zheng, N., and Estelle, M. (2010). Auxin perception--structural insights. Cold Spring Harb Perspect Biol *2*, a005546.

Calderon Villalobos, L.I., Lee, S., De Oliveira, C., Ivetac, A., Brandt, W., Armitage, L., Sheard, L.B., Tan, X., Parry, G., Mao, H.*, et al.* (2012). A combinatorial

TIR1/AFB-Aux/IAA co-receptor system for differential sensing of auxin. Nat Chem Biol *8*, 477-485.

Campillos, M., Garcia, M.A., Valdivieso, F., and Vazquez, J. (2003). Transcriptional activation by AP-2 alpha is modulated by the oncogene DEK. Nucleic Acids Research *31*, 1571-1575.

Cao, M., Chen, R., Li, P., Yu, Y., Zheng, R., Ge, D., Zheng, W., Wang, X., Gu, Y., Gelová, Z*., et al.* (2019). TMK1-mediated auxin signalling regulates differential growth of the apical hook. Nature *568*, 240-243.

Caragea, A.E., and Berleth, T. (2016). Auxin cell biology in plant pattern formation. Botany *95*, 357-368.

Castel, B., Tomlinson, L., Locci, F., Yang, Y., and Jones, J.D.G. (2019). Optimization of T-DNA architecture for Cas9-mediated mutagenesis in Arabidopsis. PLOS ONE *14*, e0204778.

Causier, B., Ashworth, M., Guo, W.J., and Davies, B. (2012). The TOPLESS Interactome: A Framework for Gene Repression in Arabidopsis. Plant Physiology *158*, 423-438.

Causier, B., Lloyd, J., Stevens, L., and Davies, B. (2014). TOPLESS co-repressor interactions and their evolutionary conservation in plants. Plant Signaling & Behavior *7*, 325-328.

Cavel, E., Pillot, M., Pontier, D., Lahmy, S., Bies-Etheve, N., Vega, D., Grimanelli, D., and Lagrange, T. (2011). A Plant-Specific Transcription Factor IIB-Related Protein, pBRP2, Is Involved in Endosperm Growth Control. Plos One *6*.

Cerna, D., and Wilson, D.K. (2005). The Structure of Sif2p, a WD Repeat Protein Functioning in the SET3 Corepressor Complex. Journal of Molecular Biology *351*, 923-935.

Chakrabarti, M., Zhang, N., Sauvage, C., Muños, S., Blanca, J., Cañizares, J., Diez, M.J., Schneider, R., Mazourek, M., McClead, J*., et al.* (2013). A cytochrome P450 regulates a domestication trait in cultivated tomato. Proceedings of the National Academy of Sciences *110*, 17125-17130.

Chambers, M., Turki-Judeh, W., Kim, M.W., Chen, K., Gallaher, S.D., and Courey, A.J. (2017). Mechanisms of Groucho-mediated repression revealed by genome-wide analysis of Groucho binding and activity. BMC Genomics *18*, 17.

Chandler, J.W. (2016). Auxin response factors. Plant Cell Environ *39*, 1014-1028.

Chen, Q.Y., Atkinson, A., Otsuga, D., Christensen, T., Reynolds, L., and Drews, G.N. (1999). The Arabidopsis FILAMENTOUS FLOWER gene is required for flower formation. Development *126*, 2715-2726.

Chen, X., Grandont, L., Li, H., Hauschild, R., Paque, S., Abuzeineh, A., Rakusová, H., Benkova, E., Perrot-Rechenmann, C., and Friml, J. (2014). Inhibition of cell expansion by rapid ABP1-mediated auxin effect on microtubules. Nature *516*, 90.

Cheng, Y.F., Dai, X.H., and Zhao, Y.D. (2006). Auxin biosynthesis by the YUCCA flavin monooxygenases controls the formation of floral organs and vascular tissues in Arabidopsis. Genes & Development *20*, 1790-1799.

Cherenkov, P., Novikova, D., Omelyanchuk, N., Levitsky, V., Grosse, I., Weijers, D., and Mironova, V. (2018). Diversity of cis-regulatory elements associated with auxin response in Arabidopsis thaliana. Journal of Experimental Botany *69*, 329-339.

Cho, H., Ryu, H., Rho, S., Hill, K., Smith, S., Audenaert, D., Park, J., Han, S., Beeckman, T., Bennett, M.J*., et al.* (2013). A secreted peptide acts on BIN2-mediated phosphorylation of ARFs to potentiate auxin response during lateral root development. Nature Cell Biology *16*, 66.

Chodaparambil, J.V., Pate, K.T., Hepler, M.R.D., Tsai, B.P., Muthurajan, U.M., Luger, K., Waterman, M.L., and Weis, W.I. (2014). Molecular functions of the TLE tetramerization domain in Wnt target gene repression. The EMBO Journal *33*, 719-731.

Choi, H.-S., Seo, M., and Cho, H.-T. (2018). Two TPL-Binding Motifs of ARF2 Are Involved in Repression of Auxin Responses. Frontiers in Plant Science *9*.

Chung, Y., Zhu, Y., Wu, M.-F., Simonini, S., Kuhn, A., Armenta-Medina, A., Jin, R., Østergaard, L., Gillmor, C.S., and Wagner, D. (2019). Auxin Response Factors promote organogenesis by chromatin-mediated repression of the pluripotency gene SHOOTMERISTEMLESS. Nature Communications *10*, 886.

Clark, S.E., Williams, R.W., and Meyerowitz, E.M. (1997). The CLAVATA1Gene Encodes a Putative Receptor Kinase That Controls Shoot and Floral Meristem Size in Arabidopsis. Cell *89*, 575-585.

Clough, S.J., and Bent, A.F. (1998). Floral dip: a simplified method for Agrobacterium -mediated transformation of Arabidopsis thaliana. The Plant Journal *16*, 735-743.

Coen, E.S., and Meyerowitz, E.M. (1991). The war of the whorls: genetic interactions controlling flower development. Nature *353*, 31-37.

Costa, M., Nobre, M.S., Becker, J.D., Masiero, S., Amorim, M.I., Pereira, L.G., and Coimbra, S. (2013). Expression-based and co-localization detection of arabinogalactan protein 6 and arabinogalactan protein 11 interactors in Arabidopsis pollen and pollen tubes. Bmc Plant Biology *13*.

Creighton, H.B., and McClintock, B. (1931). A Correlation of Cytological and Genetical Crossing-Over in Zea Mays. Proceedings of the National Academy of Sciences *17*, 492-497.

Crick, F. (1970). Central Dogma of Molecular Biology. Nature *227*, 561-563.

Csorba, T., Questa, J.I., Sun, Q., and Dean, C. (2014). Antisense COOLAIR mediates the coordinated switching of chromatin states at FLC during vernalization. Proceedings of the National Academy of Sciences *111*, 16160-16165.

Cucinotta, M., Manrique, S., Guazzotti, A., Quadrelli, N.E., Mendes, M.A., Benkova, E., and Colombo, L. (2016). Cytokinin response factors integrate auxin and

cytokinin pathways for female reproductive organ development. Development *143*, 4419-4424.

Cui, X., Lu, F., Qiu, Q., Zhou, B., Gu, L., Zhang, S., Kang, Y., Cui, X., Ma, X., Yao, Q.*, et al.* (2016). REF6 recognizes a specific DNA sequence to demethylate H3K27me3 and regulate organ boundary formation in Arabidopsis. Nat Genet.

Dalvit, C., Fogliatto, G., Stewart, A., Veronesi, M., and Stockman, B. (2001). WaterLOGSY as a method for primary NMR screening: Practical aspects and range of applicability. Journal of Biomolecular NMR *21*, 349-359.

De Lucia, F., Crevillen, P., Jones, A.M.E., Greb, T., and Dean, C. (2008). A PHD-Polycomb Repressive Complex 2 triggers the epigenetic silencing of FLC during vernalization. Proceedings of the National Academy of Sciences of the United States of America *105*, 16831-16836.

Deb, J., Bland, H.M., and Østergaard, L. (2018). Developmental cartography: coordination via hormonal and genetic interactions during gynoecium formation. Current Opinion in Plant Biology *41*, 54-60.

del Olmo, I., Lopez, J.A., Vazquez, J., Raynaud, C., Pineiro, M., and Jarillo, J.A. (2016). Arabidopsis DNA polymerase epsilon recruits components of Polycomb repressor complex to mediate epigenetic gene silencing. Nucleic Acids Research *44*, 5597-5614.

Dharmasiri, N., Dharmasiri, S., and Estelle, M. (2005). The F-box protein TIR1 is an auxin receptor. Nature *435*, 441-445.

Dombrecht, B., Xue, G.P., Sprague, S.J., Kirkegaard, J.A., Ross, J.J., Reid, J.B., Fitt, G.P., Sewelam, N., Schenk, P.M., Manners, J.M.*, et al.* (2007). MYC2 Differentially Modulates Diverse Jasmonate-Dependent Functions in Arabidopsis. The Plant Cell *19*, 2225-2245.

Drews, G.N., Bowman, J.L., and Meyerowitz, E.M. (1991). NEGATIVE REGULATION OF THE ARABIDOPSIS HOMEOTIC GENE AGAMOUS BY THE APETALA2 PRODUCT. Cell *65*, 991-1002.

Driever, W., and Nüsslein-Volhard, C. (1988). The bicoid protein determines position in the Drosophila embryo in a concentration-dependent manner. Cell *54*, 95-104.

Eberharter, A., and Becker, P.B. (2002). Histone acetylation: a switch between repressive and permissive chromatin - Second in review series on chromatin dynamics. Embo Reports *3*, 224-229.

Echeverria, P.C., and Picard, D. (2010). Molecular chaperones, essential partners of steroid hormone receptors for activity and mobility. Biochimica et Biophysica Acta (BBA) - Molecular Cell Research *1803*, 641-649.

Edwards, K., Johnstone, C., and Thompson, C. (1991). A simple and rapid method for the preparation of plant genomic DNA for PCR analysis. Nucleic Acids Research *19*, 1349-1349.

Efroni, I., Han, S.K., Kim, H.J., Wu, M.F., Steiner, E., Birnbaum, K.D., Hong, J.C., Eshed, Y., and Wagner, D. (2013). Regulation of Leaf Maturation by Chromatin-Mediated Modulation of Cytokinin Responses. Developmental Cell *24*, 438-445.

Egea-Cortines, M., Saedler, H., and Sommer, H. (1999). Ternary complex formation between the MADS-box proteins SQUAMOSA, DEFICIENS and GLOBOSA is involved in the control of floral architecture in Antirrhinum majus. Embo Journal *18*, 5370-5379.

Engler, C., Youles, M., Gruetzner, R., Ehnert, T.M., Werner, S., Jones, J.D.G., Patron, N.J., and Marillonnet, S. (2014). A Golden Gate Modular Cloning Toolbox for Plants. Acs Synthetic Biology *3*, 839-843.

Espinosa-Ruiz, A., Martínez, C., de Lucas, M., Fàbregas, N., Bosch, N., Caño-Delgado, A.I., and Prat, S. (2017). TOPLESS mediates brassinosteroid control of shoot boundaries and root meristem development in Arabidopsis thaliana. Development *144*, 1619-1628.

Eysholdt-Derzsó, E., and Sauter, M. (2017). Root Bending Is Antagonistically Affected by Hypoxia and ERF-Mediated Transcription via Auxin Signaling. Plant Physiology *175*, 412-423.

Ferrandiz, C., Liljegren, S.J., and Yanofsky, M.F. (2000). Negative regulation of the SHATTERPROOF genes by FRUITFULL during Arabidopsis fruit development. Science *289*, 436-438.

Finet, C., Berne-Dedieu, A., Scutt, C.P., and Marletaz, F. (2013). Evolution of the ARF Gene Family in Land Plants: Old Domains, New Tricks. Molecular Biology and Evolution *30*, 45-56.

Finet, C., Fourquin, C., Vinauger, M., Berne-Dedieu, A., Chambrier, P., Paindavoine, S., and Scutt, C.P. (2010). Parallel structural evolution of auxin response factors in the angiosperms. Plant Journal *63*, 952-959.

Flaus, A., Martin, D.M.A., Barton, G.J., and Owen-Hughes, T. (2006). Identification of multiple distinct Snf2 subfamilies with conserved structural motifs. Nucleic Acids Research *34*, 2887-2905.

Fletcher, J.C., Brand, U., Running, M.P., Simon, R., and Meyerowitz, E.M. (1999). Signaling of Cell Fate Decisions by CLAVATA3 in Arabidopsis Shoot Meristems. Science *283*, 1911-1914.
Francis, N.J., and Kingston, R.E. (2001). Mechanisms of transcriptional memory. Nature Reviews Molecular Cell Biology *2*, 409-421.

Franco-Zorrilla, J.M., Lopez-Vidriero, I., Carrasco, J.L., Godoy, M., Vera, P., and Solano, R. (2014). DNA-binding specificities of plant transcription factors and their potential to define target genes. Proceedings of the National Academy of Sciences of the United States of America *111*, 2367-2372.

Friml, J., Benková, E., Blilou, I., Wisniewska, J., Hamann, T., Ljung, K., Woody, S., Sandberg, G., Scheres, B., Jürgens, G.*, et al.* (2002a). AtPIN4 Mediates Sink-Driven Auxin Gradients and Root Patterning in Arabidopsis. Cell *108*, 661-673.

Friml, J., Wiśniewska, J., Benková, E., Mendgen, K., and Palme, K. (2002b). Lateral relocation of auxin efflux regulator PIN3 mediates tropism in Arabidopsis. Nature *415*, 806-809.

Friml, J., Yang, X., Michniewicz, M., Weijers, D., Quint, A., Tietz, O., Benjamins, R., Ouwerkerk, P.B.F., Ljung, K., Sandberg, G.*, et al.* (2004). A PINOID-Dependent Binary Switch in Apical-Basal PIN Polar Targeting Directs Auxin Efflux. Science *306*, 862-865.

Furey, T.S. (2012). ChIP–seq and beyond: new and improved methodologies to detect and characterize protein–DNA interactions. Nature Reviews Genetics *13*, 840.

Gallavotti, A., Long, J.A., Stanfield, S., Yang, X., Jackson, D., Vollbrecht, E., and Schmidt, R.J. (2010). The control of axillary meristem fate in the maize ramosa pathway. Development *137*, 2849-2856.

Gamble, M.J., and Fisher, R.P. (2007). SET and PARP1 remove DEK from chromatin to permit access by the transcription machinery. Nature Structural & Molecular Biology *14*, 548-555.

Gammons, M., and Bienz, M. (2018). Multiprotein complexes governing Wnt signal transduction. Current Opinion in Cell Biology *51*, 42-49.

Gao, Y., Zhang, Y., Zhang, D., Dai, X., Estelle, M., and Zhao, Y. (2015). Auxin binding protein 1 (ABP1) is not required for either auxin signaling or Arabidopsis development. Proceedings of the National Academy of Sciences *112*, 2275-2280.

Garcia, D., Collier, S.A., Byrne, M.E., and Martienssen, R.A. (2006). Specification of leaf polarity in Arabidopsis via the trans-acting siRNA pathway. Current Biology *16*, 933-938.

Gendall, A.R., Levy, Y.Y., Wilson, A., and Dean, C. (2001). The VERNALIZATION 2 gene mediates the epigenetic regulation of vernalization in Arabidopsis. Cell *107*, 525-535.

Girin, T., Paicu, T., Stephenson, P., Fuentes, S., Koerner, E., O'Brien, M., Sorefan, K., Wood, T.A., Balanza, V., Ferrandiz, C.*, et al.* (2011). INDEHISCENT and SPATULA Interact to Specify Carpel and Valve Margin Tissue and Thus Promote Seed Dispersal in Arabidopsis. Plant Cell *23*, 3641-3653.

Godoy, M., Franco-Zorrilla, J.M., Pérez-Pérez, J., Oliveros, J.C., Lorenzo, Ó., and Solano, R. (2011). Improved protein-binding microarrays for the identification of DNA-binding specificities of transcription factors. The Plant Journal *66*, 700-711.

Gray, W.M., Kepinski, S., Rouse, D., Leyser, O., and Estelle, M. (2001). Auxin regulates SCFTIR1-dependent degradation of AUX/IAA proteins. Nature *414*, 271-276.

Greenwald, W.W., Li, H., Benaglio, P., Jakubosky, D., Matsui, H., Schmitt, A., Selvaraj, S., D'Antonio, M., D'Antonio-Chronowska, A., Smith, E.N.*, et al.* (2019). Subtle changes in chromatin loop contact propensity are associated with differential gene regulation and expression. Nature Communications *10*, 1054.

Gremski, K., Ditta, G., and Yanofsky, M.F. (2007). The HECATE genes regulate female reproductive tract development in Arabidopsis thaliana. Development *134*, 3593-3601.

Gu, Q., Ferrandiz, C., Yanofsky, M.F., and Martienssen, R. (1998). The FRUITFULL MADS-box gene mediates cell differentiation during Arabidopsis fruit development. Development *125*, 1509-1517.

Gu, X.F., Xu, T.D., and He, Y.H. (2014). A Histone H3 Lysine-27 Methyltransferase Complex Represses Lateral Root Formation in Arabidopsis thaliana. Molecular Plant *7*, 977-988.

Guilfoyle, T.J., and Hagen, G. (2007). Auxin response factors. Current Opinion in Plant Biology *10*, 453-460.

Gurdon, J.B., and Bourillot, P.Y. (2001). Morphogen gradient interpretation. Nature *413*, 797-803.

Han, S.-K., Wu, M.-F., Cui, S., and Wagner, D. (2015). Roles and activities of chromatin remodeling ATPases in plants. Plant Journal *83*, 62-77.
He, H.H., Meyer, C.A., Hu, S.e.S., Chen, M.-W., Zang, C., Liu, Y., Rao, P.K., Fei, T., Xu, H., Long, H.*, et al.* (2014). Refined DNase-seq protocol and data analysis reveals intrinsic bias in transcription factor footprint identification. Nature Methods *11*, 73-+.

Hedden, P. (2003). The genes of the Green Revolution. Trends in Genetics *19*, 5-9.
Heisler, M.G.B., Atkinson, A., Bylstra, Y.H., Walsh, R., and Smyth, D.R. (2001). SPATULA, a gene that controls development of carpel margin tissues in Arabidopsis, encodes a bHLH protein. Development *128*, 1089-1098.

Hershey, A.D., and Chase, M. (1952). INDEPENDENT FUNCTIONS OF VIRAL PROTEIN AND NUCLEIC ACID IN GROWTH OF BACTERIOPHAGE. The Journal of General Physiology *36*, 39-56.

Hironaka, K.-i., and Morishita, Y. (2012). Encoding and decoding of positional information in morphogen-dependent patterning. Curr Opin Genet Dev *22*, 553-561.
Hon, G.C., Hawkins, R.D., and Ren, B. (2009). Predictive chromatin signatures in the mammalian genome. Human Molecular Genetics *18*, R195-R201.

Jennings, B.H., and Ish-Horowicz, D. (2008). The Groucho/TLE/Grg family of transcriptional co-repressors. Genome Biology *9*, 205.

Jennings, B.H., Pickles, L.M., Wainwright, S.M., Roe, S.M., Pearl, L.H., and Ish-Horowicz, D. (2006). Molecular Recognition of Transcriptional Repressor Motifs by the WD Domain of the Groucho/TLE Corepressor. Molecular Cell *22*, 645-655.

Jennings, B.H., Wainwright, S.M., and Ish-Horowicz, D. (2008). Differential in vivo requirements for oligomerization during Groucho-mediated repression. EMBO reports *9*, 76-83.

Johnston, D.S., and Nüsslein-Volhard, C. (1992). The origin of pattern and polarity in the Drosophila embryo. Cell *68*, 201-219.

Jolma, A., Kivioja, T., Toivonen, J., Cheng, L., Wei, G., Enge, M., Taipale, M., Vaquerizas, J.M., Yan, J., Sillanpaa, M.J.*, et al.* (2010). Multiplexed massively

parallel SELEX for characterization of human transcription factor binding specificities. Genome Res *20*, 861-873.

Jolma, A., Yin, Y., Nitta, K.R., Dave, K., Popov, A., Taipale, M., Enge, M., Kivioja, T., Morgunova, E., and Taipale, J. (2015). DNA-dependent formation of transcription factor pairs alters their binding specificity. Nature *527*, 384.

Kadauke, S., and Blobel, G.A. (2009). Chromatin loops in gene regulation. Biochimica et Biophysica Acta (BBA) - Gene Regulatory Mechanisms *1789*, 17-25.
Kadoch, C., and Crabtree, G.R. (2015). Mammalian SWI/SNF chromatin remodeling complexes and cancer: Mechanistic insights gained from human genomics. Science Advances *1*, e1500447.

Kagale, S., Links, M.G., and Rozwadowski, K. (2010). Genome-Wide Analysis of Ethylene-Responsive Element Binding Factor-Associated Amphiphilic Repression Motif-Containing Transcriptional Regulators in Arabidopsis. Plant Physiology *152*, 1109-1134.

Kagale, S., and Rozwadowski, K. (2011). EAR motif-mediated transcriptional repression in plants An underlying mechanism for epigenetic regulation of gene expression. Epigenetics *6*, 141-146.

Kappes, F., Waldmann, T., Mathew, V., Yu, J.D., Zhang, L., Khodadoust, M.S., Chinnaiyan, A.M., Luger, K., Erhardt, S., Schneider, R.*, et al.* (2011). The DEK oncoprotein is a Su(var) that is essential to heterochromatin integrity. Genes & Development *25*, 673-678.

Kato, H., Nishihama, R., Weijers, D., and Kohchi, T. (2018). Evolution of nuclear auxin signaling: lessons from genetic studies with basal land plants. J Exp Bot *69*, 291-301.

Kavanaugh, G.M., Wise-Draper, T.M., Morreale, R.J., Morrison, M.A., Gole, B., Schwemberger, S., Tichy, E.D., Lu, L., Babcock, G.F., Wells, J.M.*, et al.* (2011). The human DEK oncogene regulates DNA damage response signaling and repair. Nucleic Acids Research *39*, 7465-7476.

Ke, J., Ma, H., Gu, X., Thelen, A., Brunzelle, J.S., Li, J., Xu, H.E., and Melcher, K. (2015). Structural basis for recognition of diverse transcriptional repressors by the TOPLESS family of corepressors. Science Advances *1*.

Kearse, M., Moir, R., Wilson, A., Stones-Havas, S., Cheung, M., Sturrock, S., Buxton, S., Cooper, A., Markowitz, S., Duran, C.*, et al.* (2012). Geneious Basic: An integrated and extendable desktop software platform for the organization and analysis of sequence data. Bioinformatics *28*, 1647-1649.

Kelley, D.R., Arreola, A., Gallagher, T.L., and Gasser, C.S. (2012). ETTIN (ARF3) physically interacts with KANADI proteins to form a functional complex essential for integument development and polarity determination in Arabidopsis. Development *139*, 1105-1109.

Kelley, D.R., and Estelle, M. (2012). Ubiquitin-Mediated Control of Plant Hormone Signaling. Plant Physiology *160*, 47-55.

Kepinski, S., and Leyser, O. (2004). Auxin-induced SCFTIR1–Aux/IAA interaction involves stable modification of the SCFTIR1 complex. Proceedings of the National Academy of Sciences of the United States of America *101*, 12381-12386.

Kepinski, S., and Leyser, O. (2005). The Arabidopsis F-box protein TIR1 is an auxin receptor. Nature *435*, 446-451.

Kieber, J.J., and Schaller, G.E. (2018). Cytokinin signaling in plant development. Development *145*, dev149344.

Kieffer, M., Master, V., Waites, R., and Davies, B. (2011). TCP14 and TCP15 affect internode length and leaf shape in Arabidopsis. Plant Journal *68*, 147-158.
Kim, K.-C., Lai, Z., Fan, B., and Chen, Z. (2008). Arabidopsis WRKY38 and WRKY62 Transcription Factors Interact with Histone Deacetylase 19 in Basal Defense. The Plant Cell *20*, 2357-2371.

King, H.A., Trotter, K.W., and Archer, T.K. (2012). Chromatin remodeling during glucocorticoid receptor regulated transactivation. Biochimica Et Biophysica Acta-Gene Regulatory Mechanisms *1819*, 716-726.

Kondo, S., and Miura, T. (2010). Reaction-Diffusion Model as a Framework for Understanding Biological Pattern Formation. Science *329*, 1616-1620.

Korasick, D.A., Westfall, C.S., Lee, S.G., Nanao, M.H., Dumas, R., Hagen, G., Guilfoyle, T.J., Jez, J.M., and Strader, L.C. (2014). Molecular basis for AUXIN RESPONSE FACTOR protein interaction and the control of auxin response repression. Proceedings of the National Academy of Sciences of the United States of America *111*, 5427-5432.

Kornberg, R.D., and Lorch, Y. (1999). Twenty-Five Years of the Nucleosome, Fundamental Particle of the Eukaryote Chromosome. Cell *98*, 285-294.
Kouzarides, T. (2007). Chromatin modifications and their function. Cell *128*, 693-705.

Krogan, N.T., Hogan, K., and Long, J.A. (2012). APETALA2 negatively regulates multiple floral organ identity genes in Arabidopsis by recruiting the co-repressor TOPLESS and the histone deacetylase HDA19. Development *139*, 4180-4190.
Kubo, M., Furuta, K., Demura, T., Fukuda, H., Liu, Y.G., Shibata, D., and Kakimoto, T. (2011). The CKH1/EER4 Gene Encoding a TAF12-Like Protein Negatively Regulates Cytokinin Sensitivity in Arabidopsis thaliana. Plant and Cell Physiology *52*, 629-637.

Kumar, S., Stecher, G., and Tamura, K. (2016). MEGA7: Molecular Evolutionary Genetics Analysis Version 7.0 for Bigger Datasets. Molecular Biology and Evolution *33*, 1870-1874.

Kumaran, M.K., Bowman, J.L., and Sundaresan, V. (2002). YABBY polarity genes mediate the repression of KNOX homeobox genes in Arabidopsis. Plant Cell *14*, 2761-2770.

Kwon, Y., Yu, S.-i., Park, J.-h., Li, Y., Han, J.-H., Alavilli, H., Cho, J.-I., Kim, T.-H., Jeon, J.-S., and Lee, B.-h. (2012). OsREL2, a rice TOPLESS homolog functions in axillary meristem development in rice inflorescence. Plant Biotechnology Reports *6*, 213-224.

Lago, C., Clerici, E., Dreni, L., Horlow, C., Caporali, E., Colombo, L., and Kater, M.M. (2005). The Arabidopsis TFIID factor AtTAF6 controls pollen tube growth. Developmental Biology *285*, 91-100.

Langowski, L., Stacey, N., and Ostergaard, L. (2016). Diversification of fruit shape in the Brassicaceae family. Plant Reprod.

Larsson, E., Franks, R.G., and Sundberg, E. (2013). Auxin and the Arabidopsis thaliana gynoecium. Journal of Experimental Botany *64*, 2619-2627.

Larsson, E., Roberts, C.J., Claes, A.R., Franks, R.G., and Sundberg, E. (2014). Polar Auxin Transport Is Essential for Medial versus Lateral Tissue Specification and Vascular-Mediated Valve Outgrowth in Arabidopsis Gynoecia W. Plant Physiology *166*, 1998-U1237.

Le Hir, H., Gatfield, D., Izaurralde, E., and Moore, M.J. (2001). The exon-exon junction complex provides a binding platform for factors involved in mRNA export and nonsense-mediated mRNA decay. Embo Journal *20*, 4987-4997.

Le Hir, H., Izaurralde, E., Maquat, L.E., and Moore, M.J. (2000). The spliceosome deposits multiple proteins 20-24 nucleotides upstream of mRNA exon-exon junctions. Embo Journal *19*, 6860-6869.

Lee, S.H., and Cho, H.-T. (2006). PINOID Positively Regulates Auxin Efflux in Arabidopsis Root Hair Cells and Tobacco Cells. The Plant Cell *18*, 1604-1616.
Lewis, E.B. (1978). A gene complex controlling segmentation in Drosophila. Nature *276*, 565.

Leyser, O. (2018). Auxin Signaling. Plant Physiology *176*, 465-479.
Li, B., Carey, M., and Workman, J.L. (2007). The role of chromatin during transcription. Cell *128*, 707-719.

Li, C., Gu, L., Gao, L., Chen, C., Wei, C.Q., Qiu, Q., Chien, C.W., Wang, S., Jiang, L., Ai, L.F.*, et al.* (2016). Concerted genomic targeting of H3K27 demethylase REF6 and chromatin-remodeling ATPase BRM in Arabidopsis. Nat Genet.
Liao, C.-Y., Smet, W., Brunoud, G., Yoshida, S., Vernoux, T., and Weijers, D. (2015). Reporters for sensitive and quantitative measurement of auxin response. Nature Methods *12*, 207-+.

Liao, C.-Y., and Weijers, D. (2018). A toolkit for studying cellular reorganization during early embryogenesis in Arabidopsis thaliana. The Plant Journal *93*, 963-976.

Lieberman-Lazarovich, M., Yahav, C., Israeli, A., and Efroni, I. (2019). Deep conservation of cis-element variants regulating plant hormonal responses. The Plant Cell, tpc.00129.02019.

Liljegren, S.J., Ditta, G.S., Eshed, H.Y., Savidge, B., Bowman, J.L., and Yanofsky, M.F. (2000). SHATTERPROOF MADS-box genes control seed dispersal in Arabidopsis. Nature *404*, 766-770.
Liljegren, S.J., Roeder, A.H.K., Kempin, S.A., Gremski, K., Ostergaard, L., Guimil, S., Reyes, D.K., and Yanofsky, M.F. (2004). Control of fruit patterning in Arabidopsis by INDEHISCENT. Cell *116*, 843-853.

Liu, J., Hua, W., Hu, Z., Yang, H., Zhang, L., Li, R., Deng, L., Sun, X., Wang, X., and Wang, H. (2015). Natural variation in ARF18 gene simultaneously affects seed

weight and silique length in polyploid rapeseed. Proceedings of the National Academy of Sciences *112*, E5123-E5132.

Liu, X., Dinh, T.T., Li, D., Shi, B., Li, Y., Cao, X., Guo, L., Pan, Y., Jiao, Y., and Chen, X. (2014). AUXIN RESPONSE FACTOR 3 integrates the functions of AGAMOUS and APETALA2 in floral meristem determinacy. Plant Journal *80*, 629-641.

Liu, X., Galli, M., Camehl, I., and Gallavotti, A. (2019). RAMOSA1 ENHANCER LOCUS2-Mediated Transcriptional Repression Regulates Vegetative and Reproductive Architecture. Plant Physiology *179*, 348-363.

Livak, K.J., and Schmittgen, T.D. (2001). Analysis of Relative Gene Expression Data Using Real-Time Quantitative PCR and the 2−ΔΔCT Method. Methods *25*, 402-408.

Logan, C.Y., and Nusse, R. (2004). The Wnt signaling pathway in development and disease. Annual Review of Cell and Developmental Biology *20*, 781-810.

Long, J.A., Ohno, C., Smith, Z.R., and Meyerowitz, E.M. (2006). TOPLESS regulates apical embryonic fate in Arabidopsis. Science *312*, 1520-1523.

Long, Stephen P., Marshall-Colon, A., and Zhu, X.-G. (2015). Meeting the Global Food Demand of the Future by Engineering Crop Photosynthesis and Yield Potential. Cell *161*, 56-66.

Luger, K., Mäder, A.W., Richmond, R.K., Sargent, D.F., and Richmond, T.J. (1997). Crystal structure of the nucleosome core particle at 2.8 Å resolution. Nature *389*, 251-260.

Ma, M., Wang, Q., Li, Z., Cheng, H., Li, Z., Liu, X., Song, W., Appels, R., and Zhao, H. (2015). Expression of TaCYP78A3, a gene encoding cytochrome P450 CYP78A3 protein in wheat (Triticum aestivum L.), affects seed size. The Plant Journal *83*, 312-325.

Magome, H., Yamaguchi, S., Hanada, A., Kamiya, Y., and Oda, K. (2008). The DDF1 transcriptional activator upregulates expression of a gibberellin-deactivating gene, GA2ox7, under high-salinity stress in Arabidopsis. Plant Journal *56*, 613-626.
Mallo, M., and Alonso, C.R. (2013). The regulation of Hox gene expression during animal development. Development *140*, 3951-3963.

Mallory, A.C., Bartel, D.P., and Bartel, B. (2005). MicroRNA-Directed Regulation of Arabidopsis AUXIN RESPONSE FACTOR17 Is Essential for Proper Development and Modulates Expression of Early Auxin Response Genes. The Plant Cell *17*, 1360-1375.

Marin, E., Jouannet, V., Herz, A., Lokerse, A.S., Weijers, D., Vaucheret, H., Nussaume, L., Crespi, M.D., and Maizel, A. (2010). miR390, Arabidopsis TAS3 tasiRNAs, and Their AUXIN RESPONSE FACTOR Targets Define an Autoregulatory Network Quantitatively Regulating Lateral Root Growth. Plant Cell *22*, 1104-1117.

Marsch-Martinez, N., Ramos-Cruz, D., Reyes-Olalde, J.I., Lozano-Sotomayor, P., Zuniga-Mayo, V.M., and de Folter, S. (2012). The role of cytokinin during

Arabidopsis gynoecia and fruit morphogenesis and patterning. Plant Journal *72*, 222-234.

Martin-Arevalillo, R., Nanao, M.H., Larrieu, A., Vinos-Poyo, T., Mast, D., Galvan-Ampudia, C., Brunoud, G., Vernoux, T., Dumas, R., and Parcy, F. (2017). Structure of the Arabidopsis TOPLESS corepressor provides insight into the evolution of transcriptional repression. Proceedings of the National Academy of Sciences *114*, 8107-8112.

Mashiguchi, K., Tanaka, K., Sakai, T., Sugawara, S., Kawaide, H., Natsume, M., Hanada, A., Yaeno, T., Shirasu, K., Yao, H.*, et al.* (2011). The main auxin biosynthesis pathway in Arabidopsis. Proceedings of the National Academy of Sciences *108*, 18512-18517.

McCloy, R.A., Rogers, S., Caldon, C.E., Lorca, T., Castro, A., and Burgess, A. (2014). Partial inhibition of Cdk1 in G2 phase overrides the SAC and decouples mitotic events. Cell Cycle *13*, 1400-1412.

McGarvey, T., Rosonina, E., McCracken, S., Li, Q.Y., Arnaout, R., Mientjes, E., Nickerson, J.A., Awrey, D., Greenblatt, J., Grosveld, G.*, et al.* (2000). The acute myeloid leukemia-associated protein, DEK, forms a splicing-dependent interaction with exon-product complexes. Journal of Cell Biology *150*, 309-320.

Merika, M., and Orkin, S.H. (1993). DNA-binding specificity of GATA family transcription factors. Molecular and Cellular Biology *13*, 3999-4010.

Meyer, B., and Peters, T. (2003). NMR Spectroscopy Techniques for Screening and Identifying Ligand Binding to Protein Receptors. Angewandte Chemie International Edition *42*, 864-890.

Michalko, J., Dravecká, M., Bollenbach, T., and Friml, J. (2015). Embryo-lethal phenotypes in early abp1 mutants are due to disruption of the neighboring BSM gene F1000Research *4*.

Michniewicz, M., Zago, M.K., Abas, L., Weijers, D., Schweighofer, A., Meskiene, I., Heisler, M.G., Ohno, C., Zhang, J., Huang, F.*, et al.* (2007). Antagonistic Regulation of PIN Phosphorylation by PP2A and PINOID Directs Auxin Flux. Cell *130*, 1044-1056.

Mieszczanek, J., de la Roche, M., and Bienz, M. (2008). A role of Pygopus as an anti-repressor in facilitating Wnt-dependent transcription. Proceedings of the National Academy of Sciences *105*, 19324-19329.

Monforte, A.J., Diaz, A., Caño-Delgado, A., and van der Knaap, E. (2014). The genetic basis of fruit morphology in horticultural crops: lessons from tomato and melon. Journal of Experimental Botany *65*, 4625-4637.

Morgan, T.H. (1911). Chromosomes and associative inheritance. Science *34*, 636-638.

Mosimann, C., Hausmann, G., and Basler, K. (2009). β-Catenin hits chromatin: regulation of Wnt target gene activation. Nature Reviews Molecular Cell Biology *10*, 276.

Moubayidin, L., and Ostergaard, L. (2014). Dynamic Control of Auxin Distribution Imposes a Bilateral-to-Radial Symmetry Switch during Gynoecium Development. Current Biology *24*, 2743-2748.

Moubayidin, L., and Østergaard, L. (2017). Gynoecium formation: an intimate and complicated relationship. Curr Opin Genet Dev *45*, 15-21.
Mozgova, I., and Hennig, L. (2015). The Polycomb Group Protein Regulatory Network. In Annual Review of Plant Biology, Vol 66, S.S. Merchant, ed., pp. 269-296.

Mu, Q., Huang, Z., Chakrabarti, M., Illa-Berenguer, E., Liu, X., Wang, Y., Ramos, A., and van der Knaap, E. (2017). Fruit weight is controlled by Cell Size Regulator encoding a novel protein that is expressed in maturing tomato fruits. PLoS genetics *13*, e1006930-e1006930.

Müller, A., Guan, C., Gälweiler, L., Tänzler, P., Huijser, P., Marchant, A., Parry, G., Bennett, M., Wisman, E., and Palme, K. (1998). AtPIN2 defines a locus of Arabidopsis for root gravitropism control. The EMBO Journal *17*, 6903-6911.

Müller, J., Hart, C.M., Francis, N.J., Vargas, M.L., Sengupta, A., Wild, B., Miller, E.L., O'Connor, M.B., Kingston, R.E., and Simon, J.A. (2002). Histone Methyltransferase Activity of a Drosophila Polycomb Group Repressor Complex. Cell *111*, 197-208.

Muños, S., Ranc, N., Botton, E., Bérard, A., Rolland, S., Duffé, P., Carretero, Y., Le Paslier, M.-C., Delalande, C., Bouzayen, M*., et al.* (2011). Increase in Tomato Locule Number Is Controlled by Two Single-Nucleotide Polymorphisms Located Near WUSCHEL. Plant Physiology *156*, 2244-2254.

Mutte, S.K., Kato, H., Rothfels, C., Melkonian, M., Wong, G.K.-S., and Weijers, D. (2018). Origin and evolution of the nuclear auxin response system. eLife *7*, e33399.

Nakamasu, A., Takahashi, G., Kanbe, A., and Kondo, S. (2009). Interactions between zebrafish pigment cells responsible for the generation of Turing patterns. Proceedings of the National Academy of Sciences *106*, 8429-8434.

Napier, R.M. (1995). Towards an understanding of ABP1. Journal of Experimental Botany *46*, 1787-1795.

Napier, R.M. (2004). Plant Hormone Binding Sites. Ann Bot *93*, 227-233.
Napier, R.M., David, K.M., and Perrot-Rechenmann, C. (2002). A short history of auxin-binding proteins. In Auxin Molecular Biology, C. Perrot-Rechenmann, and G. Hagen, eds. (Dordrecht: Springer Netherlands), pp. 339-348.

Nemhauser, J.L., Feldman, L.J., and Zambryski, P.C. (2000). Auxin and ETTIN in Arabidopsis gynoecium morphogenesis. Development *127*, 3877-3888.

Nüsslein-Volhard, C., and Wieschaus, E. (1980). Mutations affecting segment number and polarity in Drosophila. Nature *287*, 795-801.

O'Malley, R.C., Huang, S.S.C., Song, L., Lewsey, M.G., Bartlett, A., Nery, J.R., Galli, M., Gallavotti, A., and Ecker, J.R. (2016). Cistrome and Epicistrome Features Shape the Regulatory DNA Landscape. Cell *165*, 1280-1292.

Oh, E., Seo, P.J., and Kim, J. (2018). Signaling Peptides and Receptors Coordinating Plant Root Development. Trends in Plant Science *23*, 337-351.
Oh, E., Zhu, J.Y., Bai, M.Y., Arenhart, R.A., Sun, Y., and Wang, Z.Y. (2014). Cell elongation is regulated through a central circuit of interacting transcription factors in the Arabidopsis hypocotyl. Elife *3*.

Ohno, C.K., Reddy, G.V., Heisler, M.G.B., and Meyerowitz, E.M. (2004). The Arabidopsis JAGGED gene encodes a zinc finger protein that promotes leaf tissue development. Development *131*, 1111-1122.

Olsen, A.N., Ernst, H.A., Lo Leggio, L., and Skriver, K. (2005). NAC transcription factors: structurally distinct, functionally diverse. Trends in Plant Science *10*, 79-87.
Omelyanchuk, N.A., Wiebe, D.S., Novikova, D.D., Levitsky, V.G., Klimova, N., Gorelova, V., Weinholdt, C., Vasiliev, G.V., Zemlyanskaya, E.V., Kolchanov, N.A.*, et al.* (2017). Auxin regulates functional gene groups in a fold-change-specific manner in Arabidopsis thaliana roots. Scientific Reports *7*.

Pan, Y., Liang, X., Gao, M., Liu, H., Meng, H., Weng, Y., and Cheng, Z. (2017). Round fruit shape in WI7239 cucumber is controlled by two interacting quantitative trait loci with one putatively encoding a tomato SUN homolog. Theoretical and Applied Genetics *130*, 573-586.

Parry, G., Calderon-Villalobos, L.I., Prigge, M., Peret, B., Dharmasiri, S., Itoh, H., Lechner, E., Gray, W.M., Bennett, M., and Estelle, M. (2009). Complex regulation of the TIR1/AFB family of auxin receptors. Proc Natl Acad Sci U S A *106*, 22540-22545.

Pauwels, L., Barbero, G.F., Geerinck, J., Tilleman, S., Grunewald, W., Perez, A.C., Chico, J.M., Vanden Bossche, R., Sewell, J., Gil, E.*, et al.* (2010). NINJA connects the co-repressor TOPLESS to jasmonate signalling. Nature *464*, 788-U169.
Pekker, I., Alvarez, J.P., and Eshed, Y. (2005). Auxin response factors mediate Arabidopsis organ asymmetry via modulation of KANADI activity. Plant Cell *17*, 2899-2910.

Pendle, A.F., Clark, G.P., Boon, R., Lewandowska, D., Lam, Y.W., Andersen, J., Mann, M., Lamond, A.I., Brown, J.W.S., and Shaw, P.J. (2005). Proteomic analysis of the Arabidopsis nucleolus suggests novel nucleolar functions. Molecular Biology of the Cell *16*, 260-269.

Péret, B., Swarup, K., Ferguson, A., Seth, M., Yang, Y., Dhondt, S., James, N., Casimiro, I., Perry, P., Syed, A.*, et al.* (2012). AUX/LAX genes encode a family of auxin influx transporters that perform distinct functions during Arabidopsis development. The Plant cell *24*, 2874-2885.

Petrášek, J., Mravec, J., Bouchard, R., Blakeslee, J.J., Abas, M., Seifertová, D., Wiśniewska, J., Tadele, Z., Kubeš, M., Čovanová, M.*, et al.* (2006). PIN Proteins Perform a Rate-Limiting Function in Cellular Auxin Efflux. Science *312*, 914-918.
Pi, L., Aichinger, E., van der Graaff, E., Llavata-Peris, C.I., Weijers, D., Hennig, L., Groot, E., and Laux, T. (2015). Organizer-Derived WOX5 Signal Maintains Root Columella Stem Cells through Chromatin-Mediated Repression of CDF4 Expression. Dev Cell *33*, 576-588.

Pierre-Jerome, E., Moss, B.L., Lanctot, A., Hageman, A., and Nemhauser, J.L. (2016). Functional analysis of molecular interactions in synthetic auxin response

circuits. Proceedings of the National Academy of Sciences of the United States of America *113*, 11354-11359.

Piya, S., Shrestha, S.K., Binder, B., Stewart, C.N., and Hewezi, T. (2014). Protein-protein interaction and gene co-expression maps of ARFs and Aux/IAAs in Arabidopsis. Frontiers in Plant Science *5*.

Plavskin, Y., Nagashima, A., Perroud, P.-F., Hasebe, M., Quatrano, R.S., Atwal, G.S., and Timmermans, M.C.P. (2016). Ancient trans-Acting siRNAs Confer Robustness and Sensitivity onto the Auxin Response. Developmental Cell *36*, 276-289.

Pradeepa, M.M., Grimes, G.R., Kumar, Y., Olley, G., Taylor, G.C., Schneider, R., and Bickmore, W.A. (2016). Histone H3 globular domain acetylation identifies a new class of enhancers. Nat Genet.

Questa, J.I., Song, J., Geraldo, N., An, H.L., and Dean, C. (2016). Arabidopsis transcriptional repressor VAL1 triggers Polycomb silencing at FLC during vernalization. Science *353*, 485-488.

Quinet, M., Angosto, T., Yuste-Lisbona, F.J., Blanchard-Gros, R., Bigot, S., Martinez, J.P., and Lutts, S. (2019). Tomato Fruit Development and Metabolism. Frontiers in Plant Science *10*, 23.

Rademacher, E.H., Lokerse, A.S., Schlereth, A., Llavata-Peris, C.I., Bayer, M., Kientz, M., Rios, A.F., Borst, J.W., Lukowitz, W., Juergens, G.*, et al.* (2012). Different Auxin Response Machineries Control Distinct Cell Fates in the Early Plant Embryo. Developmental Cell *22*, 211-222.

Rademacher, E.H., Moller, B., Lokerse, A.S., Llavata-Peris, C.I., van den Berg, W., and Weijers, D. (2011). A cellular expression map of the Arabidopsis AUXIN RESPONSE FACTOR gene family. Plant Journal *68*, 597-606.

Rajani, S., and Sundaresan, V. (2001). The Arabidopsis myc/bHLH gene ALCATRAZ enables cell separation in fruit dehiscence. Current Biology *11*, 1914-1922.

Raven, J.A. (1975). TRANSPORT OF INDOLEACETIC ACID IN PLANT CELLS IN RELATION TO pH AND ELECTRICAL POTENTIAL GRADIENTS, AND ITS SIGNIFICANCE FOR POLAR IAA TRANSPORT. New Phytologist *74*, 163-172.

Ream, T.S., Haag, J.R., Wierzbicki, A.T., Nicora, C.D., Norbeck, A.D., Zhu, J.-K., Hagen, G., Guilfoyle, T.J., Paša-Tolić, L., and Pikaard, C.S. (2009). Subunit Compositions of the RNA-Silencing Enzymes Pol IV and Pol V Reveal Their Origins as Specialized Forms of RNA Polymerase II. Molecular Cell *33*, 192-203.

Reyes-Olalde, J.I., Zuniga-Mayo, V.M., Montes, R.A.C., Marsch-Martinez, N., and de Folter, S. (2013). Inside the gynoecium: at the carpel margin. Trends in Plant Science *18*, 644-655.

Ringrose, L. (2007). Polycomb comes of age: genome-wide profiling of target sites. Current Opinion in Cell Biology *19*, 290-297.

Ripoll, J.-J., Zhu, M., Brocke, S., Hon, C.T., Yanofsky, M.F., Boudaoud, A., and Roeder, A.H.K. (2019). Growth dynamics of the Arabidopsis fruit is mediated by cell expansion. Proceedings of the National Academy of Sciences *116*, 25333-25342.

Robert, S., Kleine-Vehn, J., Barbez, E., Sauer, M., Paciorek, T., Baster, P., Vanneste, S., Zhang, J., Simon, S., Čovanová, M.*, et al.* (2010). ABP1 Mediates Auxin Inhibition of Clathrin-Dependent Endocytosis in Arabidopsis. Cell *143*, 111-121.

Robson, F., Costa, M.M.R., Hepworth, S.R., Vizir, I., Pin˜eiro, M., Reeves, P.H., Putterill, J., and Coupland, G. (2001). Functional importance of conserved domains in the flowering-time gene CONSTANS demonstrated by analysis of mutant alleles and transgenic plants. The Plant Journal *28*, 619-631.

Rodríguez-Leal, D., Lemmon, Z.H., Man, J., Bartlett, M.E., and Lippman, Z.B. (2017). Engineering Quantitative Trait Variation for Crop Improvement by Genome Editing. Cell *171*, 470-480.e478.

Rodríguez, G.R., Muños, S., Anderson, C., Sim, S.-C., Michel, A., Causse, M., Gardener, B.B.M., Francis, D., and van der Knaap, E. (2011). Distribution of SUN, OVATE, LC, and FAS in the Tomato Germplasm and the Relationship to Fruit Shape Diversity. Plant Physiology *156*, 275-285.

Roeder, A.H.K., Ferrándiz, C., and Yanofsky, M.F. (2003). The Role of the REPLUMLESS Homeodomain Protein in Patterning the Arabidopsis Fruit. Current Biology *13*, 1630-1635.

Roeder, A.H.K., and Yanofsky, M.F. (2006). Fruit development in Arabidopsis. The Arabidopsis book / American Society of Plant Biologists *4*, e0075.

Rokhsar, D.S., Fazo, J., Putnam, N., Hayes, R.D., Neupane, R., Howson, R., Shu, S., Mitros, T., Hellsten, U., Dirks, W.*, et al.* (2011). Phytozome: a comparative platform for green plant genomics. Nucleic Acids Research *40*, D1178-D1186.

Sablowski, R. (2015). Control of patterning, growth, and differentiation by floral organ identity genes. Journal of Experimental Botany *66*, 1065-1073.

Sammons, M., Wan, S.S., Vogel, N.L., Mientjes, E.J., Grosveld, G., and Ashburner, B.P. (2006). Negative regulation of the RelA/p65 transactivation function by the product of the DEK proto-oncogene. Journal of Biological Chemistry *281*, 26802-26812.

Sangster, T.A., Bahrami, A., Wilczek, A., Watanabe, E., Schellenberg, K., McLellan, C., Kelley, A., Kong, S.W., Queitsch, C., and Lindquist, S. (2007). Phenotypic Diversity and Altered Environmental Plasticity in Arabidopsis thaliana with Reduced Hsp90 Levels. PLOS ONE *2*, e648.

Sangster, T.A., and Queitsch, C. (2005). The HSP90 chaperone complex, an emerging force in plant development and phenotypic plasticity. Current Opinion in Plant Biology *8*, 86-92.

Sato, A., and Yamamoto, K.T. (2008). Overexpression of the non-canonical Aux/IAA genes causes auxin-related aberrant phenotypes in Arabidopsis. Physiologia Plantarum *133*, 397-405.

Sato, S., Tabata, S., Hirakawa, H., Asamizu, E., Shirasawa, K., Isobe, S., Kaneko, T., Nakamura, Y., Shibata, D., Aoki, K.*, et al.* (2012). The tomato genome sequence provides insights into fleshy fruit evolution. Nature *485*, 635-641.

Scheres, B. (2007). Stem-cell niches: nursery rhymes across kingdoms. Nature Reviews Molecular Cell Biology *8*, 345.

Scheres, B., Wolkenfelt, H., Willemsen, V., Terlouw, M., Lawson, E., Dean, C., and Weisbeek, P. (1994). Embryonic origin of the Arabidopsis primary root and root meristem initials. Development *120*, 2475-2487.

Schiessl, K., Muiño, J.M., and Sablowski, R. (2014). Arabidopsis JAGGED links floral organ patterning to tissue growth by repressing Kip-related cell cycle inhibitors. Proceedings of the National Academy of Sciences *111*, 2830-2835.

Schneider, C.A., Rasband, W.S., and Eliceiri, K.W. (2012). NIH Image to ImageJ: 25 years of image analysis. Nature Methods *9*, 671-675.

Schoof, H., Lenhard, M., Haecker, A., Mayer, K.F.X., Jürgens, G., and Laux, T. (2000). The Stem Cell Population of Arabidopsis Shoot Meristems Is Maintained by a Regulatory Loop between the CLAVATA and WUSCHEL Genes. Cell *100*, 635-644.

Schübeler, D. (2015). Function and information content of DNA methylation. Nature *517*, 321.

Schuster, C., Gaillochet, C., and Lohmann, J.U. (2015). Arabidopsis HECATE genes function in phytohormone control during gynoecium development. Development (Cambridge, England) *142*, 3343-3350.

Scutt, C.P., Vinauger-Douard, M., Fourquin, C., Finet, C., and Dumas, C. (2006). An evolutionary perspective on the regulation of carpel development. Journal of Experimental Botany *57*, 2143-2152.

Sekiya, T., and Zaret, K.S. (2007). Repression by Groucho/TLE/Grg Proteins: Genomic Site Recruitment Generates Compacted Chromatin In Vitro and Impairs Activator Binding In Vivo. Molecular Cell *28*, 291-303.

Sessions, A., Nemhauser, J.L., McColl, A., Roe, J.L., Feldmann, K.A., and Zambryski, P.C. (1997). ETTIN patterns the Arabidopsis floral meristem and reproductive organs. Development *124*, 4481-4491.

Sessions, A.Z. (1995). Arabidopsis gynoecium structure in the wild type and ettin mutants.

Sessions, R.A. (1997). Arabidopsis (Brassicaceae) flower development and gynoecium patterning in wild type and Ettin mutants. American Journal of Botany *84*, 1179-1191.

Seymour, G.B., Ostergaard, L., Chapman, N.H., Knapp, S., and Martin, C. (2013). Fruit Development and Ripening. In Annual Review of Plant Biology, Vol 64, S.S. Merchant, ed. (Palo Alto: Annual Reviews), pp. 219-241.

Shima, Y., Kitagawa, M., Fujisawa, M., Nakano, T., Kato, H., Kimbara, J., Kasumi, T., and Ito, Y. (2013). Tomato FRUITFULL homologues act in fruit ripening via

forming MADS-box transcription factor complexes with RIN. Plant Molecular Biology *82*, 427-438.

Shin, R., Burch, A.Y., Huppert, K.A., Tiwari, S.B., Murphy, A.S., Guilfoyle, T.J., and Schachtman, D.P. (2007). The Arabidopsis transcription factor MYB77 modulates auxin signal transduction. Plant Cell *19*, 2440-2453.

Shogren-Knaak, M., Ishii, H., Sun, J.-M., Pazin, M.J., Davie, J.R., and Peterson, C.L. (2006). Histone H4-K16 Acetylation Controls Chromatin Structure and Protein Interactions. Science *311*, 844-847.

Siegfried, K.R., Eshed, Y., Baum, S.F., Otsuga, D., Drews, G.N., and Bowman, J.L. (1999). Members of the YABBY gene family specify abaxial cell fate in Arabidopsis. Development *126*, 4117-4128.

Simon, J.A., and Tamkun, J.W. (2002). Programming off and on states in chromatin: mechanisms of Polycomb and trithorax group complexes. Curr Opin Genet Dev *12*, 210-218.

Simonini, S., Bencivenga, S., Trick, M., and Ostergaard, L. (2017). Auxin-Induced Modulation of ETTIN Activity Orchestrates Gene Expression in Arabidopsis. The Plant Cell.

Simonini, S., Deb, J., Moubayidin, L., Stephenson, P., Valluru, M., Freire-Rios, A., Sorefan, K., Weijers, D., Friml, J., and Ostergaard, L. (2016). A noncanonical auxin-sensing mechanism is required for organ morphogenesis in Arabidopsis. Genes & Development *30*, 2286-2296.

Simonini, S., Mas, P.J., Mas, C.M.V.S., Østergaard, L., and Hart, D.J. (2018a). Auxin sensing is a property of an unstructured domain in the Auxin Response Factor ETTIN of Arabidopsis thaliana. Scientific Reports *8*, 13563.

Simonini, S., Stephenson, P., and Østergaard, L. (2018b). A molecular framework controlling style morphology in Brassicaceae. Development *145*.

Singh, K.B. (1998). Transcriptional regulation in plants: The importance of combinatorial control. Plant Physiology *118*, 1111-1120.

Smith, Z.R., and Long, J.A. (2010). Control of Arabidopsis apical-basal embryo polarity by antagonistic transcription factors. Nature *464*, 423-U121.

Smyth, D.R., Bowman, J.L., and Meyerowitz, E.M. (1990). EARLY FLOWER DEVELOPMENT IN ARABIDOPSIS. Plant Cell *2*, 755-767.

Soares, L.M.M., Zanier, K., Mackereth, C., Sattler, M., and Valcarcel, J. (2006). Intron removal requires proofreading of U2AF/3 ' splice site recognition by DEK. Science *312*, 1961-1965.

Sorefan, K., Girin, T., Liljegren, S.J., Ljung, K., Robles, P., Galvan-Ampudia, C.S., Offringa, R., Friml, J., Yanofsky, M.F., and Ostergaard, L. (2009). A regulated auxin minimum is required for seed dispersal in Arabidopsis. Nature *459*, 583-U114.

Soyk, S., Lemmon, Z.H., Oved, M., Fisher, J., Liberatore, K.L., Park, S.J., Goren, A., Jiang, K., Ramos, A., van der Knaap, E.*, et al.* (2017). Bypassing Negative Epistasis on Yield in Tomato Imposed by a Domestication Gene. Cell *169*, 1142-+.

Steffen, P.A., and Ringrose, L. (2014). What are memories made of ? How Polycomb and Trithorax proteins mediate epigenetic memory. Nature Reviews Molecular Cell Biology *15*, 340-356.

Stepanova, A.N., Robertson-Hoyt, J., Yun, J., Benavente, L.M., Xie, D.-Y., Doležal, K., Schlereth, A., Jürgens, G., and Alonso, J.M. (2008). TAA1-Mediated Auxin Biosynthesis Is Essential for Hormone Crosstalk and Plant Development. Cell *133*, 177-191.

Stigliani, A., Martin-Arevalillo, R., Lucas, J., Bessy, A., Vinos-Poyo, T., Mironova, V., Vernoux, T., Dumas, R., and Parcy, F. (2018). Capturing Auxin Response Factors Syntax Using DNA Binding Models. Molecular Plant.

Stoeger, T., Battich, N., and Pelkmans, L. (2016). Passive Noise Filtering by Cellular Compartmentalization. Cell *164*, 1151-1161.

Sun, X., Cahill, J., Van Hautegem, T., Feys, K., Whipple, C., Novák, O., Delbare, S., Versteele, C., Demuynck, K., De Block, J.*, et al.* (2017). Altered expression of maize PLASTOCHRON1 enhances biomass and seed yield by extending cell division duration. Nature Communications *8*, 14752.

Swarup, K., Benková, E., Swarup, R., Casimiro, I., Péret, B., Yang, Y., Parry, G., Nielsen, E., De Smet, I., Vanneste, S.*, et al.* (2008). The auxin influx carrier LAX3 promotes lateral root emergence. Nature Cell Biology *10*, 946.

Szemenyei, H., Hannon, M., and Long, J.A. (2008). TOPLESS mediates auxin-dependent transcriptional repression during Arabidopsis embryogenesis. Science *319*, 1384-1386.

Tabata, R., Ikezaki, M., Fujibe, T., Aida, M., Tian, C.-e., Ueno, Y., Yamamoto, K.T., Machida, Y., Nakamura, K., and Ishiguro, S. (2009). Arabidopsis AUXIN RESPONSE FACTOR6 and 8 Regulate Jasmonic Acid Biosynthesis and Floral Organ Development via Repression of Class 1 KNOX Genes. Plant and Cell Physiology *51*, 164-175.

Tan, X., Calderon-Villalobos, L.I.A., Sharon, M., Zheng, C.X., Robinson, C.V., Estelle, M., and Zheng, N. (2007). Mechanism of auxin perception by the TIR1 ubiquitin ligase. Nature *446*, 640-645.

Tao, Y., Ferrer, J.-L., Ljung, K., Pojer, F., Hong, F., Long, J.A., Li, L., Moreno, J.E., Bowman, M.E., Ivans, L.J.*, et al.* (2008). Rapid Synthesis of Auxin via a New Tryptophan-Dependent Pathway Is Required for Shade Avoidance in Plants. Cell *133*, 164-176.

ten Hove, C.A., Lu, K.J., and Weijers, D. (2015). Building a plant: cell fate specification in the early Arabidopsis embryo. Development *142*, 420-430.

Thomas, M.C., and Chiang, C.M. (2006). The general transcription machinery and general cofactors. Critical Reviews in Biochemistry and Molecular Biology *41*, 105-178.

Tie, F., Banerjee, R., Conrad, P.A., Scacheri, P.C., and Harte, P.J. (2012). Histone Demethylase UTX and Chromatin Remodeler BRM Bind Directly to CBP and

Modulate Acetylation of Histone H3 Lysine 27. Molecular and Cellular Biology *32*, 2323-2334.

Tiwari, S.B., Hagen, G., and Guilfoyle, T. (2003). The roles of auxin response factor domains in auxin-responsive transcription. Plant Cell *15*, 533-543.

Tromas, A., Paque, S., Stierlé, V., Quettier, A.-L., Muller, P., Lechner, E., Genschik, P., and Perrot-Rechenmann, C. (2013). Auxin-Binding Protein 1 is a negative regulator of the SCFTIR1/AFB pathway. Nature Communications *4*, 2496.

Tsai, M., and O'Malley, B.W. (1994). Molecular Mechanisms of Action of Steroid/Thyroid Receptor Superfamily Members. Annual Review of Biochemistry *63*, 451-486.

Tsuzuki, M., Nishihama, R., Ishizaki, K., Kurihara, Y., Matsui, M., Bowman, J.L., Kohchi, T., Hamada, T., and Watanabe, Y. (2016). Profiling and Characterization of Small RNAs in the Liverwort, Marchantia polymorpha , Belonging to the First Diverged Land Plants. Plant and Cell Physiology *57*, 359-372.

Turing, A.M. (1952). The chemical basis of morphogenesis. Philosophical Transactions of the Royal Society of London Series B, Biological Sciences *237*, 37-72.

Turki-Judeh, W., and Courey, A.J. (2012). Chapter three - Groucho: A Corepressor with Instructive Roles in Development. In Current Topics in Developmental Biology, S. Plaza, and F. Payre, eds. (Academic Press), pp. 65-96.

Uchida, N., Takahashi, K., Iwasaki, R., Yamada, R., Yoshimura, M., Endo, T.A., Kimura, S., Zhang, H., Nomoto, M., Tada, Y.*, et al.* (2018). Chemical hijacking of auxin signaling with an engineered auxin–TIR1 pair. Nature Chemical Biology *14*, 299.

Ulmasov, T., Hagen, G., and Guilfoyle, T.J. (1997a). ARF1, a Transcription Factor That Binds to Auxin Response Elements. Science *276*, 1865-1868.

Ulmasov, T., Hagen, G., and Guilfoyle, T.J. (1999a). Activation and repression of transcription by auxin-response factors. Proceedings of the National Academy of Sciences of the United States of America *96*, 5844-5849.

Ulmasov, T., Hagen, G., and Guilfoyle Tom, J. (1999b). Dimerization and DNA binding of auxin response factors. The Plant Journal *19*, 309-319.

Ulmasov, T., Murfett, J., Hagen, G., and Guilfoyle, T.J. (1997b). Aux/IAA proteins repress expression of reporter genes containing natural and highly active synthetic auxin response elements. The Plant Cell *9*, 1963-1971.

Vakoc, C.R., Sachdeva, M.M., Wang, H., and Blobel, G.A. (2006). Profile of Histone Lysine Methylation across Transcribed Mammalian Chromatin. Molecular and Cellular Biology *26*, 9185-9195.

van Amerongen, R., and Nusse, R. (2009). Towards an integrated view of Wnt signaling in development. Development *136*, 3205-3214.

van der Knaap, E., Chakrabarti, M., Chu, Y.H., Clevenger, J.P., Illa-Berenguer, E., Huang, Z., Keyhaninejad, N., Mu, Q., Sun, L., Wang, Y.*, et al.* (2014). What lies

beyond the eye: the molecular mechanisms regulating tomato fruit weight and shape. Frontiers in Plant Science *5*.

van Tienen, L.M., Mieszczanek, J., Fielder, M., Rutherford, T.J., and Bienz, M. (2017). Constitutive scaffolding of multiple Wnt enhanceosome components by Legless/BCL9. Elife *6*.

Vanhaeren, H., Inzé, D., and Gonzalez, N. (2016). Plant Growth Beyond Limits. Trends in Plant Science *21*, 102-109.

Vanneste, S., and Friml, J. (2009). Auxin: A Trigger for Change in Plant Development. Cell *136*, 1005-1016.

Varaud, E., Brioudes, F., Szecsi, J., Leroux, J., Brown, S., Perrot-Rechenmann, C., and Bendahmane, M. (2011). AUXIN RESPONSE FACTOR8 Regulates Arabidopsis Petal Growth by Interacting with the bHLH Transcription Factor BIGPETALp. Plant Cell *23*, 973-983.

Vercruyssen, L., Verkest, A., Gonzalez, N., Heyndrickx, K.S., Eeckhout, D., Han, S.K., Jegu, T., Archacki, R., Van Leene, J., Andriankaja, M.*, et al.* (2014). ANGUSTIFOLIA3 Binds to SWI/SNF Chromatin Remodeling Complexes to Regulate Transcription during Arabidopsis Leaf Development. Plant Cell *26*, 210-229.

Vernoux, T., Brunoud, G., Farcot, E., Morin, V., Van den Daele, H., Legrand, J., Oliva, M., Das, P., Larrieu, A., Wells, D.*, et al.* (2011). The auxin signalling network translates dynamic input into robust patterning at the shoot apex. Molecular Systems Biology *7*.

Vukasinovic, N., and Russinova, E. (2018). BRexit: Possible Brassinosteroid Export and Transport Routes. Trends Plant Sci *23*, 285-292.

Waidmann, S., Kusenda, B., Mayerhofer, J., Mechtler, K., and Jonak, C. (2014). A DEK Domain-Containing Protein Modulates Chromatin Structure and Function in Arabidopsis. Plant Cell *26*, 4328-4344.

Wang, R.-L., Stec, A., Hey, J., Lukens, L., and Doebley, J. (1999). The limits of selection during maize domestication. Nature *398*, 236-239.

Wang, R., Zhang, Y., Kieffer, M., Yu, H., Kepinski, S., and Estelle, M. (2016). HSP90 regulates temperature-dependent seedling growth in Arabidopsis by stabilizing the auxin co-receptor F-box protein TIR1. Nature Communications *7*, 10269.

Watanabe, K., and Okada, K. (2003). Two discrete cis elements control the abaxial side-specific expression of the FILAMENTOUS FLOWER gene in Arabidopsis. Plant Cell *15*, 2592-2602.

Watson, J.D., and Crick, F.H.C. (1953). Molecular Structure of Nucleic Acids: A Structure for Deoxyribose Nucleic Acid. Nature *171*, 737-738.

Weigel, D., and Jürgens, G. (2002). Stem cells that make stems. Nature *415*, 751-754.

Weijers, D., Benkova, E., Jäger, K.E., Schlereth, A., Hamann, T., Kientz, M., Wilmoth, J.C., Reed, J.W., and Jürgens, G. (2005). Developmental specificity of auxin response by pairs of ARF and Aux/IAA transcriptional regulators. The EMBO Journal *24*, 1874-1885.

Weijers, D., Schlereth, A., Ehrismann, J.S., Schwank, G., Kientz, M., and Jurgens, G. (2006). Auxin triggers transient local signaling for cell specification in Arabidopsis embryogenesis. Developmental Cell *10*, 265-270.

Weiste, C., and Droege-Laser, W. (2014). The Arabidopsis transcription factor bZIP11 activates auxin-mediated transcription by recruiting the histone acetylation machinery. Nature Communications *5*.

Went, F.W.T., K. V. (1937). Phytohormones. (New York, USA: MacMillan Company, New York.).

Wetmore, R.H., and Wardlaw, C.W. (1951). Experimental Morphogenesis in Vascular Plants. Annual Review of Plant Physiology *2*, 269-292.

Whitehouse, I., Flaus, A., Cairns, B.R., White, M.F., Workman, J.L., and Owen-Hughes, T. (1999). Nucleosome mobilization catalysed by the yeast SWI/SNF complex. Nature *400*, 784-787.

Whittaker, C., and Dean, C. (2017). The FLC Locus: A Platform for Discoveries in Epigenetics and Adaptation. In Annual Review of Cell and Developmental Biology, Vol 33, R. Schekman, ed. (Palo Alto: Annual Reviews), pp. 555-575.

Wolpert, L. (1969). Positional information and the spatial pattern of cellular differentiation. Journal of Theoretical Biology *25*, 1-47.

Woo, E.-J., Marshall, J., Bauly, J., Chen, J.-G., Venis, M., Napier, R.M., and Pickersgill, R.W. (2002). Crystal structure of auxin-binding protein 1 in complex with auxin. The EMBO Journal *21*, 2877-2885.

Wu, M.-F., Sang, Y., Bezhani, S., Yamaguchi, N., Han, S.-K., Li, Z., Su, Y., Slewinski, T.L., and Wagner, D. (2012). SWI2/SNF2 chromatin remodeling ATPases overcome polycomb repression and control floral organ identity with the LEAFY and SEPALLATA3 transcription factors. Proceedings of the National Academy of Sciences of the United States of America *109*, 3576-3581.

Wu, M.-F., Yamaguchi, N., Xiao, J., Bargmann, B., Estelle, M., Sang, Y., and Wagner, D. (2015). Auxin-regulated chromatin switch directs acquisition of flower primordium founder fate. eLife *4*.

Wu, S., Xiao, H., Cabrera, A., Meulia, T., and van der Knaap, E. (2011). SUN Regulates Vegetative and Reproductive Organ Shape by Changing Cell Division Patterns. Plant Physiology *157*, 1175-1186.

Wu, S.Y., Zhou, T.Y., and Chiang, C.M. (2003). Human mediator enhances activator-facilitated recruitment of RNA polymerase II and promoter recognition by TATA-binding protein (TBP) independently of TBP-associated factors. Molecular and Cellular Biology *23*, 6229-6242.

Wunderlich, Z., and Mirny, L.A. (2009). Different gene regulation strategies revealed by analysis of binding motifs. Trends in Genetics *25*, 434-440.

Xiang, D.Q., Yang, H., Venglat, P., Cao, Y.G., Wen, R., Ren, M.Z., Stone, S., Wang, E., Wang, H., Xiao, W*., et al.* (2011). POPCORN Functions in the Auxin Pathway to Regulate Embryonic Body Plan and Meristem Organization in Arabidopsis. Plant Cell *23*, 4348-4367.

Xiao, J., and Wagner, D. (2015). Polycomb repression in the regulation of growth and development in Arabidopsis. Current Opinion in Plant Biology *23*, 15-24.

XU, F., FANG, J., OU, S., GAO, S., ZHANG, F., DU, L., XIAO, Y., WANG, H., SUN, X., CHU, J*., et al.* (2015). Variations in CYP78A13 coding region influence grain size and yield in rice. Plant, Cell & Environment *38*, 800-811.

Xu, T., Dai, N., Chen, J., Nagawa, S., Cao, M., Li, H., Zhou, Z., Chen, X., De Rycke, R., Rakusová, H*., et al.* (2014). Cell Surface ABP1-TMK Auxin-Sensing Complex Activates ROP GTPase Signaling. Science *343*, 1025-1028.

Xu, X.P., Chen, C.H., Fan, B.F., and Chen, Z.X. (2006). Physical and functional interactions between pathogen-induced Arabidopsis WRKY18, WRKY40, and WRKY60 transcription factors. Plant Cell *18*, 1310-1326.

Yamaguchi, N., Wu, M.-F., Winter, Cara M., Berns, Markus C., Nole-Wilson, S., Yamaguchi, A., Coupland, G., Krizek, Beth A., and Wagner, D. (2013). A Molecular Framework for Auxin-Mediated Initiation of Flower Primordia. Developmental Cell *24*, 271-282.

Yang, H.C., Berry, S., Olsson, T.S.G., Hartley, M., Howard, M., and Dean, C. (2017). Distinct phases of Polycomb silencing to hold epigenetic memory of cold in Arabidopsis. Science *357*, 1142-1145.

Yang, H.C., Howard, M., and Dean, C. (2014). Antagonistic Roles for H3K36me3 and H3K27me3 in the Cold-Induced Epigenetic Switch at Arabidopsis FLC. Current Biology *24*, 1793-1797.

Zhang, X.-C., Millet, Y.A., Cheng, Z., Bush, J., and Ausubel, F.M. (2015). Jasmonate signalling in Arabidopsis involves SGT1b–HSP70–HSP90 chaperone complexes. Nature Plants *1*, 15049.

Zhang, Y., Iratni, R., ErdjumentBromage, H., Tempst, P., and Reinberg, D. (1997). Histone deacetylases and SAP18, a novel polypeptide, are components of a human Sin3 complex. Cell *89*, 357-364.

Zhao, B., Dai, A., Wei, H., Yang, S., Wang, B., Jiang, N., and Feng, X. (2016). Arabidopsis KLU homologue GmCYP78A72 regulates seed size in soybean. Plant Molecular Biology *90*, 33-47.

Zhao, Y. (2010). Auxin Biosynthesis and Its Role in Plant Development. Annual Review of Plant Biology *61*, 49-64.

Zheng, Y., and Liu, X. (2019). Review: Chromatin organization in plant and animal stem cell maintenance. Plant Science *281*, 173-179.

Zhou, V.W., Goren, A., and Bernstein, B.E. (2010). Charting histone modifications and the functional organization of mammalian genomes. Nature Reviews Genetics *12*, 7.

Zhu, G., Wang, S., Huang, Z., Zhang, S., Liao, Q., Zhang, C., Lin, T., Qin, M., Peng, M., Yang, C.*, et al.* (2018). Rewiring of the Fruit Metabolome in Tomato Breeding. Cell *172*, 249-261.e212.

Zhu, Z., Xu, F., Zhang, Y., Cheng, Y.T., Wiermer, M., Li, X., and Zhang, Y. (2010). Arabidopsis resistance protein SNC1 activates immune responses through association with a transcriptional corepressor. Proceedings of the National Academy of Sciences *107*, 13960-13965.

Zilberman, D., Cao, X., Johansen, L.K., Xie, Z., Carrington, J.C., and Jacobsen, S.E. (2004). Role of Arabidopsis ARGONAUTE4 in RNA-Directed DNA Methylation Triggered by Inverted Repeats. Current Biology *14*, 1214-1220.